University of Brighton

School of Pharmacy and Biomolecular Sciences

Improving Flurbiprofen brain-permeability and targeting in Alzheimer's disease by using a novel dendronised ApoE-derived peptide carrier system

Shafq K. Al-azzawi

A thesis submitted in fulfilment of the requirements of the University of Brighton for the degree of Doctor of Philosophy

October 2017

Abstract

Alzheimer disease (AD) is a neurodegenerative and age related disease characterised by gradual decrease in memory, caused by the abnormal accumulation of beta-amyloid (Aβ) in the brain. Recently, the incidence of AD has increased with 47 million people worldwide having this disease. Current available drugs are only capable of improving symptoms, but do not have profound effects on the underlying cause of the disease. Lack of a true treatment is due to limitations imposed by the blood brain barrier (BBB) that blocks the passage of drugs to the brain. Flurbiprofen is an example of a drug that has the potential to be used in the treatment of AD as it has shown to decrease the formation of Aβ, but the drug's efficacy is hampered due to its poor permeability across the BBB. A promising approach for improved drug permeability is the integration of the drug with specific carriers, such as dendrimers, that have the ability to pass through the BBB. Dendrimers are hyper branched macromolecules, have a unique structure that can be easily bifunctionalised with both the drug and a ligand such as ApoE derived peptide facilitating the biochemical integration with cell membranes. This favours the recognition by the low density lipoprotein receptors on the brain endothelial cells, enhancing cellular uptake and brain targeting of the carrier system. The present project aims to improve brain permeability of Flurbiprofen by developing novel, biocompatible and biodegradable dendrimer-based carrier systems utilising an ApoE-derived peptide to facilitate brain delivery and targeting.

The novel dendronised molecules and the functionalisation with ApoE-derived peptide were produced and integrated with the Flurbiprofen using solid phase peptide synthesis. Mass spectra, Fourier transform infra-red spectroscopy, high performance liquid chromatography (HPLC) and thin layer chromatography were used for characterisation and verifying the purity of the products. A bEnd.3 brain endothelial cell line was used as an *in vitro* BBB model to determine the biocompatibility, uptake and permeability of the synthesised molecules. The cellular biochemical response upon exposure to the novel materials was studied using MTT, LDH, and Hoechst-propidium iodide assays. The cellular permeability of each material was assessed using an *in vitro* model based on a monolayer system utilising bEnd.3 cells grown in a Transwell support, while confocal microscopy, flow cytometry and HPLC were used for quantitative and qualitative analysis. In addition, the activity of the drug conjugates was investigated biochemically by

quantification of γ-secretase enzyme and the biodegradability of these conjugates was also verified.

The results of this study indicated that the dendronised carrier systems were successfully produced and efficiently conjugated with the Flurbiprofen via amide linkage. These dendrons, both denuded and functionalised with the drug and ApoE peptide, were also found non-toxic. Moreover, the uptake and permeability results demonstrated the potential of the dendronised ApoE peptide to improve the drug permeability significantly across the *in vitro* model of the BBB after the validity of this model was verified. Furthermore, the results showed that the Flurbiprofen-bound carriers still retain the drug action in decreasing the activity of γ-secretase enzyme on C6 glial cells alongside with evidence of the biodegradability of the drug conjugates into their building units.

This novel study provides the first demonstration of drug-laden, ApoE peptide-functionalised dendrimers with the potential ability to cross the BBB and targeting the brain via receptor mediation for enhanced drug therapy of AD.

Contents

Abbreviations

ABC transporters	ATP-binding cassette transporters
AD	Alzheimer disease
AEP	Apolipoprotein E derived peptide
AEP-K-FP	Apolipoprotein E derived peptide- Generation 0 lysine- 2 Flurbiprofen
AICD	Cytoplasmic domain
AJs	Adheren junctions
AMT	Adsorptive-mediated transcytosis
Apo E	Apolipoprotein E
APP	Amyloid precursor protein
Aβ	Beta-amyloid
bEnd.3	Immortalised brain capillary endothelial cells
BACE	β-secretase
BBB	Blood brain barrier
Boc	Tert-butoxycarbonyl
CL	Cardiolipine
CNS	Central nervous system
COX	Cyclooxygenase
CLSM	Confocal laser scanning microscope
CSF	Cerebro-spinal fluid
CTF	C-terminal fragment
Da	Dalton
DDS	Drug delivery system
DIPEA	N,N-Diisopropylethylamine
DMEM	Dulbecco's Modified Eagle's Medium

DMF	N,N-Dimethylformamide
DMSO	Dimethylsulfoxide
DTR	Diphtheria toxin receptor
DW	Distilled water
EC	Endothelial cells
ESI	Electrospray ionisation
ELISA	Enzyme-linked immune-sorbent assay
F	Phenylalanine
FBS	Foetal bovine serum
FSC	Forward scattering
Fmoc	9-Fluorenylmethyloxycarbonyl
FP	Flurbiprofen
FTIR	Fourier Transform Infra-Red
FITC	Fluorescein-5-isothiocyanate (isomer I)
G0K	Phenylalanine-Generation 0 lysine dendron
G0K-FP	Phenylalanine-Generation 0 lysine- 2Flurbiprofen
G1K	Phenylalanine-Generation 1 lysine dendron
G1K-FP	Phenylalanine-Generation 1 lysine- 4Flurbiprofen
GLUT	Glucose-transporter
GSM	Gamma secretase modulator
HBTU	N,N,N′,N′-Tetramethyl-O- (1H-benzotriazol-1-yl) uronium hexafluorophosphate
HF	Hydrogen flouride
HPI	Hoechst-propidium iodide
HPLC	High performance liquid chromatography
HRP	Horseradish peroxidase
HUVECs	Human umbilical vein endothelial cells

JAMs	Junctional adhesion molecules
K	Lysine
LDH	Lactate dehydrogenase
Lf	Lactoferrin
m/z	Mass to charge ratio
MDR	Multidrug resistance protein
MS	Mass spectrometry
MTT	3-(4,5-Dimethylthiazol-2-yl)-3,5-diphenylformazan (Thiazolyl blue tetrazolium)
MW	Molecular weight
ND	Neurodegenerative disease
NFTs	Neurofibrillary tangles
NLs	Nanoliposomes
NMs	Nanomaterials
NPs	Nanoparticles
NSAIDs	Nonsteroidal anti-inflammatory drugs
PA	Phosphatidic acid
PAMAM	Poly amido amine dendrimers
PEG	Poly ethylene glycol
P-gp	P-glycoproteins
PPI	Poly propylene imine
PSEN	Presenilin
PMT	Photo multiplier tube
Rf	Retention factor
RMT	Receptor-mediated transcytosis
RPM	Rotation per minute
SLCs	Solute carriers

SPPS	Solid phase peptide synthesis
SPs	Senile plaques
SSC	Side scattering
T2D	Type 2 diabetes
TEER	Transepithelial electrical resistance
TFA	Trifluoroacetic acid
Tf	Transferrin
TfR	Transferrin receptor
TIPS	Trisopropylsilane
TJs	Tight junctions
TLC	Thin Layer Chromatography
TMD	Transmembrane domain
TMB	Tetramethylbenzidine
TNF	Tumour necrosis factor
ZO	Zonula occludens

List of figures

List of tables

Acknowledgment

It is a genuine pleasure to express my deep thanks to my supervisors, Professor Matteo Santin, Dr. Gary Phillips, Dr. Anna Guildford and Dr. Houria Bachtarzi for their patience, guidance and support to complete this work.

I owe a deep sense of gratitude to the Ministry of Higher Education in Iraq represented by the Iraqi Cultural Attaché in the UK for offering me the grant and financial support to finish my PhD.

My sincere thanks also go to Dr. Steve Meikle for his encouragement, valuable knowledge and resources to perform my laboratory work.

I am also thankful to Dr. Valeria Perugini and Dr. Mark Best for all the help they provided during my project.

I would like to express my deepest appreciation to Chris Morris and Maurizio Valeri for guiding me during tissue culture experiments. Also, I am very grateful to Angela Quadir, Anna Blunden and Flavia Hume for their help during laboratory work.

Of course, I would not have been able to complete this thesis without the invaluable loving, support, praying and blessings of my family, in particular my mother who endured my leaving away for the PhD journey.

Special thanks for my husband Dhafir for being always with me.

Finally I would like to thank the Iraqi army and public crowds (Al-Hashd Al-Shaabi) for keeping my home safe during tough times of the war against terrorism.

Declaration

I declare that the research contained in this thesis, unless otherwise formally indicated within the text, is the original work of the author. The thesis has not been previously submitted to this or any other university for a degree, and does not incorporate any material already submitted for a degree.

Signed

Chapter 1. Introduction and Literature Review

1.1 Alzheimer disease (AD)

AD is a neurodegenerative (ND) and age related disease caused by the accumulation of abnormally-folding and extracellular deposits of beta-amyloid (Aβ) aggregates and tau amyloid proteins forming senile plaques (SPs) in the brain (Ballard *et al.*, 2011). AD is also characterised by increased levels of oxidative stress and inflammation, in addition to a reduction in acetylcholine levels (Banks, 2012; Meister *et al.*, 2013). AD is clinically defined by gradual impairment in memory (dementia) and one or more of other intellectual functions. Recently, the incidence of AD has increased with 47 million people worldwide suffering from this disease. It is expected for this number to increase to be more than 131 million by 2050 with increasing population's age (Prince *et al.*, 2016). The successful treatment of AD needs drugs that can negotiate the blood-brain barrier (BBB) which is considered the main obstacle in ND therapeutic development (Wyss, 2016).

1.1.1 History and Discovery

AD was discovered by a German physician Dr. Alois Alzheimer in 1907, although, until the 1970s it was not considered a major disorder or disease. Alzheimer reported the case of Auguste, a woman in her fifties who experienced severe memory loss (Habeck, 2002).

Alzheimer performed an autopsy on the patient's brain after her death and during the process he found unusual features of accumulation and lesions that might be the cause or effect of this disorder which was later (in 1910) named Alzheimer by Emil Kraepelin, a German psychiatrist who worked with Alzheimer. Before the discovery of Alzheimer, the scientists and the community identified dementia as natural age progression and considered plaques as a part of aging. In 1931, the electron microscope was invented enabling scientists for further brain cells studies (Habeck, 2002; Holstein, 1996). The Alzheimer's Association was founded in 1985 and gradually AD has been accepted as a disease rather than a natural function of aging (Holstein, 1996).

1.1.2 Stages of AD

The structure and chemistry of the brain alters as the disease progresses. According to these changes, AD is mainly divided into three stages; early, middle, and late.

Early stage: AD begins gradually so the early symptoms are often mistaken as normal signs of aging. These signs may include forgetfulness, decrease in judgment, difficulties in making decisions, communication difficulties, being slow to understand new ideas, and changes in mood and behavior ("Alzheimer's Society," 2016; Jakob *et al.*, 2009; Lovestone, 1998).

The middle stage: This is also called "moderate Alzheimer's disease." In this stage, memory and thinking deteriorate more but sufferers are still aware of their condition. Most people in this stage of AD need help with daily tasks such as eating, dressing or washing. The common signs of this stage are: inappropriate behaviours, extreme emotion, confusion, and sometimes hallucinations ("Alzheimer's Society," 2016; Jakob *et al.*, 2009).

The late stage: This stage is also called severe or advanced Alzheimer's. People in late stage of AD need 24 hr care as they become physically frail, with decreased mental ability and an inability to communicate verbally. The aim of care at this stage is to support the person for the highest quality of life. The main signs and symptoms representing this stage are; increase in unsteady gait, loss of speech or repetition, weight loss, and sometimes loss of bladder and bowel control ("Alzheimer's Society," 2016; Jakob *et al.*, 2009).

1.1.3 Prevalence and Incidence of AD

The Alzheimer's society considers the disease to be the most expensive condition in the UK ("Alzheimer's Society," 2016). Alzheimer's statistics revealed that the global cost of Alzheimer's and dementia is estimated to be £200 billion. The significant costs of AD and other related disorders and dementias are direct, including medical care and therapy, and indirect involving lost wages by caregivers and decreased business productivity, in addition to the costs carried by patients relatives (Alzheimer's, 2017). It is difficult to quantify these intangible costs which represent an additional burden to the whole community (Colucci *et al.*, 2014). Suehs *et al*, (2014) found that AD has a significant clinical and financial impact on individuals who are taking care of patients diagnosed with AD in which the findings revealed higher healthcare resource use, medical condition burden and direct healthcare costs than for those of others with no AD (Suehs *et al.*, 2014).

Studies have shown that the incidence of AD in females is more than in males. For race differences, it has been found that AD is more prevalent in blacks, while the type of community and culture has no any effect on the prevalence (Richard *et al.*, 2012).

Current reports from Alzheimer's association revealed that two-thirds of older people living with AD are women. Of the 5.3 million, 3.3 million people age 65 and older with AD in the United States of America are women, and the rest are men. Therefore, females are considered at the epicenter of the Alzheimer's crisis (Alzheimer's, 2017). It is estimated that the lifetime risk of developing AD in women over age 65 is 1 in 6, in comparison to nearly 1 in 11 for men. As real a concern as breast cancer is to female's health, they are about twice as likely to develop AD during their lives as they are to develop breast cancer (Seshadri *et al.*, 2006).

The number of people with AD and other dementias is predicted to increase rapidly in coming years as the baby boom generation ages. It is expected that the number of people over 65 years with this disease will continue to increase and may triple by 2050, unless there are medical breakthroughs developed to stop, slow or prevent the occurrence of AD (Alzheimer's, 2017; Chêne *et al.*, 2015; Seshadri *et al.*, 2006) (Fig.1.1).

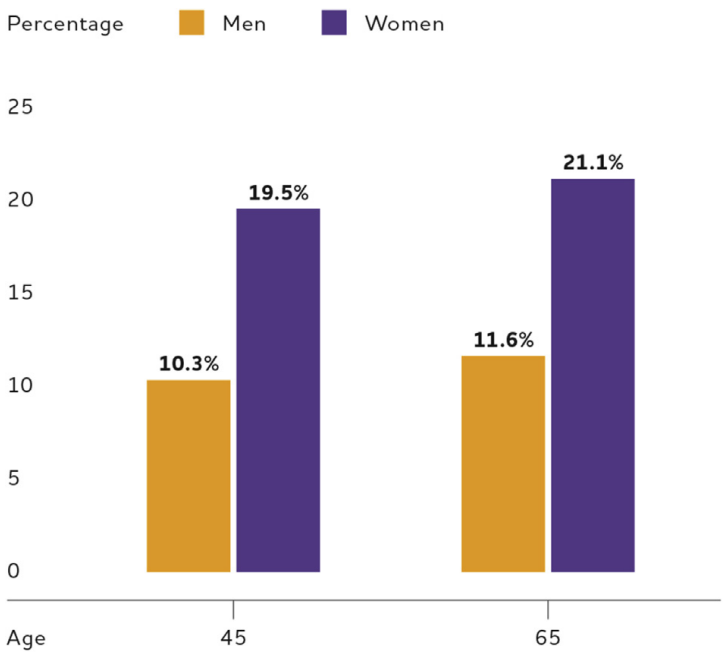

Fig.1.1: AD lifetime risks graph according to age and sex (Chêne *et al.*, 2015)

1.1.4 Mortality and Morbidity

In general, AD is considered the sixth leading cause of death, and for those aged over 65, it is listed to be the fifth leading cause (Murphy *et al.*, 2013). A recent report of the Office for National Statistics has shown that AD is the first leading cause of death in England and

Wales ("Alzheimer's Society," 2016). AD is also considered a cause of poor health and disability (morbidity) during years of the disease progress ("Alzheimer's Society," 2016).

In the United States, it is estimated that about 700,000 people aged 65 years or older died with AD in 2014 (Reitz, 2014). Regardless the reason of death, among older people, 61% of those suffering from AD are expected to die before reaching the age of 80 years in comparison to 30% of people of same age without AD ("Alzheimer's Association," 2014).

The population-attributable risk could describe the impact of AD on mortality. This risk represents the proportion of deaths in a population in a definite amount of time that might be preventable if a disease was eliminated. It has been found that the population-attributable risk of Alzheimer's on mortality for 5 years is between 5% and 15% in people aged 65 years and older (Alzheimer's, 2017; Ganguli *et al.*, 2005). That means for the next 5 years, AD is likely to be responsible for 5% to 15% of all deaths in older people (Alzheimer's, 2017).

1.1.5 Risk factors

1.1.5.1 Cerebrovascular disease

Hemorrhagic infarcts, vasculopathies, small and large ischemic cortical infarcts, and white matter changes are the cerebrovascular changes that may elevate the risk of dementia. Infarcts or white matter hyperintensies can cause direct damage to brain regions and increase the deposition of Aβ that, in turn, might lead to cognitive decline or induce inflammatory responses that is impairing cognitive function (Cheung, 2008).

1.1.5.2 Blood pressure

Data from observational and cohort studies suggest that elevated levels of blood pressure in mid-life (40-60 years of age) and in late-life could increase the risk of later-life cognitive impairment, dementia and AD (Alzheimer's, 2017; Whitmer *et al.*, 2005). Hypertension might increase the risk of AD by effecting on the vascular integrity of the BBB, leading to more protein extravasation inside brain tissue (Kalaria, 2010). In turn, this results in a reduction in neuronal or synaptic function, cell damage, apoptosis, and an increase in the accumulation of Aβ (Deane *et al.*, 2004).

1.1.5.3 Type 2 diabetes

It has been found that type 2 diabetes (T2D) approximately doubles the risk of AD (Luchsinger *et al.*, 2001). Evidences from recent studies have stated the impact of insulin resistance in the disturbance of different signaling pathways in addition to biological processes. Defect in insulin signals and impaired glucose metabolism contributes in the deposition of Aβ plaques and dysfunctioning of cognitive abilities (Khyati *et al.*, 2016; Watson *et al.*, 2003).

1.1.5.4 Plasma lipid levels

Studies have indicated a harmful effect of elevated lipids in mid-life on the risk of AD incidence. These findings are backed up by genetic linkage and have identified different genes involved in the metabolism of cholesterol or in its transport as AD susceptibility genes. These include ATP-binding cassette A7 (ABCA7), apolipoprotein-E (ApoE), apolipoprotein-J (APOJ), and sortilin-related receptor. Further functional cell biology studies have verified a potential involvement of cholesterol in the alteration of Aβ production due to modulation of Aβ precursor protein processing by secretase enzymes (Michikawa, 2003; Reitz, 2014).

1.1.5.5 Metabolic syndrome

Various studies have demonstrated a positive association between metabolic syndrome (obesity associated with diabetes and high blood pressure) as a whole and the AD risk or cognitive dysfunction (Alzheimer's, 2017; Yaffe *et al.*, 2009).

1.1.5.6 Smoking

Smoking could trigger the risk of AD through different mechanisms. Potentially through the generation of free radicals, yielding a high oxidative stress state, or have an impact on the inflammatory immune system, resulting in activation of phagocytes and more oxidative damage. Also, smoking could increase AD risk by promoting cerebrovascular disorders (Reitz, 2014; Traber *et al.*, 2000).

1.1.5.7 Traumatic brain injury

Results of various studies have suggested that the risk of AD is higher in people with a history of traumatic brain injury than those with no history of this injury (Reitz, 2014; Schofield, 1997).

1.1.6 Biochemistry and Pathogenesis of AD

The primary cause of AD is the extracellular deposition of Aβ which is the main component of SPs. The secondary cause is the intracellular accumulation of tau protein which is the component of neurofibrillary tangles (NFTs). Both of these compounds are insoluble. Aβ deposition is considered specific for AD, whereas tau accumulation can be occurred in other ND diseases, such as Parkinson and Pick's diseases (Reitz, 2014). SPs are characterised as spherical lesions measuring nearly 100 microns found mostly in the cerebral cortex. They are divided in to two types: the Aβ plaques, which are spherical in shape and deposited extracellularly and the neuritic plaques which are diffuse Aβ plaques with abnormal neuronal processes and tau filaments (Nelson *et al.*, 2012; Solfrizzi *et al.*, 2011).

1.1.6.1 Beta amyloid Aβ

Aβ is a peptide composed of 36-43 amino acids. The peptide is generated following the sequential processing of a larger molecule called amyloid precursor protein (APP) by the β-secretase (BACE) and the γ-secretase complex enzymes (Canter *et al.*, 2016). APP is a transmembrane protein made by brain cells and neurons and penetrates through the neuronal membrane. APP is important for normal brain function and is involved in neuron growth, survival and repair (Turner *et al.*, 2003).

There are 3 main parts of the APP (Fig.1.2); an extracellular domain forms the major part followed by a transmembrane domain (TMD) and a small cytoplasmic domain of only 50 amino acids length (AICD). It has been proposed that the extracellular domain might act as a neurotrophic factor, while the AICD may serve as a regulator of gene transcription (Cao, 2004; Turner *et al.*, 2003). Proteolytic protease enzymes for APP are; α, β, and γ-secretase (Dillen, 2006). Cleavage by either α or β secretase happens at APP's extracellular site near the TMD and leads to a shedding of the extracellular site into the extracellular space. Each one forms a short C-terminal fragment (CTF) either CTFα of 83 amino acids or CTFβ of 99 amino acids length, that remain presented in the cell membrane with its TMD. Both CTFs can be further cleaved by γ-secretase enzyme and in the case of CTFβ results in the generation of the Aβ peptides, while CTFα produces the shorter peptides which are rapidly and easily degraded and without any pathological role (Kojro *et al.*, 2005; Lichtenthaler *et al.*, 2004). The APP protein levels are highly expressed in the central nervous system (CNS), and are also formed in other tissues to a lesser extent. Its level can elevate

following traumatic brain injuries resulting in higher expression (Klein, 2007; Maloney *et al.*, 2007)

1.1.6.2 The β-Secretase

BACE (type-1) is one of the aspartyl proteases group and it is similar to APP in having extracellular, transmembrane and intracellular domains (Fig.1.2). The highest levels have been found in the CNS, but lower levels of expression are also documented in peripheral tissues (Jakob *et al.*, 2009).

In addition to APP, there are other BACE1 substrates, including the amyloid precursor-like proteins (APLP) 1 and 2, the sialyl transferase, the P-selectin glycoprotein ligand and the growth factor neuregulin (Jakob *et al.*, 2009; Lichtenthaler *et al.*, 2003).

BACE2 (type 2) has also been identified to be mainly expressed in the peripheral tissues. This enzyme plays an essential role in myelination of central and peripheral nerves (Jakob *et al.*, 2009).

1.1.6.3 The γ-Secretase

The CTFβ fragment generated from APP by the cleavage reaction of BACE is further cleaved by γ-secretase into the Aβ peptides. These peptides in turn are released into the extracellular space and the cytoplasmic domain AICD is liberated from the anchor of membrane into the cytoplasm (Haass, 2004; Jakob *et al.*, 2009).

Gamma-secretase differs from other proteases by a number of specific features including:

1) It hydrolyses its substrates within the TMD's lipophilic environment.
2) It is firmly integrated into the membrane of the cell via multiple TMDs.
3) It is a complex of 4 different proteins, namely, presenilin 1 or 2 (PSEN1 or PSEN2), anterior pharynx defective (aph-1), nicastrin and presenilin enhancer 2 in an equal ratio (Haass, 2004; Selkoe, 2007).

It is believed that PSEN1 and PSEN2 form the catalytic subunit of the complex of the γ-secretase enzyme. They have 8 or 9 TMDs, and they are cleaved by autoproteolysis into an N- and C-terminal fragment when they are in an active state (Jakob *et al.*, 2009; Selkoe, 2007).

The γ-cleavages that release the Aβ peptides occur in the middle of the transmembrane domain of APP and they are preceded by a proteolytic cut at the line between the cytoplasm and the TMD. Other γ-secretase substrates, such as CD44, Delta, APLP1 and 2, and Notch, undergo a similar cleavage pattern (Hecimovic *et al.*, 2004).

The most important of these substrates are the Notch receptors. After cleavage by γ-secretase, Notch intracellular domain (NICD) is released and directed to the nucleus to serve as a regulator of transcription. This action plays different essential roles including maintenance of the epithelia of the gut and skin and development of B- and T-cells. Therefore inhibition of γ-secretase activity leads to reduce a Notch signalling and, thus severely affects the homeostasis of these tissues (Jakob *et al.*, 2009; Nelson *et al.*, 2012).

1.1.6.4 Aβ peptide clearance

Normally the CNS contains a high steady state of Aβ peptide level and does not lead to the formation of amyloid aggregates or amyloid plaques in healthy subject. In a healthy brain, the freshly formed Aβ peptides are rapidly cleared, their half-life is a few hours (Bateman *et al.*, 2006; Cirrito *et al.*, 2003). The most important brain proteases that are responsible for the removal of peptides are neprilysin (endopeptidase or enkephalinase) and the insulin degrading enzyme (insulysin) (Bateman *et al.*, 2006; Jakob *et al.*, 2009).

A second major pathway for Aβ peptide clearance is by the transporter-mediated efflux across the BBB into the periphery via low density lipoprotein-related protein receptor (LRP1) (Deane *et al.*, 2007). ATP binding transporter P glycoprotein (P-gp) can provide additional efflux for Aβ peptides (Cirrito *et al.*, 2005).

In AD, the fragments of APP form dense clumps and deposits outside neurons this gives rise to SPs, which are made up of small peptides of different Aβ isoforms depending on numbers of amino acids (Kuo *et al.*, 1996). The most prevalent variant isoforms of Aβ are Aβ40 and Aβ42. The increased generation or abnormal accumulation of Aβ42 fibrils and plaques inside the brain is the primary event in the pathogenesis of Alzheimer's (Fig.1.2) (Ballard *et al.*, 2011; Meister *et al.*, 2013).

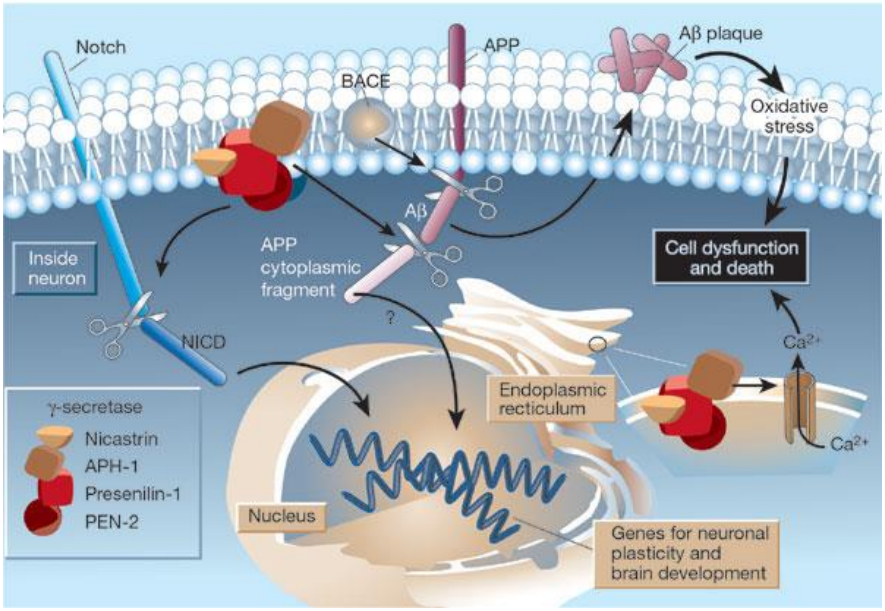

Fig.1.2: Formation of Aβ plaque from APP protein extracellularly. It is showing the action of β-secretase and the γ-secretase complex enzymes in the neuron (picture taken from www.biowiki.ucdavis.edu)

Moreover, the accumulation of both isoforms (Aβ40 and Aβ42) inside the cells, and specifically in the mitochondria, might explain the remarkable mitochondrial damage and oxidative stress levels elevation in AD (Borger *et al.*, 2013).

Aβ accumulation is highly toxic to neurons (Fig.1.3). In the brain this accumulation causes loss of long-term potentiation, synapse damage and neuron death. Furthermore, it shows selective neurotoxicity for the entorrhinal cortex (areas that are severely affected in AD) and for the hippocampus. This damage is mediated by the generation of free radicals, due to complex formation of Aβ with Zn^{2+}, Cu^{2+} and Fe^{3+}. It has been found that there is a significant correlation between the level of Aβ and the severity of neurotoxicity and the neurological dysfunction in AD (Heather *et al.*, 2011; Jakob *et al.*, 2009).

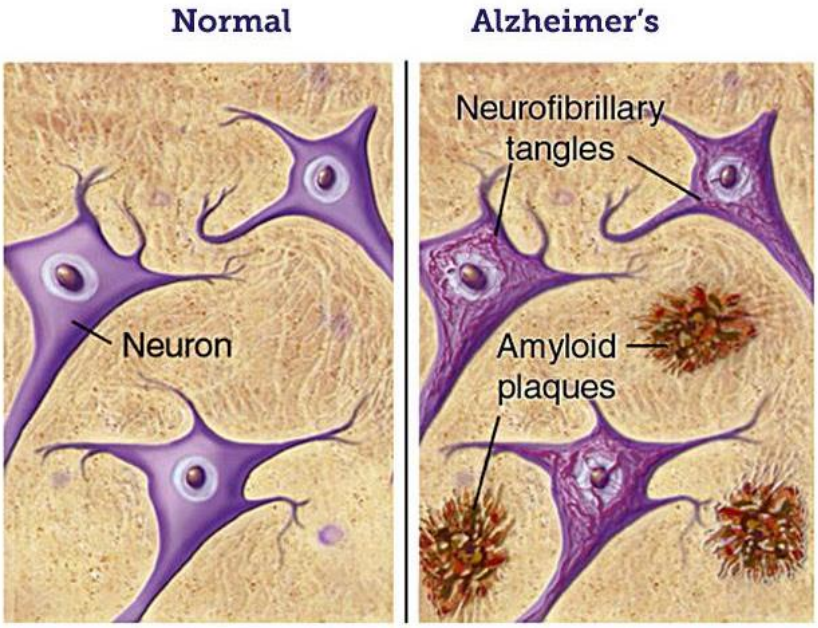

Fig.1.3: The brain images of normal versus AD. It is showing the plaques aggregates surrounding the neurons and the NFT inside the cells in the AD (picture taken from www.brightfocus.org/alzheimers).

1.1.6.5 Tau

Generally in AD, two main lesions appear; the first are SPs and the second are Tau proteins. Tau is formed during splicing of the microtubule associated protein and is abundant in mature neurons. The abnormal deposition of insoluble polymers of "highly-phosphorylated microtubule associated-tau protein" in the neuronal body leads to neurofibrillary degeneration (Liu *et al.*, 2012).

Tau aggregates as paired helical filaments twisted around each other. It is proposed that tau deposition could interfere with cellular functions through organelle displacement (Liu *et al.*, 2012). Due to their distorting the spacing of microtubules, the axonal transport will be impaired, resulting in an insufficient nutrition of axon terminals and its dendrites (Nelson *et al.*, 2012).

Tau filaments are NFTs deposited in the neuronal body. In late stage of AD, the hippocampus mostly contains high extracellular NFTs which are integrated with the neuropil. The prevailing opinion is that NFTs are secondary lesions after the Aβ accumulation in AD (Ballard *et al.*, 2011; Solfrizzi *et al.*, 2011).

NFTs are also observed in other ND condition in addition to AD, such as prion diseases, the frontotemporal dementias and myotonic dystrophy, whereas SPs are only observed in

AD. Both SPs and NFTs are found in most cases of AD, but in some cases there is a predominance to one of them (Nelson *et al.*, 2012; Solfrizzi *et al.*, 2011).

1.2 Discovery of drugs for AD

The poor penetrability of drugs across the BBB accounts to a great extent for the high attrition rate for drugs under development for treatment of most brain disorders including AD. The BBB hinders free access of most drugs to CNS leading to insufficient brain exposure for these drugs to be effective, and using high therapeutic doses could be toxic to the brain. Furthermore, drug development intended for the treatment of most brain disorders is associated with a higher failure rate than that for other disorders and mostly occurs in the later stages (at Phase 3 or after registration) (Aparicio *et al.*, 2016).

1.2.1 The first generation (symptomatic treatments)

The aim of these drugs is to improve the symptoms or delay the progression of the disease. The first drugs marketed were piracetam, nootropics and aniracetam (Jakob *et al.*, 2009). Clinics started using these drugs in the 1990s due to their ability to provide symptomatic relief and target the cognitive impairments. These drugs act as inhibitors of acetylcholine esterase but without addressing the underlying pathology. They most likely have moderate therapeutic effects and these decrease after a certain time (Martin *et al.*, 1993). Currently, there are three compounds on the market: donepezil, galantamine and rivastigmine (Jakob *et al.*, 2009). Memantine is another drug in this class that blocks glutamate receptor, in turn lowers the excitotoxic activity in CNS when brain cells are damaged (Schmitt *et al.*, 2007).

1.2.2 The second generation (disease-modifying treatments)

The second generation of drug discovery is mostly based on amyloidosis and targets various steps in the production pathway of amyloid. In contrast to symptomatic therapy, this is aimed to retard and prevent AD progression (Jakob *et al.*, 2009).

1.2.2.1 Immunotherapy

As therapeutics, antibodies have been mainly used in two ways in AD; either direct targeting pathologic agents or as delivery vehicles (Jakob *et al.*, 2009). The treatment of AD by immunotherapy was originated from a research work in 1999. The findings of this study suggested that the vaccination of AD patients with amyloid could increase anti-Aβ antibodies and result in a significant reduction of brain Aβ peptide (Schenk *et al.*, 1999). In addition, the immunised animal brain has revealed lower neuro inflammation and signs of

neuro synaptic loss (Hawkes *et al.*, 2007). Reduction in the Aβ peptide levels by vaccination also improved performance in various learning activities (Morgan *et al.*, 2000). In addition, injection of antibodies specific for Aβ peptides directly into the CNS can reduce the amyloid deposits in the brain and improve signs of synaptic loss and relief impairments in special learning activities (Hartman *et al.*, 2005). It has recently been found that the generation of aducanumab, a human monoclonal antibody, can selectively target the aggregated Aβ. Aducanumab has shown to enter the brain of a transgenic mouse model of AD and reduced the soluble and insoluble Aβ in a dose-dependent manner (Sevigny *et al.*, 2016).

The most important mechanisms that explain the action of antibodies on Aβ plaques are:

- Antibodies can be administered to the brain by local injection, and bind directly to the brain amyloids (Banks *et al.*, 2007). After that, the bound molecules will be gradually degraded by intracellular lysosomal proteolysis.
- A binding of antibodies with the circulating Aβ in the blood (DeMattos *et al.*, 2002) preventing their aggregation to fibrils and reducing the plaque levels in blood and, in turn, in brain. Therefore, antibodies here act as direct aggregation inhibitors (Jakob *et al.*, 2009).

The antibody-based therapy is considered a promising avenue in AD despite the risks and associated adverse effects of the active vaccination approach, such as stroke and encephalitis, and unproven therapeutic efficacy (DeMattos *et al.*, 2002).

1.2.2.2 Inhibition of β-secretase

The first generation of BACE inhibitors developed were a class of aspartyl proteases including statines, norstatins, hydroxyethylamines and hydroxyethylenes (Cole *et al.*, 2007). In cell-free assays, these compounds have shown high binding affinities, while in cellular activity assays they were poorly active (Jakob *et al.*, 2009). The potent and effective compound that has been used clinically is CTS-21166 (Ghosh *et al.*, 2012). Several other compounds have also been identified to be BACE inhibitors with better pharmacological activities which are derived from peptidomimetics (Hills *et al.*, 2007). Some of these compounds have been active *in vivo* after application together with a P-gp inhibitor, but with disadvantages related to their ability to compete with other substrates of P-gp (Jakob *et al.*, 2009).

1.2.2.3 Inhibition of γ-secretase

Gamma-secretase is one of the most attractive targets for the discovery of AD therapy, and it is more advanced in clinical development than that of BACE inhibitors. Scientific literature and patents have identified several highly potent and structurally diverse γ-secretase inhibitors. Some of these inhibitors have reached clinical trials stages for the AD treatment (Jakob *et al.*, 2009).

Dovey *et al.* (2001) have provided the first proof of an effective γ-secretase inhibitor *in vivo* which was DAPT (Dovey *et al.*, 2001). Oral application of this substance in mouse has led to a significant decrease in the brain Aβ levels with rapid turnover of pre-aggregate, soluble peptides in the CNS. However, these results were only found in young, pre-amyloid animals (Lanz *et al.*, 2006).

LY-411575 is another compound described and widely used as a γ-secretase inhibitor for *in vivo* studies. This compound was found to be active in cellular assays, and reduced the Aβ level in the brain at low concentrations (Best *et al.*, 2005). In addition LY-450139, a compound structurally related to LY-411575, has been identified in phase I and phase II studies. The results revealed that this substance showed a dose-dependent slight decrease in the Aβ levels in the brain, CSF, and plasma. These compounds had shown Notch-related adverse effects which are considered a serious problem with γ-secretase inhibitors and limit their use (Lanz *et al.*, 2006).

BMS-299897 is another active *in vivo* enzyme inhibitor with different structure. A study showed that its action to decrease Aβ in the brain, CSF, and plasma in young mice is a dose and time dependent. Similar to LY-411575, no changes were observed in the Aβ levels in the brain of older animals after acute treatment (Barten *et al.*, 2005). MRK-560 has also been reported to be a potent γ-secretase inhibitor drug. Three months of treatment in a mouse model was shown to reduce the brain Aβ levels without adverse effects of Notch inhibition (Best *et al.*, 2006). It was noted that different γ-secretase inhibitors could cause goblet cells hyperplasia in rat gut epithelia after long-term treatment and thus consider a drawback in this type of therapy (Jakob *et al.*, 2009).

The main limitation of secretase inhibitors (γ and β) in general, is the physiological and biological functions of secretases that could be affected after treatment (Lee *et al.*, 2007).

1.2.2.4 Modulation of γ-secretase

Recently, γ-secretase modulators (GSM) have received a considerable amount of attention. This concept was initiated when observation showed that some nonsteroidal anti-inflammatory drugs (NSAIDs) including ibuprofen, flurbiprofen (FP), indomethacin and sulindac sulphide, could change the pattern of production of Aβ peptides in cellular assays in a way that decreased the Aβ42 level, whereas Aβ38 levels increased. In addition, the ε site cleavage, that liberates the intracellular domain, remained unchanged (Jakob *et al.*, 2009; Lleo *et al.*, 2004). This was considered an ideal result, as Aβ42 is considered the harmful one among other Aβ isomers that leads to the generation of toxic aggregates and deposits (Reitz, 2014). The NSAIDs have a direct action on the γ-secretase enzyme that is not related to their inhibitory effect on the inflammatory enzymes, cyclooxygenase (COX 1 and 2) (McGeer *et al.*, 2007). Studies have showed that binding of NSAIDs to γ-secretase in the cell membranes is at the allosteric site so their binding was non-competitive antagonism with other inhibitors (Weggen *et al*., 2003). Another study has suggested that NSAIDs can act by direct targeting the PSEN site of the enzyme (Lleo *et al.*, 2004). However, the difficulty associated with the use of NSAIDs as a treatment for AD is their poor penetration across the BBB with very low potency as GSM, as their effective concentration is usually >50 µM (Pissarnitski, 2007).

1.2.2.4.1 Flurbiprofen (FP)

This drug is one of the phenylalkanoic acid (arylpropionic acid) derivative groups of NSAIDs (Fig.1.4). FP, also known as tarenflurbil or Flurizan® has a γ-secretase modulating activity (Eriksen *et al.*, 2003). A number of years' investigations and trials for the drug have been conducted and have concluded its potential as a drug for AD treatment (Gasparini *et al.*, 2004; Green *et al.*, 2009). However, development of the drug for the treatment of AD was discontinued due its poor permeability for the BBB (Green *et al.*, 2009; Meister *et al.*, 2013).

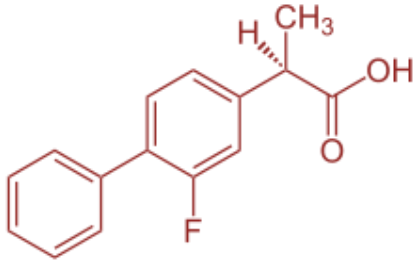

Fig.1.4: FP chemical structure.

FP has antipyretic and analgesic properties in addition to anti-inflammatory activity by inhibition of COX1 or 2 (Carreras *et al.*, 2013; Eriksen *et al.*, 2003). FP is FDA-approved and commercially available. It is well absorbed orally and its rate of absorption is not altered with increasing age. Peak plasma levels can be achieved in approximately 2 hr after a single 100 mg oral dose (Davies, 1995; Eriksen *et al.*, 2003). The elimination half-life of drug is about 4 hr and its steady state concentrations are achieved with no accumulation when the drug is administered daily; in addition, excretion is completed after 24 hr intake of the final dose (Davies, 1995).

In cell-based and animal studies, FP has been shown to reduce Aβ42 without affecting γ-secretase cleavage of other substrates, such as Notch (Weggen *et al.*, 2003). It mostly acts on the PSEN site of the γ-secretase complex of the membrane and it can significantly reduce the levels of both Aβ40 and Aβ42 isomers in CNS as well as improve the cognitive performance (Eriksen *et al.*, 2003). FP was found to decrease the formation of both Aβ40 and Aβ42 in neuroblastoma cells and in cell cultures of rat neurons (Gasparini *et al.*, 2004).

Reid *et al*. (2003) have reported that FP and some other NSAIDs are able to interact with, and inhibit, MRP4 which is an ABC- transporter (Reid *et al.*, 2003). It has been postulated that the MRP4 substrates, such as cAMP or unconjugated estradiol, are able to regulate the metabolism of APP/ Aβ. Therefore, FP can also indirectly influence the metabolism of Aβ by altering MRP4 (Gasparini *et al.*, 2004; Lleo *et al.*, 2004).

The gastrointestinal and renal toxicity of NSAIDs mediated by their COX inhibition are thought to be potential side effects associated with their clinical use as anti-inflammatory medications and as Aβ42 lowering agents (Eriksen *et al.*, 2003).

It is also reported that FP is able to inhibit the "nuclear factor kappa-light-chain-enhancer of activated B cells" (NF-κB). This NF-κB inhibition has been suggested to decrease the inflammatory response in the AD brain. However, both effects of FP, the Aβ42 lowering and NF-κB inhibition seem to be independent of each other (Eriksen *et al.*, 2003).

Randomised phase II and III studies and placebo-controlled trials evaluated results of using FP in patients with mild AD and they concluded that the drug significantly failed to improve learning and thinking ability or cognition decline (Green *et al.*, 2009; Wilcock *et*

al., 2008). These studies also have revealed that FP had a very low brain permeability and this very low amount of drug that was achieved in the brain appears to be far from the therapeutic concentration (150-250 μM) needed to exert the inhibitory effect on γ-secretase activity (Green *et al.*, 2009; Meister *et al.*, 2013; Wilcock *et al.*, 2008).

1.2.2.5 Further Therapeutic Targets

Aβ peptides in healthy and young people, are rapidly cleaved by proteases, degraded and not accumulated to levels that can form stable and neurotoxic plaques (Jakob *et al.*, 2009). Substantial *in vivo* data has found that some gene manipulations could prevent or reduce the amount of amyloid accumulation. Thus, activation of the proteases such as neprilysin and insulin-degrading enzyme could enhance the Aβ degradation (Saito *et al.*, 2005).

Using aggregation inhibitors is a potential alternative mean to prevent the toxicity of Aβ peptides. Some of these inhibitors are plant-derived compounds such as Exebryl®, whereas others are designed products such as tramiprosate (Alzhemed®), however, they have failed to provide clear positive results (Jakob *et al.*, 2009).

Tau plaques are pathological factors that play an essential role in disease progression, and provide further targets for therapeutic intervention in AD. The protein kinases, that are responsible for the over-phosphorylation of tau protein, are viewed as amenable drug targets (Kojro *et al.*, 2005; Liu *et al.*, 2012). A major obstacle in this approach is the unknown phosphorylation site that is important for the transformation of native protein into its pathologic form and the unknown protein kinase that accomplishes this reaction (Liu *et al.*, 2012). It has been described that some kinases have important activity in tau-phosphorylation including proline-directed protein kinases (Cdk and GSK) and the mitogen-activated protein kinases (ERK and JNK) (Cheung, 2008; Liu *et al.*, 2012).

Epidemiological studies have postulated that thiazolidinedione (TZD) drugs that are commonly used in the treatment of T2D disease can improve cognition in AD patients through increasing the number of mitochondria and their metabolic efficiency and reducing the expression of BACE1 (Strum *et al.*, 2007).

Other studies have revealed that long-term use of NSAIDs can decrease the risk of AD developing, as the neuroinflammation, particularly activated microglia, is a regular feature of lesions associated with the disease (McGeer *et al.*, 2007).

Due to the extensive oxidative stress that is observed in the AD brain, the intake of antioxidants including vitamin C and E, as preventative or therapeutic agents, has a considerable effect (Mourtas *et al.*, 2011; Reitz, 2014). Some studies have demonstrated a protective antiamyloid effect of using polyphenolic substances derived from plants, such as catechin and quercin (the green-tea constituents) and curcumin (Mourtas *et al.*, 2011; Rezai *et al.*, 2005). However, recent study has shown dementia incidence did not differ after vitamin E and selenium supplement trial in elderly people (Kryscio *et al.*, 2017).

Furthermore, phosphatidic acid (PA) and cardiolipin (CL), which are essential for cell membrane integrity can reverse the oxidative stress and lipid peroxidation that result in neuronal loss and mitochondrial dysfunction associated with AD (Gobbi *et al.*, 2010).

The development of drugs to combat AD is hampered due to the presence of the BBB, which prevents the crossing of more than 98% of all small molecule drugs and nearly 100% of all large molecule drugs (Banks, 2012).

1.3 The Blood Brain Barrier (BBB)

In order to keep normal brain function, the neural environment should be maintained within a narrow homeostatic range. Therefore, a robust regulation of transportation of cells, ions and molecules between the brain and the blood is required. This regulation is preserved by very specific physiological and anatomical barriers, formed together in the CNS (Abbott, 2014). There are three barrier layers responsible for the separation of the neural tissues and blood:

1) Highly specialised endothelial cells layer (ECL) which comprises the BBB and separates the brain interstitial fluid from the blood.
2) The blood-cerebro spinal fluid (CSF) barrier (BCSFB) contains the choroid plexus epithelium that secretes the CSF into the cerebral ventricles.
3) The arachnoid epithelium partitioning the blood and the subarachnoid CSF (Hansson *et al.*, 2006).

1.3.1 Development of the BBB

The BBB develops and matures during foetal life and is well characterised by birth (Abbott, 2014). The vascular endothelium development is stimulated by neuro-epithelial signalling to initiate a central nervous-specific vascular system and particularisation of the BBB (Liebner *et al.*, 2010).

The first feature of the development of the BBB is tight junctions (TJs) formation. It has been found that a brain of a 14-week human foetus expresses claudin-5 and occludin in the capillary endothelium with the same adult distribution at cell margins (Serlin *et al.*, 2015).

1.3.2 Histology of the BBB

The BBB is composed of the ECL with its basement membrane; it is supported by TJ proteins in between cells with highly particular transport mechanisms. The brain ECL is surrounded by cellular elements forming an extra continuous stratum which separates brain tissue from blood vessels (Lawther *et al.*, 2011). The BBB is supported by specific cells, such as pericytes, astrocyte end-feet, and a discontinuous basal lamina (Fig.1.5). The basal lamina separates the brain capillaries from the pericytes, serving as an extracellular matrix and providing a scaffold for cell migration, mechanical support for cell attachment and isolation from the adjacent tissue (Hansson *et al.*, 2006).

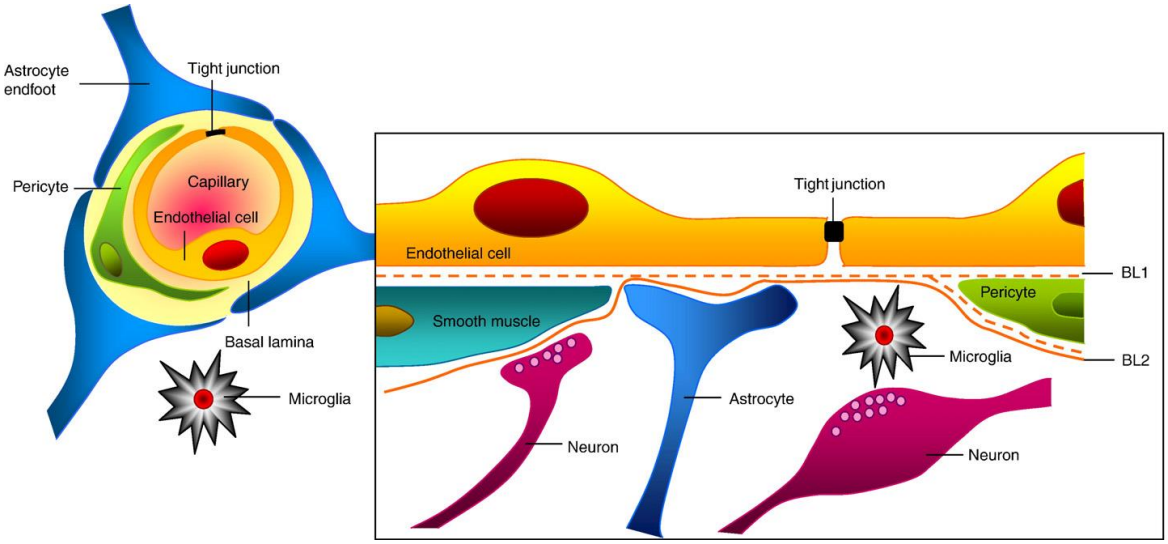

Fig.1.5: BBB structure. it shows the TJs in between adjacent endothelial cells, and pericyte cells distributed along the line of the capillaries of the brain and to some extent embrace the endothelium. Both the pericytes and the cerebral endothelial cells are enclosed by basal lamina (BL1), (BL2). End feet of astrocyte cells form a network surrounding the blood vessels and neurons (Hansson *et al.*, 2006).

Pericytes are small capillary wall-associated cells originating from the mesoderm. They enfold microvessels and capillaries of the brain and are present in close proximity to neurons and astrocytes (Fig.1.6). These cells play an essential role in the BBB formation and maturation and in regulation of tissue-survival (Daneman *et al.*, 2010). Furthermore, pericytes can regulate the mediation of inflammation and control the capillary-like

structure formation through actin fibres that are found in the cell body. Therefore, they are responsible for the maintenance of the BBB integrity and brain homeostasis (Peppiatt *et al.*, 2006). Pericytes dysfunction may appear due to aging and lead to blood flow reduction in cerebral region (Armulik *et al.*, 2010).

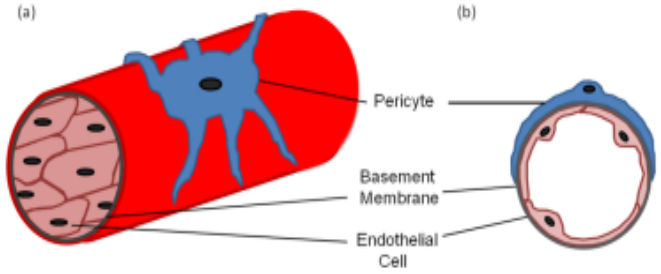

Fig.1.6: Pericyte cell. It is showed to embrace the cerebral endothelia cell membrane of the blood vessel. a. Longitudinal section. b. Cross section (Mills *et al.*, 2013).

Two types of pericytes have been identified; one is located at straight section of the capillary, whereas the other one is placed at capillary connections (Daneman *et al.*, 2010). The second type of cells is the astrocytes which are star-shaped and derived from the ectoderm of the neural tube. There are approximately 11 phenotypes of astrocytes, 8 of which are correlated with blood vessels (Hansson *et al.*, 2006). The 2 main types of astrocyte cells found in the brain are protoplasmic and fibrillary cells. Protoplasmic astrocytes are found in the grey matter and distinguished from other cells by their large nuclei and several thick cytoplasmic appendices which produce the end-feet (Bernacki *et al.*, 2008).

Fibrillary cells are present in the white matter and characterised by long unbranched end feet. These end feet are tightly attached to neurons on one side and blood vessels on the other (Fig.1.7). Due to their localisation and specific features, astrocytic end feet are important for BBB integrity (Hansson *et al.*, 2006; Serlin *et al.*, 2015). Astrocytes play an essential role in keeping normal neural metabolism, nutrition, and discharge of waste substrates. In addition, astrocytes that are attached to the apial matter are capable of transcytosis and support the active transport of ions (Bernacki *et al.*, 2008).

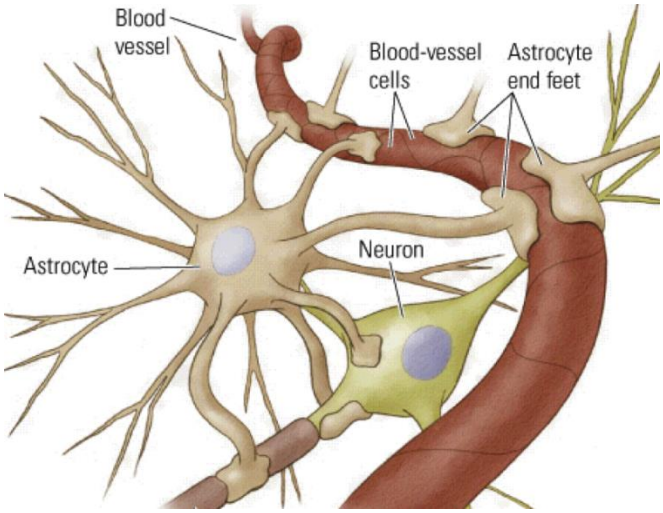

Fig.1.7: Astrocyte cells. It is a star shape in which their end-feet are attached to neurons on one side and membrane of blood vessels on the other (picture taken from www.faithfulbrain.com).

1.3.3 Physiology of the BBB

Each interfaced layer in the CNS, including the BBB, acts as a metabolic, physical, transport and immunologic barrier. Their functions are dynamic with regulatory signals received from both brain and blood (Abbott *et al.*, 2010). Diffusion of polar substances across the intercellular cleft is restricted because of TJs between adjacent cells. These barriers allow O_2 and CO_2 to pass through and are also permeable to other gaseous molecules such as xenon, N_2, helium and numerous anaesthetic gases. The barriers are permeable to small lipid soluble particles through diffusion (Serlin *et al.*, 2015). Moreover, the BBB is permeable to water, while the specific carriers present in the membranes, together with endoenzymes and ectoenzymes, can regulate the entry and efflux of small solute (Lawther *et al.*, 2011). Multidrug transporters can regulate passage of some molecules so can limit their amount within the CNS (Pardridge, 2005). The BBB plays an important role in ion regulation by providing several particular ion channels and transporters that preserve the ionic content optimal for neuronal signalling function. The BBB can also support in isolation of central transmitter pools from the peripheral, so that it minimises any unwanted transfer of signals (Bernacki *et al.*, 2008).

In addition, the BBB prevents many neurotoxic materials circulating in the blood (such as proteins, endogenous metabolites or ingested xenobiotics with the diet) from entering the CNS. These substances might damage the nervous tissue, leading to cellular activation and apoptosis (Gingrich *et al.*, 2000). The BBB has specific transport systems for nutrients and

metabolites required by nervous tissue so that it ensures a sufficient supply to the CNS (Ballabh *et al.*, 2004).

Macromolecules, with specific roles in growth and signalling within the CNS, cross the BBB by restricted and regulated mechanisms, while smaller peptides might enter the brain via either endocytosis or receptor mediated manners. Therefore, high percentage of small molecules cannot freely cross the BBB (Pardridge, 2005). Furthermore, the BBB regulates the penetration of leukocytes and innate immune elements and in turn, it contributes to the CNS immunity functions (Greenwood *et al.*, 2003) (more details in Section 1.4).

1.3.4 The tight junctions (TJs)

Brain endothelial cells are unlike other endothelial cells of the peripheral circulation in the fact that they produce TJs with no pores (Ballabh *et al.*, 2004). TJs are junctional complexes existing in between the endothelial cells of brain micro vessels and are formed by the interaction of multiple cerebral transmembrane proteins that mostly project into, and seal, the paracellular pathways which are responsible for BBB impermeability (Abbott *et al.*, 2010) (Fig.1.5). TJs act as a border cleft for protein and lipid molecules diffusion across the barrier and account for the polarity differentiation of endogenous transporters between the luminal and abluminal membranes (Wolburg *et al.*, 2002).

Because of the complete and tight fusion of the TJs between adjacent endothelial cells, they close the paracellular pathway that will force transport of substances through the cellular membrane (Serlin *et al.*, 2015).

Moreover, TJs are positioned in between brain endothelial cells dividing their membranes into two poles; a blood-facing and a brain-facing membrane. The type of proteins present at each site also effect this division of membranes, and the distinctive interactions of these membranous proteins with each other, determining the speed and the pathway of particles to cross the BBB (Hawkins *et al.*, 2006).

There are different TJs-associated protein components forming cerebral endothelial cell TJs which include; occludin protein, claudin protein, and adherens junction molecules. Zonula occludin (ZO) proteins such as ZO1, ZO2, ZO3 and cingulin are also recognized as sub-membranous components of TJs that link trans-membranous proteins with actin, and

this is considered the primary scaffold maintaining the normal structure and functional integrity of the brain endothelium (Abbott *et al.*, 2010; Bauer *et al.*, 2016) (Fig.1.8).

1.3.4.1 Occludin

Occludin was the first discovered tight junctional transmembrane protein (Furuse *et al.*, 1993). It is a phosphoprotein that consists of 4 transmembrane domains with molecular weight (MW) 60 kDalton (Da). The paracellular architecture of the TJ is complex with two extracellular loops of both occludin and claudin, and the cytoplasmic domain is tightly attached to ZO proteins (Fig.1.8). Occludin molecules have been identified in adult humans and mice and in a highest expression in comparison to other TJ proteins. It regulates the cellular function and restricts the paracellular transport (Hirase *et al.*, 1997).

It has been demonstrated that occludin phosphorylation could regulate the permeability of TJ by either a G protein-dependent or -independent way, depending on the receptor involved in the process, and independently on changes of the cytoskeleton (Hirase *et al.*, 2001). The external loops with both the transmembrane and the cytoplasmic domains of occludin play an important role in the regulation of endothelial paracellular permeability. The cytoplasmic domain is also important for the regulation of trans-epithelial movement of neutrophils (Huber *et al.*, 2000). Studies have reported that occludin is responsible for resealing of TJs and it is involving in preserving BBB electrical resistance and formation of aqueous pores (Tsukita *et al.*, 2001).

1.3.4.2 Claudins

These proteins are considered as integral membrane proteins of 22 kDa MW and appear to complete the task of constructing barrier properties (Furuse *et al.*, 2001). They are also phosphoproteins consisting of four transmembrane domains shared with occludin without any sequence homology to occludin. Twenty four members of this protein family have been identified in both mice and humans (Balda *et al.*, 2016). These proteins are essential for permeability restriction in the brain (Tsukita *et al.*, 2001). The claudin protein from one cell attaches to another claudin from an adjacent cell producing the “primary closure” of the TJ (Fig.1.8), whereas the carboxylic end of each one links to cytoplasmic ZO1, ZO2, or Z3 (Wolburg *et al.*, 2002).

Occludins and claudins produce hetero-polymers and transcellular tracts consisting of several channels for ionic and hydrophilic molecule transport (Matter *et al.*, 2003). In fact,

the relationships existing between these 2 proteins suggest they contribute to the selective diffusion across cell membrane. Therefore, their presence appears to be critical for the optimum function of TJs and for integrity of the BBB (Tsukita *et al.*, 2001).

1.3.4.3 Junctional adhesion molecules (JAMs)

The junctional adhesion molecules, in addition to other endothelial cellular selective adhesion molecules, are membranous proteins localised at TJs skeleton with molecular masses about 40 kDa. JAMs belong to the immunoglobulin family and promote homophilic and heterophilic interactions in the cellular region of TJ (Wolburg *et al.*, 2002). They are characterised by having one transmembrane domain associated with the extracellular part as well as containing 2 "immunoglobulin-like" loops (Fig.1.8) (Petty, 2002). Study in the rodent brain has identified only three members of this family including JAM1, JAM2, and JAM3. Both JAM1 and JAM3 are found in endothelial membranes of brain vessels, while the human cerebral cortex was found to contain only JAM1 (Vorbordt, 2004). They are mainly involved in organizing the structure TJ of the cell membrane as well as playing an important role in leukocyte extravasation (Van *et al.*, 2014; Wolburg *et al.*, 2002).

1.3.4.4 Sub-membranous TJ-associated proteins

Sub-membranous TJ-associated proteins (or called cytoplasmic proteins) are parts of the TJ constriction, these include ZO proteins (ZO1, 2, and 3), cingulin, and 7H6. The ZO proteins are members of the "membrane-associated guanylate kinase" family which share three distinct core regions composed of different protein-containing domains (Fig.1.8). These domains play important role in BBB permeability regulation, protein arrangements, and maintaining the integrity of plasma membrane (Vorbordt, 2004).

The protein 7H6 is a phosphoprotein with 155 kDa molecular mass and is responsible for membrane impermeability to ions and macromolecules (Satoh *et al.*, 1996). In contrast to ZO1, 7H6 can detach from the TJ region when cellular ATP levels decrease; eventually this detachment process leads to enhanced membrane paracellular permeability and hence influences the junctional function (Mitic *et al.*, 1998).

Another phosphoprotein found at the cytoplasmic part of TJs is cingulin with molecular mass of about 150 kDa. Cingulin acts as a critical scaffold between transmembranous

proteins and the cytoskeleton through its binding to ZO proteins and actin (Wolburg *et al.*, 2002).

Other TJ-cytoplasmic proteins, such as "Ca^{2+}-dependent serine protein kinase", partitioning defective proteins, and G-protein signalling serve as cellular signalling regulators (Abbott *et al.*, 2012). Hence, it appears that the function of TJ proteins not only keep the integrity of the brain endothelial membrane but also provide constructional support for this endothelium owing to their complex interconnection networks. Therefore any disturbances in this order can alter cell structure and TJ integrity. In turn these events may lead to the alteration in BBB physiological functions and to some extent CNS homeostasis (Ballabh *et al.*, 2004).

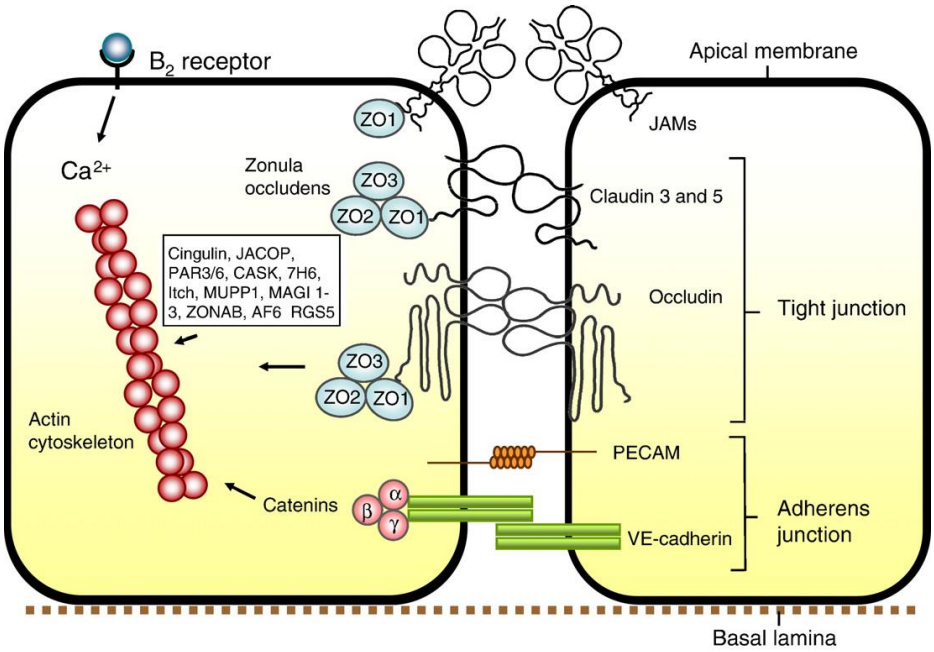

Fig.1.8: Structure of BBB with TJs. The TJs complex consists of occludin, claudins, and JAMs. Each side in claudins and occludin associates and bind to its analogue on the other side across the intercellular cleft, both of them are attached to the cytoskeletal proteins ZO1, ZO2 and ZO3, and then attached via cingulin-actin cytoskeletal system within the endothelial cell (Abbott *et al.*, 2010).

1.3.5 Adheren junctions (AJs)

In addition to TJs, AJs are the second type of junctional complexes that tighten structures in between endothelial cells (Bauer *et al.*, 2016). They are transmembranous proteins of a large family of cadherins proteins. These proteins present at the intercellular cleft and are interconnected to the cytoplasm via the specific scaffolding proteins including α, β and γ

catenin in the presence of calcium ions (Takeichi, 1995). They hold the endothelial cells together providing a strict tissue structural support (Fig.1.8), and any defect in their function results in barrier disruption (Van *et al.*, 2014). Studies have revealed that cadherin and catenin proteins are highly expressed in the human cerebral cortex (Vorbordt, 2004; Wolburg *et al.*, 2002).

1.4 Transport across the BBB

1.4.1 Passive diffusion into the brain

1.4.1.1 Transcellular pathway

Some small lipid-soluble particles can enter the brain by passive diffusion though the BBB (Liu *et al.*, 2004). The rate of the solute entering to the CNS is generally correlated with its lipid solubility (Clark, 2003). Some factors may restrict substances entry into the brain such as high polar surface area and the ability to form 6 hydrogen bonds or more, which mostly increases the free energy required to move from an aqueous into the lipid phase of the cellular membrane (Abbott *et al.*, 2010; Gleeson, 2008). Furthermore, a MW greater than 400 Da and existence of molecular rotatable bonds can limit BBB penetration. Binding to plasma proteins with high affinity and low dissociation rate can also lower brain permeability (Serlin *et al.*, 2015).

The crossing of blood gases, O_2 and CO_2, through the BBB is diffusive, while other dissolved gases mainly move according to their concentration gradients (Gleeson, 2008). Supply of O_2 to the brain and removal of CO_2 are blood-flow dependent. Therefore, gas transport is efficient as long as blood flow to the CNS remains within physiological limits (Abbott *et al.*, 2010) (Fig.1.9.a).

1.4.1.2 Paracellular aqueous pathway

This pathway allows small water-soluble molecules to be simply diffused through the TJ but only to a limited extent (Hirase *et al.*, 2001).

1.4.2 ATP-binding cassette transporters in the BBB (ABC transporters)

ABC transports are also known as efflux pumps. In humans, ABC transporters are a superfamily of proteins including 48 members and further grouped into 7 subfamilies depending on their structure (Dean *et al.*, 2001). The main important ABC transporters in the BBB are; P-gp (such as multidrug resistance protein (MDR)), the breast cancer resistance protein (BCRP/ABCG2) and multidrug resistance-associated proteins (MDRs/

ABCC) (Dauchy *et al.*, 2008). Additionally, ABCA1and ABCG1 which transport cholesterol and ABCA2 which is associated with drug resistance are also expressed in the BBB (Dean *et al.*, 2001). The ABC transporters act as active efflux pumps utilising ATP which transports a wide range of lipid-soluble molecules out of the CNS. They are considered neuro-protective and detoxifying agents by extruding neurotoxic endogenous or xenobiotic substances from the brain (Dallas *et al.*, 2006). Moreover many drugs are also substrates for these transporters, so their permeability to the brain is lowered (Begley, 2004) (Fig.1.9.b).

1.4.3 Solute carriers in the BBB (SLCs) (carrier-mediated influx)

Due to presence of the barrier, the brain is potentially isolated from many important polar substances that are necessary for metabolism such as glucose and amino acids. Therefore, to supply the brain with these materials, the endothelium of the BBB must contain specific solute transporters (carriers) (Bernacki *et al.*, 2008). The formation of TJs provides the essential characteristics of a continuous cell membrane on the BBB, and the diffusional properties influence by the lipid bilayer and the orientation of the particular transport proteins found in the cellular membrane. All cells express high numbers of these carriers in the membrane to transport polar molecules such as glucose, amino acids nucleoside, monocarboxylates and small peptides (Zhang *et al.*, 2002). Some of these transport proteins are found integrated with either the luminal or abluminal membrane of the endothelial cells; others are integrated with both membranes (Bernacki *et al.*, 2008). The directionality of these transporters regulates the transport of solutes into or across the endothelium preferentially, so the direction of the transport can be from brain to blood or the reverse (Abbott *et al.*, 2010).

Several characterised BBB transport systems are found to meet the brain metabolic demand, such as glucose-transporter 1 (GLUT1), the A-system, and L-system amino acid carriers (Lawther *et al.*, 2011). It has been reported that GLUT1 is positioned in endothelium of the brain capillaries, astrocytes, and the choroid plexus (Carruthers *et al.*, 2009). It is responsible for the brain uptake of glucose via insulin independent manner. There are also GLUT3 and GLUT4 which serve as glucose carrier in the neurons (Lawther *et al.*, 2011) (Fig.1.9.c).

The SLC also consists of a family of transporters including organic cation transporters (Oct/OCT, SLC22A1), organic anion transporters (Oat/OAT, SLC22A6-8, -10, -11) and

organic anion transporting polypeptides (OATP/SLCO). They play a role in the transport of organic compounds across the BBB and act together with MRPs in the removal of xenobiotics from the brain. Different organic solutes including steroid conjugates, thyroid hormones, dehydroepiandrosterone, histamine and morphine are known to be transported across cellular membranes by these carriers (Bernacki *et al.*, 2008).

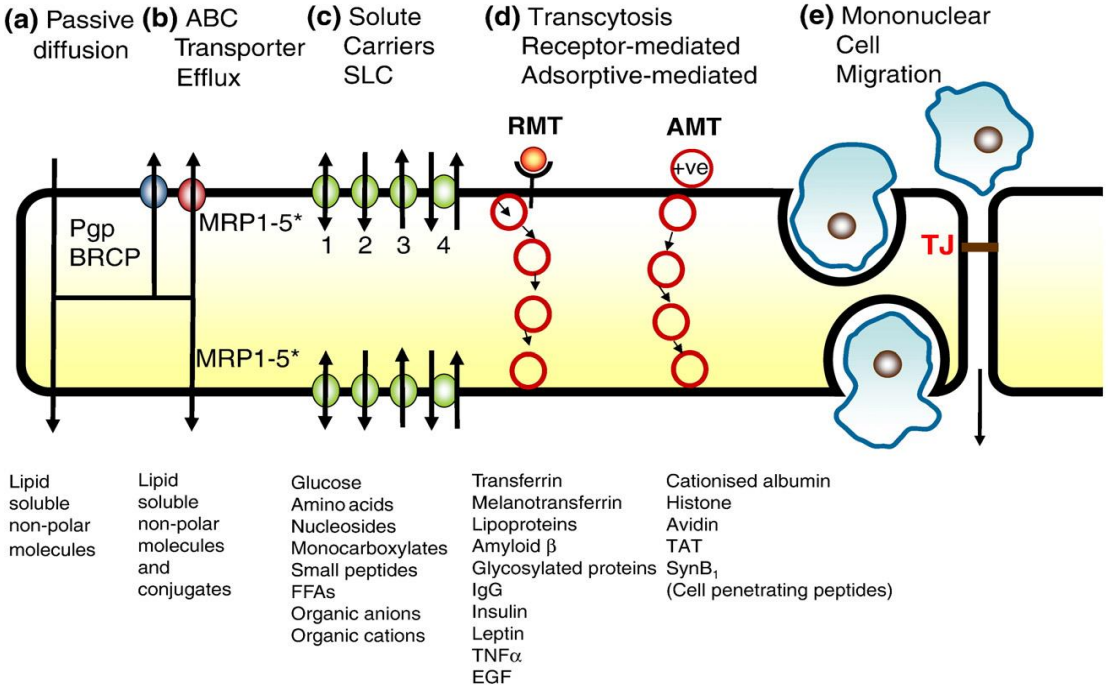

Fig.1.9: Transport across BBB. a. Lipophilic molecules cross the BBB by passive diffusion through the cell membrane. b. ABC transportes intercept the entry of some solutes and dragged them out of the brain endothelial cell. c. Solute carriers (SLCs) or carrier mediated influx transport many important polar substances into the CNS. d. RMT includes binding of ligand to the receptor and can transport different macromolecules (such as proteins and peptides) through the BBB (transcytosis), while AMT is another way to transport positively charged substances by adsorption across the endothelium. e. Leukocytes can pass through the BBB either via diapedesis through the membrane, or through modified TJs (Abbott *et al.*, 2010).

1.4.4 Transport of macromolecules in BBB (transcytosis)

Transcytosis is the main route by which macromolecules (large MW molecules) such as proteins and peptides can penetrate and enter the brain intact (Serlin *et al.*, 2015).

Although the presence of the BBB and TJs physically prevent brain entry of a majority of large molecules, several transcytotic mechanisms are known to transport a diverse range of these molecules across the BBB. These particular vesicular mechanisms include; receptor-

mediated transcytosis (RMT) and adsorptive-mediated transcytosis (AMT) (Dean *et al.*, 2001) (Fig.1.9.d).

RMT is the selective uptake of macromolecules in which the ligands bind to specific receptors on the cellular membrane initiating an endocytotic event (Bernacki *et al.*, 2008). After that, the bound ligand with receptor gather with each other forming a caveolus, and then a vesicle. This is followed by internalisation of both ligand and receptors into the cell and directed through the cytoplasm to be exocytosed to the opposite side of the cell. Dissociation of these receptors and ligands probably happens during the exocytotic event or during cellular transit (Abbott *et al.*, 2012).

RMT is extensively studied for pharmaceutical applications and brain targeting (Pardridge, 2005). The well-characterised systems present in the brain are transferrin receptor (TfR), lipoprotein receptors, insulin receptor, scavenger receptors class B, glutathione transporter and diphtheria toxin receptor (Rip *et al.*, 2009).

AMT is also known as the pinocytosis route which is induced by an electrostatic interaction between a positively charged molecule and the negatively charged proteoglycans and phospholipid ends of the outer site of the cell membrane leading to endocytosis and followed by transcytosis. This process, therefore, requires cationic substance with excess surface positive charge (Sauer *et al.*, 2005). In comparison with RMT, AMT has lower affinity and higher capacity of surface binding (Herve *et al.*, 2008).

Basic molecules have higher BBB penetrance than acids. Their cationic nature and the ability to interact with the negatively charged membrane surface may enhance entry. The bicarbonate ion, which carries a negative charge, has very low passive brain permeability (Ballabh *et al.*, 2004).

The caveolae-mediated transcytosis such as in RMT, has a protein coat composed of caveolins. Caveolins are integral membrane proteins and they are essential for the stability of the formed caveolae. Transport by caveolae-dependent endocytosis can bypass lysosomes and thus avoid a degradative fate. Therefore the cargo can be released to extracellular matrix and enhances the delivery to the target, which is critical for improvement of therapeutic delivery. In contrast, clathrin-dependent endocytosis and other endocytic pathways lack this property in which the endocytic vesicles are destroyed after

fusion with early endosome which gradually mature into late endosomes, and then into lysosomes (Kou *et al.*, 2013; Xiao *et al.*, 2013). This process is associated with the lowering of the internal pH to be acidic, triggering digestion and releasing of contents into the cytosol (Cooper, 2000; Godlee *et al.*, 2013).

In both RMT and AMT, the lysosomal compartment in the cell should be avoided via routing the primary endosome away from this degradative compartment, in order to achieve an intact protein or peptide transcytosis. This process of avoiding lysosomal degradation seems not to happen in other peripheral endothelia, thus it might be a particular characteristic of the BBB where a high number of intact molecules is necessary to be transported (Abbott *et al.*, 2010; Serlin *et al.*, 2015).

According to advanced electron microscopic examination of BBB endothelium, there are relatively few endocytotic vesicles observed in their cytoplasm in comparison with the other types of endothelial cells (Abbott, 2014). In addition, the endothelia of brain capillaries are very thin cells; the distance separating luminal and abluminal membranes is less than 500 nm (Abbott *et al.*, 2010).

Many examples are exist employing the receptors at the cell surface for specific ligand transport such as TfR for transferrin (Tf), LfR for lactoferrin (Lf), Apolipoprotein E receptor 2 ApoER2 (for lipoproteins and molecules bound to ApoE), LRP 1 and 2 (for lipoproteins and Aβ), receptors for advanced glycosylation end-products RAGE (for glycosylated proteins), immunoglobulin G for IgG, insulin, leptin, tumour necrosis factor (TNFα), epidermal growth factor EGF, diphtheria toxin (DTR), cationised proteins (for cationised albumin) and cell penetrating peptides (Abbott *et al.*, 2010; Hawkins *et al.*, 2006).

1.4.5 Cell movement across the BBB (cell-mediated transcytosis)

This transport pathway depends on immune cells such as monocytes or macrophages entering the CNS through the BBB. In contrast to other transport pathways which permit passage of solutes with specific properties, this way offers the possibility to transport different types of molecules (Park, 2008). In this transport type, the circulating mononuclear cells and neutrophils are attracted to sites of inflammation in the BBB, then cross the barrier forming holes in the perivascular space, encircling venules and other small vessels; these spaces serve as a particular niches for specific immune responses

(Konsman *et al.*, 2007). The CNS is an immune privileged system, whereas the infiltration of neutrophils into the brain is lower than into other tissues owing to the presence of the BBB and the well-regulated immune cell to BBB interaction. Free brain penetration could happen only in trauma or ischemia after pathologic disorders when the BBB is destroyed by activated neutrophils (Scholz *et al.*, 2007).

1.5 Strategies used to deliver drugs to the brain in AD

Due to the presence of the BBB, drug delivery to the brain requires specific approaches to be adopted in order to treat CNS disorders. These approaches include four main categories:

1) Direct or local injection inside the brain and implantation.
2) Disruption or a temporary opening of the BBB by chemical or physical methods.
3) Drug modification to be lipophilic.
4) Using specific endogenous transport systems, such as carrier-mediated transporters (Khawli *et al.*, 2013).

It is essential that the drugs used in AD must cross the BBB and reach deep targets in the brain. Nevertheless, most trials that have been conducted have failed due to the inefficient trial design which neglected the BBB penetration (Becker *et al.*, 2008). In AD, the BBB represents the biggest challenge in delivering drugs to the CNS and the following strategies have been developed, by which some potential drugs used in AD can cross the BBB.

1.5.1 BBB disruption

Local BBB disruption or opening of TJs can be stimulated providing a temporary pathway for drug entry. These stimuli can be either chemical such as hyperosmolar solution, or physical such as ultrasound, or biological such as inflammatory mediators (Chen *et al.*, 2012).

Although any disruption in the BBB could enhance drug delivery into the brain, this could lead to barrier leakage and many circulating substances in the blood, potentially neurotoxic, will enter the brain. Therefore, BBB disruption to deliver drugs or biomaterials must be cautiously controlled (Banks, 2012). Previous studies have found that large molecules such as dextran and antibodies could enter mouse brain when it was opened by the action of adenosine on the BBB (Carman *et al.*, 2011).

Some micro-punctate disruptions of the BBB which have been seen in AD animal models may not be adequate for drugs to reach their therapeutic levels (Banks, 2012). This is due to the restriction of the disrupted BBB in comparison to other peripheral tissue beds. Furthermore, poor diffusion in brain tissue limits the drug ability to reach lesion areas of the brain (Begley, 2004). One study has found that BBB disruption in AD animal models was not sufficient to improve small molecules entry to the brain and did not provide an acceptable cost and benefit values for drug delivery especially for chronic diseases such as AD (Cheng *et al.*, 2010).

1.5.2 Lipid solubility

Recent CNS studies were addressed to the development of small and lipid soluble molecules such as phenserine and posiphen which are cholinesterase inhibitors to improve BBB penetration (Maloney *et al.*, 2007). However, the presence of ABC transporters, such as P-gp, prevents many of these molecules from accumulating in the brain to their therapeutic concentration (Banks, 2012). Indeed, it was found that NNC 26-9100, a non-peptide somatostatin agonist with high lipid solubility (MW=556 Da) has given positive effects on cognition improvement in an AD animal model (Sandoval *et al.*, 2011).

1.5.3 Transport systems

Endogenous transport systems are considered the greatest potential strategy used in brain drug delivery (Banks, 2012). The vascular BBB is rich with well-known transporters and still many of BBB transporters have not yet been discovered (Barres *et al.*, 2010). Many transporters of proteins and peptides have a heterogeneous distribution leading to a possibility of targeting drugs and specific delivery to the brain areas (Banks, 2012).

Preclinical and clinical studies have shown that few drugs used in AD treatment take advantage of these transport systems. Some cholinesterase inhibitors, such as Donepezil®, are transported through the BBB utilising an organic cation transporter, such as choline transporter, that is mostly used for choline molecules (Banks, 2012; Kim *et al.*, 2010).

Trojan horse approaches tend to use these systems, such as RMT, not only to transport their endogenous ligands, but also to deliver the attached drugs. Many endogenous substances are used as ligand, such as glucose and lipoprotein (Chen *et al.*, 2012). Furthermore, antibodies with their attached cargos can be directed at Tf or

melanotransferrin transporters, which are located on the brain endothelial luminal surface, and can be used in the delivery of drugs for the AD treatment (Begley, 2004).

1.6 Drug delivery systems

During the past two decades, studies regarding the development of pharmaceuticals have mainly focused on ways of delivering drugs to the brain, and therefore a wide range of drug delivery systems (DDS) or carrier systems have been designed (Carlotta *et al.*, 2017; Sahoo *et al.*, 2007). Ideally, the DDS would optimise the physico-chemical properties of the drug such as stability, solubility, absorption, cellular entry and therapeutic concentration within the target tissue, and permit reproducible and long-term release of the drug at the target site (Tiwari *et al.*, 2012). Furthermore, DDS can reduce the frequency of drug administration and thus improve patient comfort (Sahoo *et al.*, 2007).

Some drug carrier systems such as micelles, vesicles, liposomes, polymers, dendrimers and nanoparticles provide great promise for targeted drug delivery. The goal of designing these systems is to improve drug loading and release properties with optimum shelf-life and low cytotoxicity (Safari *et al.*, 2014; Sahoo *et al.*, 2007; Xing *et al.*, 2014) (Fig.1.10).

1.6.1 Micelles

Micelles are produced by the assembly of amphiphilic copolymers in aqueous solutions (Tiwari *et al.*, 2012). The drugs can be loaded by entrapping them into the micellar core. The hydrophilic sites are able to form hydrogen bonds with the external aqueous sites resulting in a strong shell around the core of micelle. Micelle size and morphology can be controlled as their chemical components, molecular weight and length ratios of the block can be easily altered (Tiwari *et al.*, 2012).

1.6.2 Liposomes and Nanolipsomes (NLs)

These are small artificial and spherical shaped vesicles made of phospholipids that self-assembled into a bilayer with a hydrophilic end and an opposite hydrophobic end. Water-soluble drugs are incorporated into the aggregation of the hydrophobic ends while lipid-soluble drugs are trapped inside the phospholipid layer (Akbarzadeh *et al.*, 2013). Some liposomes can attach and fuse with membranes of the cells, releasing their cargos within the cell. Other liposomes are taken up by phagocytic cells and the phospholipid layers are lysed by lysosomes, releasing the drug (Akbarzadeh *et al.*, 2013). However, difficulty to be removed from circulation, the low solubility, short half-life, oxidation and hydrolysis of

the cellular membrane phospholipid, leakage and fusion of encapsulated molecules and high production cost are all reasons behind their limitation (Tiwari *et al.*, 2012).

1.6.3 Nanoparticles (NPs)

NPs are colloidal particles between 10-100 nm in size (Sahoo *et al.*, 2007). NPs and microparticles can be formed using polymers such as poly lactic-co-glycolic acid (PLGA) and PLA which are being suggested as potential gene delivery systems owing to their sustained-release properties, and ability to protect DNA from lysosomal degradation (Panyam *et al.*, 2003). There are different types of NP such as gold NP, quantum (Q) dots, superparamagnetic iron oxide NP and paramagnetic lanthanide ions.

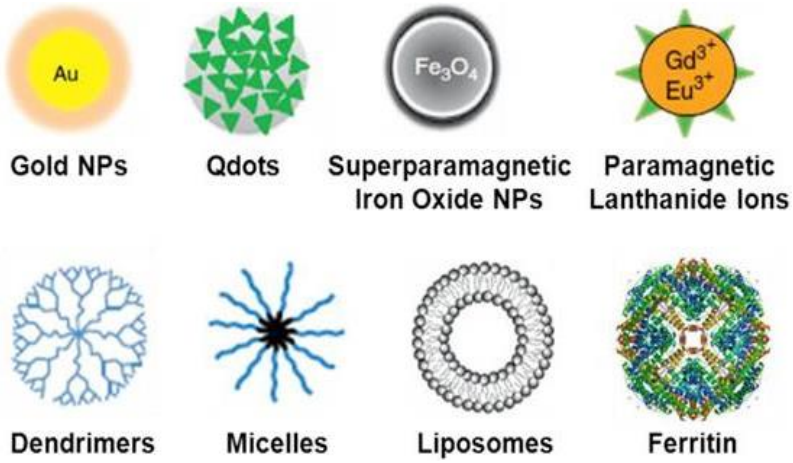

Fig.1.10: Some examples of DDS. Different types of nanoparticles (NP) including gold NP, Q dots, superparamagnetic iron oxide NP and paramagnetic lanthanide ions, in addition to some other types of DDS, including dendrimers, micelles, liposomes and ferritin (Xing *et al.*, 2014).

1.6.4 Dendrimers

Dendrimers are hyperbranched polymeric macromolecules. They have a "unique molecular architecture with distinctive characteristics" making them different from other polymers; particularly the gradual assembly method of the constituents so that they have a well-defined size and structure (Heather *et al.*, 2011). Their high density of terminal functional groups is the key property in terms of their potential use in drug and gene delivery. This mostly contributes to the molecular surface properties which provide multiple attachment sites for the integration and loading of drugs or other bioactive targeting moieties (Sadekar *et al.*, 2013).

The term dendrimer was first identified by Tomalia in 1985 (Tomalia *et al.*, 1985) which derived from the Greek word "dendron", means tree and "meros", means part and it represents the highly ordered, hyper branched and three-dimensional features that resemble the architecture of a tree at the molecular level (Menjoge *et al.*, 2010).

1.6.4.1 Types of dendrimers

Different types of dendrimers have become available with defined nanosize and numbers of functional terminal groups (Prashant, 2014; Srinivas *et al.*, 2014) (Fig.1.11).

1. Poly amido amine dendrimers (PAMAM): these are the first identified dendritic structures synthesised via the divergent strategy (see Section 2.3) using ethylenediamine or ammonia initiator core as starting material.
2. Poly (propylene imine)/ poly (propylene amine) dendrimers (PPI /POPAM): They are hyperbranched macromolecules with terminal amines which are mostly formed using the divergent strategy and its core consisting of 3˚-propylene amines as the interior entity.
3. Liquid crystalline dendrimers (LC): These dendrimers consist of LC monomers such as mesogen-functionalised carbosilane. They are mainly synthesised by disk-like (discotic) molecules or rod-like (calamitic) materials. It has been suggested that these dendrimers can be used in bioactive agent's delivery (Pedziwiatr *et al.*, 2013; Prashant, 2014).
4. Tecto dendrimers: These are also called core-shell and considered a highly ordered polymeric architecture formed by the controlled coupling of dendrimers building units (Schilrreff *et al.*, 2012). They are composed of a dendrimer as a core, which might contain drug molecule, surrounded by multiple dendrimers.
5. Chiral dendrimers: These dendrimers are formed by the chiral core attaching to chemically similar, but constitutionally different, branches. They have potential applications in chiral molecular recognition and asymmetric catalysis.
6. Peptide dendrimers: These are hyper and radical branched macromolecules which contain amino acids as branching or interior units or consist of a peptidyl branching core with terminal peptide chains. They are frequently synthesised by divergent or convergent methods. These dendrimers have been mostly utilised in industry as surfactants, and in biomedical fields as carriers for drug and gene delivery, multiple antigen peptides, and protein mimics.

7. Glycodendrimers: These molecules involve sugar moieties in their construction such as glucose, mannose, and galactose. Most of them have sugar moieties on their outer layer, and some of them also contain a saccharide unit in the central core. They are mostly applied to the delivery of drugs to specific sites, particularly the lectin-rich parts.
8. Hybrid dendrimers: are combinations of both linear and dendritic polymers in forms of either graft copolymer or hybrid block. Their small segments are linked to several reactive chain ends allows them to be used as hybrid dendritic linear polymers or surface active agents or adhesives.
9. PAMAM-organosilicon dendrimers (PAMAMOS): are inverted unimolecular micelles containing nucleophilic or hydrophilic PAMAM as interiors and their exteriors are hydrophobic organosilicon (OS). They have the potential for multiple applications such as chemical catalysis, electronics, photonics and nanolithography.

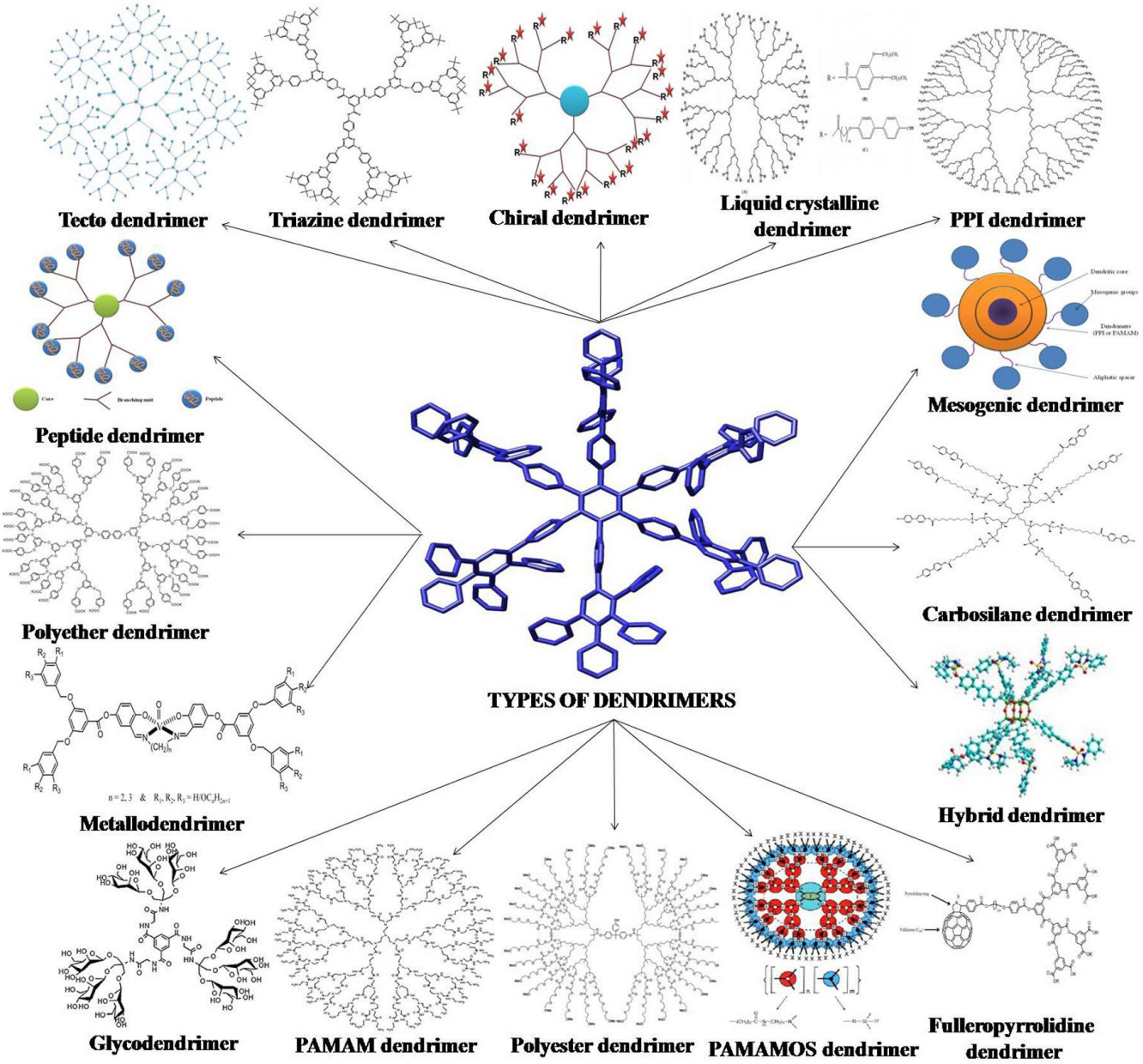

Fig.1.11: Different types of dendrimers with different core units and different terminal functional groups (Prashant, 2014).

1.6.4.2 Dendronised polymers for biomedical applications

The use of dendronised polymers in numerous biomedical applications such as in drug and gene delivery and in imaging has increased due to the adaptability of dendrimer chemistry, allowing the synthesis of a broad range of molecules with different functionality (Boas *et al.*, 2004; Gagliardi, 2017).

The highly controlled level of their structural design clearly differentiates those dendrimers as optimum and unique carriers in clinical applications (Longmire *et al.*, 2011). Bioactive agents such as drugs can either be encapsulated within the branches or attached to the

terminal groups of dendrimers (Patri *et al.*, 2012). The distinct properties of these molecules, including biocompatibility and biodegradability are beyond their success as carriers or biomaterials (Tomalia *et al.*, 2005).

It has been demonstrated that dendronised polymers can be used in pharmaceutical and skin care applications (Sahoo *et al.*, 2007). Functionalisation of PAMAM with antiperspirant deodorant constituents has been documented to successfully enhance their efficacy on skin (Menjoge *et al.*, 2010). Moreover, dendrimer-based products have been utilised for different cancer therapies such as for glioblastoma, prostate cancer, and bone metastases (Lee *et al.*, 2012).

A recent research has shown a significant improvement in the bioavailability of pilocarpine in the eye by using surface-modified dendrimers (Srinivas *et al.*, 2014). Positively charged dendrimers have been postulated to relatively increase the bioavailability of encapsulated enoxaparin in pulmonary drug delivery (Bai *et al.*, 2007). Moreover, it has been found that dendrimers complexes with ketoprofen and indomethacin could improve the skin permeation of these drugs (Cheng *et al.*, 2007).

In oral drug delivery experiments, it has been postulated that low-generation dendrimers can successfully cross cell membranes, possibly via adsorptive endocytosis (Patri *et al.*, 2012). Furthermore, a controlled release of adriamycin and methotrexate (anticancer drugs) were achieved after encapsulating into polyethyleneglycol (PEG)-modified dendrimers (Xu *et al.*, 2014).

It was found that the loading of folic acid to modified PAMAM dendrimers with carboxymethyl PEG can control its release rate and lower its haemolytic effect (Choi *et al.*, 2005). While ibuprofen complexed with dendrimer was found to enter lung cells rapidly compared with free drug, implying that dendrimers can efficiently carry the encapsulated drug through cell membrane (Kolhe *et al.*, 2003). Sadekar *et al* (2013) have used PAMAM dendrimer conjugated with the anticancer drug, camptothecin, to improve the drug solubility and to increase its bioavailability at target tissue (Sadekar *et al.*, 2013).

The data of a recent study have shown the ability of generation 3 poly lysine dendron, with diphenylalanine as core and peptide at branches [FFG3K $(WHLPFKC)_{16}$], to regulate angiogenesis in tissue regeneration (Perugini, 2013).

Many studies have utilised dendrimers as a drug carrier system targeting the brain owing to their distinctive properties and ability to cross BBB by AMT (Xu *et al.*, 2014). It was found that a conjugation of the drug doxorubicin (anticancer) to a dendrimer decorated with PEG triggered drug release efficiently under weak acidic conditions, enhancing transport across the BBB and reducing tumour volume of glioma *in vitro* (Li *et al.*, 2012).

In order to improve targeting and penetration of a drug delivery system to the site of action, these carrier systems can be decorated with a specific ligand such as Tf and ApoE-peptide which can be recognized by a specific receptor on BBB (Gao *et al.*, 2010). For instance, it has been found that decorated PAMAM with Tf or Lf, enhanced delivery and targeting of doxorubicin to the brain (Huang *et al.*, 2008).

1.6.5 Using DDS in AD therapy

DDS and nanobased carrier systems have been extensively used to overcome the low permeability of drugs to the CNS (Safari *et al.*, 2014). One study has successfully found that liposomes complexed with PA or CL have the ability to reduce toxicity of Aβ deposits (Bereczki *et al.*, 2011). In another study, Gobbi *et al* (2010) have developed NLs by their complexation with CL or PA, and functionalisation with ApoE-derived peptides (fragment 141-150) and found the NLs could interact with brain endothelial cells cultured *in vitro* and able to target the aggregations of Aβ peptide (Gobbi *et al.*, 2010).

A further study showed that decorated NLs with an anti-Aβ monoclonal antibody were found to have a high affinity for brain fibrils of Aβ both *in vitro* and in *ex vivo* samples of AD brain (Canovi *et al.*, 2011). Results from previous studies revealed that decorated NLs with a curcumin derivative are able to interact with Aβ in newly formed plaques with high affinity and prevent its aggregation *in vitro* (Mourtas *et al.*, 2011; Re *et al.*, 2011; Taylor *et al.*, 2011).

Other researchers have taken several different approaches in the development of NPs for the treatment of AD. For instance, fluorinated NPs capable of increasing the α-helical constituents of Aβ have been found to prevent the formation of Aβ oligomers and inhibit its aggregation (Saraiva *et al.*, 2010). Alternatively, conjugation of NPs with iron chelators might have the potential to inhibit the formation the oligomers of Aβ; in turn they protect the neurons from Aβ-induced oxidative toxicity (Liu *et al.*, 2009).

Interestingly studies of AD patients revealed that the Aβ42 lowering drug, FP, failed to improve the cognitive decline after 18 months of treatment, due to its low penetration across the BBB and, consequently, inadequate target engagement in the brain (Green *et al.*, 2009). On the other hand, FP embedding in polylactide NPs enables it to exert its biological function in high concentration (Meister *et al.*, 2013). However, the study had recommended some improvements and optimisations of the NPs for future research that could lead to a higher bioavailability or a specific targeting to the brain.

One of the limitations of the above studies is the lack of clinical trials and the fact that they relied on *in vitro* cell culture models. Therefore, there is not enough data available to ensure a successful AD treatment in human. As a result further trials are needed to improve FP penetration across BBB and to retain its pharmacological activity in AD within its therapeutic dose.

A promising approach for improved FP permeability is by loading it to specific carriers, such as dendrimers, that have biocompatible and biodegradable properties and the ability to cross the BBB. Dendrimers have a unique structure that can be easily bifunctionalised with both the drug and a ligand such as ApoE derived peptide that can be recognised by the LDL receptors on the brain endothelia, enhancing targeting and cell uptake of the carrier system. This study is testing the hypothesis of the ability of dendronised-ApoE-derived peptide in facilitating cellular uptake and delivery of FP to the brain.

1.7 Aims of the study

The present study uniquely integrates state of the art in between a therapeutic agent and biomaterial to offer a novel efficacious treatment of AD. The study aims to:

1. Improve cellular membrane permeability of FP into the brain by designing a novel dendronised carrier system, and to achieve high bioavailability by integrating the drug (for the first time) through a coupling reaction with multiple terminal functional groups of the dendronised carrier system.
2. Study the cytotoxicity of the designed dendronised carrier systems using bEnd.3 cell line as a BBB model to ensure their biocompatibility.
3. Enhance the brain targeting and permeability via functionalising this drug-carrier system with an ApoE-derived peptide of 10 amino acids that acts as a ligand to be recognized by lipoprotein receptors at the brain.
4. Examine the cellular uptake of the synthesised products and to study their potential to cross a validated *in vitro* model of the BBB.
5. Investigate the activity of the drug conjugates on γ-secretase enzyme secreted by the glial cells biochemically and to ensure the conjugates biodegradability.

Chapter 2. Design and Characterisation of Dendronised Carrier System integrated With FP

2.1 Introduction

Drugs with a potential in the treatment of AD have clinically failed to reach their targets and resolve the underlying pathogenesis because they lack the BBB permeability; FP is one of these drugs. It is therefore essential to incorporate these active molecules into appropriate carrier systems capable of ensuring their pharmacological activity.

Several carrier systems including nanomaterials (NMs) have been designed to overcome the problems regarding BBB permeability. NMs are considered the most promising strategies to interact with the endothelial cells of the BBB at the molecular level, without interfering with the normal physiological function of the barrier or its integrity (Bhaskar *et al.*, 2010). The most commonly used NMs for therapy and diagnosis of ND are liposomes, polymers, micelles, nanogels, nanofibers, nanotubes and dendrimers, these are plain or decorated with ligands for specific transporters (Re *et al.*, 2012).

A number of properties of NMs should be considered in order to achieve this aim, including (i) surface functionalisation for drug loading, (ii) targeting and crossing of the BBB, (iii) prolonged half-life in blood (enough for drug to exert its action, by avoiding the reticuloendothelial system; 'stealth' NMs). Finally, NMs should be non-toxic, biodegradable and biocompatible, they should not induce inflammatory reactions and be non-immunogenic (Re *et al.*, 2012). One of the promising NMs in delivering drugs is the dendrimers (Khawli *et al.*, 2013). Some other NMs such as polymers and liposomes have many disadvantages such as difficulty in preparation, more immunogenicity and more toxicity in comparison to dendrimers (Boas *et al.*, 2004).

2.1.1 Dendrimers and Dendrons

Dendrimer was one of the most frequently seen terms in the scientific literature in the nanotechnologies formative years (Srinivas *et al.*, 2014). They have numerous advantages over other polymers and NMs in clinical applications (Heather *et al.*, 2011; Patri *et al.*, 2012; Srinivas *et al.*, 2014).

1) They have nanoscale particle size of less than 100 nm that reduces uptake by macrophages and their high density of 2^{o} and 3^{o} amines in PAMAM or

other dendrimers with branching amino groups, facilitates their escape from reticulum endothelium.

2) Addition further layers increases the peripheral branches with lower density core forming hollow spaces that can be used for entrapment of drugs or other bioactive molecules.
3) Multiple outer surface functional groups offer multiple attachment sites for the bioactive molecules, targeting moieties and the loading of high number of the drug molecules so it can increase its bioavailability (Fig.2.1).
4) Their synthesis can be modified in a manner that facilitates their biodegradation and drug release.
5) They enhance permeability and retention action so that they can target specific cells effectively with rapid cellular entry, in addition to the ability to cross the cellular membrane.
6) They are ideal drug delivery systems due to their unique functionality, dimensions and their biocompatibility and biodegradability (Patri *et al.*, 2012; Srinivas *et al.*, 2014).

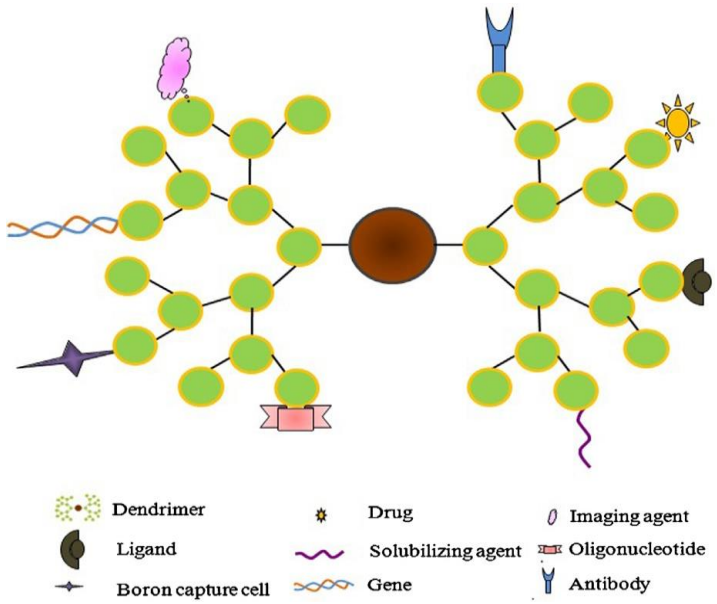

Fig.2.1: Dendrimers offer multiple attachments to different bioactive molecules and a tool for various applications (Prashant, 2014).

2.1.2 Dendrimers structure and synthesis

A typical structure of a dendrimer consists of three distinct regions: a central poly functional core; repeated branched monomeric units organised in layers called "generations" (G); and peripheral groups designed to give functionality to the dendrimers (Fig.2.2). Dendrimers are normally synthesised from the central poly-functional core by repetitive addition of the monomers. The size and molecular weight of a dendrimer increase as the generation number increases (Boas *et al.*, 2004).

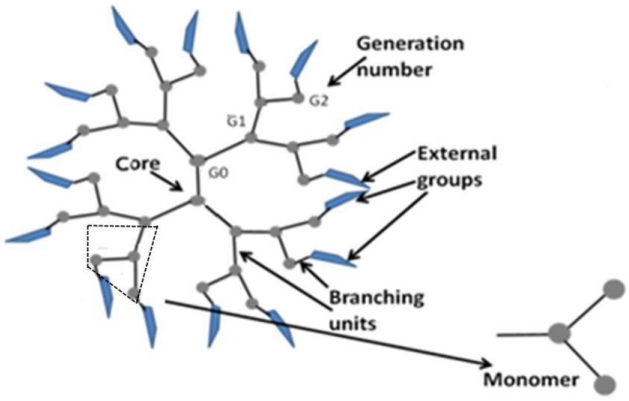

Fig.2.2: General basic structure of a dendrimer. The dendrimer size and shape relies on the number of monomer layers and generation (G) refers to every layer added (Perugini, 2013).

Dendrons are identical subunits formed the layers of the dendrimer (Aulenta, 2003) (Fig. 2.3). The central core and peripheral functional subunits are interdependent and able to create a distinct macromolecule with a particular shape, size, functionality and flexibility (Tomalia *et al.*, 2005).

The size and generation number of dendrimers increases systematically and their size can also contribute to their three-dimensional shape; dendrimer structures with lower generations tend to be open and amorphous while those with higher generations present a spherical conformation able to incorporate drug molecules (Prashant, 2014).

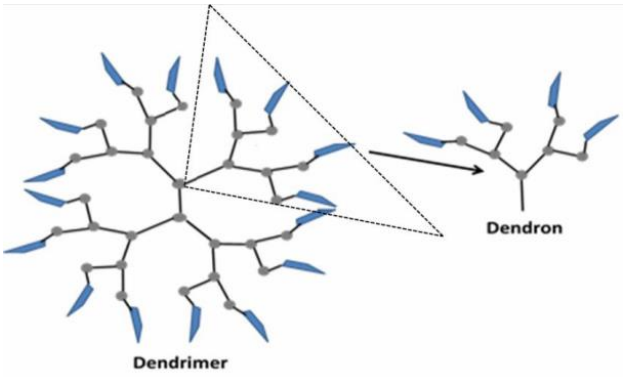

Fig.2.3: Dendrimers and dendrons. The dendron is considered as a subunit and its repetitive addition form dendrimers in different generations (Perugini, 2013).

Generally, dendronised macromolecules are synthesised by two techniques known as the convergent or divergent assembly approaches. In the convergent approach, dendrimers are built up starting from the periphery branches to the core unit, an outside inwards strategy (Abbasi *et al.*, 2014). Alternatively, synthesis by the divergent approach starts at a central core unit and grows outwards radially by stepwise addition of monomers (Carlmark, 2009). A dendrimer generation can be controlled during synthesis by adding monomers to each active functional group on the surface in turn leaving the terminal groups available for further reaction (Biricova *et al.*, 2009) (Fig.2.4). Other strategies used for the formation of new structures of dendrimers, tend only to be modifications or combinations of these two basic methods (Touzani, 2011).

The most widely used strategy is the divergent based on solid phase peptide synthesis (SPPS) (Merrifield, 1965). SPPS is the stepwise protocol by addition of amino acids (monomers) to a growing peptide chain that is fixed to a solid phase particulate support via a linker molecule which allows cleavage and purification after achieving the desired peptide (Mitchell, 2008). SPPS-assisted microwave peptide synthesis has been demonstrated to be a valuable technique in the synthesis of different generations of dendronised carrier systems. Despite the length and branching, dendronised polymers and other peptides have been routinely produced and efficiently analysed by this method (Made, 2014; Perugini, 2013).

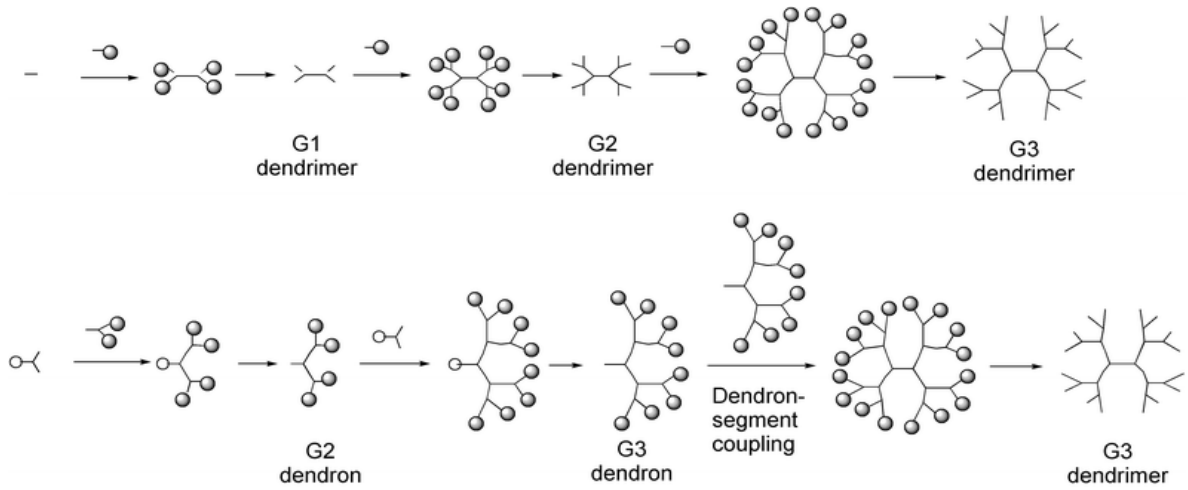

Fig.2.4: Synthesis of different generations of dendrimers. The Divergent method is shown at the top, with the addition of monomers to the starting central core, and the convergent method is at the bottom, which shows addition of synthesised branches to the core (picture taken from pubs.rsc.org).

It is apparently that the utilisation of dendronised polymers has been explored in numerous biomedical applications (Abbasi *et al.*, 2014). Their easy synthesis, controlled design and functionalisation or loading with drugs as well as the ability to cross physiological barriers behind their using as successful carrier system (Tomalia *et al.*, 2005). However, further research is needed to elucidate the role of low generation dendrons, with loaded drug, in integrating with cell membrane and increasing cellular uptake and brain delivery. These investigations can potentiate the crucial use and industrial benefit of these products as novel carrier systems for drugs and imaging or diagnostic agents in AD or other ND diseases.

2.2 Aim of the chapter

1. To design low generations lysine dendrons (G0K and G1K) with phenylalanine (F) as a core molecule using a modified microwave-based SPPS method.
2. To integrate a widely accepted drug for AD treatment, FP, into this carrier system to improve its passage across the BBB and to increase its bioavailability by coupling one molecule for each uppermost amino groups of the branched molecules through amide linkage.
3. To characterise the designed molecules and confirm the successful attachment of the drug to the dendrons using a range of analytical techniques (Mass Spectrometry (MS), Fourier Transform Infrared Spectroscopy (FTIR)), and to confirm their purity by an optimised thin layer chromatography (TLC) and High performance liquid chromatography (HPLC).

2.3 Materials and Experimental methods

2.3.1 Solid phase peptide synthesis (SPPS) by microwave synthesiser

SPPS is the widely used method for peptide production. It provides the assembly of amino acids from the C-terminus of carbonyl-group side to the N-terminus of the amino-group side of an amino acid chain via a series of steps including coupling and deprotection (Meikle *et al.*, 2011; Perugini, 2013) as outlined in Fig.2.5.

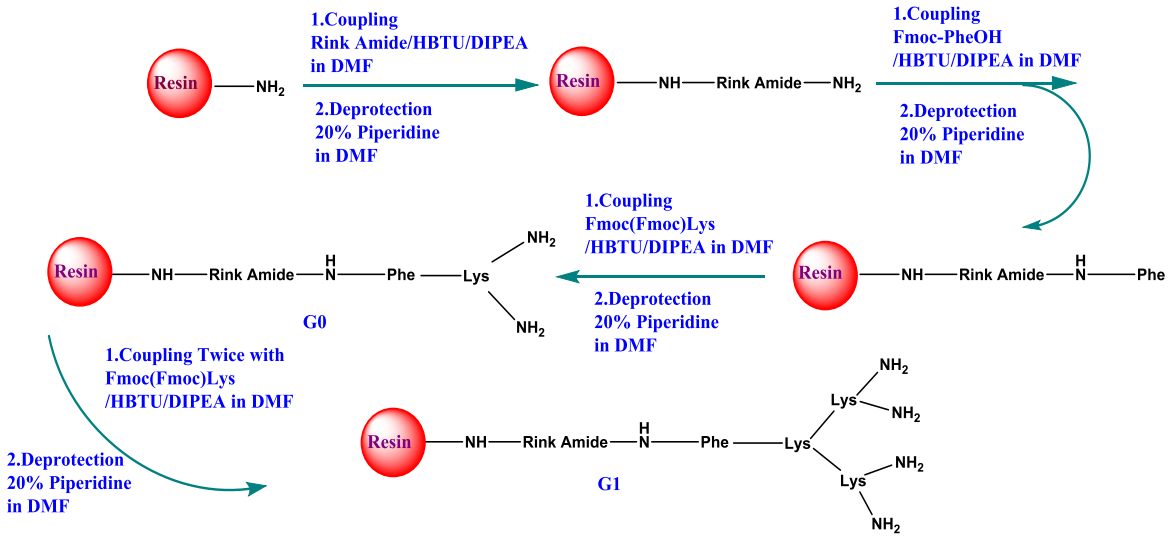

Fig.2.5: SPPS synthesis. This protocol is based on using a TentaGel NH_2 resin as a support with using Fmoc-α-amine-protected amino acid as monomer unit. The free active N-terminal of an amino acid is bound to the COOH group of the next amino acid by coupling reaction; then the Fmoc is removed by deprotection revealing a new free active N-terminal amine to react with the carboxyl group of a new amino acid. This cycle of coupling and deprotection is repeated to achieve the desired dendrimer.

This procedure is developed to achieve a high percentage completion of each amino acid coupling reaction guaranteeing high productivity and purity of the interested dendronised molecule. This method was used to:

1. Synthesise phenylalanine-lysine dendron G0K (chemical formula: $C_{15}H_{23}N_3O_3$, exact mass: 293.174, MW: 293.367 Da) (Fig.2.6).
2. Synthesise phenylalanine-2lysine dendron G1K (chemical formula: $C_{27}H_{47}N_7O_5$, exact mass: 549.364, MW: 549.717 Da) (Fig.2.7).

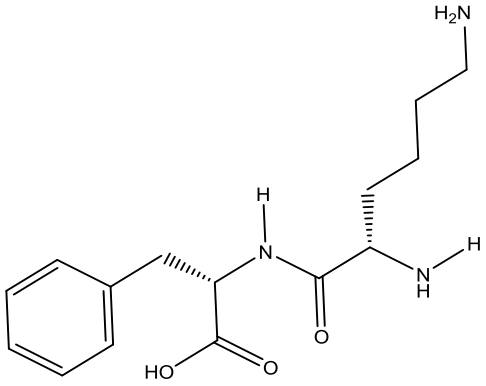

Fig.2.6: Chemical structure of G0K showing two terminal amine groups.

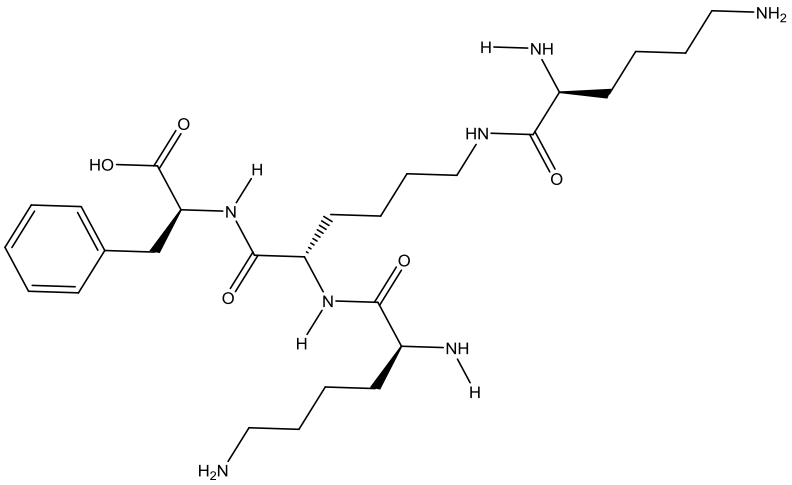

Fig.2.7: Chemical structure of G1K showing four terminal amine groups.

2.3.1.1 Assembly of dendron (hyper branched peptide)

All amino acids (Novabiochem), Rink amide and TentaGel resin (Iris Biotech GmbH) were allowed to reach ambient temperature for approximately 30 min. Prior to peptide assembly, 100 mL of 20% $^{v}/_{v}$ piperidine (Sigma Aldrich) in N, N–dimethylformamide (DMF) ((anhydrous solvent - synthesis grade) (Fisher Scientific)) was prepared and 0.5 g of TentaGel NH_2 resin was put into a reaction vessel that was attached to a vacuum pump. DMF (5 mL) was added to a reaction vessel containing the resin then left to swell for 15 min. The DMF was then removed from the reaction vessel using the vacuum pump. A magnetic stirring bar was added to the reaction vessel to improve reaction.

In a separate glass vial, 0.4 mmol of both Rink amide linker and 2-(1H-benzotriazol-1-yl)-1,1,3,3-tetramethyluronium hexafluorophosphate (HBTU) (Novabiochem) were weighed and 140 µL of N,N–diisopropylethylamine (DIPEA) (Sigma Aldrich), which is used as activation agent, and 3 mL DMF were added then sonicated for a few seconds until solubilised. This solution was then added to the reaction vessel and covered with the lid.

Reaction conditions were set up on a peptide synthesis microwave synthesiser (Biotage Initiator, UK) following the instructions in Table 2.1 for coupling reaction conditions. Once the cycle was complete, the solvent was removed from the reaction vessel by vacuum pump. The resin was then washed with 3 mL DMF 3 times and the solution was removed under the vacuum pump.

Table 2.1: List of reaction conditions for microwave synthesis

Step	**Duration (min)**	**Power (W)**	**Initial power (W)**	**T (^{o}C)**	**Stirring rate (rpm)**
Coupling	5	50	10	50	900
Initial deprotection	0.5	0	0	Off	900
Deprotection	2	0	0	Off	900
Final deprotection	30	0	0	Off	900

To remove the basic Fmoc-group, deprotection was performed by the addition of 3 mL of 20% $^{v}/_{v}$ piperidine in DMF to the reaction vessel and the program was set up on initial deprotection conditions (Table 2.1). Washing steps were then repeated and deprotection started, which was repeated 3 times, by the addition of 3 mL of 20% $^{v}/_{v}$ piperidine in DMF to the reaction vessel using conditions described in Table 2.1.

After each deprotection step, washing steps were repeated. The exposure of a new N-terminal amine allowed the assembly of a series of Fmoc-amino acids (Fig.2.8).

For coupling of phenylalanine, 0.4 mmol Fmoc-Phe-OH and 0.4 mmol HBTU were weighed in a new glass vial with 140 µL DIPEA and 3 mL DMF, then sonicated and added

to the reaction vessel, and subjected to the same protocols in coupling and deprotection steps.

For the coupling of the lysine dendron, 0.4 mmol of Fmoc-Lys(Fmoc)-OH was used as shown in Table 2.2 then the required number of coupling steps and initial deprotection and deprotection steps were carried out as shown in Table 2.2.

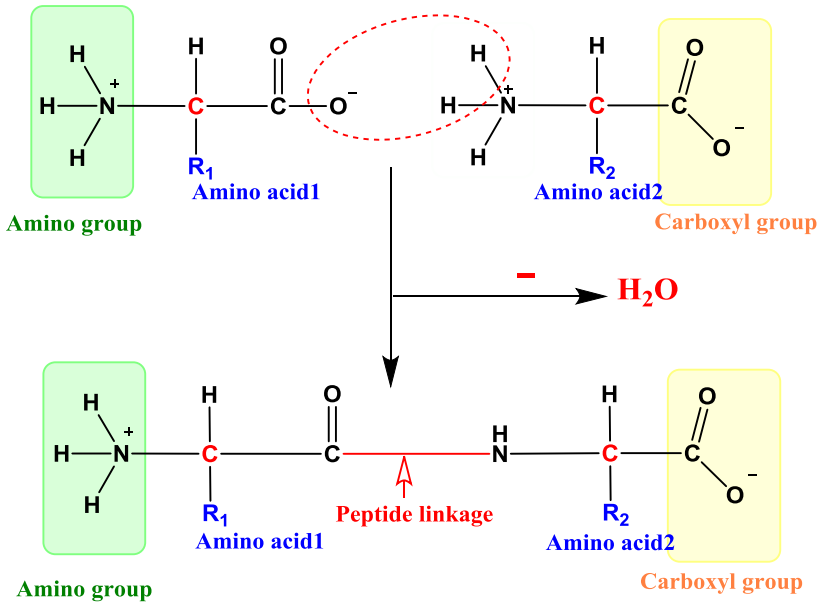

Fig.2.8: Formation of a peptide. Reaction of the amino group of amino acid 2 with the carboxylic acid moiety of amino acid 1 forms peptide linkage (amide linkage bond).

After all desired amino acids were added by a series of coupling and deprotection steps, the peptide was allowed to stand for 30 min for final deprotection. It was then transferred to a fritted 10 mL syringe to be washed through a series of washes with 40 mL of each dichloromethane, methanol and diethylether (HPLC Grade). The product of synthesis was finally left a few hours to dry inside a flow hood and weighed prior to being cleaved from the resin.

Table 2.2: Assembly sequence of G0K and G1K dendrons.

Addition step	Amino acid	No. cycles (0.4 mmol)	Reactive sites at start/ end of cycle	Molar excess (mmol)
Rink Amide	Fmoc Rink Amide Linker	1	1 / 1	4
F	Fmoc-Phe- OH	1	1 / 1	4
G0K	Fmoc-Lys(Fmoc)-OH	1	1 / 2	4
G1K	Fmoc-Lys(Fmoc)-OH	2	2 / 4	4

2.3.1.2 Cleavage of peptide from resin

The remaining protecting groups were cleaved from the peptide when all cycles of synthesis were complete. This cleavage resulted in the removal of the N-terminal protecting group of the first amino acid attached to linker and any side-chain protecting groups (Fig.2.9). A relatively mild acid such as trifluoroacetic acid (TFA) is usually used, this acid is mixed with the free radical scavengers (such as triisoprpylsilane (TIPS)) to prevent any aggregation or modification of the reactive sites of the peptide (Made, 2014; Shin *et al.*, 2005).

The cleavage cocktail consisted of 95% $^{v}/_{v}$ TFA (99.5% Acros Organics), 2.5% $^{v}/_{v}$ deionised H_2O, and 2.5% $^{v}/_{v}$ TIPS (99% Sigma Aldrich). All cleavage mixtures were prepared fresh prior to use and added as 2 mL to each 100 mg of the synthesised peptide with resin. The mixture was left for 3 hr with occasional shaking. The solution was then passed through a Pasteur pipette filled with 1 cm of a glass wool and the peptide was collected in a tube containing 20 mL of diethylether kept on ice.

The collected solution was then centrifuged at 3500 rpm for 5 min to precipitate the peptides. The diethylether was decanted from the tube, 20 mL of fresh diethylether was added and the sample tube was vortexed to disrupt the pellet. The procedure was repeated 3 times and the diethylether was subsequently decanted off. The product was then freeze dried, dissolved in ethanol and filtered through a syringe filter with a pore diameter of 0.22 µm prior to characterisation.

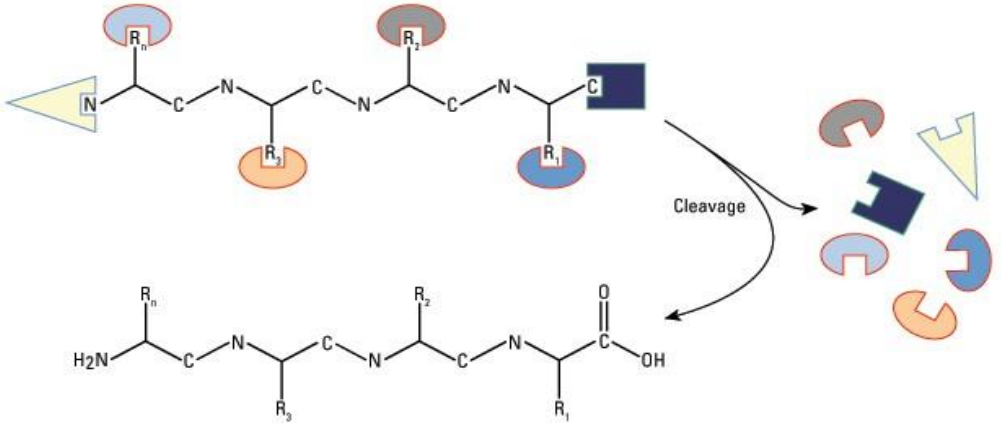

Fig.2.9: Peptide cleavage after synthesis is completed. All remaining N-terminal protecting groups, the C-terminal protecting group and side-chain protecting groups or solid support are removed by addition of cleavage mixture (picture taken from https://www.thermofisher.com/uk).

2.3.1.3 Integration of the FP onto the dendronised carrier systems

For synthesising G0K dendron-2drug (chemical formula: $C_{45}H_{45}F_2N_3O_5$, exact mass: 745.333, sodium salt MW: 767.5 Da), 0.4 mmol of FP (Sigma Aldrich) was weighed in a glass vial and 0.4 mmol HBTU, 3 mL DMF and 140 µL of DIPEA were added and sonicated to solubilise. Coupling and washing steps with DMF without deprotection were then performed, further coupling step with another 0.4 mmol of FP was repeated to produce G0K-FP (Fig.2.10). After that, washing and cleavage were performed as detailed previously for dendrons (Table 2.3).

Table 2.3: Integration of FP to G0K and G1K dendrons.

FP addition step	**No. of coupling (0.4mmol)**	**No. of NH_2 reactive sites / No. of FP**
G0 Lys-NH_2	2	2 / 2
G1 Lys-NH_2	4	4 / 4

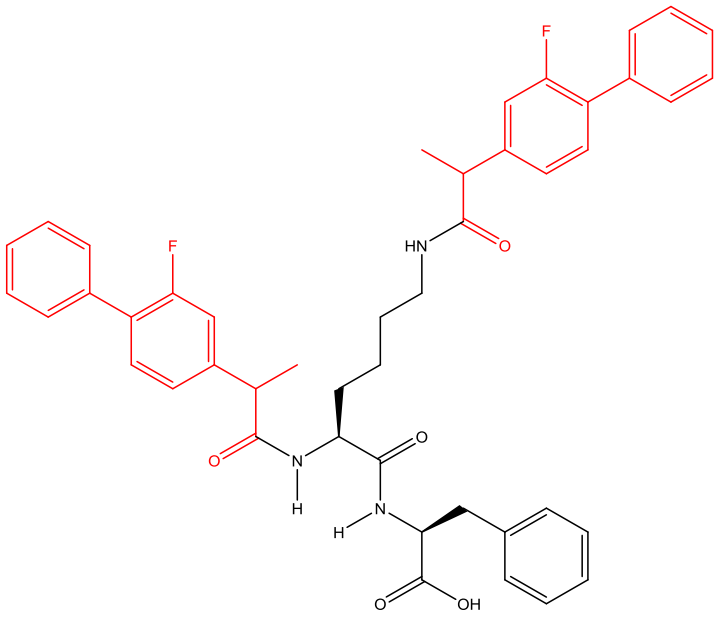

Fig.2.10: Chemical structure of G0K-FP. Two FP molecules (presented in red) attached to dendron via amide linkage.

For G1K dendron-4drug (chemical formula: $C_{87}H_{91}F_4N_7O_9$, exact mass: 1454.6, sodium salt MW: 1475.7 Da), the coupling step was repeated 4 times with 0.4 mmol of FP as indicated for G0K-FP (Fig.2.11).

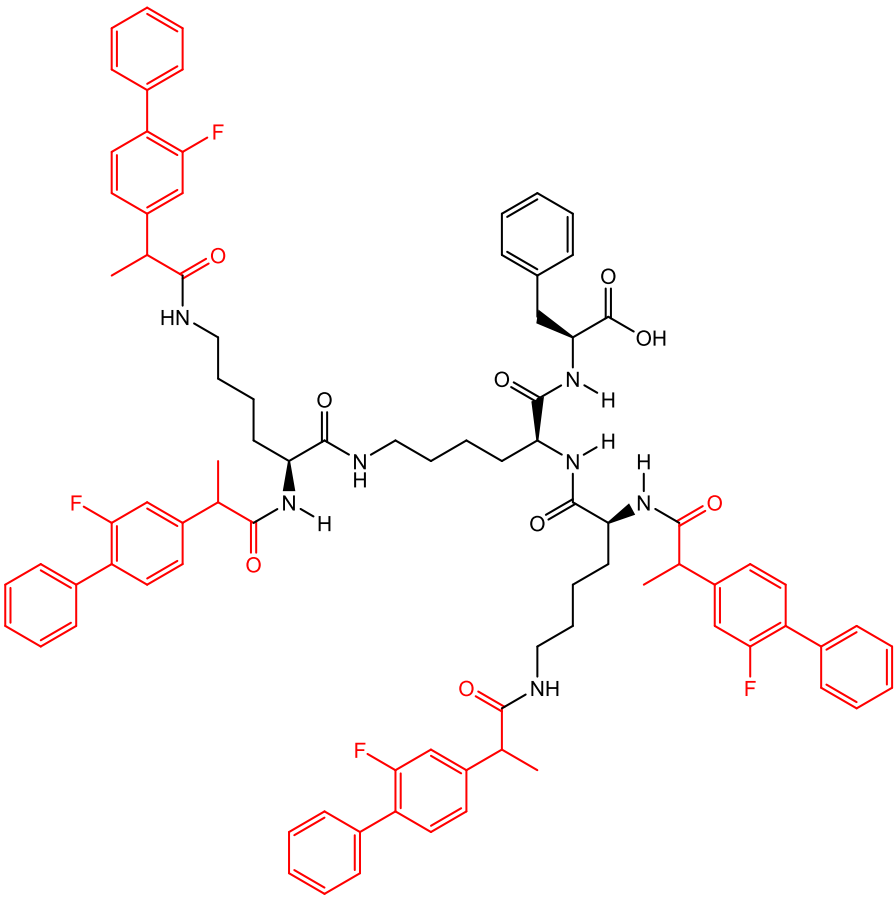

Fig.2.11: Chemical structure of G1K-FP. Four FP molecules (presented in red) attached to dendron via amide linkage.

2.3.1.4 Purification of the synthesised molecules

In order to remove impurities, the synthesised molecules were purified using Zeba spin desalting columns (0.5 mL) (Fisher Scientific). These columns contain a high-performance size-exclusion chromatographic resin which provides desalting or buffer exchange for peptide samples, with ≥ 95% retention of salts and other small molecules according to their mass.

The columns were washed with methanol (0.3 mL), and then centrifuged for 1 min at 1500 rpm 3 times, then 130 µL of the sample was added to the column and the filtrate was collected after centrifugation for 2 min.

2.3.2 Characterisation of dendrons with and without drug

2.3.2.1 Mass spectrometry

Mass spectrometry (MS) is an analytical technique used for identifying materials in terms of their molecular mass and to demonstrate the structure and chemical properties of

different molecules. In general, mass spectrometers have three main essential events known as ion production, ion transmission and ion detection. The injected sample is first ionised through an ionisation source in the gas-phase in order to move freely to the detector via a series of electric and magnetic lenses. This process requires a vacuum pump system to efficiently maintain the pressure within a constant range and limit the production of unwanted side reaction products. Once completed, the mixture of ions is moved to a mass analyser which separates ions and passes information to a data station to be characterised (Downard, 2004; "Mass Spectrometry," 2015) (Fig.2.12).

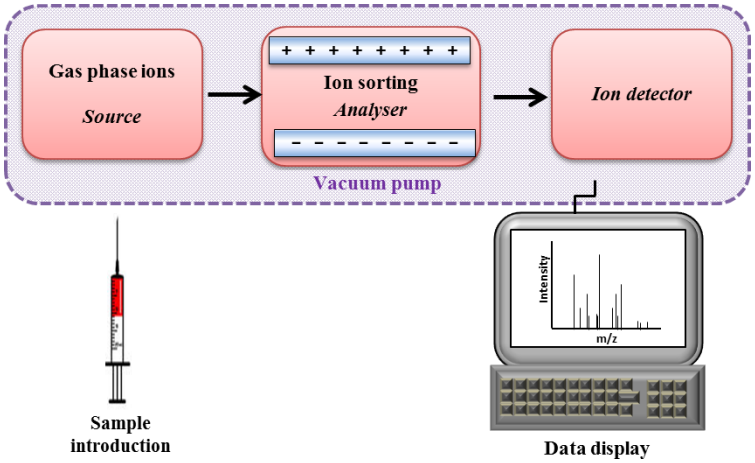

Fig.2.12: Overview of MS principle.

For peptides, this process mostly includes electrospray ionisation (ESI). The movement of the ions within the MS is controlled by the charge state (z) and the mass (m), therefore it measures a combination of these two parameters in a ratio of m/z. The data appears in a mass spectrum represents "the relative intensity of all ions detected in the MS within a defined period of time versus their m/z" (Downard, 2004; Edmond *et al.*, 2007).

Here, the dendrons with and without drug were characterised by electrospray/ionisation-time of flight ((ESI-TOF MS) (Bruker Daltonics)), according to a standard method. Briefly, the dried molecule was dissolved in 2 mL of methanol at a concentration of 1mg/mL, then filtered with a 0.22 µm filter to avoid clusters, and pumped through a stainless steel capillary.

A voltage of 4 kV was applied to the tip of the capillary leading to dispersion of the sample into a highly-charged droplet chamber. This process was supported by introducing a nebulising nitrogen gas flowing around the capillary at 0.4 Bar. These charged droplets

were de-solvated via a series of steps of decreasing pressure and then directed to form different products including positive ions. These were pulled in to the anode on the opposite side and moved to a TOF mass analyser. TOF has the potential to control the upper mass limit of ions and then measure their transmission and resolution. The group of ions corresponding to each specific molecule was processed and translated to a molecular weight via data detector systems. Mass measurements were performed in a range of 50-3,000 m/z.

In ESI mode, samples mass gives rise to multiple charged molecular-related ions and labelled either with their charges (i.e. +2, +3) or as:

$$Equation\ 1.1 \qquad m/z = (MW + nH)/n$$

Where:

MW = molecular weight of the sample,

n = No. of charges on the ions,

H = mass of proton (1.008 Da).

2.3.2.2 Fourier Transform Infra-Red (FTIR)

In order to investigate the structural changes in drug-dendron conjugates, FTIR spectroscopy was used. FTIR-spectroscopy is an analytical technique based on electromagnetic-wave absorption due to molecule vibrations. It can provide qualitative and semi-quantitative measurements for solid and liquid samples. It is a powerful tool for identifying different types of chemical groups or bonds in a molecule by producing an infrared absorption spectrum (Doyle, 1992) (Fig.2.13).

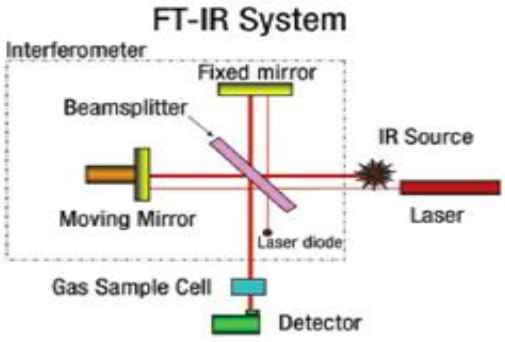

Fig.2.13: Principle of FTIR (picture taken from http://iitk.ac.in).

Before adding the sample, the diamond and sample screw of FTIR (Perkin Elmer Spectrum 65) were cleaned with ethanol. The diamond surface was covered with a few milligrams of the dried sample and scanned in the range 550-4000 cm^{-1} and 32 scans.

2.3.2.3 Thin Layer Chromatography (TLC)

TLC is an analytical chromatographic technique used to separate the components of a mixture or identify the purity of a product using a thin stationary phase supported by an inert backing. TLC is widely used because of its simplicity, relative low cost, high sensitivity and speed of separation. TLC's principle is based on affinity differences of the compound for the mobile and stationary phases, and in turn the speed at which it migrates differs.

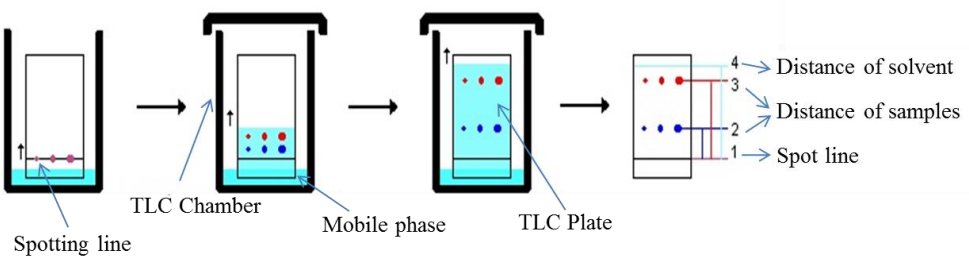

Fig.2.14: TLC principle. It is showing the mobile (solvent) and stationary phase (plate) with spotting line where the sample is added, and example of data results (picture was modified from www.bio-rad.com)

The aim of TLC is to obtain well defined and well separated spots. Each spot has a retention factor (Rf) that can be calculated by the distance migrated by sample over the total distance covered by the solvent (Sherma *et al.*, 2003) (Fig.2.14).

The procedure was performed by dissolving the dried molecules in methanol with a concentration of 1mg/mL, and then filtered with a 0.22 µm filter to avoid clusters. Each sample of 5 µL was added to a silica gel TLC plate (stationary phase) using a thin capillary tube. The plate was placed vertically in a TLC chamber containing 40% $^{v}/_{v}$ deionised water and 60% $^{v}/_{v}$ acetonitrile (mobile phase). The solvent was left to move up the plate and when it reached the top, the plate was removed from the chamber and left to dry. The plate was then visualised with the aid of a UV light chamber (UVP Chromato-vue Cabinet, USA) at 230 nm. The detected spots under UV light which appeared as dark spots were used to calculate the Rf as shown in equation 1.2. The optimal ratio of any spot was considered between 0.2 and 0.8.

$$Equation\ 1.2 \qquad R_f = \frac{Distance\ traveled\ by\ sample}{Distance\ traveled\ by\ solvent}$$

2.3.2.4 High Performance Liquid Chromatography (HPLC)

HPLC is one of the analytical techniques used to determine the purity of peptide. It separates components of any mixture of samples depending on their affinities to the stationary and mobile phases (Pare *et al.*, 1997).

The dissolved sample is injected in a mobile phase consists of either one or more solvents at a specific ratio that is forced under high pressure through a column (stationary phase). The column contains small particles (such as alkyl hydrocarbon (C) and silica) which interact with the mobile phase and retard the flow of different molecules in the sample leading to their separation over time. The corresponding electrical signals of flow of the eluted compounds through a UV detector are detected and sent to a computer data station as a series of peaks separated with different retention times and appears as a chromatogram (Fig.2.15).

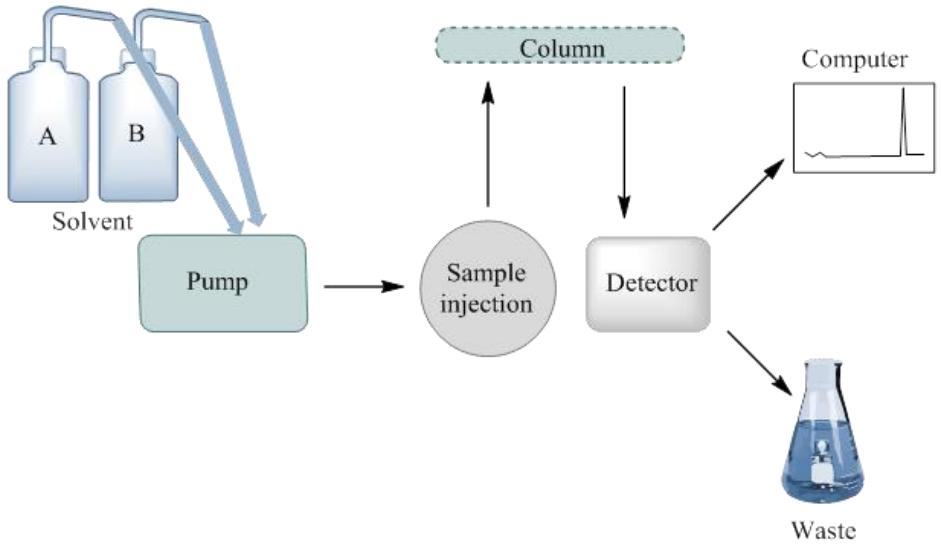

Fig.2.15: HPLC principle. It is showing the parts of the analysis.

For the analysis of FP, G0K-FP and G1K-FP, the dried powder was dissolved in methanol, and then filtered with a 0.22 µm filter to avoid clusters before injection using HPLC, diode array detector, autosampler (Agilent technology/1260 infinity, UK).

The analytical HPLC method was performed using a hydrophobic C18 column (150*4.6 mm (Fortis)) at 25°C, and 20 µL of injection volume. The flow rate used was 0.6 mL/min,

while the UV-detection wavelength was 248 nm (the absorbance wave length of FP) (Meister *et al.*, 2013).

The wave length was also confirmed spectrophotometrically (ParkinElmer lambda 25, UV/VIS) using quartz cuvette and sample solutions of FP, G0K, G1K, G0K-FP and G1K-FP in methanol. Methanol was used as blank background and the range of wave length was 200-400 nm.

The HPLC mobile phase solvents consisted of water/acetonitrile in which the gradient of eluent was run from 75:25 to 25:75 water: acetonitrile over 20 min.

2.4 Results

2.4.1 Characterisation of G0K and G1K and their integration with FP by MS

The results that have been given by mass spectra for G0K and G1K dendrons indicated the successful synthesis of both molecules by giving the exact MW. The main peak (293.2) of intensity $6.3x10^5$ in the mass spectra of G0K (Fig.2.16. a) matches the calculated MW of 293.17 Da.

Similarly, the spectra produced by G1K (Fig.2.16. b) at 549.36 peak with an intensity of $4.5x10^4$ represents its calculated MW of 549.36 Da.

A MS has also been used to analyse the crude drug (FP) which is known to have MW of 244.26 Da. The spectra obtained revealed a peak at 266.73 with an intensity of $0.68x10^5$ representing the sodium salt of the drug resulting from normal ionisation during the process of analysis (Fig.2.16. c).

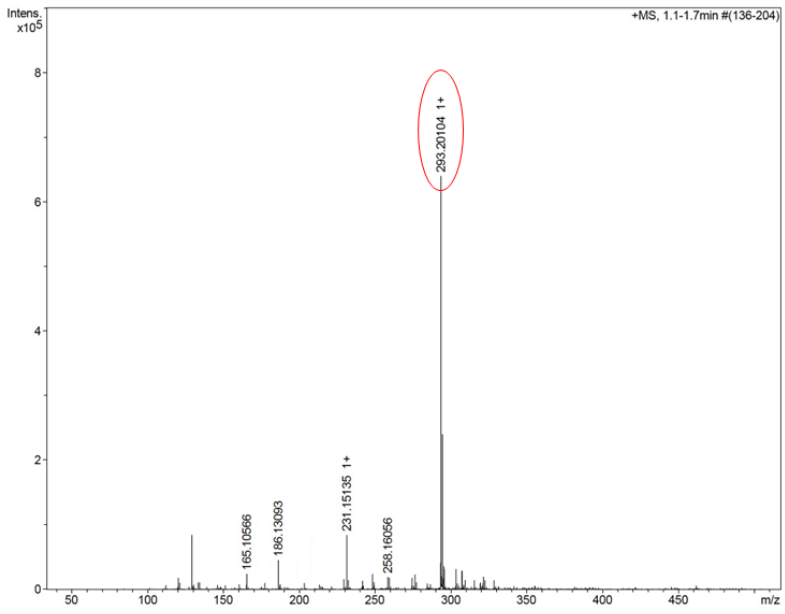

Fig.2.16. a: MS of G0K. it is showing the main peak of 293.2 represents the exact MW of product.

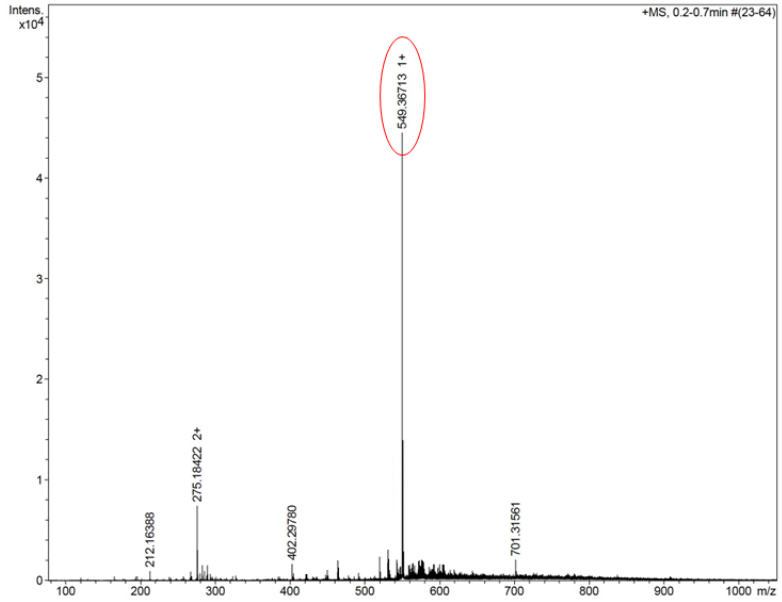

Fig.2.16 b: MS of G1K. It is showing the peak of 549.39 represents the exact MW of product with double-charged ion at 275.18.

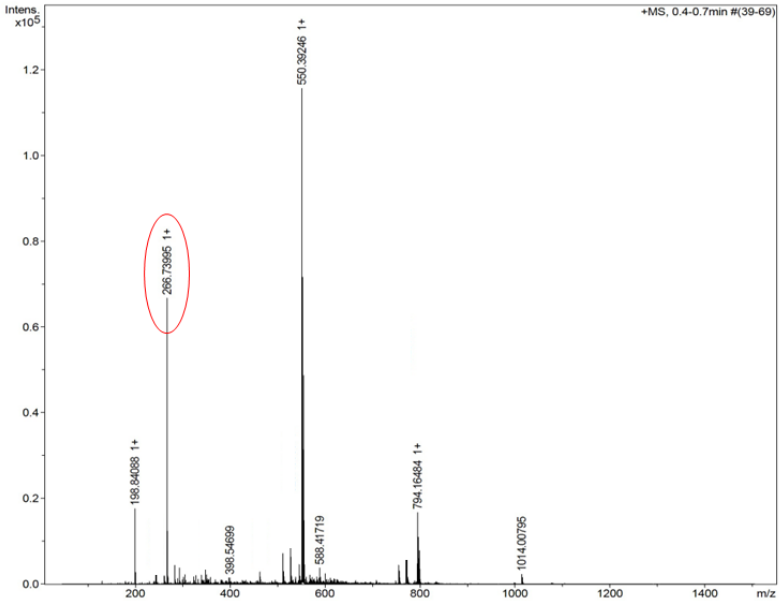

Fig.2.16. c: MS of crude FP. It is showing the peak of 266.7 represents the MW of sodium salt.

Mass spectra have also demonstrated the successful loading of FP to both G0K- and G1K-dendron with peaks corresponding to the expected MW (745.33 Da for G0K-FP and 1454.7 Da for G1K-FP) as demonstrated in Fig.2.17 and 2.18 respectively.

The data from mass spectra of G0K-FP reveals a peak at 745.33 with $0.1x10^4$ intensity, represents the exact MW of product and a second peak at 767.31 represents the sodium salt of product (Fig.2.17).

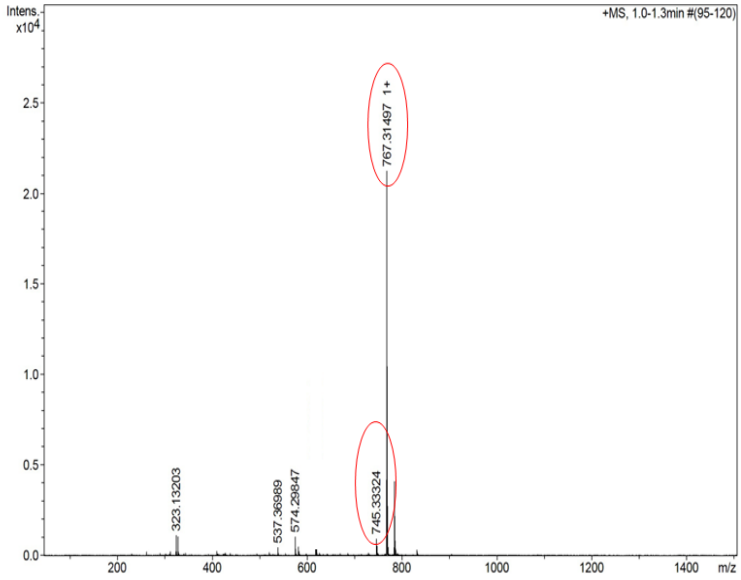

Fig.2.17: MS of G0K-FP. it is showing the peak of 745.33 represents the exact MW of product and the highest intensity peak of 767.31 represents the sodium salt of product yield due to normal ionisation in the system.

Analysis of G1K-FP shows a peak at 1454 with $0.6x10^3$ intensity matches the calculated MW of the product and its sodium salt at 1476 with intensity of $1x10^3$.

The other peaks that appeared in the graphs might be attributed to possible fragments for the indicated sequence and/or system noise or may be due to sodium salt formation resulting normally from ionisation and reaction with glass vessels (MW of Na=22.9 Da in displacement of H of MW=1 Da). However, the mass spectrum clearly shows a main broad peak corresponding to the desired product.

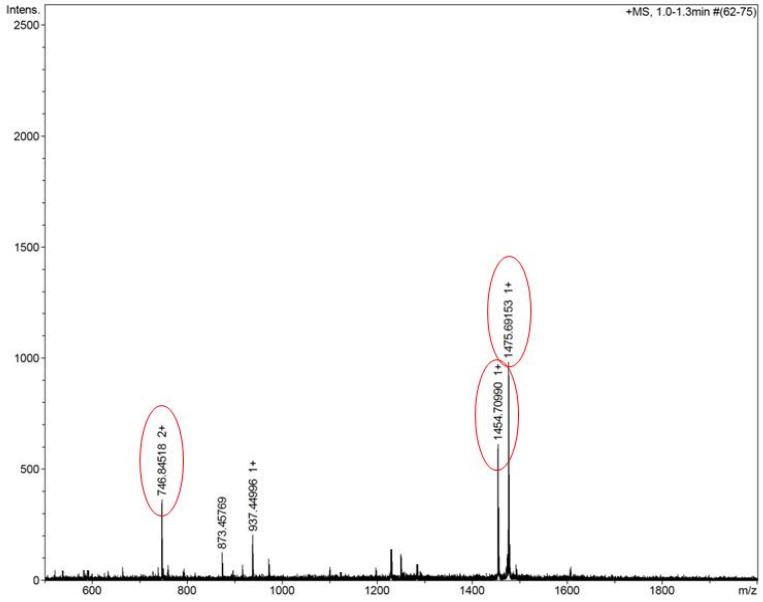

Fig.2.18: MS of G1K-FP. It is showing the peak of 1454.6 representing the exact MW of product and the highest intensity peak of 1475.7 representing the sodium salt of product yield due to normal ionisation in the system, in addition to the double-charged ion appeared in 746.84.

2.4.2 Characterisation of FP-integrated G0K- and G1K-dendrons by FTIR

FTIR analysis has revealed shifting of peaks due to the formation of an amide linkage at 3200 cm^{-1} and 1640 cm^{-1} that also confirm the attachment of drug to both G0K- and G1K-dendrons (Fig.2.19.a, b and c, 20.a, b and c).

The FTIR spectra of G0K-FP (Fig.2.19) showed strong N–H deformation vibration at 1676 cm^{-1} whereas it appeared in very high intensity in G0K as a result of unattached terminal amine groups. Furthermore, a carbonyl band can be seen at 1700 cm^{-1} in FP's spectra, which corresponds to COOH functional group of the drug that is not found in G0K's spectra. In addition to the disappearance of peaks at 1700 and 1676 cm^{-1} and appearance of a new peak at 1640 cm^{-1}, in G0K-FP's spectra, related to the amide linkage formation between drug and dendron. Moreover, the appearance of peak at 782 cm^{-1} corresponding to the aromatic ring of FP with its C=C peak at 910 cm^{-1} in the G0K-FP's spectra confirms the attachment of the drug to the dendron (Fig.2.19.a, b and d).

Results of the FTIR analysis of G1K-FP have given a same indication to that of G0K-FP in which the deformation of N–H peak related to terminal amine groups occurs at 1661 cm^{-1}. Moreover, the absence of a peak at 1700 cm^{-1} of the COOH functional group of the drug and appearance of a new peak at 1650 cm^{-1} in the G1K-FP spectra indicates the formation

an amide linkage resulting from the interaction between the free peripheral amine groups of the dendron and the carboxyl group of FP. In addition, the appearance of a peak at 782 cm^{-1} which is related to the aromatic ring of FP in the conjugated molecule's spectra gives further evidence of the attachment of drug to the dendron. At 910 cm^{-1}, a peak related to the C=C of FP appeared in the spectra of the conjugated molecules and in FP only (Fig.2.20.a, b and d) also confirm the attachment of the drug to the dendron.

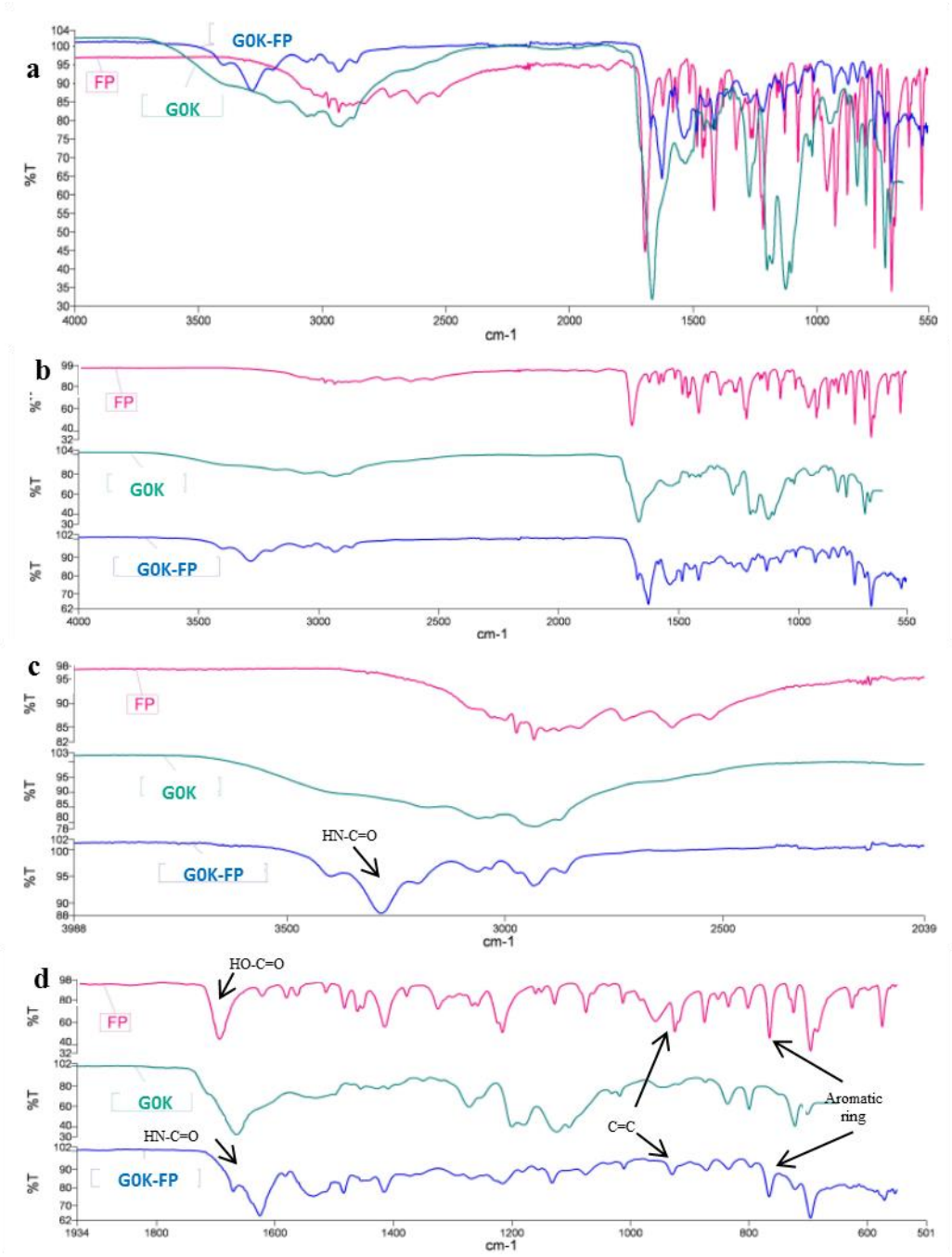

Fig.2.19: FTIR spectrum of free FP and G0K with and without FP. a. overall spectrum (overlay), b. overall spectrum (separated), c: spectrum 2000-4000cm^{-1}, d. spectrum 500-2000cm^{-1}. FTIR analysis is presenting the successful attachment of drug to G0K. Strong N–H deformation vibration representing the terminal amine groups occurs at 1676 cm^{-1}. FP spectra shows a strong carbonyl band that can be seen at 1700 cm^{-1}, which is related to the COOH functional group of FP. Disappearance of peaks at 1700 and 1676 cm^{-1} and appearance of a new peak at 1640 cm^{-1} which is related to the carboxylate ion and amide linkage formation, and appearance of peak at 782 cm^{-1} corresponded to the aromatic ring of FP with its C=C peak at 910 cm^{-1}.

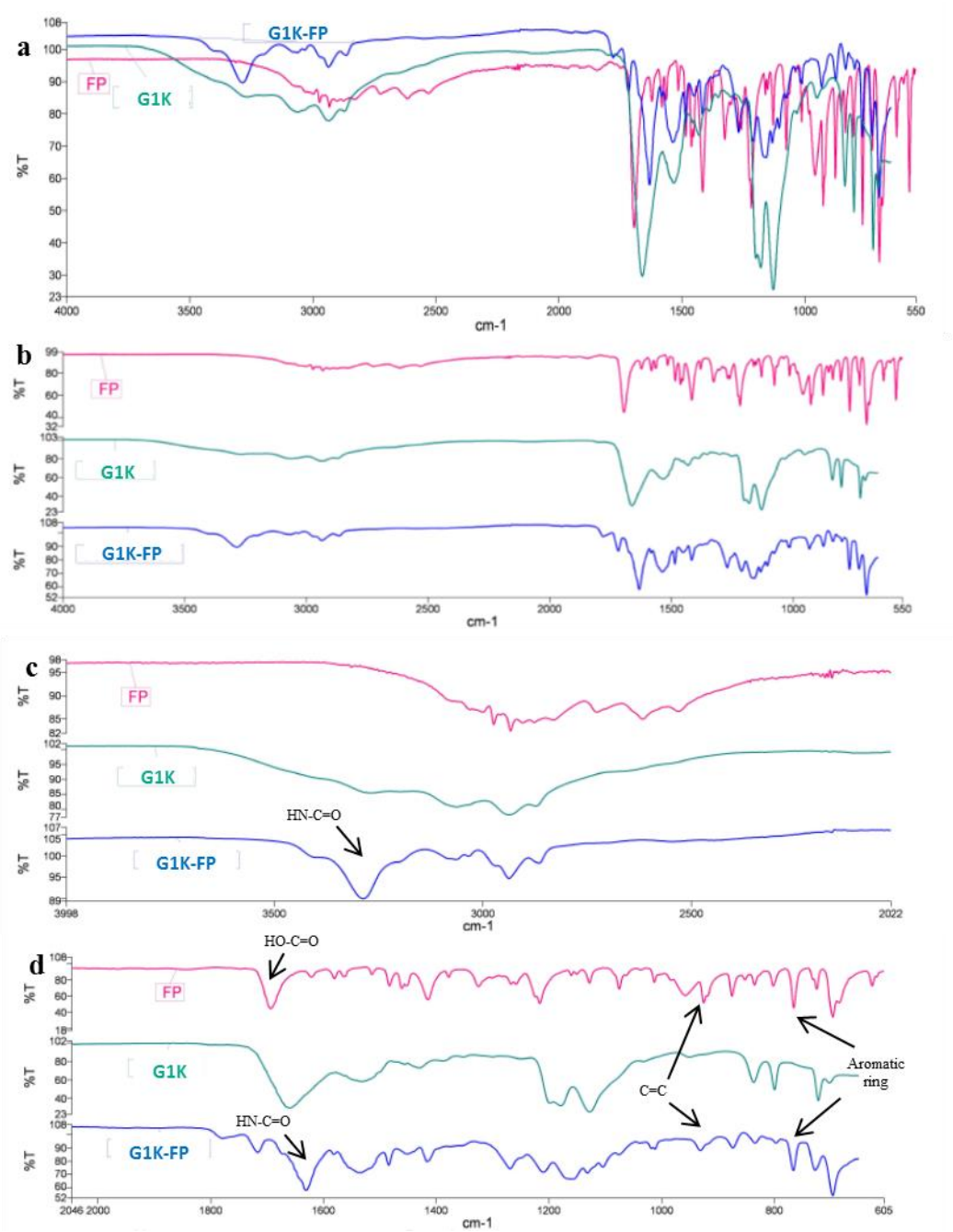

Fig.2.20: FTIR spectrum of free FP and G1K with and without FP. a. overall spectrum (overlay), b. overall spectrum (separated), **c**: spectrum 2000-4000cm^{-1}, d. spectrum 500-2000cm^{-1}. FTIR analysis is presenting the successful attachment of drug to G1K. N–H deformation related to surface amine groups can be seen at 1661 cm^{-1}. The absence of the peaks at 1703 and 1661 cm^{-1} and appearance of a new peak at 1650 cm^{-1} indicate the formation of an amide linkage which results from the interaction between the free terminal amine groups of the dendron and carboxyl group of FP and the appearance of a strong peak at 782 cm^{-1} related to the aromatic ring of FP with its C=C peak at 910 cm^{-1}.

2.4.3 Characterisation of FP-integrated dendrons by TLC and HPLC

The purity of the individual drug and drug-loaded dendrons products was confirmed by TLC. Using this technique, only one spot was observed on each TLC plate under UV light for each product and the Rf values were calculated. The Rf value of free FP was 0.5 (Fig.2.21a), whereas the integrated molecules (G0K-FP and G1K-FP) both gave a similar Rf value of 0.6 (Fig.2.21 b and c respectively), indicating that the products were pure and the G0K and G1K had been successfully synthesised and attached to the drug (Fig.2.21).

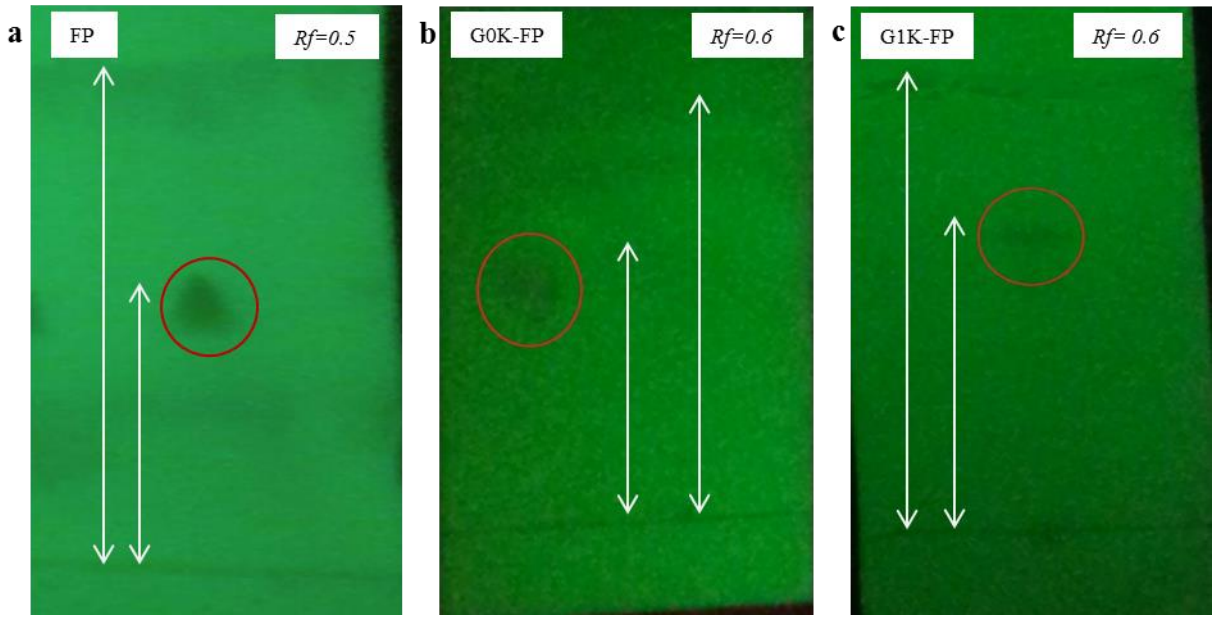

Fig.2.21: TLC characterisation of free drug and drug laden dendrons. a. TLC of free FP with only one spot with Rf = 0.5. b. TLC of G0K-FP one spot appearance with Rf = 0.6. c. TLC of G1K-FP showed only one spot with Rf = 0.6.

In the same regards, the synthesised products including G0K-FP and G1K-FP as well as the solvent (methanol) and the crude drug (FP) were analysed by HPLC to ensure their purities. The analysis was done at wave length absorbance 248 nm according to the results of the spectrophotometry which revealed that the maximum absorbance wave lengths (λ_{max}) of FP-conjugated dendrons are similar to that of free FP (Fig.2.22).

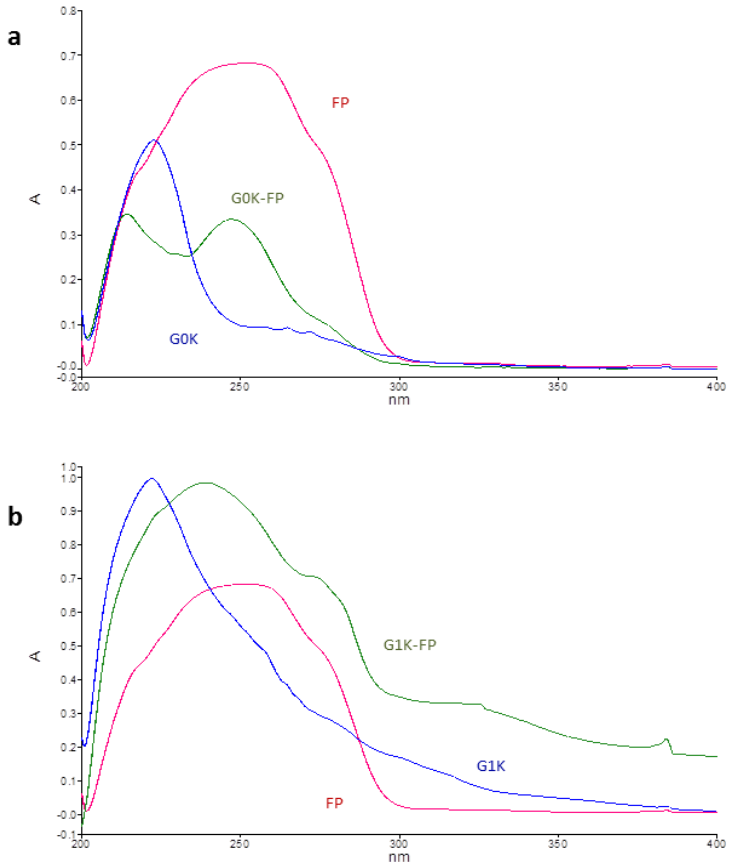

Fig.2.22: Spectrophotometric analysis. It demonstrates the maximum wave length of absorbance (λ) of: a. FP, G0K and G0K-FP and b. FP, G1K and G1K-FP.

Fig. 2.23 demonstrates the elution of FP and both drug-attached dendrons. It can be seen that for the G0K-FP and G1K-FP, only one large peak with retention times of 16.3 and 13.4 min respectively were observed (Fig.2.23. c and d), while FP was eluted at 13.1 min (Fig.2.23. b). Other small peaks are attributed to the solvent as shown in the elution of methanol alone (the background) (Fig.2.23. a). Hence, the absence of impurities in entire HPLC analysis suggested the complete synthesis of product and successful cleavage of linker and resin from peptide.

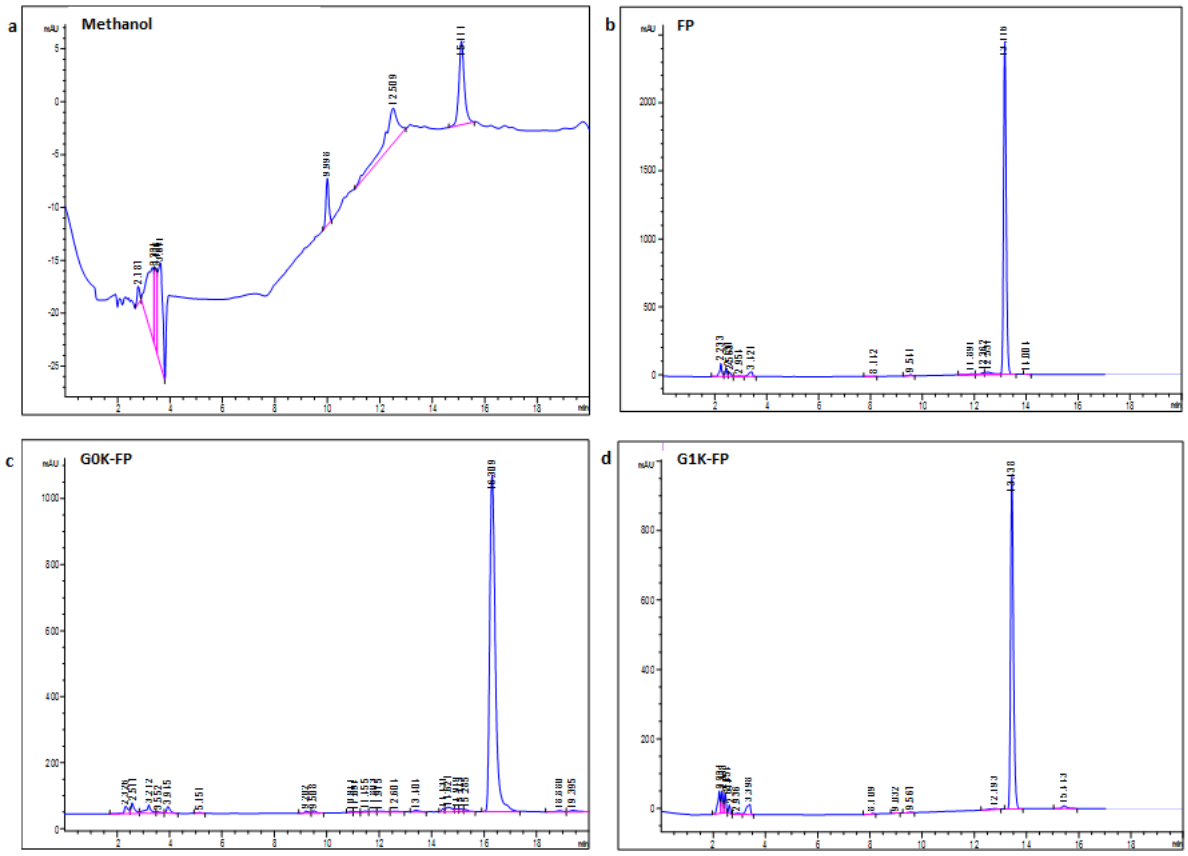

Fig.2.23: HPLC analysis. a. For Methanol only (background), b. For FP in methanol with retention time at 13.17min. c. For G0K-FP in methanol with retention time at 16.3 min and d. For G1K-FP in methanol with retention time at 13.43 min.

2.5 Discussion

In the last few decades, dendrimers and dendrons have been shown to be a promising tool in drug and gene delivery (Gagliardi, 2017). Dendronised polymers are mainly synthesised by either the convergent or divergent assembly strategies each of which have their own synthetic advantages and limitations (Carlmark, 2009). A steric crowding effect that occurs during synthesis of dendrimers when using convergent methods is the main limitation, so it tends to be used only for developing high generation products (Tomalia, 1991). However, the divergent method on which this work is based is successfully employed in the production of dendronised molecules (Carlmark, 2009; Tomalia, 1991). In contrast to the convergent, this strategy is implemented stepwise from a functionalised central core outwards. The main advantage of this strategy is the possibility of performing the repeating steps automatically and achieving unique attainable high-molecular structures, this is supported by the method is also being straightforward and controllable (Bracci *et al.*, 2003; Calderon *et al.*, 2013).

To address some problems associated with peptide synthesis such as low product yield and impurities, SPPS was applied and used. After SPPS discovery, it has become the standard strategy for peptide synthesis (Merrifield, 1965). However, there are some limitations associated with this technique such as intermolecular aggregation, truncated sequence, steric hindrance and time-consuming steps (Shin *et al.*, 2005). Microwave-based synthesis has been introduced to improve this process, and consequently become widely accepted in performing chemical reactions with higher efficiency (Merrifield, 1965; Rodriguez, 2010).

Therefore, in this work, SPPS on Tenta Gel-NH_2 resin by an adapted microwave method with a typical Fmoc chemistry was used to synthesise the branched dendrons (G0K and G1K) with and without FP (Fig.2.5). This combined method provided a high degree of accuracy, purity and reproducibility as confirmed by general outcomes of this study. The use of the microwave peptide synthesiser reduced reaction times to 5 min per coupling step and 2 min for deprotection step (as listed in Table 2.1). In addition, it enhanced coupling rates preventing the formation of truncated and deleted peptide sequences as observed in previous studies (Perugini, 2013; Rodriguez, 2010).

Successful peptide synthesis relies on multiple issues which need consideration including the type of α-amino protecting group, and side-chain protection of amino acids, class of

solid support and linker, the choice of coupling reagents and the cleavage mixture. There are two main forms of α-amino protecting group in SPPS; Fmoc (9-fluorenylmethyloxycarbonyl) and *t*-Boc (tert-butyloxycarbonyl) which require specific chemical conditions to be removed. Fmoc form of amino acids and linker were used in the synthesis of G0K and G1K (Table 2.2) for its advantages over the *t*-Boc one. Permanent and side-chain protectors of Fmoc amino acids ensure the reaction in the site of interest only to form the amide linkage. Thus, preventing secondary reactions, like the formation or incorporation of dipeptide derivatives (Fields *et al.*, 2014; White *et al.*, 2000). Fmoc is also preferred over *t*-Boc, as it can be easily removed under mild conditions, specifically *1piperidine:4DMF* solution. DMF is the most widely used solvent for both coupling and deprotection in SPPS; as it can be heated by microwaves (Made, 2014; White *et al.*, 2000). While the *t*-Boc strategy requires TFA for repetitive removal of the Boc groups, and often it uses hydrofluoric acid (HF) for release of the assembled peptide from the solid support (Made, 2014; White *et al.*, 2000). Thus this method normally requires the use of corrosive and toxic HF and requires special equipment (Fig.2.24).

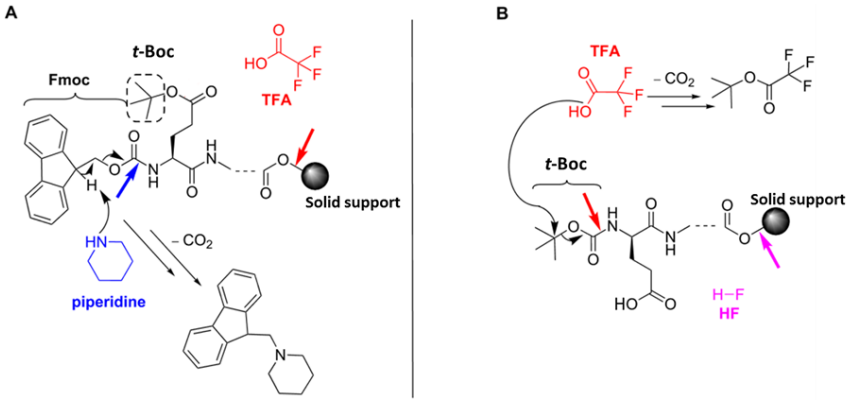

Fig.2.24: Removal of protecting group in SPPS. (A) The Fmoc protecting group is removed by using piperidine and then cleaved by TFA. (B) *t*-Boc protecting group is released by treating with TFA and cleaved with excess TFA and HF (picture was modified from Made, 2014).

The solid resin (TentaGel) that has been used in this synthesis, is a PEG hybrid polystyrene resin; it is an insoluble and inert support which swells easily in DMF. While the Rink amide linker was used as a support for the solid phase, and to decrease the degradation by linking to the amino group of the resin (Albericio, 2000), in turn it facilitates amino acids coupling. Prior to any coupling process, the amino acid was mixed with 0.4 mmol HBTU and 140 µL DIPEA. Aminium or phosphonium salts, such as

HBTU, are the methods of choice to achieve the coupling of the carboxylic acid moiety of the amino acid with the α-amino group of the growing peptide; whereas DIPEA is used to deprotonate the acid group of the Fmoc amino acids (Ye *et al.*, 1999). Consequently, using both DIPEA and HBTU in this synthesis helped reduce coupling time and epimerisation.

The cleavage process and choosing a suitable cleavage mixture is a critical step in peptide synthesis which leads to the removal of the resin and the side chains protecting groups (Albericio, 2000). In this study, concentrated TFA 95% was used as a typical reagent in the cleavage mixture in addition to TIPS and water; these act as scavengers to cut off the reactive carbocations formed during the reaction, avoiding any undesired reaction with amino acids (White *et al.*, 2000).

The analysis of synthesised peptides using MS, FTIR, TLC and HPLC was performed in order to confirm the successful production of the desired molecules and to assess their purity. The outcomes generated from MS (Fig.2.16. a and b) indicate that the protocol used was efficient and the dendronised carrier systems (G0K and G1K) were successfully synthesised. The results match previous studies in which G3K-dendrimers were efficiently produced using this method (Issa *et al.*, 2015; Meikle *et al.*, 2011). Therefore a wide range of dendronised polymers can be designed and created with the optimum chemical, physical and biological properties to be used in various clinical applications for future work.

These synthesised dendrons were successfully grafted onto FP by coupling reactions. The chemical structure of FP (Fig.1.4) which includes a carboxyl group allows it to interact with the amine group at the terminal branches of dendrons to form an amide linkage and produce the conjugated molecules (G0K-FP and G1K-FP) as confirmed by MS (Fig.2.17 and 2.18). Moreover, the comparison of the FTIR spectra of G0K-FP and G1K-FP with that of free FP and dendrons (Fig.2.19 and 2.20) also confirms the attachment of FP. Changes in certain peaks relating to the active groups such as the carboxylate and amine, and the amide linkage formation from the interaction between the amine groups of dendrons and the carboxyl group of FP, and the appearance of the aromatic ring and C=C group of FP in the integrated spectra, indicate the successful attachment of the drug to the dendrons. These findings are further supported by the ability of dendrimers that successfully attached to ibuprofen, a NSAID that is structurally related to FP, to enhance its cellular entry (Kolhe *et al.*, 2003). FP has been shown previously to form complexes with other carrier systems such as PEG-PLA micelles (Mu *et al.*, 2013) and NP (Meister *et*

al., 2013), but not via amide linkage coupling. This linkage is considered as a key in the drug release as it is hydrolysed by proteolytic enzymes (Xu *et al.*, 2014).

Using the efficient purification method and Fmoc chemistry can help in the final purification of the product with the removal of undesired products (Made, 2014). The results of TLC and HPLC confirmed the purity of the integrated products (G0K-FP and G1K-FP) (Fig.2.21 and 2.23) which indicate there are no impurities that could have implications for the cytotoxicity or the permeability of the products to be investigated in later chapters.

The low solubility of FP was the main drawback in this work because it increased the time required to solubilise the synthetic peptide, this was overcome by a using magnetic stirrer and sonication during the synthesis with evidence of its success as shown in the MS and FTIR results.

In the last few decades, modification of the dendrimers surface has become an increasingly interesting strategy to improve their properties including multi-functionality, biocompatibility and biodegradability (Song *et al.*, 2011). However, functionalisation of dendrons was a big problem, due to inappropriate modification of the last branching, in addition to the incompatible chemistries that have been used with the monomers of the dendrons (Carlmark, 2009). Recently, these dendrons have been efficiently functionalised; firstly at the core with specific amino acid such as phenylalanine, and secondly at the uppermost active amino group for attaching multiple bio-active molecules including drug and/ or ligands (Chapter 4). In this regard, dendrons were designed to interact with components at their root, and to expose a higher number of bio-active motifs, such as drug which arranged at suitable positions for recognizing target molecules. The lysine of G0 dendron has 2 terminal amino groups that allowed the attachment of 2 drug molecules while G1 offers 4 attachments. Hence, the possibility of loading 2 molecules of FP in G0K and 4 in G1K was verified, (Fig.2.10 and 2.11) and was confirmed by the MS results (Fig 2.17 and 2.18). Therefore, these functionalities of dendrons provide a platform for conjugation of high payload of the drug and to be used effectively as carrier systems for drug delivering in turn increasing its bioavailability at the target and retaining its pharmacological action in AD (Chapter 5).

From these results it can be concluded that the dendronised carrier system integrated via amide linkage with FP can be synthesised using Fmoc-SPPS optimised methods, a finding that has not yet been reported in literature. Furthermore the purity of these products is sufficient for further biological studies.

2.6 Conclusion

The use of dendronised polymers in clinical applications is mainly based on the precise control of their assembly, functionalisation and biocompatibility. Microwave Fmoc-based SPPS is a potential and fully automated device that allows for the synthesis of a range of peptides with reproducibility and minimisation of the time required. In the present work, a novel dendronised carrier system for delivery of FP has successfully been synthesised using microwave Fmoc-based SPPS. In addition, the possibility of coupling a large amount of FP which is proposed to improve its bioavailability was shown for the first time. The amine-terminated G0K- and G1K-dendrons could predominantly form a complex with the carboxylate ion from the FP via amide linkage, as shown by MS and FTIR spectroscopy.

Drug loaded dendrons at both generation G0 and G1 have been efficiently designed and characterised. Those molecules were taken forward in this study to examine their cytotoxicity *in vitro* (Chapter 3) to ensure their biocompatibility prior to further studies on the functionalisation with AEP ligand (Chapter 4) and the ability to penetrate a model of the BBB (Chapter 5)

Chapter 3. Examination of the Cytotoxicity of the FP-Integrated molecules

3.1 Introduction:

The use of synthetic biological agents in clinics relies on a robust assessment of their biocompatibility and cytotoxicity. The term toxicity is widely used in the pharmaceutical industry. It refers to the measurement of non-specific, unwanted and harmful effect of a drug towards cells, organs or indeed the patient as a multi-organ system (Ruth *et al.*, 2005). Over recent decades, the field of biomedical materials has seen an extensive development of novel biomaterials for drug delivery applications, and the term "biocompatibility" is commonly adopted by convention to describe their biological characteristics. This term was firstly described at European Society for Biomaterials in 1986 (Williams, 2008), and later the definition was updated as "the ability of a biomaterial to perform its desired function with respect to a medical therapy, without eliciting any undesirable local or systemic effects in the recipient or beneficiary of that therapy, but generating the most appropriate beneficial cellular or tissue response in that specific situation, and optimising the clinically relevant performance of that therapy" (Williams, 2008). This definition stresses the need to consider the suitability of a material in respect to both its potential effect in the body (toxicity), and the beneficial effect of the physiological surrounded environment on the performance of the material (Ruth *et al.*, 2005). Therefore the toxicity of the dendrons and the FP-loaded dendrons must be defined if they are to be used in drug delivery.

Dendrimers have been considered as 'smart' carriers owing to their ability to act as intra-cellular drug carriers, to cross biological barriers, to target specific organs or body parts and to circulate in the body for long enough to exert the required effect (Prashant, 2014). In addition, their biocompatible and biodegradable properties have been demonstrated to make them successful vehicles and biomaterials (Tomalia *et al.*, 2005). As reported earlier, a number of factors have potential impact on the biocompatibility of dendrimers such as their size, chemistry and surface property. It has previously been found that the cytotoxicity of dendrimers is increasing with concentration, generation and surface charge (Yang *et al.*, 2007). Some toxicity has been found in high generation dendrimers and attributed to high density amino branches which destabilise cell membranes leading to cell lysis (Srinivas *et al.*, 2014). For instance, IC_{50} measurements (the concentration that

induces 50% cell lysis) and cell viability for PAMAM have shown low cytotoxicity with low concentrations and generations less than 4. The study also found no cytotoxic induction upon incubation of Caco-2 cell line with G0 and G1 up to concentrations 10 mM (El-Sayed *et al.*, 2002). In earlier studies, dendrimer biocompatibility has been achieved by employing a biodegradable core subunit and branching entities or utilising intermediates of various metabolic pathways during its assembly (Heather *et al.*, 2011). The use of lysine monomer in the dendron construction facilitates the biodegradation as it can be easily metabolised in the body, making it one of the most biocompatible units (Boyd *et al.*, 2006).

On the other hand, FP has shown to have a cytotoxic concentration range of 0.5 to 2.0 mM, when quantitatively assessed by the LDH release after 20 hr incubation with hepatocytes. Moreover, hepatotoxicity has been rarely recorded with FP, and appears to be mostly related to hypersensitivity (Jurima *et al.*, 1994). Reports documented that the concentration of FP required to inhibit the secretase activity in the treatment of AD is 150-250 µM (Meister *et al.*, 2013). Hence, a range of concentration 25-400 µM was examined in this work.

To study the biocompatibility, there are three broad categories of experiments are available: *in vivo*, *in silico* and *in vitro* studies, each category has advantages and limitations. This study concentrates on *in vitro* analysis of cytotoxicity of the new molecules towards cells represent the BBB.

In vitro studies have many advantages over other types of studies. Living organisms are highly sophisticated functional systems composed of millions of essential materials such as protein, genes, small organic and inorganic molecules and other complexes in an environment that is organised by specific membranes (Alberts, 2007). Therefore, the identification of interactions between its components and the demonstration of their basic biological functions becomes a great barrier due to this complexity. The main advantage of *in vitro* work is that it simplifies the system under study, so that the research can be focused on a small number of components (Price *et al.*, 2009; Vignais *et al.*, 2010).

Another advantage of the *in vitro* methods is that human cells can be used directly. In addition, no translation from animal to human is needed so that exclude any problem related to cross-species transpositions due to species-specific cellular responses, in turn

this method can also offer replacement of unethical human trials (Quignot *et al.*, 2014). Moreover, *in vitro* testing is quite beneficial in the characterisation of some specific adsorption, distribution, metabolism and excretion (ADME) processes taking place inside the living organism (Price *et al.*, 2009). Furthermore, it is considered fast (particularly in screening), relatively inexpensive, mostly predictive of a real hazard or risk (e.g., DNA damage) and high throughput screening (Quignot *et al.*, 2014). On the other hand, the primary disadvantage of this experimental study is the challenging to extrapolate from its results back to the normal biology of the intact organism (Rothman, 2002).

3.1.1 Cell culture and Cell line

An important issue of any biotechnological work is the culture of animal cells in artificial media. The animal cell and tissue cultures are being extensively used in different areas of research such as production of vaccines, monoclonal antibodies, pharmaceutical drugs, cancer research and genetic manipulations (Alberts, 2007; Maqsood *et al.*, 2013). Two types of cell cultures are being used mainly; the primary cell culture which is derived directly from normal animal tissue, and the cell line (immortalised) which is a sub-culture of primary cell. Many studies have used the immortalised cell line as it is easily derived from a complex organism which has evaded normal cellular senescence due to mutation and can keep undergoing division. These cells can therefore be grown for prolonged periods *in vitro*, while the preparation of primary cultures is labour intensive, expensive and their growth can be maintained *in vitro* for a limited time (Maqsood *et al.*, 2013; Steinert *et al.*, 2000).

To study the cytotoxicity of G0K, G1K, G0K-FP and G1K-FP *in vitro*, immortalised brain endothelial cell line (bEnd.3) has been used. The bEnd.3 is an immortalised mouse brain endothelial cell line originally generated in 1990 (Montesano *et al.*, 1990) and it is commercially available. These cells are reported to be excellent for studies as a model of the BBB representing a stable and fully characterised cell line that maintains most of structural and biochemical properties of the human brain endothelium (Omidi *et al.*, 2003; Weksler *et al.*, 2005). Unlike cell lines obtained from human brain endothelial cells which have short life span, the mouse bEnd.3 cell lines have prolonged life span and easy to immortalise (Naik *et al.*, 2012). It has been demonstrated that TJ proteins including occludin, claudine, actin and ZO are highly expressed in the bEnd.3 cell line that producing an integral cell layer when compared to other available BBB models such as

bEnd clone and bEnd.5. In addition, bEnd.3-based BBB model has been found to give a continuous monolayer with high electrical resistance than that found in bEnd clone and bEnd.5 BBB models (Brown *et al.*, 2007; He *et al.*, 2010).

3.2 Aim of the chapter

Before using these synthesised products in BBB permeability tests, it is necessary to demonstrate that they are nontoxic. The aim of this chapter is; therefore to:

1. Determine the cytotoxic profiles of FP, G0K, G1K, G0K-FP and G1K-FP *in vitro*, using bEnd.3 as a BBB model with different assays including cell metabolic activity, lactate dehydrogenase release and cell death assessment.
2. To assess the cytotoxicity of FP, G0K, G1K, G0K-FP and G1K-FP using human umbilical vein endothelial cells (HUVECs) to ensure their non-cytotoxicity on other tissues rather than brain cells.

3.3 Materials and Experimental methods

3.3.1 Preparation of bEnd.3 cells

The bEnd.3 cells (ATCC- Manassas, USA) were cultured, according to the ATCC-product sheet, in Dulbecco's Modified Eagle's Medium (DMEM) (ATCC) high glucose medium with L-pyruvate. This media contains 10% $^{v}/_{v}$ foetal bovine serum (FBS) (heat inactivated. PAA Laboratories Ltd., UK) and 5 mL of 500 U/mL penicillin/streptomycin antibiotics (P/S) (Gibco, Germany) was added to be 1% of the final volume.

Cells were seeded at a density of $5x10^4$ cells per cm^2 in T-25 and T-75 tissue culture flasks then put in an air atmosphere incubator at 37˚C and 5% CO_2. The flasks were checked every day using light microscopy and the culture media was changed every 3 days. Experiments were performed when cells reached a confluency of 75%. The numbers of passages of bEnd.3 that have been used in all experiments were less than 20.

3.3.2 Passaging and Sub-culturing of cells

Cells were passaged once a week. All required liquids were removed from the fridge and warmed in a water bath (37˚C). Routine passaging was performed by washing culture flasks with buffer solution and treating with trypsin/EDTA solution and then incubating at 37˚C for 5 min until the cells detached from the flask as assessed by light microscopy. Trypsin was neutralised using twice its volume with FBS-containing media. Trypsinised cells were then transferred into a 30 mL universal tube and centrifuged at 500 rpm for 5 min. The supernatant was aspirated and the cells resuspended in 1 mL fresh culture media. A haemocytometer was used to count the cells for each well. A volume of counted cells was added to new T-75 tissue culture flasks containing fresh media. All works have been done in sterilised conditions under hood.

3.3.3 Counting of bEnd.3 cells

After resuspending the pellet in 1 mL culture media, only 10 µL was taken and diluted with fresh media in a small tube. A haemocytometer was cleaned gently with alcohol and allowed to dry, a coverslip was then pushed onto haemocytometer slide and 10 µl from diluted cell suspension was applied to the edge of the coverslip. The cells were counted under inverted phase-contrast microscope and the average was taken and multiplied by the dilution factor to calculate the number of cells.

3.3.4 Freezing and Storage cell stocks

Cells were cryopreserved in a freezing solution containing the cryoprotectant dimethyl sulfoxide (DMSO) (Sigma-Aldrich). This freezing solution was prepared by mixing 95% $^{v}/_{v}$ complete culture medium and 5% $^{v}/_{v}$ DMSO (according to the ATCC-product sheet). Aliquots of cells were suspended in a freezing solution in sterile cryovials. Cells were frozen slowly up to -70˚C and then transferred to liquid nitrogen for long term storage.

3.3.5 Thawing cells from cold storage

Frozen cells were thawed according to the ATCC-product sheet, by gentle agitation in a water bath at 37˚C until the contents are thawed and then the contents were transferred to a centrifuge tube containing complete culture medium to be spun at 125 x g for 5 min. The cell pellet was then re-suspended with the recommended complete culture media and transferred to a T-25 polystyrene flask containing culture media.

3.3.6 Preparation and Culturing of HUVECs

The synthesised molecules were further tested on human umbilical vein endothelial cells (HUVECs) (ATCC-UK) and were used from passages 35 to 39. HUVECs were routinely cultured in endothelial basal medium (F-12K) containing 0.05 mg/mL of endothelial cell growth supplement (ECGS), 0.1 mg/mL of heparin and adjusted to a final concentration of 10% $^{v}/_{v}$ of FBS according to the manufacturer's recommendations.

3.3.7 Treatment protocols for assays

Before each experiment, cells were cultured into 6- or 24-well plates, depending on the demand of the proposed experiment and multi-well plates of 96-well were used for cytotoxicity experiments according to each protocol.

The toxic effects of FP, G0K, G1K, G0K-FP and G1K-FP on brain endothelial cells were investigated in a series of experiments. Samples were made by preparing stock solutions containing concentration of 1 mg of each molecule dissolved in 1 mL culture media then filtered by micro unit filter of 0.22 µm pore size. All dilutions were prepared under aseptic conditions to ensure sterility.

The cells were cultured in well plates at a density of $5x10^4$ cells per cm^2 and after reaching confluence, were treated with 25, 50, 100, 200, 300 and 400 µM concentrations of each FP, G0K, G1K, G0K-FP and G1K-FP. Cell metabolic activity using MTT was measured at

24 and 48 hr time points. Cytotoxicity was assessed by detection of LDH release after 24 and 48 hr. HPI test was performed to evaluate the occurrence of apoptotic and necrotic cells after treatment.

3.3.8 Cytotoxic examination of dendrons and FP-integrated dendrons

3.3.8.1 MTT assessment of cell metabolic activity

The 3-(4,5-dimethylthiazol-2-yl)-2,5-diphenyltetrozolium bromide (MTT) assay is used to measure cell metabolic activity. This assay depends on mitochondrial reductase enzymes which are present in viable (healthy) cells, to reduce a tetrozolium salt. MTT is a yellow-coloured compound converts to a purple formazan product via reduction reaction (Mosmann, 1983). This reaction is accomplished by specific co-factors to the dehydrogenase enzymes in metabolically active cells, including nicotinamide adenine dinucleotide phosphate (NADP) or NAD hydrogenase (NADH) (Berridge *et al.*, 1993). Solubilisation of cells in an organic solvent releases the purple colour of the formazan reagent (Fig.3.1), the intensity of which is measured spectrophotometrically, and is directly proportional to the number of living cells.

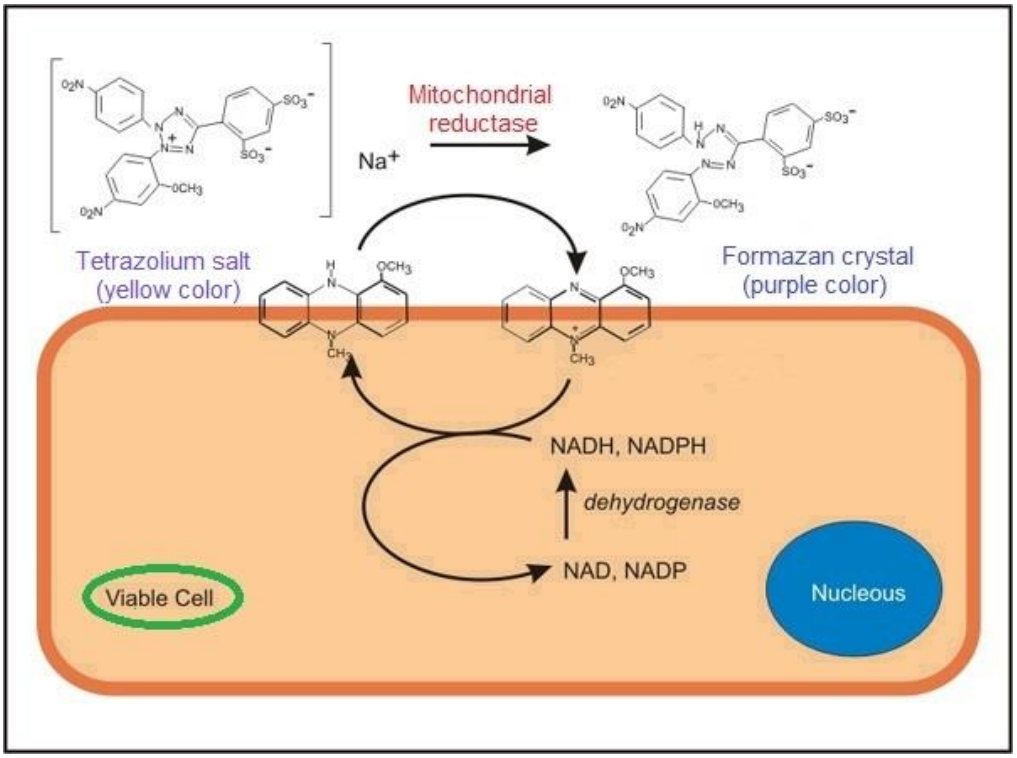

Fig.3.1: MTT principle. It is showing the formation of formazan salt (purple colour) from a yellow colour tetrazolium salt with reduction of NADH or NADPH in mitochondria (picture was modified from www.biotek.com).

MTT solution (98% Sigma-Aldrich) was prepared at a 0.2 mg/mL concentration in supplemented culture medium (DMEM) without FBS, and sterilised using a 0.2 µm filter prior to use, and then incubated in water bath at 37˚C for 10 min. Due to sensitivity to light, all work was undertaken in the dark.

After 24 and 48 hr treatment exposure, the supernatant was removed and the MTT solution was added to the cells. At least 4 wells were not exposed to any treatment, to be used as control. Each well was treated with 500 µL of the warm MTT/DMEM solution, then incubated for 1 hr in a 37˚C and 5% CO_2 incubator. MTT/DMEM solution was then removed from each well and treated with 125 µL of DMSO, with gentle agitation to dissolve the formazan crystals and a purple colour was observed. From the contents of each well, 50 µL was transferred into new 96-well plate in duplicate. The absorbance was measured at wavelength 540 nm in a spectrophotometer (Thermo Multiskan Ascent 354). MTT absorption readings were expressed as percentage of the control (untreated cells) on each plate, and converted into cell metabolic activity percentages using the following equation:

Equation 3.1: Percentage of cell metabolic activity from MTT absorption.

$$Cell\ viabilty\ \% = \left(\frac{S - B}{C - B}\right) \times 100\%$$

Where:

S = Sample absorbance (treated cells).

C = Control = average non-treated healthy population absorbance value.

B = Blank = average cell free blank absorbance.

Lower measurements than 50% were considered to be indicative of cytotoxicity (through loss of cell metabolic activity). This represents the half maximal inhibitory concentration (IC_{50}) accepted to show a drug or other materials ability to inhibit cellular biological function (Mosmann, 1983).

3.3.8.2 LDH assay evaluation of cytotoxicity

The Lactate dehydrogenase (LDH) assay is based on the work of Ulmer and co-workers (Ulmer *et al.*, 1956). LDH is a cytosolic enzyme, present in various cell species; it is responsible for the conversion of lactate to pyruvate with simultaneous reduction of NAD^+ to NADH. LDH is a stable intracellular enzyme and can only be measured when it is

released following cell lysis, thus will indicate the loss of the cell membrane integrity (Yang *et al.*, 2009). Integrity of cell membrane is crucial to cell survival and interaction with the surrounding environment (Allcock, 2011). The leakage of LDH into the supernatant is measured in conjunction with a coupled enzymatic assay that results in the conversion of a colourless iodonitrotetrazolium salt into an orange formazan product (Nachlas *et al.*, 1960) (Fig.3.2).

The intensity of colour resulted from this reaction can be measured using a spectrophotometer, and is directly proportional to the number of lysed cells. The LDH release in culture supernatants is assayed using the Promega CytoTox96® Non-Radioactive Cytotoxicity Assay Kit, UK.

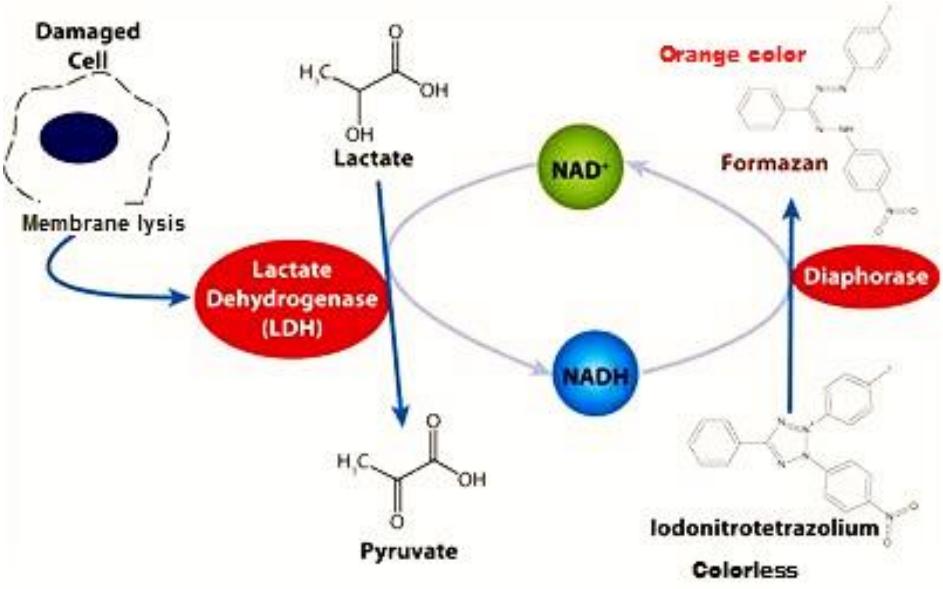

Fig.3.2: Principle of LDH assay. It is showing the formation of formazan from a colourless iodonitrotetrazolium associated with the conversion of lactate to pyruvate (picture was modified from www.test.Gbiosciences.com).

The bEnd.3 cells were cultured in 24-well plates, and treated with synthesised molecules after reaching confluence. Lysis solution (1% $^{v}/_{v}$ Triton™x100 supplied with the kit) was added to the sample to initiate complete lysis to provide a positive control and determine 100% LDH release. In each experiment at least four wells were left untreated as negative controls and determine their absorbance of normal LDH release. The experiment was carried out by the addition of lysis solution to the control sample 45 min prior to the assaying of other wells and cells were maintained in an incubator at 37˚C and 5% CO_2. A

blank sample of media only (without cells) was also incubated to be used as control against all background absorbance.

Supernatant (50 µL) was taken in duplicate and transferred to a new 96-well plate. LDH substrate mixture was prepared following the manufacturer's instructions. This was then added to equal volumes of cell supernatant from the respective sample of cells previously treated 24 and 48 hr as detailed in Section 3.3.7. The reaction was conducted at room temperature and in the dark. After 30-minutes incubation, the reaction was stopped by adding solution of an equal volume (50 µl) of 1M acetic acid (supplied with the kit). Absorbance was read using a spectrophotometer (Thermo Multiskan Ascent 354) at 490 nm. The readings were converted to a measurement of cytotoxicity as a percentage of the LDH released from the treated cells in relation to the complete lysis (positive control), using the following equation.

Equation 3.2 . Calculation of percent of cytotoxcity from LDH release.

$$\%\ cytotoxicity\ from\ LDH\ release = \left(\frac{(S-B)-(C-B)}{(L-B)-(C-B)}\right) \times 100\%$$

Where:

S = Sample absorbance.

B = Average cell free blank absorbance.

C = Average negative control, or non-treated healthy population absorbance value

L = Average positive control, or complete lysed cell population absorbance value.

Values higher than 50% of the positive control were considered to be indicative of a toxic response. This represents the median lethal dose (LD_{50}), which can be used as a measure of acute toxicity that relates to the dose or concentration (LC_{50}) required to kill half the cells of tested population over a given treatment period (Zbinden *et al.*, 1981).

3.3.8.3 Cell death assessment

Hoechst 33342 and propidium iodide (PI) salt (HPI) are intracellular organelle specific dyes. The test can be used for monitoring biological processes in living cells and thus they are useful in assessment of cell death. The dyes are cell permeable, and immediately stain cells when added to culture medium of the cell (Wallen *et al.*, 1983) in which the Hoechst 33342 binds to DNA so it is staining the nuclei whereas PI stains the cytoplasm, resulting in emission of light observed under a fluorescent microscopy. These reactions will give

distinct cell morphologies depending on the state of the cell (Majno *et al.*, 1995; Wallen *et al.*, 1983). Live cells appear blue with intact membranes on microscopic examination, and those at early and late apoptotic phase appear bright blue with shrinkage. On the other hand, necrotic or damaged cells appear red with ruptured membranes (Majno *et al.*, 1995) (Fig.3.3).

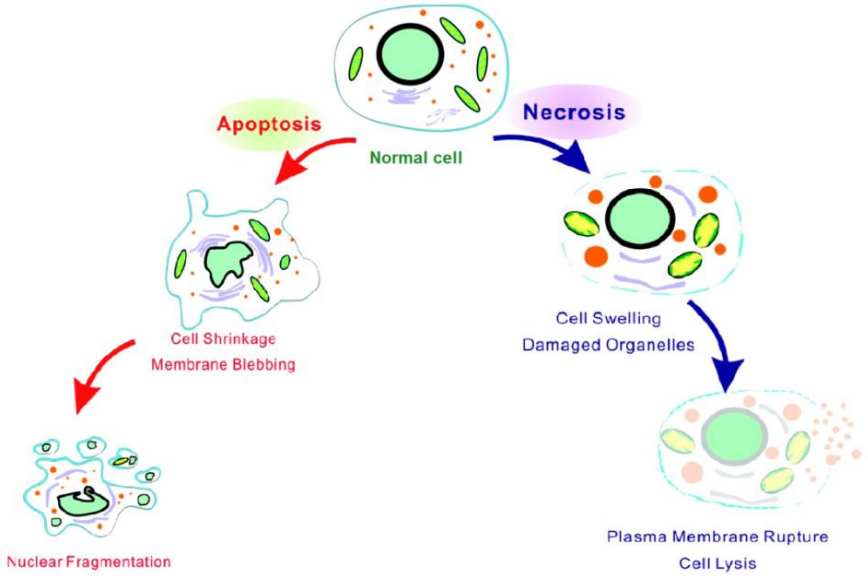

Fig.3.3: Cell death process. It is showing different steps of the apoptosis and necrosis of normal cell (picture was modified from www.pubs.rsc.org).

HPI dye was prepared by adding 900 µL of DMEM to a mixture solution of 50 µL of 1mg/mL Hoechst 33342 (98% Sigma-Aldrich) and 50 µL of 2 µg/mL PI (Sigma-Aldrich) in a glass vial. After 24 hours of treatment and incubation in 6-well plate as detailed in Section 3.3.7, culture medium was removed and 100 µL HPI dye solution were added in each well then incubated for 10 min. Control wells containing cells without treatment were also included. To identify and count the cells with distinct morphologies, an epi fluorescent microscopy (Olympus microscope equipped with a Nikon D1X camera) was used; the images were captured at 20X magnification. Cell counts for healthy (living), apoptotic, or necrotic cells were obtained from the same treatment in duplicate wells, and from three different fields for each well. Counting of the cell were measured according to their appearance, then averaged and expressed as percent of total cell number (Fig.3.4).

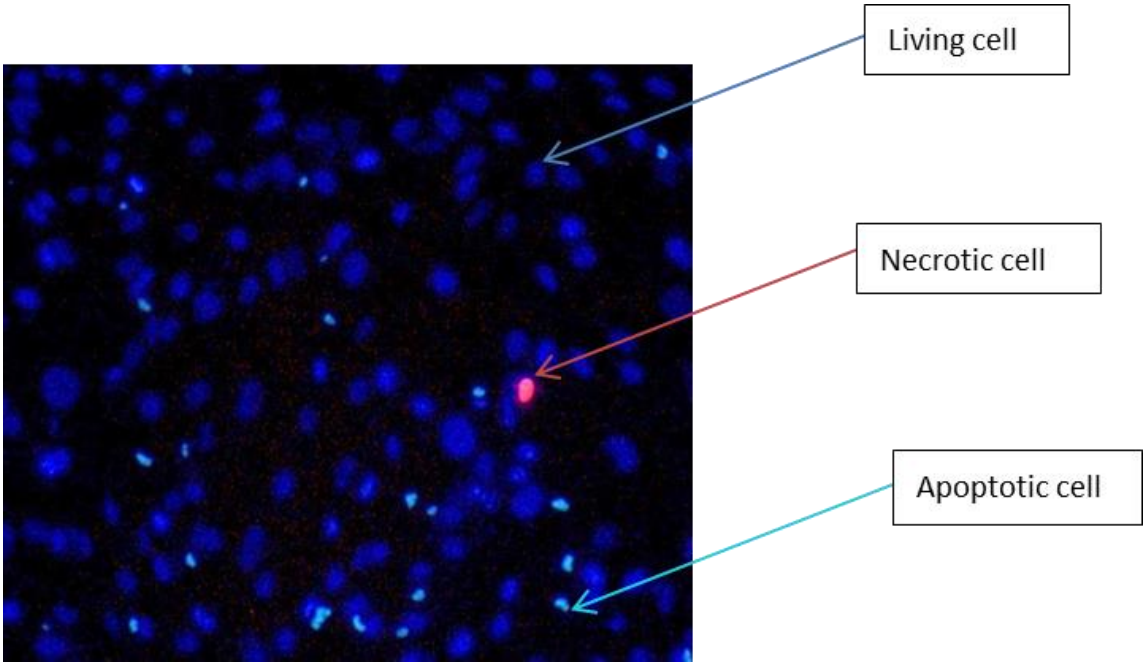

Fig.3.4: Microscopic picture of HPI assessment. The blue cells represent the healthy living cells while the bright blue refers to apoptotic cell and the red is necrotic cell; the images were captured at 20X magnification and 200 μm scale bar.

3.3.9 Statistical analysis

Mean values were calculated for the number of readings (n) in each experiment (as have been given in the figure legends) and the error bars represent the standard division (SD).

Results were statistically analysed using one-way ANOVA with Tukey's tests. Any significant difference was identified by a P-value <0.05, and the degrees of significance are indicated on figure legends where appropriate.

3.4 Results

3.4.1 Culturing of bEnd.3

Light microscopic picture of the cultured bEnd.3 cell line revealed a spindle shape cells reaching 70-80 % confluency after 3-4 days of seeding (Fig.3.5).

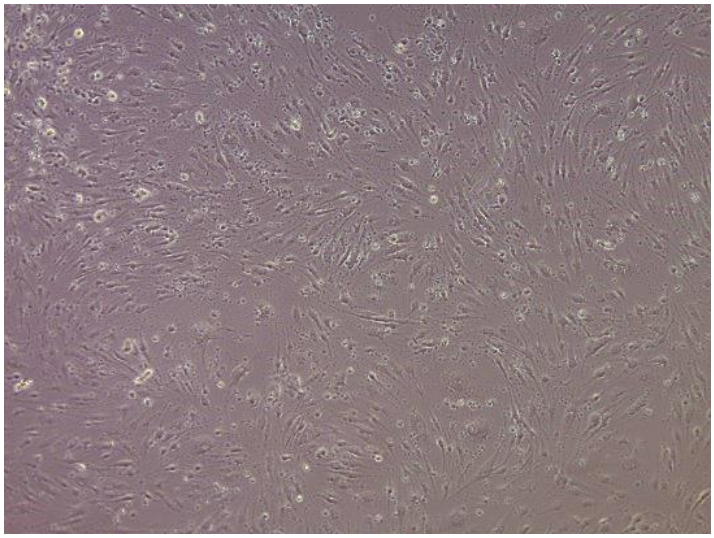

Fig.3.5: Light microscopic picture of cultured bEnd.3 (20X magnification and 200 µm scale bar).

3.4.2 MTT cells metabolic activity results

Results of MTT analysis have indicated that there is no cytotoxic effect over 24 hr for FP, G0K, G1K, G0K-FP and G1K-FP at the range of concentrations used (25-400 µM) indicating no reduction in cell metabolic activity by giving values more than 50% in relation to the control untreated cells (Fig.3.6. a).

The results after 48 hr treatment have followed similar pattern to those seen after 24 hr treatment (Fig.3.6. b) with no significant difference ($P>0.05$) to those of 24 hr results. The cell metabolic activity levels were seen decreased with increasing molecule concentration where the lowest value showed by G1K-FP at 400 µM to be 77.2% and 76.9% after 24 hr and 48 hr exposure respectively. Whilst, the 25 µM of all molecules showed a range of cell metabolic activity levels 95-100%.

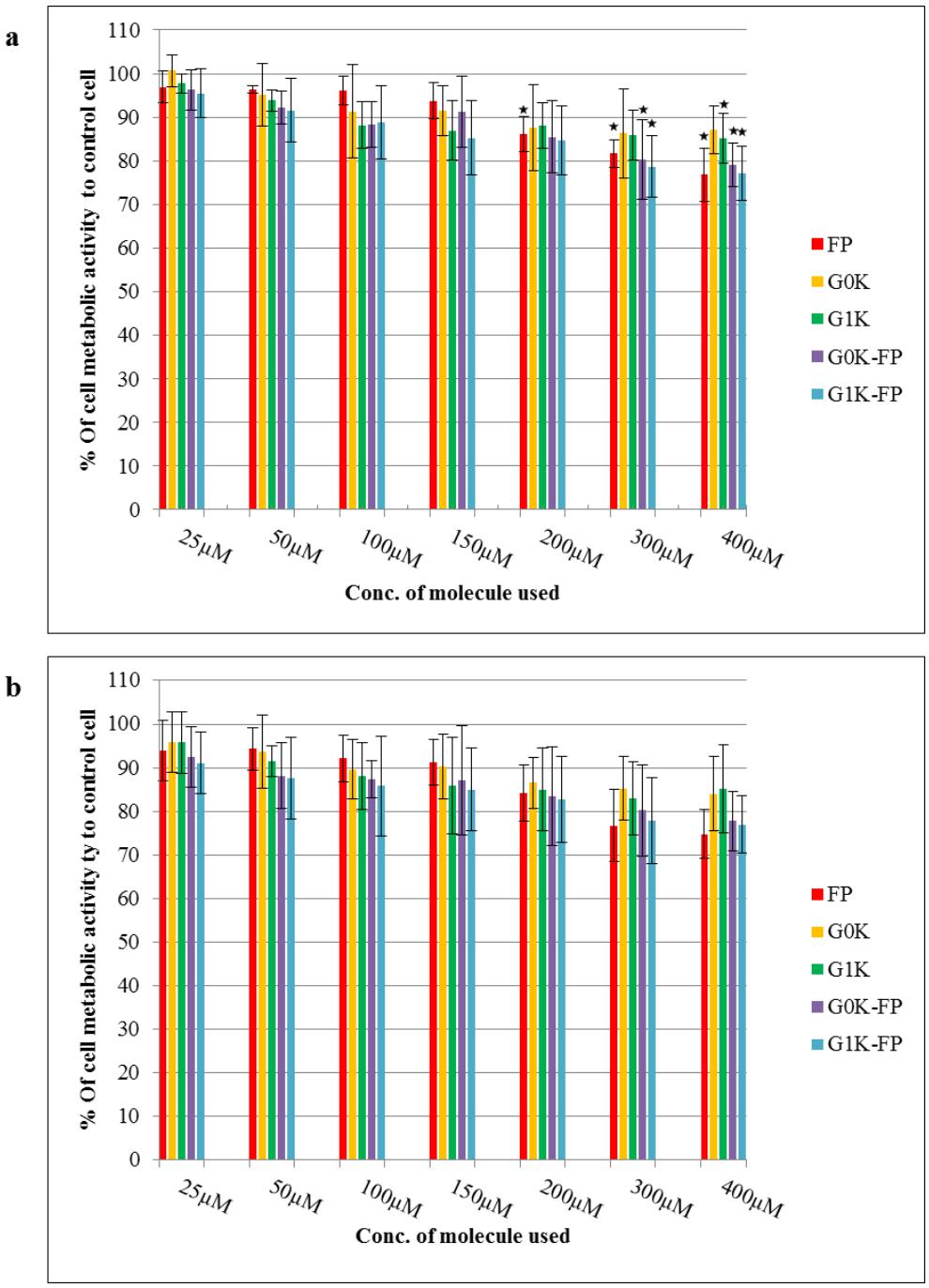

Fig.3.6: MTT results of bEnd.3 cells treated with free FP and G0K, G1K- dendrons with and without FP. a. after 24 hr treatment. b. after 48 hr treatment. The absorbance was measured and the cell metabolic activity was calculated as a percentage of absorbance in relation to control untreated cells. Values marked asterisk are with significant difference to control ($P<0.05$). The data represent mean ± SD of n = 6.

3.4.3 LDH assay for evaluation of cytotoxicity

No cytotoxicity was apparent using the LDH assay in the concentration range used (25, 50, 100, 200, 300 and 400 µM) of FP, G0K, G1K, G0K-FP and G1K-FP after 24 hr of treatment (Fig.3.7. a). The results of 48 hr treatment remained within acceptably low toxicity range for all dendrons with and without drug and free drug as all levels were less than 50% of positive control (100% complete lysis cells) (Fig.3.7. b). In similar pattern to MTT assay, the lowest LDH release was with lowest concentration of molecules and increased with increasing concentration to be 12.8% and 14.8% for G1K-FP after 24 hr and 48 hr of treatment respectively.

Both time interval treatment results are significantly different to the positive control ($P<0.001$). Whereas no significant difference ($P>0.05$) between 24 and 48 hr LDH levels.

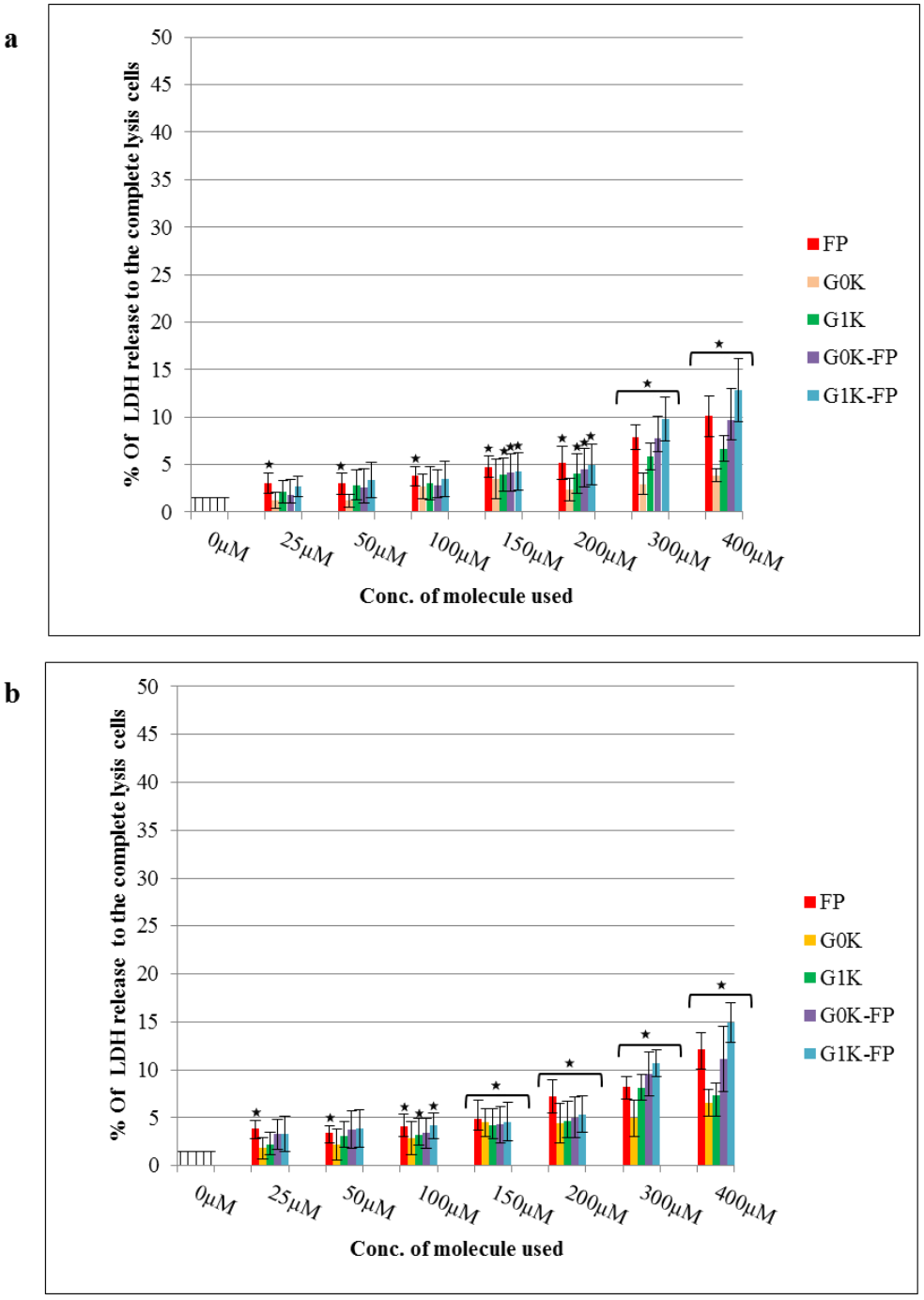

Fig.3.7: LDH results of bEnd.3 cells treated with free FP and G0K, G1K- dendrons with and without FP. a. after 24 hr treatment. b. after 48 hr treatment. The absorbance was measured and the LDH release of each was calculated as a percentage of absorbance in relation to control and complete lysis untreated cells. There is a significant difference to positive control ($P<0.001$) in all values. Values marked asterisk are significantly different to negative control ($P<0.05$). The data represent mean ± SD of n = 6.

3.4.4 HPI Cell death assessment

Results of staining the cells with HPI revealed results consistent with those obtained from the MTT and LDH assays, after treatment with each synthesised molecules. The percentage of healthy cells at all concentration used (100, 300 and 400 µM) for FP, G0K, G1K, G0K-FP and G1K-FP, were not less than 89%. The G1K-FP at a concentration of 400 µM showed the lowest value of healthy cells and the highest level of apoptotic and necrotic cells. While the highest value of healthy cells appeared with 100 µM of G1K. Regarding apoptosis and necrosis, G0K with concentration 100 µM, showed the lowest values (Fig.3.8, 3.9).

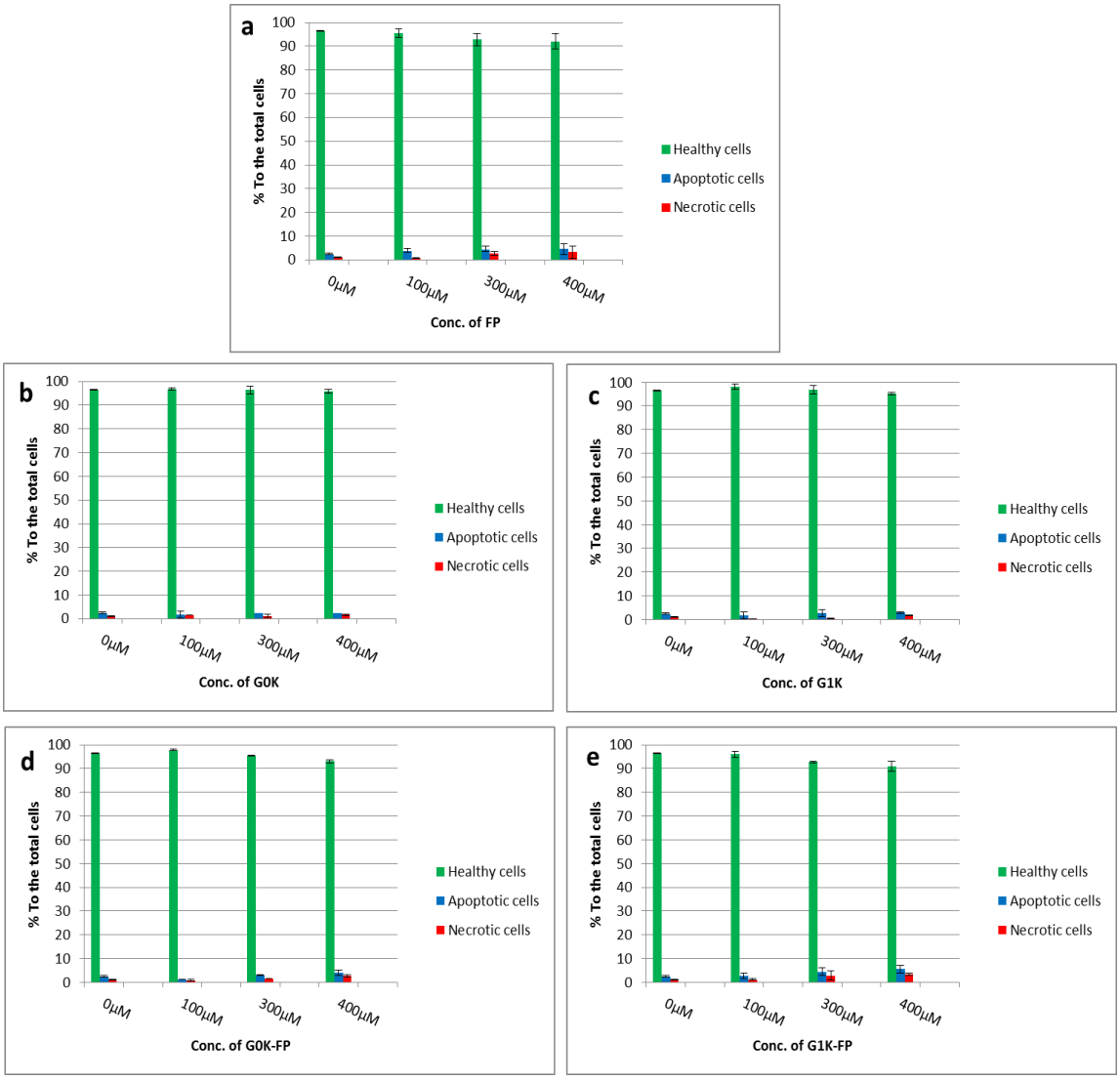

Fig.3.8: HPI staining of bEnd.3 cells. a. For the FP alone. b. For the G0K. c. For the G1K. d. For the G0KFP. e. For the G1KFP. The microscopic pictures were taken and the healthy, apoptotic and necrotic cells of each were calculated as a percentage to the total number of cells in each field. No significant differences from the control ($P>0.05$) were seen. The data represent mean ± SD of n = 6.

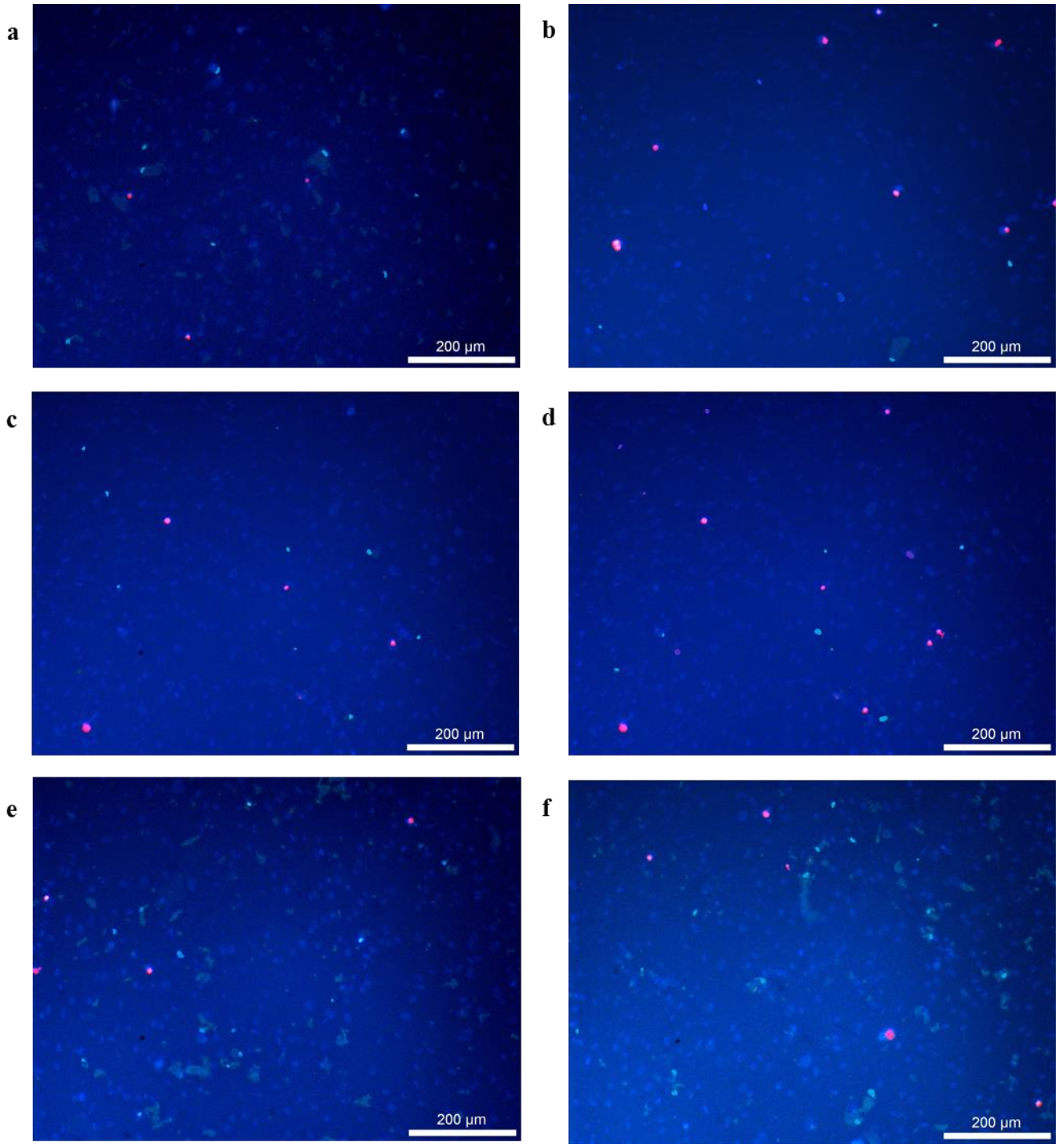

Fig.3.9: Examples of microscopic pictures of HPI-stained bEnd.3 cells. a. Control untreated cells. b. Treatment with the FP alone. c. Treatment with the G0K. d. Treatment with the G1K. e. Treatment with the G0K-FP. f. Treatment with the G1K-FP. The blue cells represent the healthy living cells while the bright blue refers to apoptotic cell and the red is necrotic cells.

3.4.5 Cytotoxicity related to HUVEC

Biochemical investigation of FP, G0K, G1K, G0K-FP and G1K-FP has been also undertaken on HUVEC cells to ensure their non-cytotoxicity on different tissues.

The MTT results after 24 and 48 hr treatment revealed no cytotoxicity even with the highest concentration used (400 µM) as it still giving more than 50% of cell metabolic activity (Fig.3.10. a and b).

Furthermore, no cytotoxicity was seen in the results of LDH assays undertaken on HUVEC cells after 24 and 48 hr treatment with FP, G0K, G1K, G0K-FP and G1K-FP as the values of LDH release were less than 50% in relation to the positive controls, with a significant difference ($P<0.001$) (Fig.3.11. a and b).

In addition, for both MTT and LDH assays, the results after 48 hr showed no significant difference ($P>0.05$) from those of 24 hr results.

No significant differences ($P>0.05$) were found when compared statistically the MTT and LDH values of HUVEC with that of the bEnd.3 cell line type.

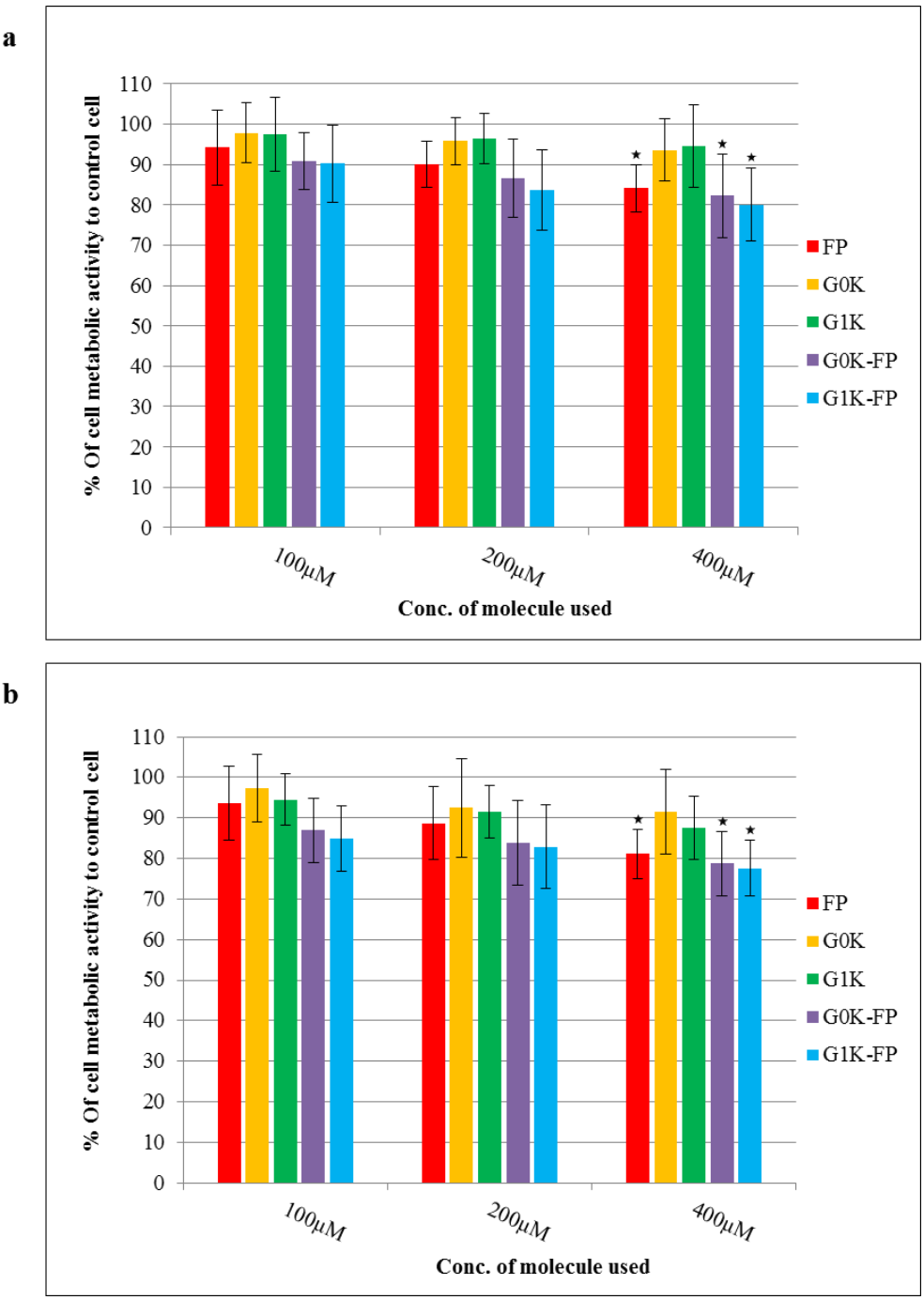

Fig.3.10: MTT results of HUVEC cells treated with free FP and G0K, G1K- dendrons with and without FP. a. after 24 hr treatment. b. after 48 hr treatment. The absorbance was measured and the cell metabolic activity was calculated as a percentage of absorbance in relation to control untreated cells. Values marked asterisk are with significant difference to control ($P<0.05$). The data represent mean ± SD of n = 6.

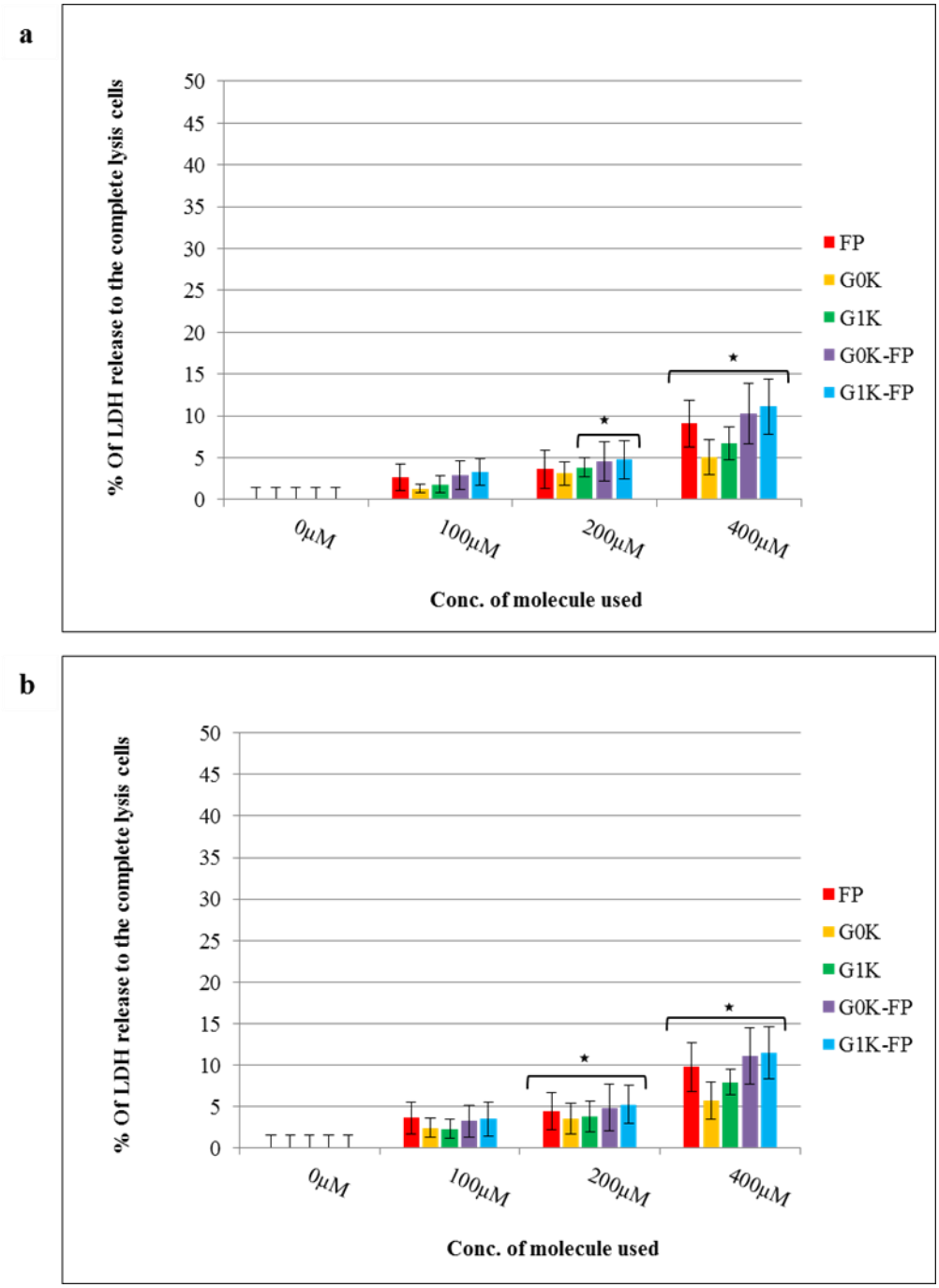

Fig.3.11: LDH results of HUVEC cells treated with free FP and G0K, G1K- dendrons with and without FP. a. after 24 hr treatment. b. after 48 hr treatment. The absorbance was measured and the LDH release of each was calculated as a percentage of absorbance in relation to control and complete lysis untreated cells. There is a significant difference to positive control ($P<0.001$) in all values. Values marked asterisk are significantly different to negative control ($P<0.05$). The data represent mean ± SD of n = 6.

3.5 Discussion

It is essential to explore the cytotoxicity of any new synthetic materials before taking forward for further examination, thus free and drug-laden dendrons were investigated to ensure their biocompatibility. The success of dendronised polymers as carriers or biomaterials is due to their biodegradability and biocompatibility properties (Tomalia *et al.*, 2005). Studies have reported that their biocompatibility properties are mostly dependent on concentration, generation and surface charge (Yang *et al.*, 2007). Results have showed that lower generation dendrimers (G0 to G3) exhibit considerably less cytotoxicity than higher generation dendrimers (Menjoge *et al.*, 2010). In this study, this issue has been taken in consideration during the design of the dendronised carrier system by choosing lower generations (G0 and G1).

The *in vitro* cytotoxicity of dendronised polymers has been extensively examined using various cell lines, diversity of incubation times, and different assays (Ruth *et al.*, 2005). Variability in conditions of cell culture makes it difficult to give a direct comparison of experiments conducted in various published studies. To determine the cytotoxicity of dendrimers with different chemical structures, it is essential to use a physiologically relevant incubation time in line with the intended use and administration on specific cells, and enough amount to determine the inhibitory concentration (Ruth *et al.*, 2005; Xu *et al.*, 2014). To study the cytotoxicity of the dendronised carrier systems produced in this study, the bEnd.3 cell line was used. This type of brain capillary cell line is considered an optimal candidate as an *in vitro* BBB model which, unlike other types of cells, maintains the same properties of *in vivo* brain endothelium (Hong *et al.*, 2004; Weksler *et al.*, 2005). BEnd.3 cells are considered fast growing cells and could reach 75-85% confluence within 3-4 days. A previous study has described the cells as elongated spindle shape under light microscopy, a similar feature was seen in our work when cultured bEnd.3 (Fig.3.5). By using highly advanced electron-micrographs, the bEnd.3 cells appear to take a squamous morphology extending peripherally to thin attenuations and forming tight junctional complexes with adjacent cells. These features are similar to that of the *in vivo* brain microvascular endothelial cells and to the primary cultured cells. Whereas using higher magnification, the observation revealed that the cells possess a high density of non-coated intracellular vesicles and at the apical plasma membrane, there were invaginations characteristic of clathrin-coated pits (Omidi *et al.*, 2003).

In this study, it has been demonstrated that the unloaded lysine-dendron with low generation (G0 and G1) and the drug-loaded molecules (G0K-FP and G1K-FP) have no significant effect on mitochondrial function using MTT assay, by giving high cell metabolic activity levels (more than 77%) in comparison to that of control cells (Fig.3.6. a and b). MTT assay measures the reduction in metabolic activity of mitochondria and it is essential to keep this function intact as it is vital source of energy, which is used by the cell for division and growth (Allcock, 2011). The levels of cell metabolic activity were high at lower concentrations of synthetic molecules than that of higher concentrations and this might be due to the increasing tendency of cytotoxicity with higher concentrations (Yang *et al.*, 2007). In addition, these synthetic molecules did not show any significant effect on cell lysis according to the results of LDH assays. Similar to the results of the MTT analysis, higher LDH release was observed at higher concentrations of the synthesised molecules (G0K, G1K, G0K-FP and G1K-FP), however, these results were far lower than the generally accepted toxic values (as they were less than 15% of positive control) with a significant difference ($P<0.001$) from the positive control (Fig.3.7. a and b). LDH is one of the cell components released when the cell membrane is lysed (Allcock, 2011). These findings demonstrate the non-cytotoxicity of these products and are consistent with previous studies that showed no cytotoxicity even with the higher generation (G3) of poly-(ε)-lysine dendron in cell culture (Issa *et al.*, 2015; Meikle *et al.*, 2011; Perugini, 2013). Perhaps the most notable consequences generated from these results, suggest that the amino acid composition including lysine, and not just the lower generation, may have a role in reducing toxicity of the dendron. Choi, *et al* (2004) showed that lysine-modified dendrimers have low cytotoxicity with high transfection efficiency on HepG2, Neuro 2A cell lines, and primary rat vascular smooth muscle cells (Choi *et al.*, 2004). Moreover, conducting the MTT assay with a hepatocellular carcinoma cell line, have indicated the low cytotoxicity of poly(L-lysine) dendrimer (Jia *et al.*, 2007).

Whereas the free FP cytotoxicity evaluation results are in agreement with what have been early reported that the drug exerts its cytotoxic potential at higher concentrations (about 400 µM and above) in different cell cultures (Eriksen *et al.*, 2003; Grosch *et al.*, 2003; Meister *et al.*, 2013).

The observations regarding increasing cellular response with higher concentrations of the synthetic molecules in this work are probably due to the cytotoxic behaviour of multiple

amine groups. These positively charged groups interact with negatively charged cell membranes, causing cell membrane damage (Prashant, 2014), in turn increasing LDH release and affecting the mitochondrial function and cell metabolic activity. These data are consistent with other studies that stated the dendron cytotoxicity increases with higher concentration and generation (Menjoge *et al.*, 2010; Yang *et al.*, 2007). This toxicity is attributed mainly to the end group present on its periphery. Generally amine-terminated dendrimers display concentration-dependent toxicity. Alternatively neutral or anionic groups terminated dendrimers have proved to be less toxic (Malik *et al.*, 2000; Prashant, 2014). Fortunately this cytotoxicity can be overcome by complete or partial modification of their surface periphery to produce glycosylated, acetylated and PEGy-lated dendrimers (Prashant, 2014). In addition, it was shown previously that quaternised PAMAM–OH derivatives have a lower level of cytotoxicity than PAMAM–NH_2 due to the hiding the cationic charges by surface COOH groups (Feliu *et al.*, 2012). Moreover, PAMAM generation 1.5-9.5 dendrimers with a carboxyl surface were found to be non-cytotoxic towards B16F10, CCRF or HepG2 cell lines after 72 hr using MTT assay, and the modified carbosilane dendrimers were generally not toxic when incubated with CCRF and Hep G2 cells (Malik *et al.*, 2000).

In order to confirm the findings of MTT and LDH assays and to investigate whether cells were undergoing apoptosis or necrosis, HPI assessment was performed. Necrosis and apoptosis are driven by a series of intracellular events including mitochondrial dysfunction, organelle disintegration, lysosomal rupture and ultimately cell membrane rupture (Majno *et al.*, 1995). A supporting pattern of results was observed in HPI assessment to those obtained from the MTT and LDH analysis. HPI results, after treatment (with FP, G0K, G1K, G0K-FP and G1K-FP), revealed that the number of apoptotic and necrotic cells is low in relation to normal healthy cells of the same treatment (Fig.3.8), with no significant differences ($P>0.05$) from the untreated control. Accordingly this gives further proof of the integrity of cell membrane and mitochondria after treatment with the synthesised molecules.

The cytotoxicity of synthetic molecules was further analysed using another endothelial cell line (HUVECs) to ensure their non-cytotoxicity with different cells. The results of MTT and LDH assays indicted their non-cytotoxicity (Fig.3.10. a and b, and Fig.3.11. a and b), with no significant differences ($P>0.05$) when compared statistically with those of the

bEnd.3 cell line type. These results are in accordance with previous studies that have tested poly-(ε)-lysine dendrons with the HUVEC cells (Perugini, 2013). These findings demonstrate acceptable levels of toxicity in the models used, giving a clear rationale to take them forward for the next stage of studying the cell uptake and penetration.

Cytotoxicity after 48 hr of treatment with the G0K, G1K, G0K-FP and G1K-FP was investigated to determine if there are any potential negative effects with longer term treatment. The data revealed no cytotoxic impact as evidenced by MTT and LDH assays with no significant difference ($P>0.05$) from that of 24 hr of treatment. This is inconsistent with other studies which have shown that the cytotoxicity of dendrons is time dependant (Ruth *et al.*, 2005). Indeed, a previous study has provided a comprehensive *in vitro* assessment of hydroxyl functional bis-MPA and cationic PAMAM dendrimers and revealed that cytotoxicity is increasing with time (Feliu *et al.*, 2012). The type of cell line and the dendron compositions could be the reasons beyond these controversial observations. As shown in a previous study, this brain endothelial cell line is more stable and less sensitive than other types (Weksler *et al.*, 2005). These results suggest that molecules may be adsorbed over time without harmful effect to cells. This property may be highly beneficial to both *in vitro* and *in vivo* concepts, allowing the carried drug to reach the target site at BBB and exert its pharmacological effect safely.

What is interesting to note, however; is the behaviour of drug-integrated molecules (G0K-FP and G1K-FP) which showed a relatively higher impact on cellular cytotoxicity than that of unloaded dendrons. These increased responses may be attributed to the amount of FP that is conjugated to the dendrons as there are more double moles of FP for each mole lysine in the integrated molecules. This in turn may alter some of physico-chemical properties of the original molecules resulting in more destructive effect (Eriksen *et al.*, 2003; Meister *et al.*, 2013). Another consideration put forward to explain these results is the possibility that the integrated molecules may have a greater penetrability into the cells due to the adsorptive effect of the dendrons leading to a reduction in mitochondrial function and more LDH release without evidence of necrosis (however, it is worth reiterating that the complexes have been shown to be non-toxic). This possibility could have the potential to support the capability of the dendronised carrier system to cross the cell membrane and thus improve the drug permeability (Prashant, 2014). It has been

previously found that the cellular entry of some drugs such as ibuprofen was enhanced when attached to the dendrimer (Kolhe *et al.*, 2003).

Ultimately, lacking the ability to decrease the cellular viability with the low values of LDH release, supported by HPI data following treatment suggest that the synthesised molecules have a low toxicity towards brain endothelial cells. The evidence presented in this study suggest that drug loaded dendrons can be used as safe carrier systems to deliver FP and can be taken forward to study their penetration across BBB (Chapter 5).

3.6 Conclusion

Taking all the currently available evidence together, the synthesised molecules have shown low levels of cytotoxicity towards BBB endothelial cells and HUVECs. Moreover, the data suggest that G0K-FP and G1K-FP are compounds that can be used safely to study FP permeability across BBB using the bEnd.3 cell line model. Furthermore, these novel dendronised carrier-systems (G0K-FP and G1K-FP) are not only non-cytotoxic but also offer the potential to improve FP's bioavailability due to coupling of dendrons with larger amounts of FP.

The synthesised and characterised dendrons will, therefore, be tested for their cell permeability *in vitro* using bEnd.3 (Chapter 5).

Chapter 4. Functionalisation of Drug-Dendron with ApolipoproteinE-Derived Peptide

4.1 Introduction

The accessibility of therapeutics to the brain in AD is highly limited by the BBB (Ballard *et al.*, 2011). The inadequate membrane permeability and low target specificity of drugs can potentially be solved by the functionalisation of the drug-carrier with targeting and uptake-mediating ligands. In previous chapters, the dendronised carrier systems were successfully synthesised and integrated with FP, a widely accepted drug that is used to lower the Aβ in AD which is in its free form has limited ability to cross BBB (Meister *et al.*, 2013).

Functionalisation of the carrier systems in their formulations to deliver drugs is challenging whether by chemical modification or by designing them with specific targeting ligands that help achieve their action at the desired site. Any successful functionalisation is mostly dependant on the functions in respect to the target organ or tissue nature and the mechanisms of the transport (Bhaskar *et al.*, 2010). In addition, the BBB's sensitivity to this targeting ligand functionalisation and its potential toxicity and biocompatibility should be taken in consideration (Chen *et al.*, 2012).

Dendrimer chemistry offers the opportunity to design and engineer a functionalised drug carrier system. The three dimensional architecture of dendrons that consists of various structural components including core, branches and terminal groups make them useful for targeted drug delivery by providing multiple attachment sites for drug molecules and/or targeting ligands at the same time (Najlah *et al.*, 2006) (Fig.4.1) .

Using transport vectors is one of the promising strategies to deliver molecules with low BBB permeability by utilising natural transport routes. The considerable pathways of entry for these circulating molecules to the brain are the endogenous carriers for nutrients or solutes, RMT for specific ligands and AMT for hydrophobic molecules (Chen *et al.*, 2012).

To utilise endogenous carriers for the enhanced passage of therapeutics across the BBB, the drugs should have a molecular structure similar to that of the endogenous nutrients. Also the size of drugs must mimic that of the endogenous ligand so that their uptake is

enhanced and can be transferred across the BBB as the nutrient carriers stay in the cell membrane (Banks, 2012).

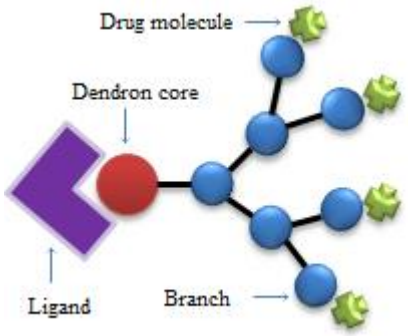

Fig.4.1: Bi-functionalisation of dendron with drug molecules and targeting ligand.

Alternatively, cationic peptides have been used to deliver molecules into the brain by exploiting the AMT route (Herve *et al.*, 2008). These peptides have the potential to enter cells rapidly via adsorptive effect without causing lysis to the cell membrane. Nevertheless, its lack of selectivity and targeting is a drawback in their use, which could lead to some drug-associated side effects in non-target sites (Chen *et al.*, 2012).

However, transport across the BBB via endogenous RMT provides selective and active targeting in which it transports the cargo molecules across the barrier by conjugating with a specific ligand at the brain endothelium (Pardridge, 2005). Different cargos such as macromolecules and drug-laden nanocarriers can be transported by this approach (Khawli *et al.*, 2013; Rip *et al.*, 2009; Rocha, 2013)

Recently, many studies have shown that an enormous number of receptors are highly expressed at the BBB which can be employed in enhancing the delivery of drugs (Mager *et al.*, 2017; Rip *et al.*, 2009; Tuma *et al.*, 2003). In general, the following three steps are involved in the RMT across the BBB (Fig.4.2):

1. Endocytosis at the blood-faced side of cell membrane (luminal side) following the binding of the receptor to the ligand.
2. Movement of the bound molecules across the cytoplasm of the endothelia, which might involve endosomal and lysosomal processes that can degrade some molecules. Cationic molecules (such as amino compounds) or pH-sensitive liposomes can be applied to avoid this degradation (Bartsch *et al.*, 2005; Shir *et al.*, 2006).

3. Exocytosis of the drug molecule or drug-integrated ligand or other types of cargos, at the brain-faced side of the cell membrane (abluminal side) (Pardridge, 2005).

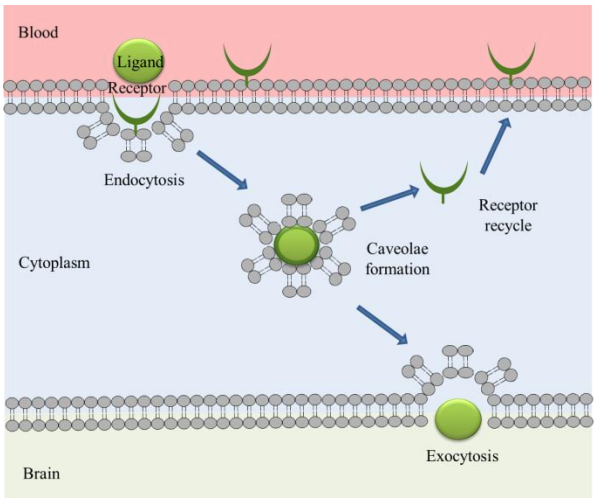

Fig.4.2: Diagram showing the RMT pathway. It is beginning with endocytosis after binding of ligand with receptor to form vesicle (caveolae), then its movement across the cytoplasm and ending with exocytosis at the abluminal side.

There are various potential endogenous receptors systems that have been exploited for a range of applications including:

1. Insulin receptors: This is a vastly utilised RMT system for transporting molecules across the BBB. Nevertheless, it is considered the riskiest system as its mechanism interferes with glucose homeostasis (Chen *et al.*, 2012; Pardridge *et al.*, 1985; Xia *et al.*, 2009).
2. Transferrin receptor (TfR): This receptor mediates the transport of iron bound to Tf in to the cell. Tf is a transmembrane polypeptide of 679 amino acids (Sawyer *et al.*, 1986). This system can be utilised to transport drugs and genes across the BBB either by using Tf as ligand for brain targeting or by using a specific antibody against the TfR (such as OX26) (Cruz *et al.*, 2004). However, its large size and difficulty in synthesising hinder its use (Chen *et al.*, 2012).
3. Diphtheria toxin receptor (DTR): This is a transmembrane receptor with no particular endogenous ligand. Diphtheria toxin binds to DTR and crosses the cell membrane through endocytosis but it is not widely used because of its toxicity (Chen *et al.*, 2012; Giannini *et al.*, 1984).
4. Low-density lipoprotein receptor (LDLr) related proteins 1 and 2 (LRP1r and LRP2r): These receptors can be also utilised to target drugs or genes to the brain

(Boer *et al.*, 2007). Numerous molecules are capable of interacting with LRP1r and 2r including melanotransferrin, Lf, α2-macroglobulin, ApoE, APP, tissue plasminogen activator and plasminogen activator inhibitor 1 (Boer *et al.*, 2007; Gabathuler, 2010) (Fig.4.3).

LDLr-mediated transcytosis is considered a promising strategy to enhance the brain permeability for drugs and genes by functionalisation of carrier systems with a particular ligand (Molino *et al.*, 2017; Sauer *et al.*, 2006; Xiao *et al.*, 2013). The upregulated expression of these receptors on capillary endothelia of the BBB in respect to other species of endothelial cells provides a rationale to take advantage of this system (Molino *et al.*, 2017).

It has been reported that NPs decorated with ApoE enhanced their brain uptake via LDLr-mediated transcytosis (Zensi *et al.*, 2009). Moreover, NPs were successfully found to interact with the LRPr and cross the BBB by functionalising with a specific amino acid sequence of ApoE (Sauer *et al.*, 2005).

The ApoE peptide's ability to interact with LDLr at brain endothelia has been extensively studied. The evidence from previous literatures suggest that the ApoE derived peptide of sequence (141-150) is the appropriate candidate to be used as a permeability enhancing and brain targeting ligand (Bana *et al.*, 2014; Gobbi *et al.*, 2010; Re *et al.*, 2010; Sauer *et al.*, 2005).

ApoE is a 34 kDa protein consisting of 299 amino acid residues; it mediates the endocytotic process of triglyceride-rich lipoproteins leading to their uptake and metabolism via high-binding affinity to the membrane's LDLr (Mahley, 1988). The receptor-binding sequence of the ApoE and its isoforms were identified to be in the region of 136-150 residues, located at the amino terminal domain (Weisgraber, 1994) (Fig.4.3). The chemical structure of the ApoE sequence that binds to the LDLr has been rather investigated by various studies (Datta *et al.*, 2000; Re *et al.*, 2011). It was found that the peptide (141-155) amino acid sequence can be recognized by the LDLr (Dyer *et al.*, 1995). However, the shorter residue (141-150 of sequence -LRKLRKRLLR-) which is derived from the human ApoE binding domain is able to induce an endocytotic process via LDLr-engagement in a primary neuronal cultures of brain tissue (Wang *et al.*, 1997). The influence of this residue was investigated using electron and fluorescence microscopies

and found it was sufficient to interact with receptor and activate the endocytosis (Sauer *et al.*, 2005).

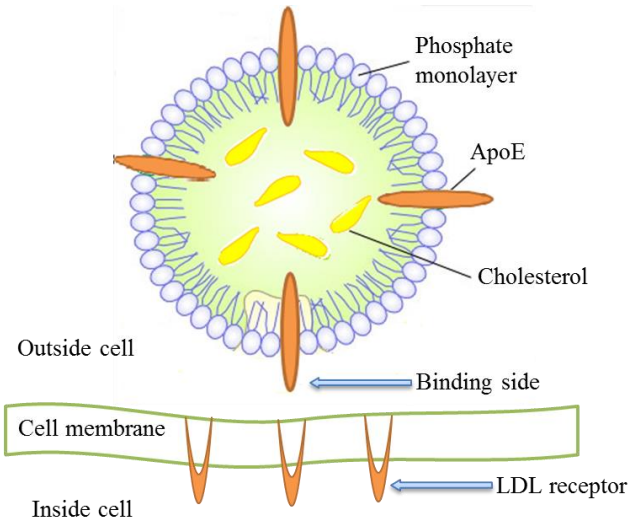

Fig.4.3: Binding site of the ApoE molecule with LDLr at the cell membrane.

Liposomes decorated with this peptide sequence (141-150) have been shown to be efficiently taken up by brain endothelium of rats (Sauer *et al.*, 2005). The ApoE-derived residue (141-150) has been successfully synthesised and functionalised with different carriers system such as NLs to deliver drugs and evidently enhanced the brain uptake of antioxidant drugs and curcumin (Gobbi *et al.*, 2010; Re *et al.*, 2010).

Due to the ability of the ApoE-derived peptide to enhance particulate uptake, a 10 amino acid sequence (LRKLRKRLLR) peptide was selected for this study to improve the cellular uptake and brain targeting of FP-loaded dendron.

4.2 Aim of the chapter

This chapter describes the synthesis of the ApoE-derived peptide, its characterisation before and after functionalisation on the FP-loaded dendron and evaluation of the peptide functionalised molecule toxicity against bEnd.3 cells. Therefore this chapter aims to:

1. Synthesise ApoE-derived peptide (AEP), a 10 amino acid sequence using a modified microwave-based SPPS method.
2. Functionalise the G0 lysine dendron at its core with this AEP, and attach FP drug molecules at its peripheral branching via coupling reactions.
3. Characterise the product (AEP-K-FP) by MS and FTIR and to confirm the purity of the product by TLC and HPLC.
4. Test the biochemical response of bEnd.3 after treatment with the AEP-K-FP using MTT, LDH and HPI cytotoxicity assays to ensure the conjugate non-cytotoxicity.

4.3 Materials and Experimental methods

4.3.1 Synthesis of AEP-K-FP using SPPS by microwave synthesiser

The linear AEP and its attachment to the drug-dendronised carrier system were synthesised using a modified SPPS by microwave synthesiser as previously described for dendron synthesis (Chapter 2).

The first step was the assembly of AEP (LRKLRKRLLR) of a chemical formula: $C_{60}H_{118}N_{24}O_{11}$ (exact mass: 1350.941, MW: 1351.76 Da) (Fig.4.4). As previously described in Section 2.3.1, the required number of coupling steps and initial deprotection and deprotection steps were carried out for the assembly of AEP. After coupling of rink amide, 0.4 mmol of each desired amino acid (Novabiochem, UK) was coupled in a sequence of; Fmoc-Leu-OH, Fmoc-Arg-OH, Fmoc-Lys(Boc)-OH, Fmoc-Leu-OH, Fmoc-Arg-OH, Fmoc-Lys(Boc)-OH, Fmoc-Arg-OH, Fmoc-Leu-OH, Fmoc-Leu-OH, Fmoc-Arg-OH consecutively as shown in Table 4.1. This sequence of amino acids corresponds to that of human ApoE peptide (141-150 residues). Then, the dendronised-FP was functionalised with AEP to produce AEP-K-FP (chemical formula: $C_{96}H_{152}$ $F_2N_{26}O_{14}$, exact mass: 1931.19, MW: 1932 Da) (Fig.4.5). This step was implemented by attaching dendron G0K (a branched lysine) with 2 drug molecules (FP) to this synthesised peptide via coupling reactions after deprotection of the final amino acid (R) of the peptide.

4.3.1.1 Capping

In order to remove any unreacted amino group after the coupling steps, these functional groups should be “capped” (blocked) so that the formation of deletion peptide sequences will be avoided and the loading of a resin also be reduced. A capping step is added during the synthesis of long linear chain peptides, such as AEP, to easily remove any separated truncated sequence that might be formed. The capping is achieved by treating the peptide on the resin, after coupling, with a high excess (approximately 50 fold molar) of a reactive derivative of acid and a base. Acetic anhydride and pyridine or DIPEA are the widely used mixture (Fields *et al.*, 2014). In this work, when the coupling solution was removed, the resin was washed with DMF then the capping mixture was added. This mixture was freshly prepared by dissolving 20 mM of acetic anhydride and DIPEA in DMF. The reaction on the resin was left to stand at room temperature for 30 min. After that the resin was filtered and washed with DMF and isopropyl alcohol before the next deprotection process.

Table 4.1: Assembly sequence of AEP to produce AEP-K-FP.

Addition step	Amino acid	No. cycles (0.4 mmol)	Reactive sites at start: end of cycle	Molar excess
Rink Amide	Fmoc Rink Amide Linker	1	1:1	4
L	Fmoc-Leu-OH	1	1:1	4
R	Fmoc-Arg-OH	1	1:1	4
K	Fmoc-Lys(Boc)-OH	1	1:1	4
L	Fmoc-Leu-OH	1	1:1	4
R	Fmoc-Arg-OH	1	1:1	4
K	Fmoc-Lys(Boc)-OH	1	1:1	4
R	Fmoc-Arg-OH	1	1:1	4
L	Fmoc-Leu-OH	1	1:1	4
L	Fmoc-Leu-OH	1	1:1	4
R	Fmoc-Arg-OH	1	1:1	4
G0K	Fmoc-Lys(Fmoc)-OH	1	1:2	4
Drug	FP	2	-	8

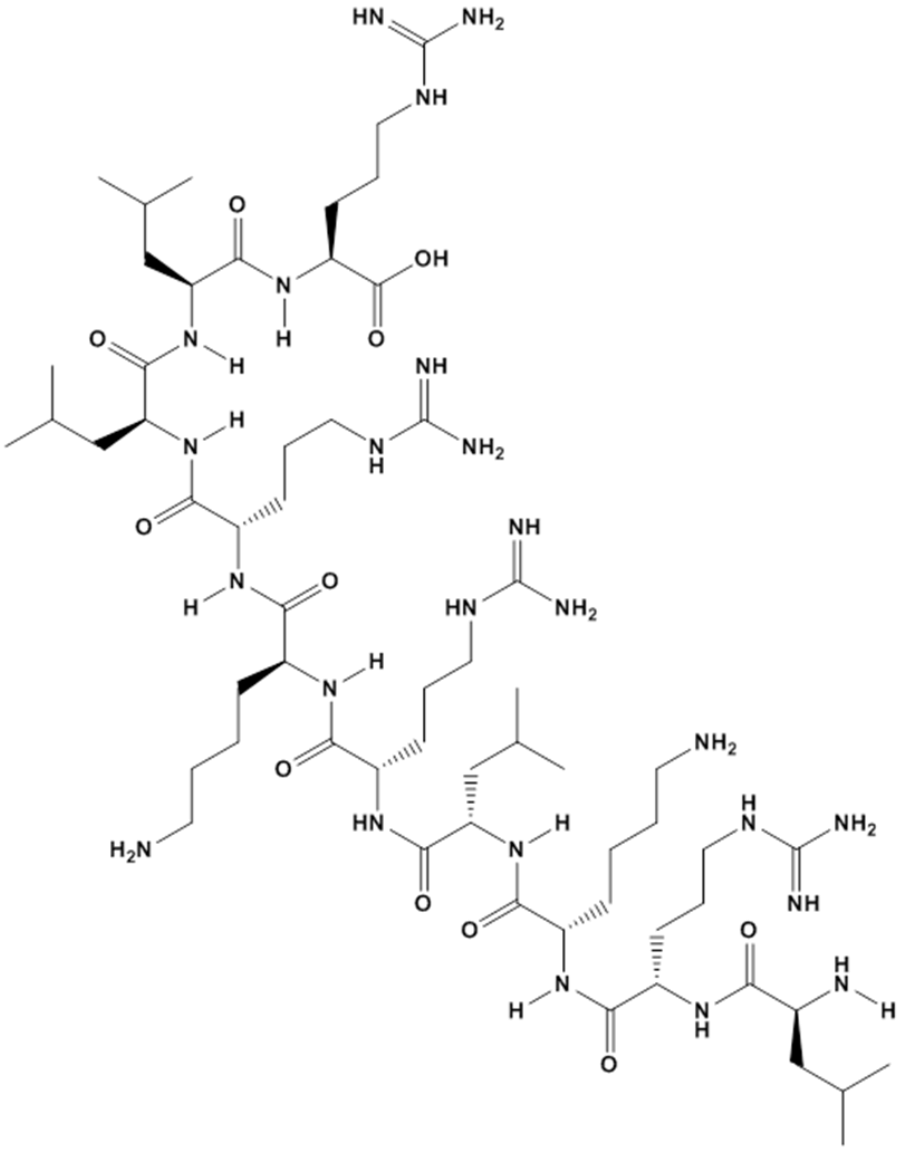

Fig.4.4: Chemical structure of linear AEP of sequence (LRKLRKRLLR) (MW: 1351.76 Da).

a

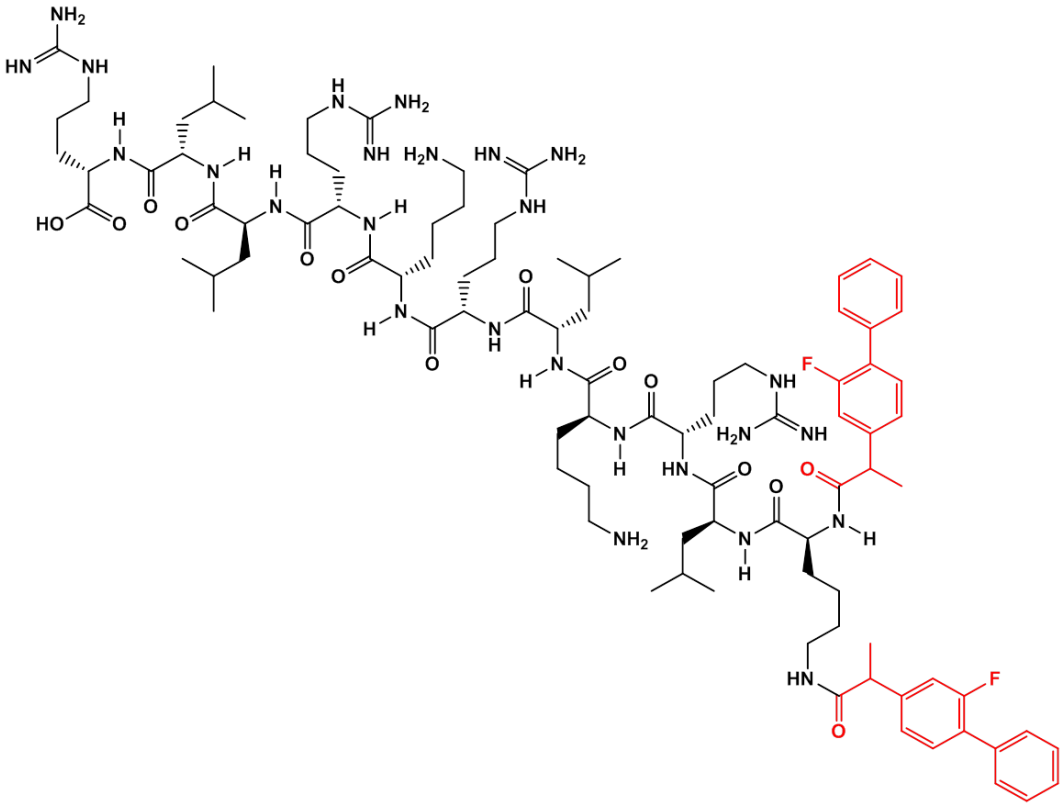

b

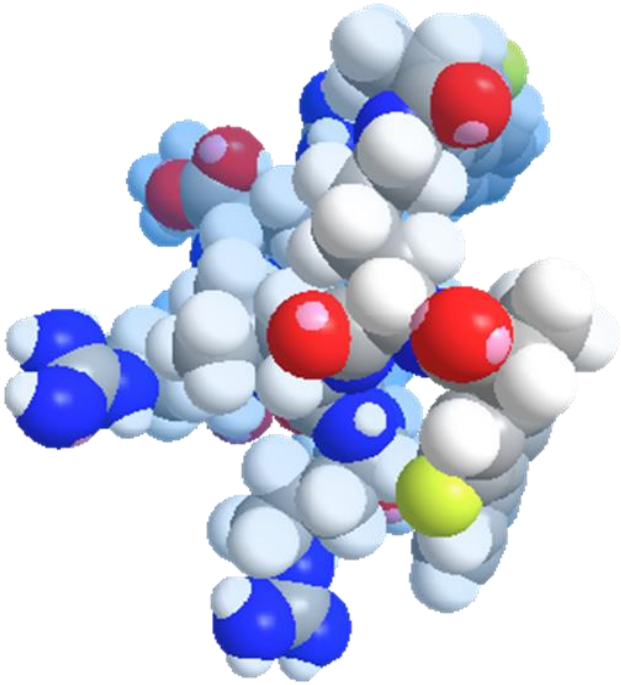

Fig.4.5: Structure of AEP-K-FP (MW: 1932 Da). a. chemical structure. b. 3-dimension chemical structure using ChemDraw Professional 15.

4.3.1.2 Cleavage and Purification

When the assembly of AEP and AEP-K-FP was accomplished, cleavage of the peptide from the resin and purification of the synthesised molecule were performed following the same protocols as described in Sections 2.3.1.2 and 2.3.1.4 to obtain the final products.

4.3.2 Characterisation of AEP and AEP-K-FP

For the characterisation of the AEP and AEP-dendronised drug peptides, MS, FTIR, TLC and HPLC were used as detailed in Section 2.3.2.

4.3.3 Cytotoxicity of AEP and AEP-K-FP

To test the cytotoxicity of the synthesised products (AEP and AEP-K-FP) with brain endothelial cells, MTT and LDH assays and HPI assessment were carried out on the bEnd.3 cell line in addition to the HUVEC according to the same protocols used in Section 3.3.8.

4.3.4 Statistical analysis

Mean values were calculated for the number of readings (n) for each experiment (given in the appropriate figure legends) and the error bars represent the standard division (SD).

Results were statistically analysed using one-way ANOVA with Tukey's tests. Significant differences were identified by a P-value <0.05, and the degrees of significance are indicated on figures where appropriate.

4.4 Results

4.4.1 Characterisation of the AEP and AEP-K-FP by MS

The final products (AEP and AEP-K-FP) were characterised by MS to ensure the successful assembly of the peptides. The MS results presented in Fig.4.6 and 4.7 for the produced peptides indicating the successful synthesis for both by giving the same theoretical and actual MW.

According to the principle of the MS (outlined in Chapter 2) which includes ionisation of molecules during the processing of analysis, different peaks were detected in the MS spectra representing related ions of the molecules.

For the AEP, the MS successfully confirmed the assembly of the 10 amino acids peptide with a theoretical MW1350.9 Da which appeared in as a peak of intensity $0.22*10^5$. The main peak of 450.9 triple positive-charged with intensity $6.8*10^5$, clearly represents the related ion of AEP according to the equation 1.1 (m/z = (1351+1.008*3)/3). While the double positive-charged ion with m/z 675.9 at intensity $2.2 *10^5$, theoretically corresponds to the AEP related ion (m/z = (1351+1.008*2)/2) (Fig.4.6).

In case of AEP-K-FP, the spectrum has proved a successful functionalisation of dendron. The dominant peak (645 with triple positive charge) of intensity $6.9*10^3$ refers to the theoretical MW (m/z = (1932+1.008*3)/3). Alternatively, the peaks 484 with quaternary charge at $3*10^3$ intensity and 967 with double charge at $1.7*10^3$ intensity, represent the related ions of AEP-K-FP (m/z = (1932+1.008*4)/4 and m/z = (1932+1.008*2)/2 respectively (Fig.4.7).

The results also demonstrated the presence of additional peaks, which although in trace amounts, are mostly attributed to fragments of the indicated sequence and system noise, or may due to sodium salt formation resulting normally from ionisation with glassware used in procedure. However, these results confirmed the successful synthesis of each of the desired molecules.

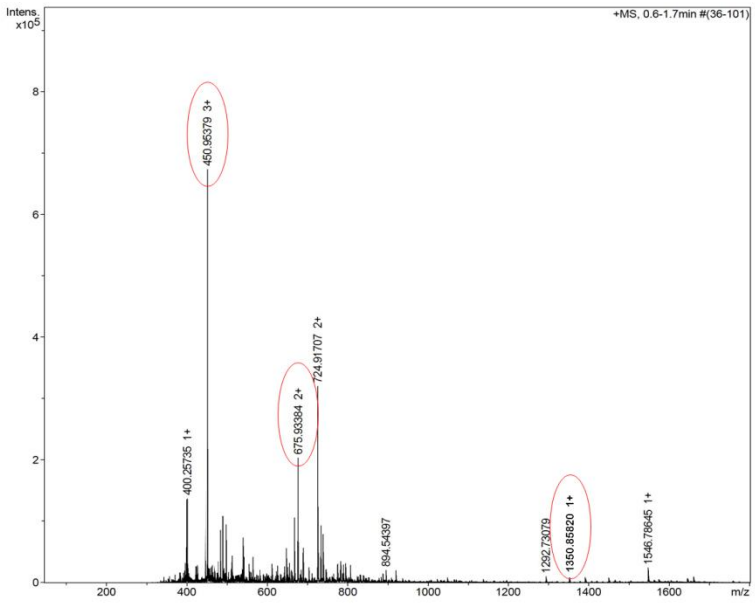

Fig.4.6: MS of AEP. It demonstrates the successful synthesis of the peptide with a theoretical MW = 1351Da.

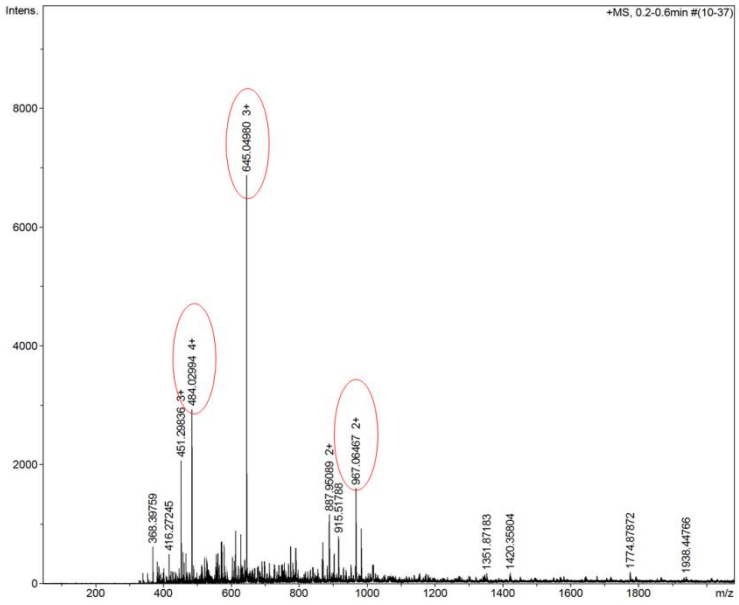

Fig.4.7: MS of AEP-K-FP. It demonstrates the successful attachment of the AEP with dendronised drug with a theoretical MW = 1932 Da.

4.4.2 Characterisation of AEP and AEP-K-FP by FTIR

FTIR has revealed a shifting of peaks due to the formation of amide linkages at 3200 and 1646 cm^{-1} that confirm the assembly of AEP and its attachment to the dendronised drug (Fig.4.8). Furthermore, the peak at 697 cm^{-1} in the conjugated molecule (AEP-K-FP)

spectra, which relates to the aromatic ring of FP, provides further evidence of the successful attachment.

The spectra of AEP-K-FP (Fig.4.8.a, c and d) showed a deformation vibration in N–H at 1646 and 3200 cm^{-1} referring to the peptide linkage formation. Furthermore, a new carbonyl band occurred at 1040 cm^{-1} in the AEP-K-FP spectra, which corresponds to C-O functional group of the FP. In addition to the disappearance of the peak at 1700 cm^{-1} that represents the carboxylate ion of FP, and appearance of new peak at 1646 cm^{-1} in AEP-K-FP spectra signifies the amide linkage formation between free surface amine groups of the AEP and carboxyl group of FP. In this regard, the appearance of a peak at 782 cm^{-1} related to the aromatic ring of FP in the conjugated molecule spectra, demonstrated successful drug attachment (Fig.4.8.a, b and d).

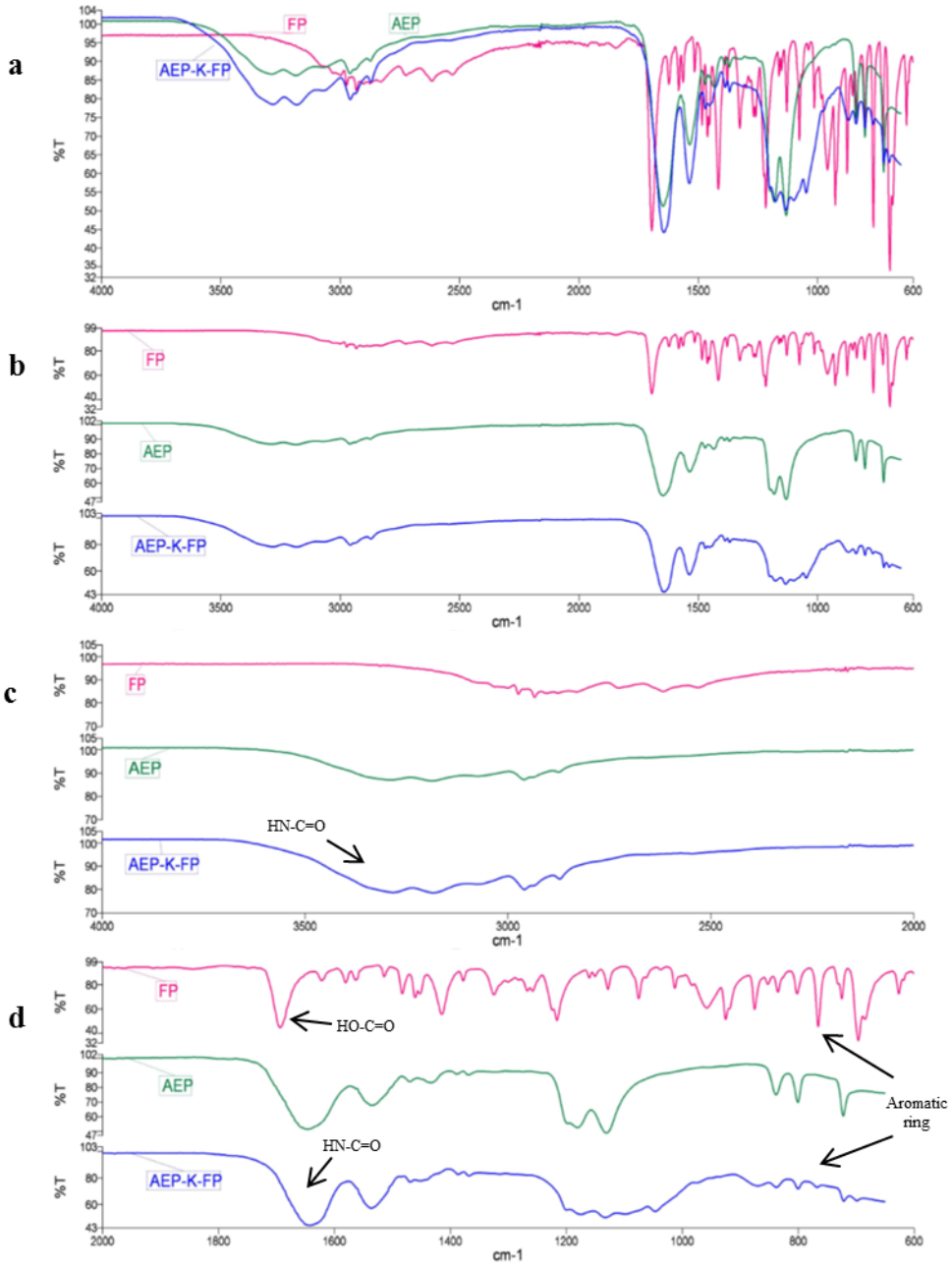

Fig.4.8: FTIR spectrum of free FP and AEP with and without FP. a: overall spectrum (overlay), b: overall spectrum (separated), c: spectrum 2000-4000 cm^{-1}, d: spectrum 600-2000 cm^{-1}. FTIR analysis is presenting the successful attachment of drug. Strong N–H deformation vibration corresponding to amide linkage formation can be seen at 3200 and 1646 cm^{-1}. AEP-K-FP spectra showed disappearance of peak at 1700 cm^{-1}, which corresponds to the COOH functional groups of FP due to peptide linkage formation, and appearance of a peak at 782 cm^{-1} related to the aromatic ring of FP.

4.4.3 Characterisation of AEP-K-FP by TLC and HPLC analysis

The purity of the AEP-K-FP was confirmed by TLC, only single spot was observed on the TLC plate under UV light signifying its purity and the Rf was 0.5 (Fig.4.9).

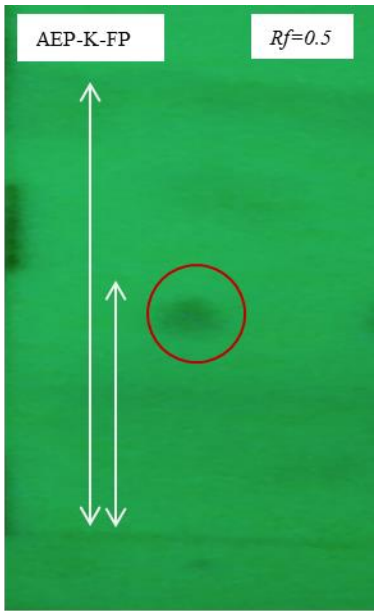

Fig.4.9: UV light irradiation of the TLC characterisation of AEP-K-FP. Only one spot appeared (Rf = 0.5).

Prior to HPLC analysis, AEP and AEP-K-FP were analysed spectrophotometrically to verify the λ_{max} (Fig.4.10) which shows the λ_{max} at 248 nm wave length. The HPLC-UV/VIS analysis of the purified AEP-K-FP showed the elution of a single peak at 9.8 min (Fig.4.11), supporting the finding of high purity from MS and TLC analysis. The HPLC analysis of the control and the back ground solvent are presented in the Section 2.4.3.

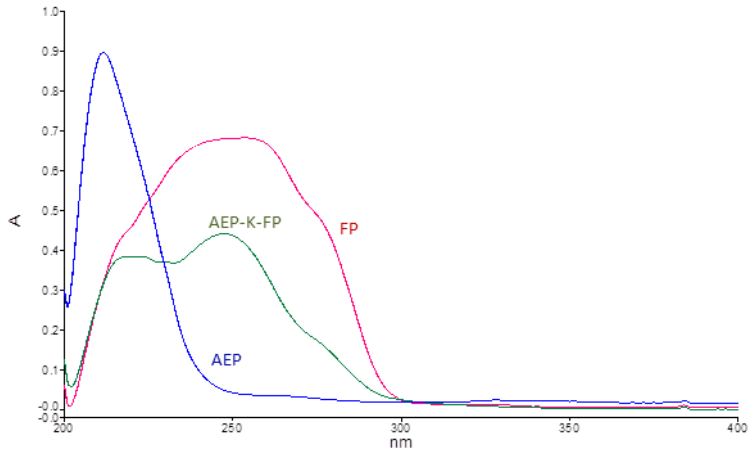

Fig.4.10: Spectrophotometric analysis. It is demonstrating the λ_{max} of FP, AEP and AEP-K-FP.

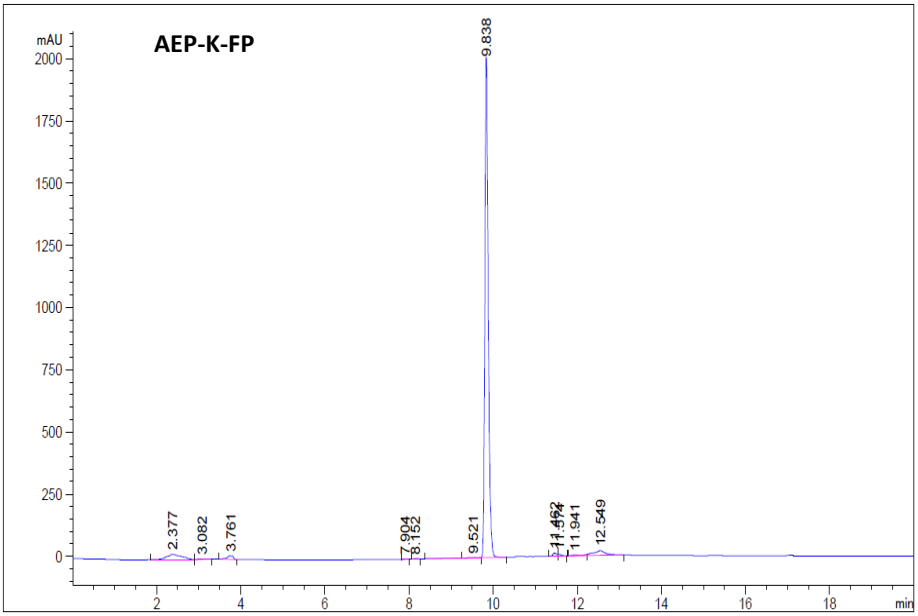

Fig.4.11: HPLC analysis of AEP-K-FP. The retention time is at 9.8 min. The analysis was performed on a hydrophobic C18 column, at 25^{o}C, 20 µL of injection volume, the flow rate was 0.6 ml/min and the wavelength was 248 nm.The HPLC mobile phase solvents gradient was 75:25 to 25:75 water: acetonitrile over 20 min.

4.4.4 MTT assays of AEP and AEP-K-FP

Results of MTT analysis have showed that there is no cytotoxic effect over 24 hr for the range of concentrations used in experiments (25-400 µM) for both AEP and AEP-K-FP, thus indicating no reduction in cell metabolic activity by giving values more than 50% in relation to the control untreated cells (Fig.4.12.a). The values decreased with increasing concentration of molecules, as were seen with the highest concentration (400 µM) to be 85.2% and 78.7% for AEP and AEP-K-FP respectively.

The results after 48 hr treatment were similar to those seen at 24 hr (Fig.4.12.b). The AEP-K-FP at concentration 400 µM showed the lowest levels of cell metabolic activity to be 76.8%. In addition there was no significant differences ($P>0.05$) in the levels of cell metabolic activity at the same concentration in different exposure periods (24 and 48 hr treatment).

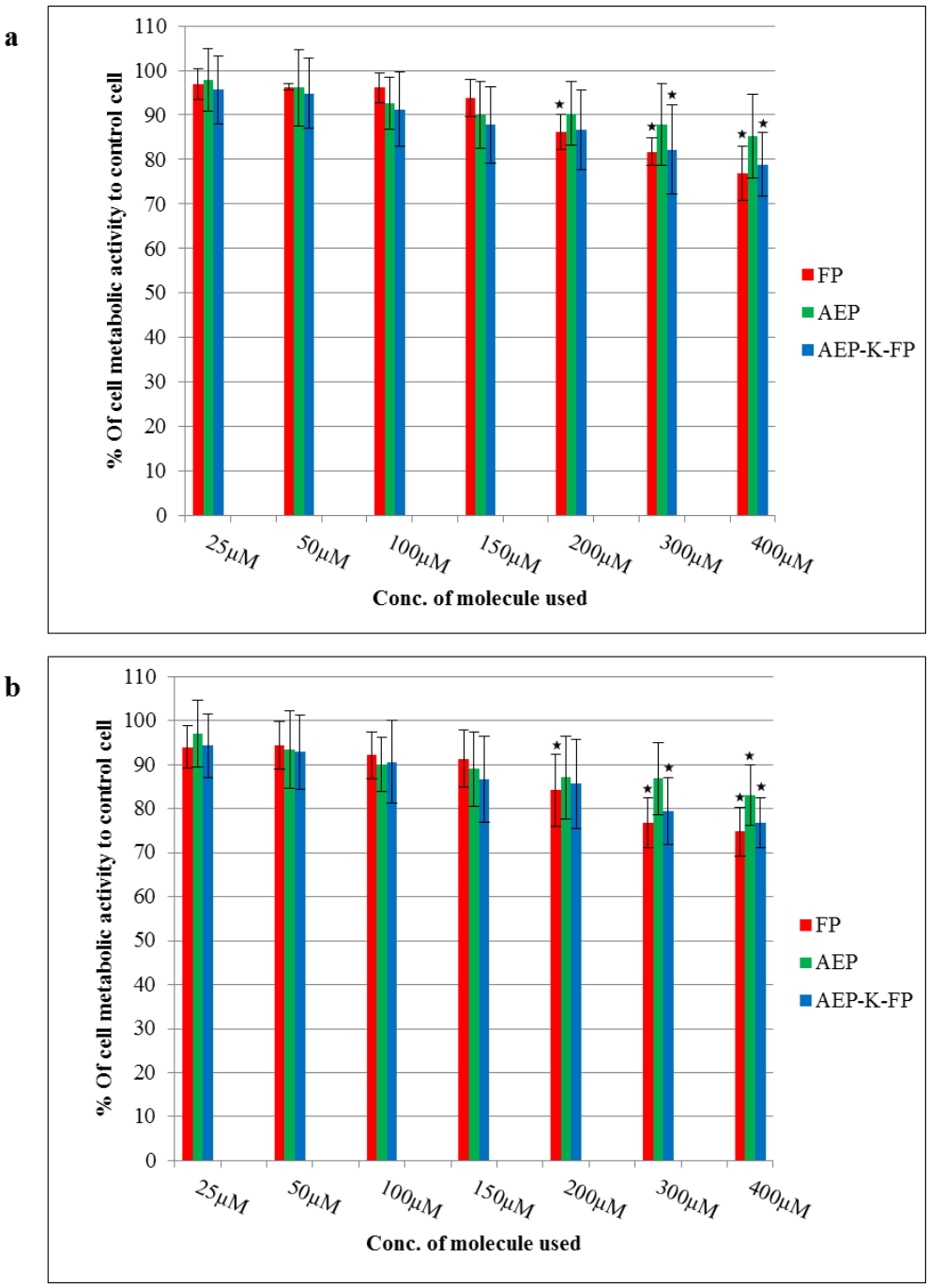

Fig.4.12: MTT results of bEnd.3 cells treated with free FP and AEP with and without FP. a. after 24 hr treatment. b. after 48 hr treatment. The absorbance was measured and the cell metabolic activity was calculated as a percentage of absorbance in relation to control untreated cells. Values marked asterisk are with significant difference to control ($P<0.05$). The data represent mean ± SD of n = 6.

4.4.5 LDH assay for evaluation of cytotoxicity of AEP and AEP-K-FP

Using the LDH assay, again, no cytotoxicity was apparent in the concentration range used (25, 50, 100, 200, 300 and 400 µM) of AEP and AEP-K-FP after 24 hr of treatment (Fig.4.13. a). The results of 48 hr treatment remained within acceptably low toxicity range for all peptides with and without drug as all levels were less than 50% of positive control (Fig.4.13. b). The highest LDH release was accompanied with the 400 µM concentration of molecules in which the AEP-K-FP showed 8.3% after 24 hr and 9.9% after 48 hr. Both results for 24 and 48 hr are significantly different to positive control (complete lysis) ($P<0.001$). Whereas no significant differences ($P>0.05$) were found between 24 and 48 hr exposure period at the corresponding concentration.

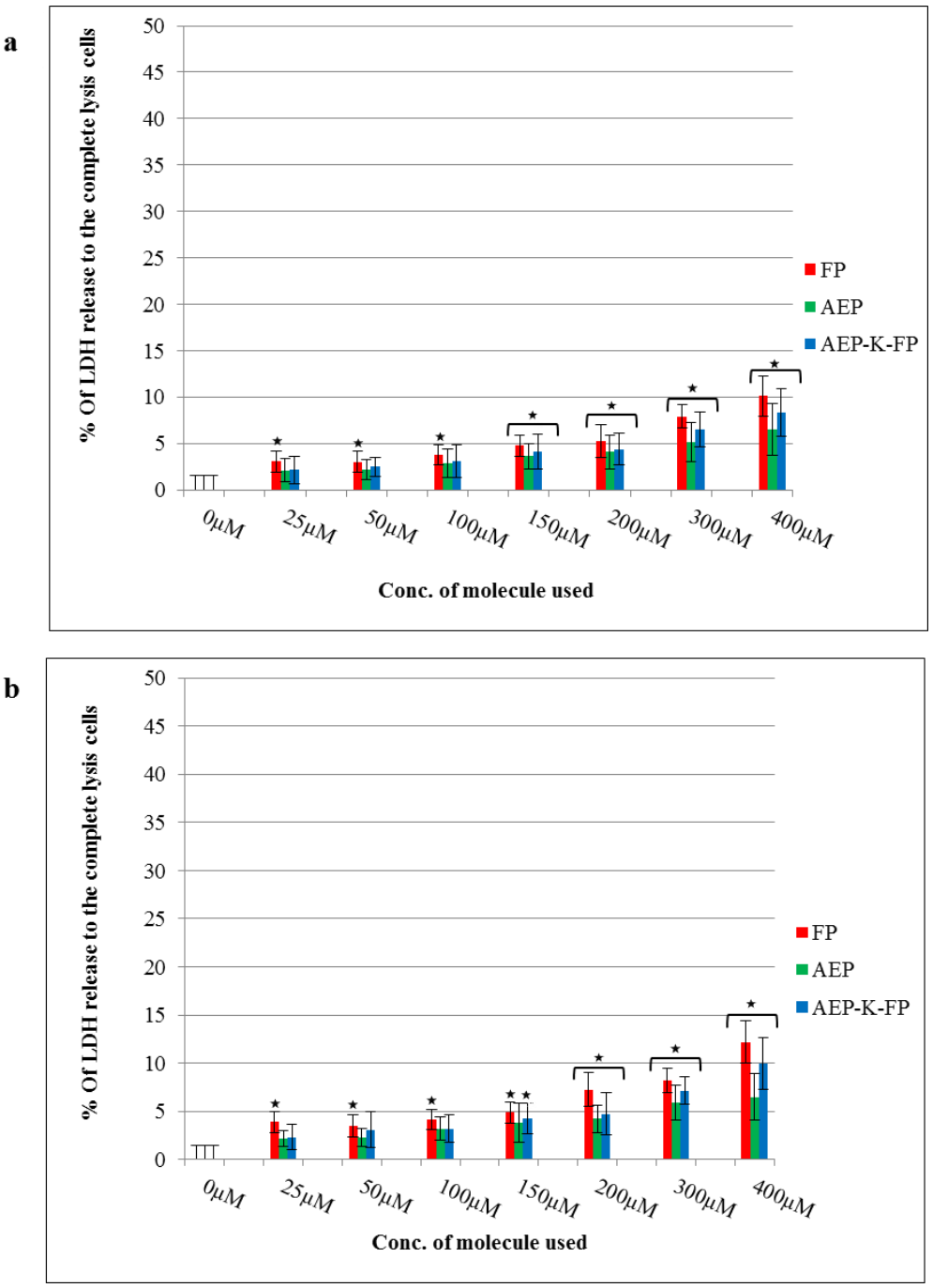

Fig.4.13: LDH results of bEnd.3 cells treated with free FP and AEP with and without FP. a. after 24 hr treatment. b. after 48 hr treatment. The absorbance was measured and the LDH release of each was calculated as a percentage of absorbance in relation to control and complete lysis untreated cells. There is a significant difference to positive control ($P<0.001$) in all values. Values marked asterisk are significantly different to negative control ($P<0.05$). The data represent mean ± SD of n = 6.

4.4.6 HPI Cell death assessment of the AEP and AEP-K-FP

HPI staining revealed no cytotoxicity was apparent and is consistent with those obtained from both MTT and LDH assays, following treatment with AEP and AEP-K-FP. The percentage of healthy cells at all concentrations used (100, 300 and 400 µM), for both products, were not less than 91%. While the values of apoptotic and necrotic cells did not exceed 4.7% and 3.4% respectively that showed by the AEP-K-FP at a concentration of 400 µM (Fig.4.14 and 4.15). Hence, there is no significant differences (P>0.05) from the control samples at all concentrations.

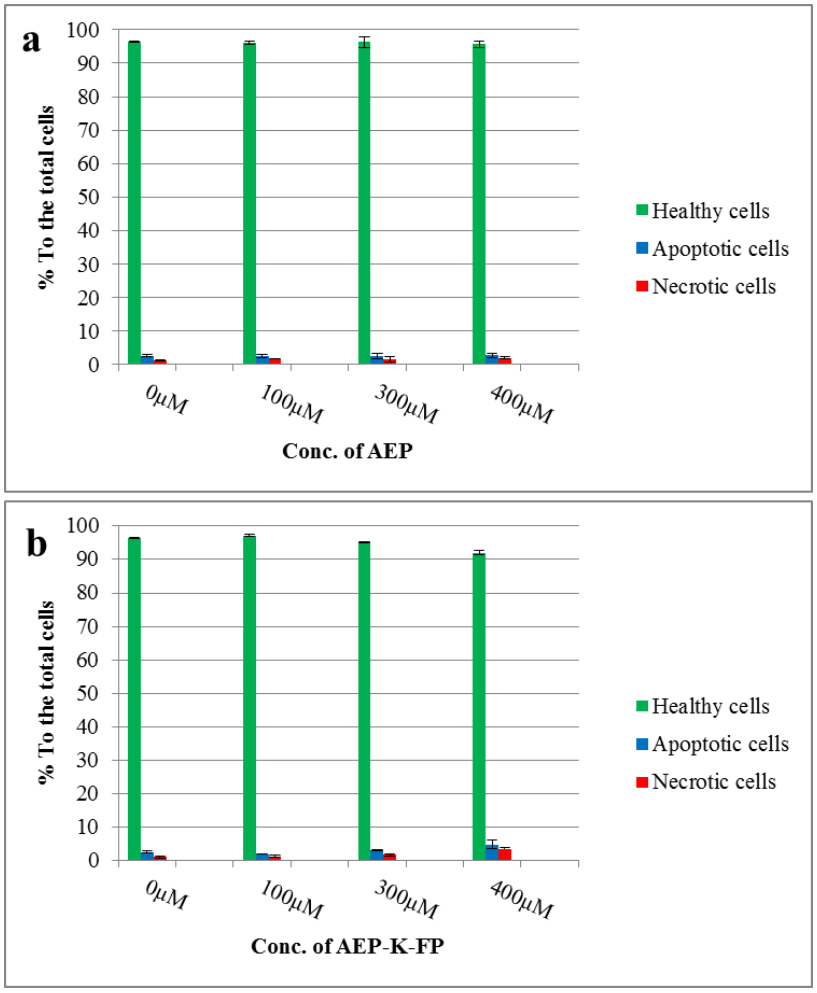

Fig.4.14: HPI results on bEnd.3 cells. a. For the AEP. b. For the AEP-K-FP. The microscopic pictures were taken and the healthy, apoptotic and necrotic cells of each were calculated as a percentage to the total number of cells in each field, no significant differences from the control (P>0.05) appeared. The data represent mean ± SD of n = 6.

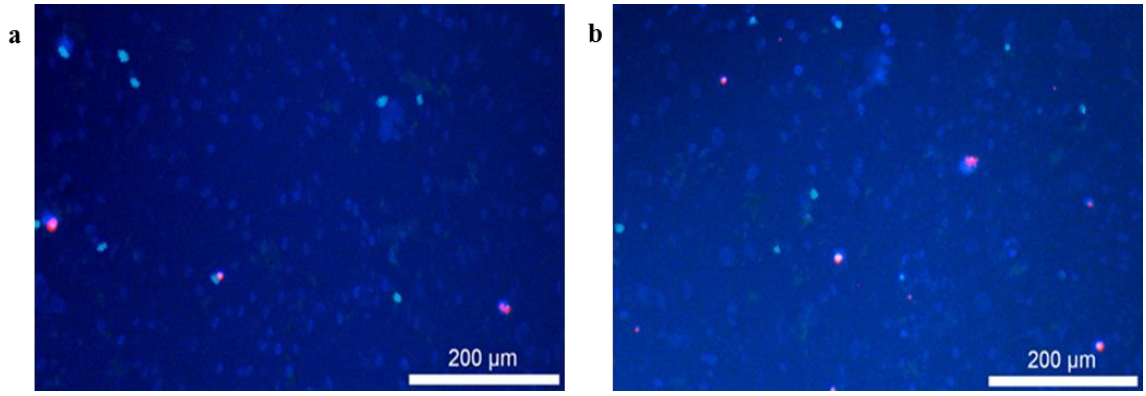

Fig.4.15: Examples of microscopic pictures after HPI staining. a. For the AEP. b. For the AEP-K-FP. The blue cells represent the healthy living cells while the bright blue refers to apoptotic cell and the red is necrotic cells.

4.4.7 Cytotoxicity related to HUVEC

Biochemical investigation of FP, AEP and AEP-K-FP has been also undertaken on HUVEC cells to ensure their non-cytotoxicity on different tissues.

The MTT results after 24 and 48 hr treatment revealed no cytotoxicity even with the highest concentration used (400 µM) as it is still giving more than 50% of cell metabolic activity to be 83% and 80.2% after 24 and 48 hr treatment respectively with AEP-K-FP (Fig.4.16. a and b).

Furthermore, no cytotoxicity was seen in the results of LDH assays undertaken on HUVEC cells after 24 and 48 hr treatment with FP, AEP and AEP-K-FP as the values of LDH release were less than 50% in relation to the positive controls, with a significant difference ($P<0.001$) (Fig.4.17. a and b). Again, the highest values of LDH release were seen with the highest concentration of treatment (400 µM) of AEP-K-FP which showed 8.5% and 8.7% after 24 and 48 hr exposure period respectively.

No significant differences ($P>0.05$) were found when both MTT and LDH values compared statistically with those of the bEnd.3 cell line type.

In addition, for both MTT and LDH assays, the results after 48 hr showed no significant difference ($P>0.05$) from those of 24 hr results.

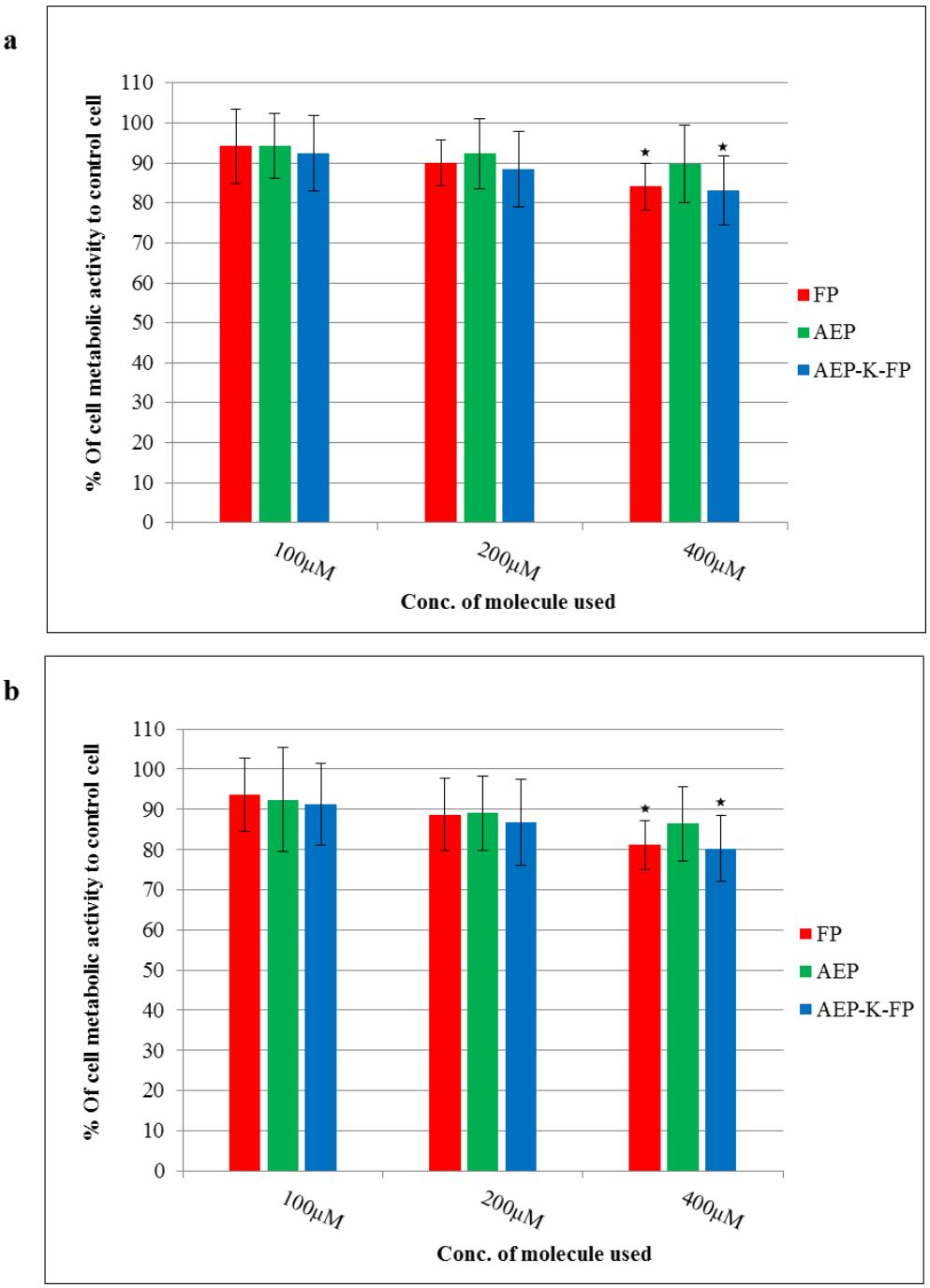

Fig.4.16: MTT results of HUVEC cells treated with free FP and AEP with and without FP. a. after 24 hr treatment. b. after 48 hr treatment. The absorbance was measured and the cell metabolic activity was calculated as a percentage of absorbance in relation to control untreated cells. Values marked asterisk are with significant difference to control ($P<0.05$). The data represent mean ± SD of n = 6.

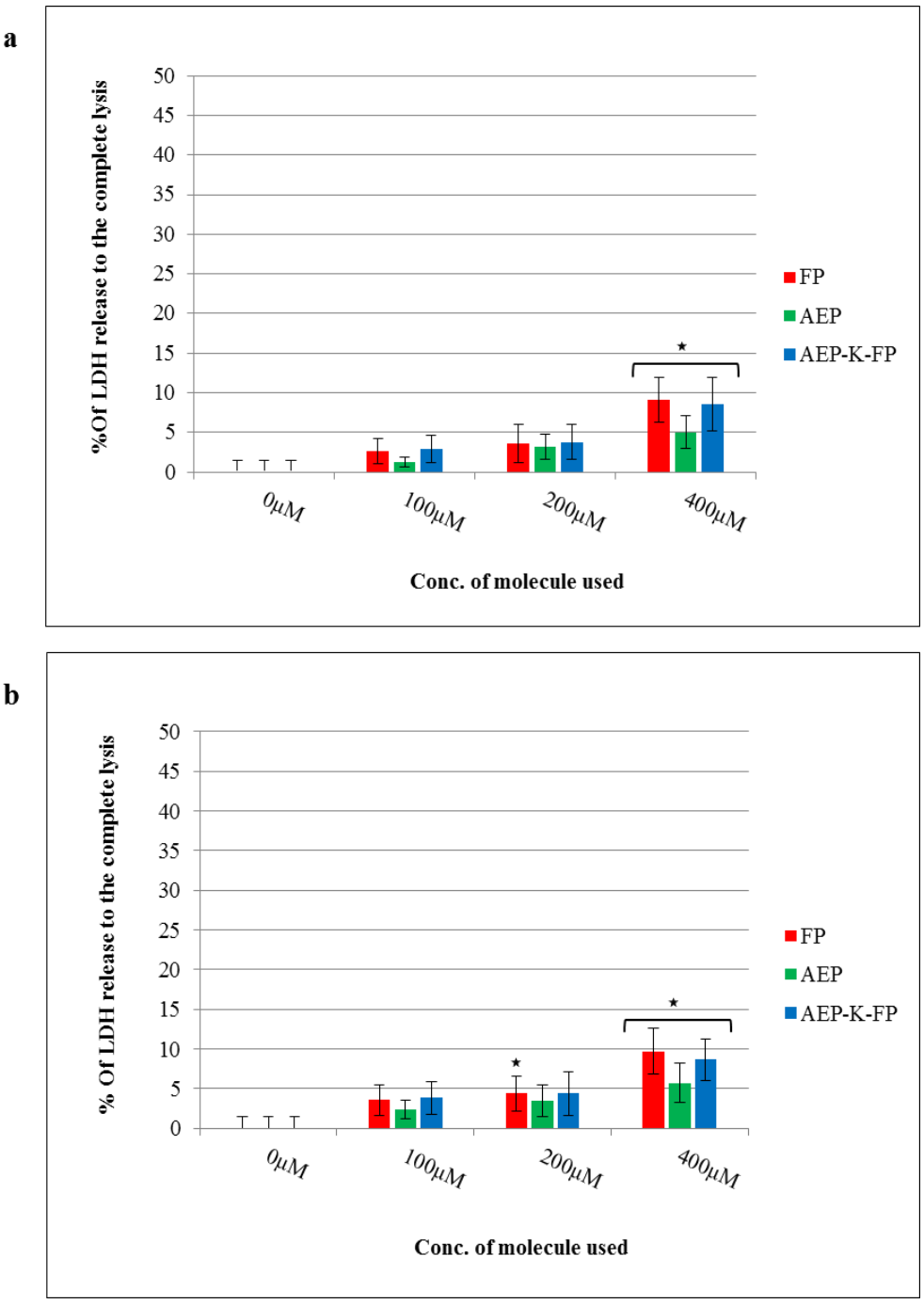

Fig.4.17: LDH results of HUVEC cells treated with free FP and AEP with and without FP. a. after 24 hr treatment. b. after 48 hr treatment. The absorbance was measured and the LDH release of each was calculated as a percentage of absorbance in relation to control and complete lysis untreated cells. There is a significant difference to positive control ($P<0.001$) in all values. Values marked asterisk are significantly different to negative control ($P<0.05$). The data represent mean ± SD of n = 6.

4.5 Discussion

AD is one of the most prevalent NDs worldwide in which the effective therapy and targeting remain a huge unsolved problem (Re *et al.*, 2010). Most large bioactive compounds cannot penetrate through cellular membranes, hindering their transport across the highly tight and compact endothelial layer of the BBB. The delivery of potential therapeutic agents therefore requires active-transport mechanisms to enable these molecules to cross the BBB and exert their biological action. In common with other therapeutics, FP is unable to efficiently permeate through the BBB. Several strategies to improve the delivery to the CNS have been developed including local injection or BBB opening, enhancing the drug permeability and targeting delivery to the brain (Boer *et al.*, 2007).

More recently, it has been recognised that dendrons as carriers equipped with penetration facilitating and targeting ligands are effective tools for the delivery of the drugs to the brain as a function of their structural properties that allow multifunctionalistion (Madaan *et al.*, 2014; Srinageshwar *et al.*, 2017; Srinivas *et al.*, 2014).

In the last decay, brain drug delivery has focused on mechanisms that can use endogenous endothelial receptors in promoting BBB passage for specific particles by RMT (Re *et al.*, 2011). This pathway employs the endothelial vesicular trafficking mechanism to transport molecules from blood to brain. With an appropriate receptor targeting ligand, RMT systems can shuttle a variety of drugs into the brain noninvasively (Jones *et al.*, 2007). Upregulation of the LDLr gene family in the BBB region in comparison with other endothelia can support this hypothesis through the recognition of endogenous ligands such as ApoE. The evidence from different studies have shown that the LDLr participated in the transport of a wide range of substances from the blood to the brain following functionalisation of the carrier system with peptide derived from the binding site of ApoE (Molino *et al.*, 2017).

In the present study, the dendron was functionalised with drug (FP) at the amine ends, and at its root with AEP (the 141-150 amino acids sequence) which corresponds to the ApoE-binding domain with cell surface LDLr (Re *et al.*, 2011). To achieve this, microwave Fmoc-based SPPS was employed and the AEP was synthesised followed by its coupling to the dendronised drug. According to the dendron's architecture, it can be efficiently

functionalised at its core with specific bioactive molecules such as ligands, and at its uppermost branching with drug molecules.

The AEP and AEP-K-FP synthesis were obtained by employing typical Fmoc chemistry for amino acids assembly by SPPS that efficiently synthesises difficult peptide sequences with a high degree of purity. The type of α-amino protecting group and the type of side-chain protection of amino acids should be taken into consideration to obtain the desired peptide synthesis. For this reason, Fmoc-Lys(Boc)-OH, has been used to obtain a linear chain of AEP, whereas Fmoc-Lys(Fmoc)-OH has been used for branched dendron. Thus ensures the formation of the amide linkage in the site of interest only and prevents unwanted reactions that could result in the formation or incorporation of dipeptide derivatives (Albericio, 2000). However, there are some of limitations associated with this technique, especially with long chain peptides, such as intermolecular aggregation and truncated sequence (Shin *et al.*, 2005). In order to overcome this issue, capping steps have been introduced after each amino acid coupling. Using acetic anhydride as a terminating agent helps block the amino acids chain that have failed to couple and permanently stop their up growing during the synthesis. Eventually, any short chain sequences formed are easily separated and isolated from the desired one, in turn leading to more purified product, as confirmed by MS, TLC and HPLC results of this work (shown in Fig.4.7, 4.9 and 4.11). Subsequently, Fmoc chemistry and capping can help in the purification of the final product to be used efficiently in the following experiments.

The superior architecture features of dendron which offers bifunctionalisation elucidate its immense versatility in various applications including drug and gene delivery (Ebelegi *et al.*, 2017). Previously studied drug delivery has shown an efficient functionalisation of PAMAM dendrimers with both carboxymethyl PEG5000 and folic acid leading to a highly cell-specific targeting and more folic acid delivering (Srinivas *et al.*, 2014). Moreover, it has been shown that the ability of a bifunctionalised PAMAM with ligands (Tf or Lf) to deliver doxorubicin to the brain was enhanced in comparison to the unfunctionalised dendrimer (Huang *et al.*, 2008). In addition the brain permeability of opioid peptide improved when integrated to a OX26-functinalised dendrimer (Yuan *et al.*, 2011), whereas the angiopep-functinalised PAMAM was used efficiently in gene delivery (Xu *et al.*, 2014).

Furthermore, the results of a recent study showed that functionalised VEGF-bound magnetic NPs conjugated with poly-lysine dendron tethered with carboxybetaine at uppermost branching could control the delivery of VEGF (Meikle *et al.*, 2016).

Prior to use these synthesised molecules as delivery systems, their biocompatibility should be assured (Tomalia *et al.*, 2005). In this work, the peptide and its coupling to dendronised drug up to 400 µM concentration were not accompanied with a significant reduction in cell metabolic activity after 24 hr and 48 hr exposure periods (Fig.4.12. a and b and Fig.4.16. a and b) in both bEnd.3 and HUVEC cell lines. Hence, these values signify there is no considerable effect on mitochondrial function when compared to control cells.

However, the observations regarding fewer viable cells with the higher concentrations of the peptide are probably attributed to the increasing cytotoxic behaviour with excessive positively charged amino groups or to the increased permeability across the cell membrane via RMT. Consequently, these could cause more cell membrane damage and affect the mitochondrial function and cell viability (Prashant, 2014). Current data are consistent with previous toxicity studies which demonstrated that the toxic effect of ApoE peptide rises with higher concentrations. It has been found that the cell metabolic activity of primary rat brain capillary endothelial cells, RBCECs, was dependent on the peptide concentrations (Sauer *et al.*, 2005).

Furthermore, both coupled and uncoupled AEP molecules did not show any significant effect on cell membrane integrity according to the LDH assay results (Fig.4.13.a and b and Fig.4.17.a and b). In same pattern seen in the MTT assay results, higher LDH release values were observed with higher concentrations of AEP-K-FP even though these values remain within the acceptable toxicity range and were far lower than that obtained from the positive control. Cell death assessment by HPI staining also confirmed the findings of MTT and LDH assays where the treated cells have undergone very low apoptosis and necrosis (Fig.4.14). This is perhaps due to the ability of the peptide to cross the cells via transcytosis process without affecting their nuclei (Majno *et al.*, 1995).

These findings indicate the non-cytotoxicity of the synthesised molecules (AEP and AEP-K-FP) and are in agreement with other studies that showed no cytotoxic impact when investigating the AEP. Re *et al* (2011) have illustrated that ApoE and ApoE-decorated NLs (at tested concentrations) were nontoxic after up to 48 hr of incubation with brain

endothelial cells using the MTT assay and the reported neurotoxicity at higher concentration was attributed to liposomes rather than the peptide (Re *et al.*, 2011). A further study demonstrated that the cytotoxic effect of ApoE-modified NPs was excluded after cell metabolic activity determination when incubated with bEnd.3 cells at different concentrations for 24 hr using cell proliferation and viability WST-1assays (Zensi *et al.*, 2009).

Interestingly, the impact of AEP-K-FP molecule on the cellular cytotoxic response in this work was relatively higher than that of AEP alone. This increased effect may be owed to the amount of FP that was integrated into the peptide (as it bears 2 molar excess of drug molecules) which could change some of the physico-chemical behaviours of this conjugate (Eriksen *et al.*, 2003; Meister *et al.*, 2013) resulting in more cytotoxic effect. Another hypothesis to explain this issue could be the penetrability of the peptide via cell surface receptor engagement leading to more bound drug entry into the cells, which in turn could have more influence on mitochondrial function or LDH release levels. In a previous *in vitro* study, the transendothelial permeability of curcumin was found higher when incorporated into ApoE-NLs which is attributed to the transcytosis process occurred as a subsequent of interaction with cell surface through LDLr binding. Therefore, functionalisation of NLs with ApoE-peptide enabled curcumin to cross the BBB and consequently elevate its brain bioavailability (Re *et al.*, 2011). A supported observation from further study showed the improvement in transport of drug (dalargin)-loaded NP coated with ApoE across the barrier via LDLr binding transcytosis (Sauer *et al.*, 2005).

The evidence in the current study of the successful bifunctionalisation of dendrons with AEP and conjugation of the drug with good biocompatibility suggests this system can provide a noninvasive and safe carrier system for drug targeting to the brain. In addition, it is expected to improve cell permeability of FP through RMT increasing its bioavailability with fewer doses that is highly preferred to decrease patient compliance.

Moreover, the targeting ability of the carrier system can reduce the adverse effects associated with non-targeting carriers which lead to distributing the drug to all body tissues. Therefore, the selective delivery of the drug in conjugation with dendronised AEP could result in less drug loss throughout the circulation and less destructive effects to other organs.

Accordingly, the designed carrier system in this work (dendronised AEP) has a promising possibility to be used for the targeting the brain to deliver not only FP but also other poor-penetrating drugs, genes and diagnostic agents.

4.6 Conclusion

In conclusion, the dendron presented here have been shown to be efficiently bifunctionalised with FP at their upper branches and at its root with APE using Fmoc-SPPS optimised methods, yielding a novel brain targeting carrier system. Furthermore, the purity of this product is sufficient to be taken forward for future studies.

The non-cytotoxicity of the AEP-K-FP also provides further justification to the investigation of this molecule's ability to cross the BBB and boost the drug permeability into the brain (Chapter 5).

Chapter 5. Evaluation of the Cellular Uptake and Permeability of the FP-Integrated Dendronised Molecules

5.1 Introduction

The cellular uptake, transport and performance of drugs to their target sites are unmanageable challenges in the treatment of NDs due to the presence of the BBB (Pardridge, 2005). Hence, various approaches have been developed to overcome this issue; including invasive techniques, chemical modifications and enhanced permeability via endogenous transcytosis (details in Section 1.5). Currently, enhancing permeability via endogenous transcytosis is considered the most attractive option as it enables the drug to undergo transcytosis into the brain effectively and safely (Re *et al.*, 2012).

This approach was exploited in this study using the synthesised dendrons functionalised with AEP after being successfully loaded with drug to increase its ability to cross the BBB. Currently, FP fails to reach its target inside the brain at therapeutic concentrations (150-250 μM) because of very low BBB permeability (Green *et al.*, 2009; Meister *et al.*, 2013; Wilcock *et al.*, 2008), integrating the drug with a specific carrier system will enhance its permeability. The potential of dendrimers to undergo endocytosis and carry drugs across the BBB has previously been demonstrated (Cheng *et al.*, 2007; Gagliardi, 2017; Najlah *et al.*, 2007; Teow *et al.*, 2013). Indeed, functionalisation with AEP as a ligand for LDLr can make carrier systems more efficient for selective brain drug delivery via RMT (Bana *et al.*, 2014; Re *et al.*, 2010).

5.1.1 Endocytosis and Trancytosis

Endocytosis is a process of molecule engulfment by the cells. Endocytotic pathways can be divided into phagocytosis and pinocytosis (Tuma *et al.*, 2003). Phagocytosis or "cell-eating" involves the plasma membrane engulfment of solid molecules such as nutrients and it is also used for defending the body against foreign substances such as pathogens and cell debris. In this process only specialized cells such as macrophages are capable of phagocytosis. This internalisation results in the formation of vesicles which are subsequently digested by lysosomes (Xiao *et al.*, 2013) (Fig.5.1).

Whereas, pinocytosis or "cell-drinking" or "fluid endocytosis", is a fluid-phase endocytosis in which cell membranes form vesicles to ingest small dissolved particles and fluids into the cell. These vesicles are subsequently fused with lysosomes and digested.

Another mode of pinocytosis is transcytosis which could be either RMT or AMT (Xiao *et al.*, 2013).

In fact, transcytosis occurs when the endocytic vesicles are exocytosed into the external cellular side. In RMT, a specific ligand binds with the membrane receptor, this membrane reinforcement forms "caveolae" subsequently resulting in small vesicle formation (<100 nm in diameter) followed by its exocytosis (Jones *et al.*, 2007; Xiao *et al.*, 2013) (Fig.5.1).

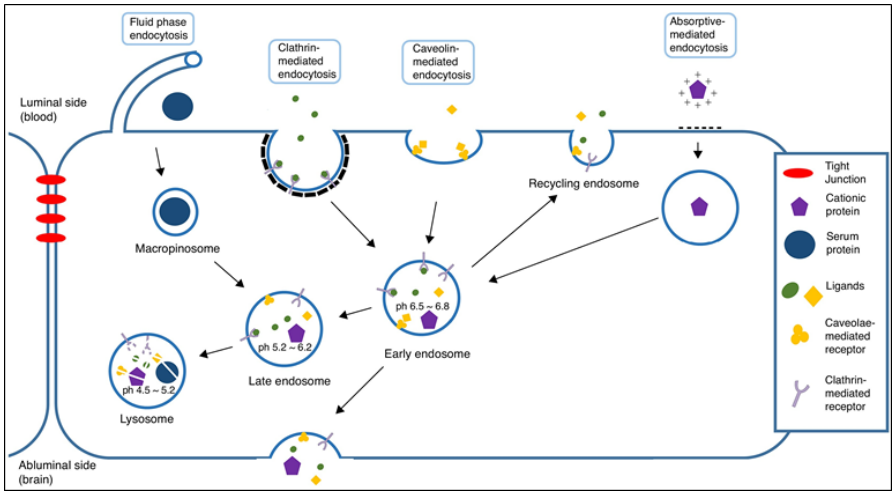

Fig.5.1: Cellular endocytosis and transcytosis pathways. It is showing the engulfment of solid materials and fluids by pinocytosis into cytoplasm following by their degradation by lysosomes. AMT and clathrin-mediated endocytosis involves the formation of vesicles which matures to early endosomes, and the cargo can subsequently be degraded or undergone transcytosis. RMT begins with the formation a caveolae followed by delivery of the receptor-ligand complex and transcytosis (Goulatis *et al.*, 2017).

In the case of AMT or marcopinocytosis, the internalisation of cationic substances occurs via clathrin-mediated, energy-dependent endocytosis following interaction with the negative charges at the cell membranes (Teow *et al.*, 2013; Tuma *et al.*, 2003). For this reason, AMT and RMT are broadly exploited in scientific research for crossing the BBB and delivering drugs to the brain (Chen *et al.*, 2012; Xu *et al.*, 2014).

It has been found that cationic dendrimers such as poly lysine and PAMAM have efficiently improved the permeability of several drugs such as paclitaxel, ketoprofen, naproxen and diflunisel across brain endothelial cells and other cellular membranes (Cheng *et al.*, 2007; Najlah *et al.*, 2007; Teow *et al.*, 2013).

In addition, bifunctionalisation of PAMAM with different types of ligands including Tf, OX26 and angiopep-2, increased BBB permeability and targeting for a variety of drugs such as doxorubicin, opioid peptide and a range of plasmids (Xu *et al.*, 2014). Besides the

aforementioned receptor-binding ligands, ApoE peptides have also been used as a ligand for improved drugs permeability and targeting of BBB via RMT (more details in Section 4.1)

To predict the brain penetration of substances and confirm the validity of transporter strategy, a number of different BBB models have been used.

5.1.2 BBB models

The developments that have occurred over the last two decades in the field of BBB modelling have been primarily affected by two factors: (1) the need to increase the understanding of the complicated mechanisms which regulate brain function and (2) to enhance the development of new and effective pharmacological protocols which target the brain. It is a highly challenging task within the development of novel CNS therapies to find a vascular environment that sufficiently mimics the functional properties of the BBB (Naik *et al.*, 2012).

For this purpose, numerous types of *in vivo*, *in vitro* and *in silico* BBB models have been developed and established for determining the brain permeability of molecules as well as understanding of the transport pathway (Shityakov *et al.*, 2013). Although *in vivo* BBB models give more reliable data for substance penetration, they are very expensive in terms of effort, resources and time. Therefore, they are only suitable at more advanced stages of the novel molecules development (Naik *et al.*, 2012). While *in silico* studies are entirely performed via computer simulation (Clark, 2003).

Alternatively, *in vitro* BBB models, based on culturing primary or immortalised brain endothelial cells on Transwell systems are considered as a bridge between *in silico* and *in vivo* models. This model has been extensively used in drug BBB permeability studies and because of its simple design became cost-efficient and high-quality screening (Eigenmann *et al.*, 2013). Several major requirements should be available in an *in vitro* BBB model to mimic the *in vivo* situation (Fig.5.2). One of the most essential of these characteristics to ensure BBB validity is its ability to form endothelial TJs in between adherent ECs resulting in a stringent and selective barrier (Shityakov *et al.*, 2013).

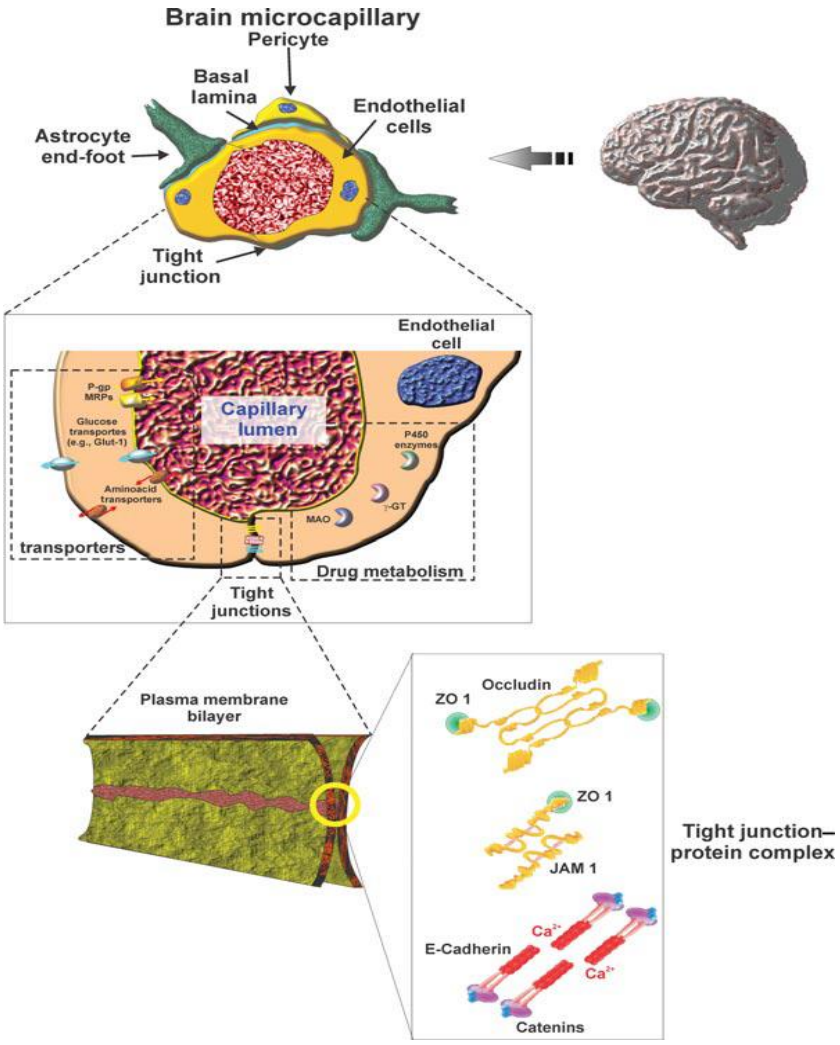

Fig.5.2: Schematic diagram represents a typical BBB. The barrier prevents crossing of substances into the brain. Presence of TJs in between cells prevents paracellular diffusion of water soluble molecules and express specific functional transport systems (Naik *et al.*, 2012).

The immortalised brain capillary endothelial cell line, bEnd.3, functionally expresses several significant features required when the cell culture is to be used to assess drug uptake and transport. Previous studies have clearly demonstrated that bEnd.3 cells expressed TJ proteins such as occludin, claudine, actin and ZO (Brown *et al.*, 2007; He *et al.*, 2010; Omidi *et al.*, 2003; Pachter *et al.*, 2003). The studies have also shown that mRNA and proteins for different TJs were highly expressed in bEnd.3 cells (Brown *et al.*, 2007; Omidi *et al.*, 2003; Pachter *et al.*, 2003). These TJ proteins are essential components that form and maintain the functional and physical paracellular barrier properties (Bauer *et al.*, 2016; Morita *et al.*, 1999) (see Section 1.3.4).

As a result, bEnd.3 culture using a Transwell system is a preferred method to be used as an *in vitro* BBB model to assess the penetrability of the FP-integrated dendronised carrier systems developed in this thesis.

5.2 Aim of the chapter

The aims of this chapter are to:

1. Validate an *in vitro* BBB model via using a culture of bEnd.3 on Transwell insert system and measuring the trans-epithelial electrical resistance (TEER).
2. Evaluate the validity of this system biochemically using sucrose as a paracellular marker, in addition to morphological evaluation by confocal laser scanning microscope (CLSM) using HUVEC cells as negative control.
3. Study the cellular uptake of dendronised molecules (G0K, G1K and AEP-K).
4. Evaluate the potential of dendron and dendronised AEP to improve FP permeability across this *in vitro* BBB model.

5.3 Materials Experimental methods

5.3.1 Validation of the in vitro BBB model

5.3.1.1 Measuring the TEER

The bEnd.3 cell line was seeded into Transwell®-clear inserts plate (membrane of 0.4 µm pore size, Fisher Scientific, UK) at a density of $5x10^4$ cells/cm^2 and incubated in a humidified atmosphere (5% CO_2/95% air) with complete culture medium as detailed in Section 3.3.1. For the assessment of TEER between the apical and basolateral chambers, an Evom voltometer (World Precision Instrument, Sarasota, USA) was used. The TEER was measured everyday starting from day 1 up to 8 to determine the day at which maximum values were obtained indicating TJ formation and therefore the model's validity for undertaking permeability experiments. The measurements were taken in triplicate and compared to HUVEC results which were also seeded into Transwell-clear inserts. Cell-free Transwell inserts were included to exclude the resistance related to the inserts membrane alone (see Section 5.3.3). TEER was also measured after 24 hr treatment with the molecules under investigation to demonstrate the effect of these molecules on the cellular monolayer integrity.

5.3.1.2 Biochemical validation using sucrose

Sucrose, a water soluble substance with limited brain penetration, is used as a marker for paracellular permeability, where low permeability values indicate the tightness of the barrier (Pierre *et al.*, 1996).

In this work, sucrose permeability was measured by the glucose oxidase (GOD)/invertase method which is based on the following biochemical reactions (Teixeira *et al.*, 2012):

$$Sucrose \xrightarrow{Invertase} Glucose + Fructose$$

$$Glucose + O_2 + H_2O \xrightarrow{Glucose\ oxidase} Gluconic\ acid + H_2O_2$$

$$H_2O_2 + Phenol \rightarrow Benzoquinone\ (Pink\ color)$$

The cells were cultured to confluence on Transwell inserts (as mentioned above), at day 6 the culture media was removed and the cells were treated with 1 mL solution of sucrose / PBS at a concentration of 2 mg/mL. Samples were collected from the lower chamber after 15 and 30 min. In separate micro-centrifuge tubes, 5 µL of sample, 85 µL distilled water

(DW) and 10 µL invertase /DW solution (of 10 mg/mL concentration) (grade VII, Sigma Aldrich, UK) were added. Control tubes that contain only PBS instead of sample were also included.

The tubes were then securely sealed and placed in a water bath at 55˚C for 10 min. the tubes were then removed and 200 µL of GOD reagent (Sigma Aldrich, UK) was added and the tubes were re-sealed and placed in a water bath at 37˚C. After 15 min, the tubes were removed, 10 µL of phenol solution added incubated at room temperature for 5 min. Samples of 50 µL were transferred to a 96-well plate in duplicate and the absorbance was read at 490 nm using a spectrophotometer.

Tubes of standard sucrose solutions at concentration range 0-5 mg/mL were also prepared and analysed to construct a calibration curve to determine the sucrose concentration in the samples.

5.3.1.3 Morphological evaluation by confocal laser scanning microscopy

CLSM is an optical imaging technique frequently used for increasing contrast and optical resolution of a microscopic image via a spatial pinhole situated at the conjugate plane in front of the lens which eliminates "out-of-focus light" (Pawley, 2006). CLSM was used here to describe the morphological differences between the brain endothelial cells and other endothelium (HUVEC) by comparing the TJ formation in between the cells using rhodamine phalloidin staining.

Phalloidin is a bicyclic peptide toxin isolated from mushrooms and it is commonly used to identify and quantitate actin filaments in the cytoskeleton by selectively labelling the F-actin. The rhodamine phalloidin (tetramethylrhodamine (TRITC)) dye acts by binding and paralysing actin fibres preventing their depolymerisation. This binding results in red-orange fluorescence which can be detected by microscope using green filter (Cooper, 1987).

Cells (bEnd.3 and HUVEC) were first seeded to confluence in 24-wells plate at a density of $5x10^4$ cells/cm^2 and incubated in a humidified atmosphere (5% CO2/95% air). The cells were washed twice with PBS before fixing with 3.7% formalin for 30 min. The cells were then washed with PBS twice, and 100 µL of rhodamine phalloidin/PBS solution (Sigma Aldrich, UK) was added. After incubation for 1 hr, the cells were washed again with PBS

twice and viewed by CLSM (Leica TCS SP5 / UK) using the green filter and 514-visible laser source. The images were captured with the following properties; format-width 1024 pixels, format-height 1024 pixels, objective HC PL FLUOTAR 20.0x0.50 dry, and emission bandwidth PMT 2 (photo multiplier tube): 546 nm-618 nm.

5.3.2 Uptake studies of dendronised carrier systems by bEnd.3

5.3.2.1 Uptake studies by CLSM

Confocal microscopy was also used to examine the cellular internalisation **(**endocytosis and uptake) of dendrons and AEP-dendron by bEnd.3 cells via labelling with a fluorescent probe, FITC.

FITC is a fluorescein-5-isothiocyanate (isomer I), (Formula $C_{21}H_{11}NO_5S$, MW 389.38) and it is a derivative of the fluorescein molecule having an isothiocyanate (-N=C=S) reactive group replacing the hydrogen (H) atom. This isomer is chemically reactive to compounds having amino and sulfhydryl groups. Spectrum peak wavelengths of excitation and emission of FITC are approximately 495 nm/519 nm (Magali *et al.*, 2009).

The FITC labelling of G0K and G1K dendrons in addition to the AEP-K conjugate was performed using a coupling reaction (Fig.5.3). Before the reaction, the terminal amine groups in these molecules were deprotected as discussed before in Section 2.3.1.

Considering the number of terminal amino groups on the compounds, 2 molar excess of FITC (Sigma Aldrich, UK) were used for each molar amino branch. Each 0.4 mmol of FITC, equal to 0.155 g, was weighed in a dark place and dissolved in 3 mL DMF and 140 µL DIPEA. The solution was added to the resin-attached deprotected peptide and the coupling reaction left for 9 hrs at room temperature to ensure attachment. Then after, 3 washes with DMF were performed and followed by washing with the 3 solvents (dichloromethane, methanol and diethyl ether) as discussed in Section 2.3.1. The samples were then left to dry over night before cleavage. The cleavage, centrifugation and washing were carried out in the same way as that used for dendrons with consideration for the light sensitivity of the molecules. The dried powder was weighed and dissolved in DMEM at a final concentration 1 mg/mL for use in cell culture experiments.

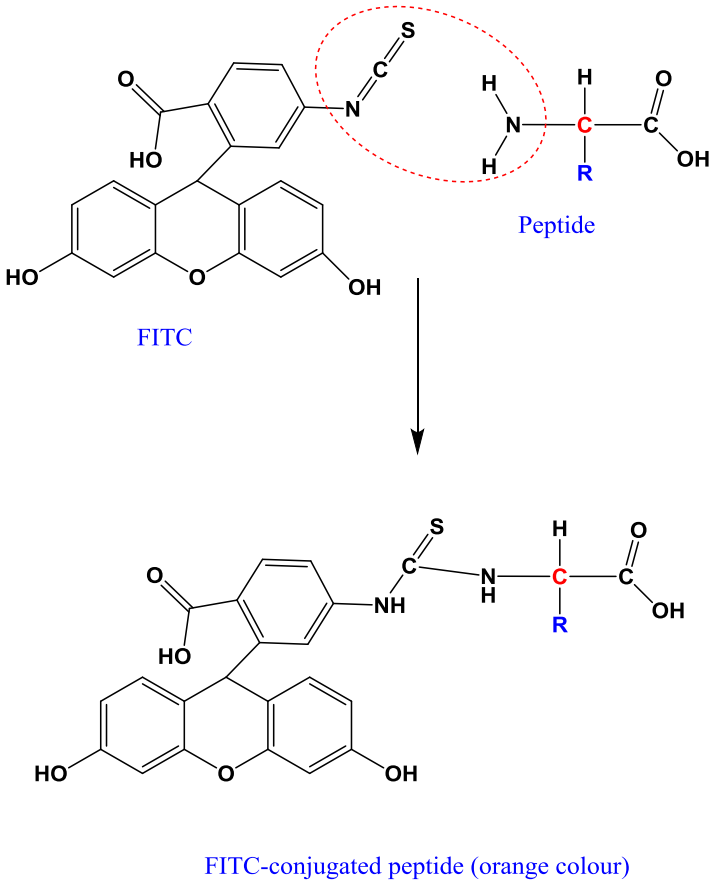

Fig.5.3: Formation of a fluorescent-labelled peptide by reaction of FITC molecule with the peptide.

The bEnd.3 cells were seeded in 24 well-plates at a density of $5x10^4$ cells/cm^2, and at confluency, cells were treated with 100 µM of FITC-labelled AEP-K and G0 and G1 dendrons solution. After 1 hr incubation, the media was removed and cells were washed twice with PBS before fixing with 3.7% formalin for 30 min, and then washed again with PBS. Wells containing untreated cells and wells treated with FITC alone were included to be used as controls.

The cells were viewed by CLSM using 488-visible laser source. The images were captured with the following properties; format-width 1024 pixels, format-height 1024 pixels, objective HC PL FLUOTAR 20.0x0.50 dry, emission bandwidth PMT 1 (photo multiplier tube): 488 nm-555 nm, with active PMT trans for bright field images.

5.3.2.2 Uptake evaluation by flow cytometry:

Flow cytometry is a simultaneous multiparametric technology that measures optical and fluorescence properties of single particles. The particles or cells are analysed by their suspension in a stream of fluid in a path of an optical-to-electronic detecting system which

records the scattering of the incident laser light as either forward scattering (FSC) or side scattering (SSC), and emission of the fluorescence will be detected according to wavelengths through photomultiplier tubes including FL(1-4) channels (Michael *et al.*, 2000) (Fig.5.4).

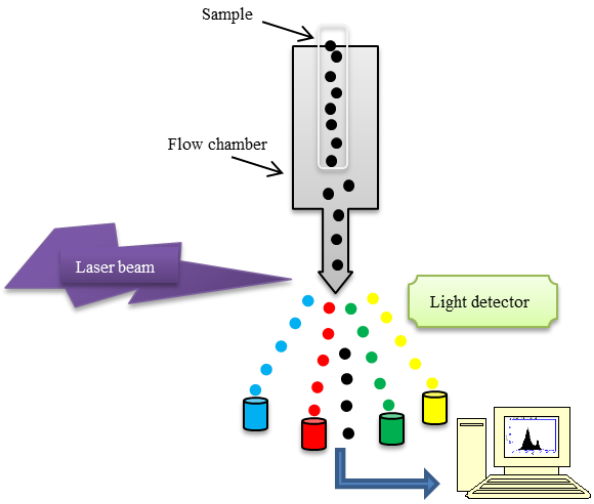

Fig.5.4: Basic principle of the flow cytometry. The cells (negative and tagged) pass across a chamber as a suspension towards the laser source, the light hit the cell and then scattered and captured by the optics according to the emission wavelength of fluorescence labelling to be directed to the detector and sorted and counted.

The bEnd.3 cells were cultured in 12 well-plates at a density of $5x10^4$ cells/cm^2, when confluency was reached, the cells were treated with 100 µM of FITC-labelled G0K, G1K and AEP-K solutions. After 1 hr incubation, the culture media was removed and the cells were washed with PBS (twice) and trypsinised prior to centrifugation for 5 min at 1000 rpm. The supernatants were then aspirated and the pellets were resuspended in 1 mL PBS, counted and analysed using a BD C6 sampler flow cytometer using 50 µL sampling run with 10000 events run limit and fast fluidity. Samples of cells without treatment were also included as a negative control. The analysis was carried out through the FL1-H channel for FITC detection and the cells were counted in relation to the negative population. The instrument settings were first adjusted and optimised using standard solutions (available with the instrument (BD Accuri C6 Sampler flow cytometer, Bioscience)) before running the samples.

5.3.3 Examination of penetration across the in vitro BBB model by HPLC

The dried powders of synthesised molecules (G0K-FP, G1K-FP and AEP-K-FP) as well as free drug (FP) were dissolved in FBS-free; phenol red-free culture media to a concentration of 200 µM. The standard curve for each molecule was obtained via running a series of dilutions (200, 100, 50, 25, 12.5 and 0 µM) using the HPLC technique, as described in Section 2.3.2.4.

To examine the penetration of molecules, bEnd.3 cells were seeded on 12-Transwell inserts with complete culture media as described in Section 5.3.1.1 (Fig.5.5). At the peak day of TEER (day 6) and prior to starting the experiment, the culture media of Transwell insert wells were removed then washed with PBS, and the apical chambers were treated with 200 µM of sample, while the basal chambers were fed with serum and phenol red-free DMEM. At pre-determined times (1 and 4 hr), 200 µL samples were collected in duplicate from the basolateral chambers.

To exclude the resistance of the membrane of the inserts itself, wells with only Transwell inserts without cells were treated with free FP and FP-attached molecules to examine the permeability through the microporous membrane.

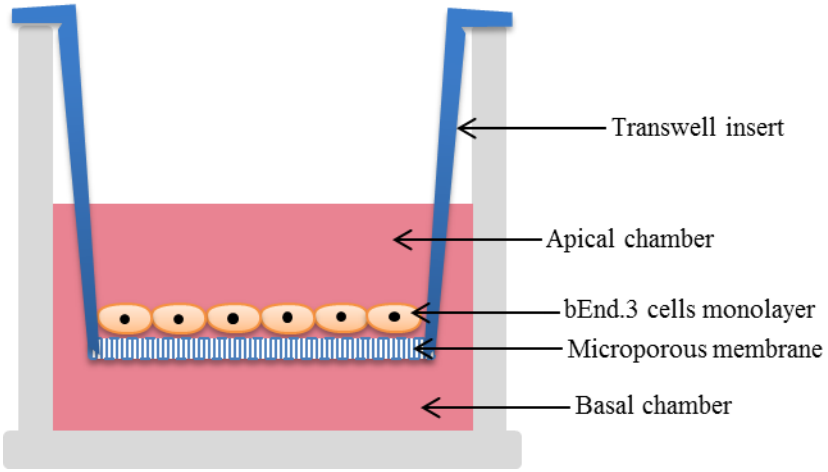

Fig.5.5: A model of an *in vitro* BBB. It is showing the culturing of bEnd.3 monolayer on the microporous membrane of the Transwell insert.

All samples were filtered with a 0.22 µm filter to avoid clusters and analysed by HPLC, the results were taken and percentage of permeability calculated according to the following (He *et al.*, 2010):

$$\boldsymbol{P}\ material\ \% = \frac{\boldsymbol{C}\ acceptor\ \times\ \boldsymbol{V}\ acceptor}{\boldsymbol{C}\ donor\ \times\ \boldsymbol{V}\ donor} \times\ 100\ \%$$

Where;

$\boldsymbol{P}_{material}\ \%$: the percentage of permeability of the tested material,

$\boldsymbol{C}_{acceptor}$: the concentration of the tested material in basal chamber,

$\boldsymbol{V}_{acceptor}$: the volume of the culture media in the basal chamber,

$\boldsymbol{C}_{donor}$: the initial concentration of the tested material in the apical chamber,

$\boldsymbol{V}_{donor}$: the volume of the culture media in the apical chamber.

5.3.4 Statistical analysis

Mean values were calculated for the number of readings (n) in each experiment and error bars represent the standard deviation (SD). Results were statistically analysed using one-way ANOVA with Tukey's tests. Significant differences were identified by a P-value < 0.05, and the degrees of significance are indicated where appropriate.

5.4 Results

5.4.1 Validation of the in vitro BBB model

5.4.1.1 TEER measurement

The electrical resistance between the apical and basal compartments of the Transwell system was measured to confirm the formation of a continuous cellular monolayer resulting from TJ formation. TEER values of cultured bEnd.3 cells increased to a highest reproducible average of 157.8 Ω cm^2 at day 6 (Fig.5.6) compared to 78.5 Ω cm^2 for cultured HUVEC cells. Whereas the inserts with media alone (cell-free) attained TEER values of an average of only 31 Ω cm^2. The day 6 TEER measurements of both cultures (bEnd.3 and HUVEC) were significantly ($P<0.05$) different from each other. The TEER values, following day 6, decreased moderately to give respective values of 153.3 and 75.1 Ω cm^2 at day 8.

In addition no significant ($P>0.05$) changes were recorded in the TEER values following 24 hr treatment with the FP-loaded molecules obtained for the bEnd.3 culture (Fig.5.7). This indicates that the treated molecules have no effects on the integrity of the endothelial monolayer

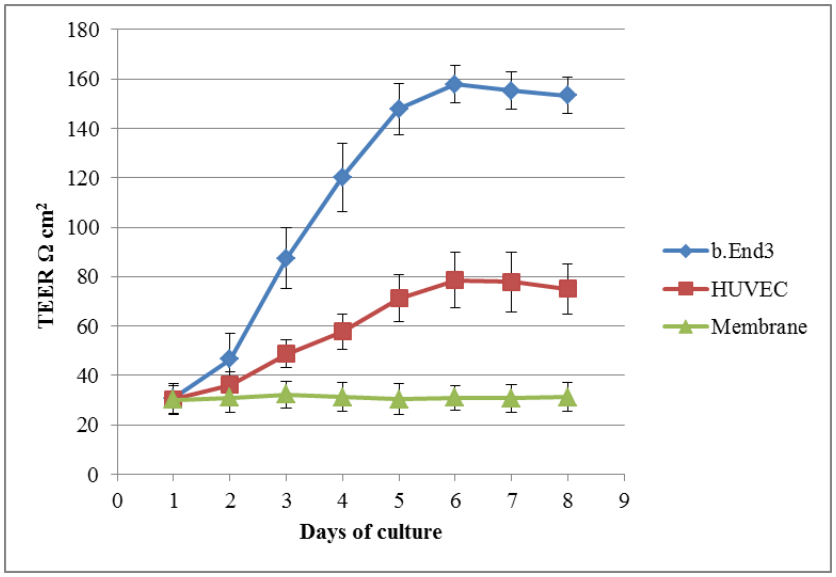

Fig.5.6: TEER measurement of the cultured bEnd.3 and HUVEC on the Transwell system. The values represent means ±SD, n = 4.

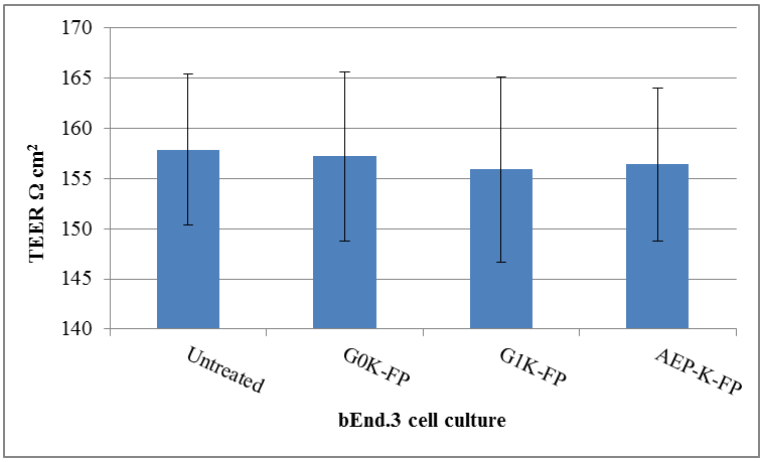

Fig.5.7: TEER measurement of the cultured bEnd.3. following 24 hr treatment with the FP-loaded molecules. The values represent means ± SD, n = 4.

5.4.1.2 Biochemical evaluation of permeability of the *in vitro* BBB model to paracellular marker

To verify that the formed monolayer culture is devoid of paracellular transport for solutes, sucrose was used as a permeability marker. The standard curve of a series of dilutions of the sucrose solution was carried out (Fig.5.8) to quantify the amount of sucrose that penetrated across the membrane and the % of permeability was calculated as shown in Table 5.1.

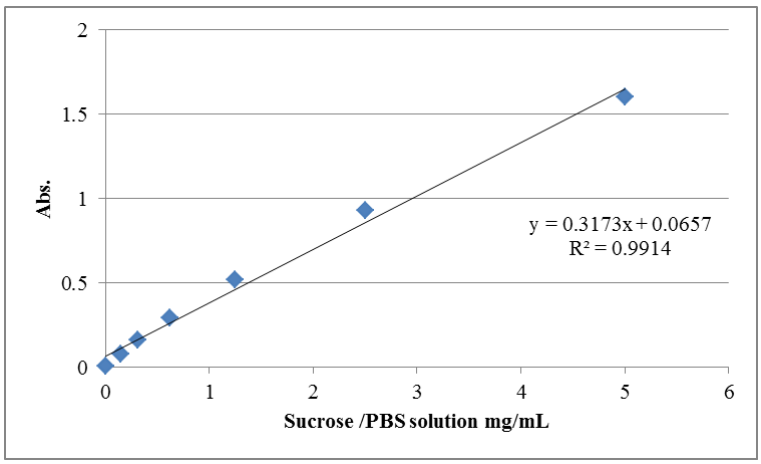

Fig.5.8: Standard curve of the sucrose solution.

After 15 min incubation of sucrose solution with the cultured cells (bEnd.3 and HUVEC) on Transwell inserts, only 6.2% of the initial amount passed across the bEnd.3 monolayer in comparison to 19.6% for that with HUVEC, whereas the amount did not increase more than 9.4% and 32.2% respectively after 30 min. The membrane alone showed free sucrose

transport to give equilibrium between the 2 chambers. These results demonstrated the resistance of the formed bEnd.3 monolayer for paracellular solute transport.

Table 5.1: Values of sucrose permeability.

Time	**No. of readings**	***% Sucrose permeability (Mean ± SD)***		
		Membrane	**HUVEC**	**bEnd.3**
15 min	4	44.7% ± 4.1	19.6% ± 2.7	6.2% ± 1.4
30 min	4	46.8% ± 3.6	32.2% ± 3.2	9.4% ± 1.8

5.4.1.3 Morphological validation of the *in vitro* BBB model

The confocal microscopic images (Fig.5.9) show bEnd.3 and HUVEC stained with phalloidine to reveal actin filaments. It is clear from the figures that bEnd.3 cells produced a continuous monolayer compared to the HUVEC that displayed gaps between the cells. These images are consistent with the results of the TEER analysis and sucrose permeability assay that revealed great resistance and reduced sucrose transport in the bEnd.3 cell culture.

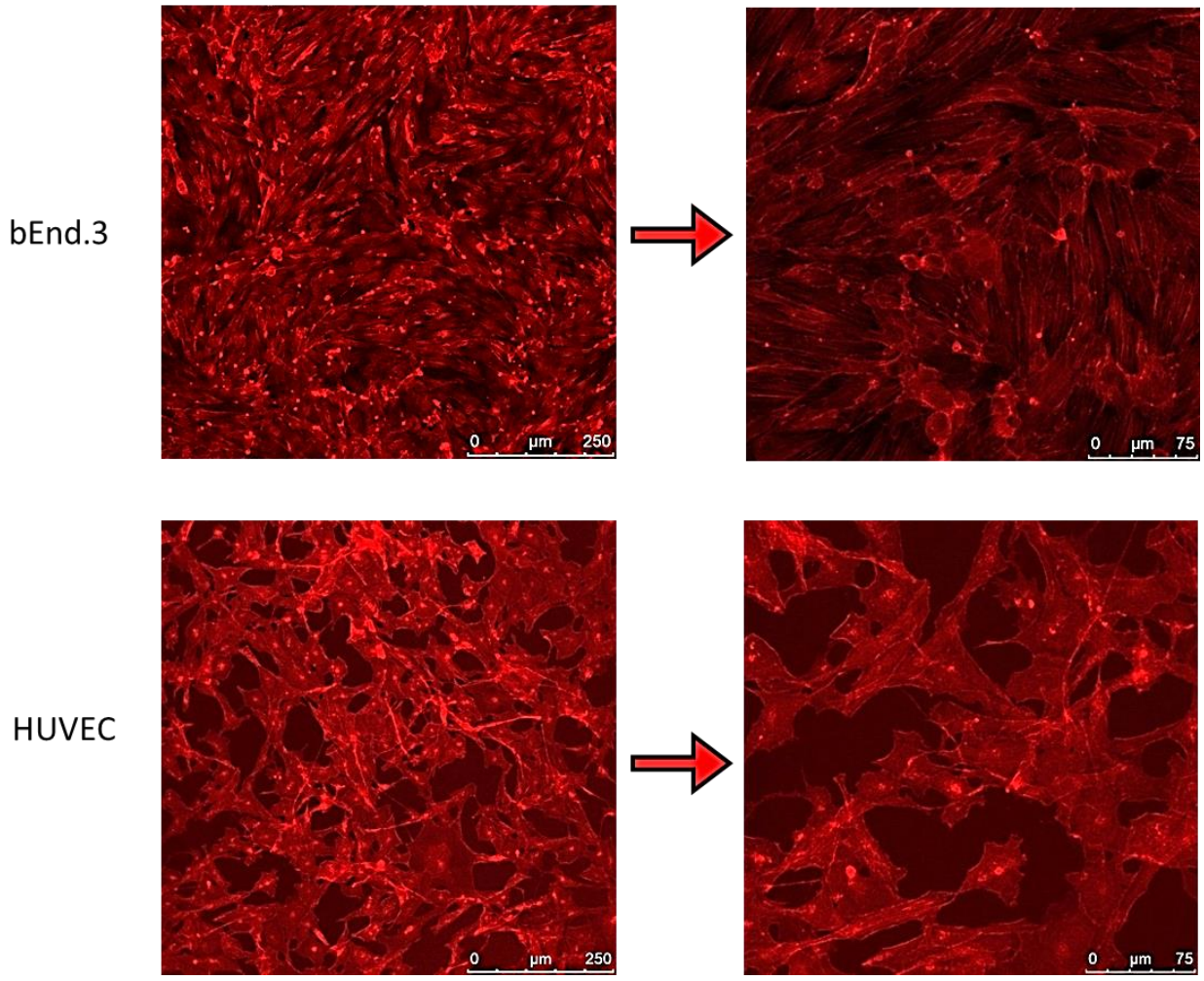

Fig.5.9: Pictures of confluent cell culture by using CLSM after rhodamine phalloidin staining. It is showing the continuous actin filaments formation in bEnd.3 whereas HUVEC containing gaps in between cells.

5.4.2 Cellular uptake of dendrons and AEP-dendron

5.4.2.1 Evaluation of cellular uptake by CLSM

The FITC-labelled dendronised carriers were viewed by CLSM to assess their uptake by brain endothelial cells. After 1 hr incubation of the tested materials with confluent bEnd.3 cell culture, the images clearly showed the accumulation of green fluorescent-tagged materials inside the cells signifying their endocytosis and uptake by the cells. The control cells (untreated) and those treated with only FITC showed no fluorescent internalisation (Fig.5.10).

5.4.2.2 Evaluation of cellular uptake by flow cytometry

The cellular uptake of G0K, G1K and AEP-K was further analysed via flow cytometry. The results of the 1 hr incubation with confluent bEnd.3 cell culture demonstrated that uptake was 38% and 67% for G0K and G1K respectively in comparison to negative control (untreated cells) which was used as a zero background. While AEP-functionalised dendron showed the highest value to reach 90% (as shown in dots blots) (Fig.5.11. a-d).

In addition, clear peaks shifting from that of control were seen in the single-parameter counting histogram (Fig.5.11. e) through the FL1-H channel for G0K, G1K and AEP-functionalised dendron as a result of high florescence intensity. The highest intensity peak was seen with AEP-functionalised dendron.

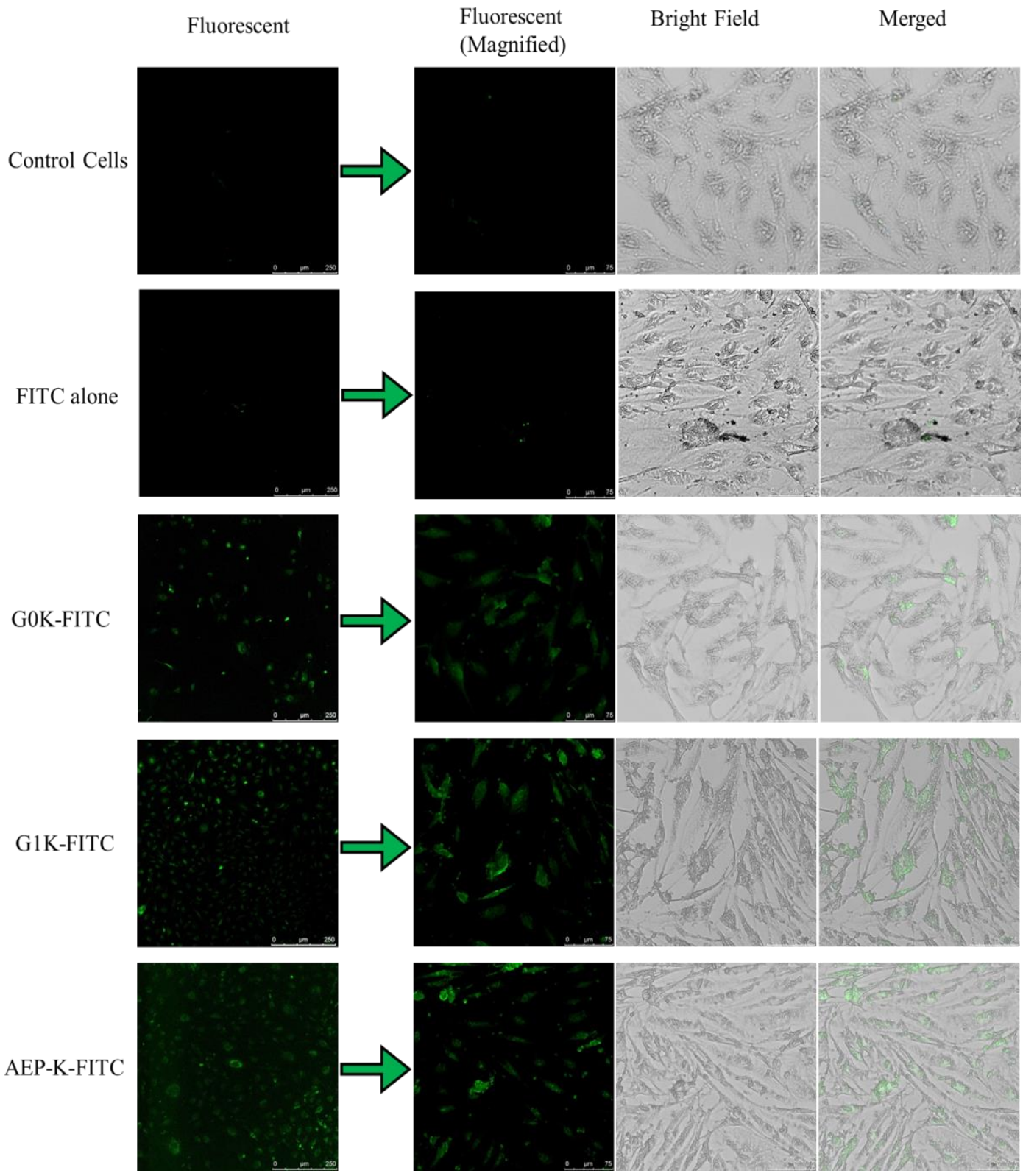

Fig.5.10: CLSM images after 1 hr incubation of FITC-labelled dendronised carriers with confluent bEnd.3 cell culture. The images of G0K, G1K and AEP-K clearly show the accumulation of green fluorescence inside the cells signifying their endocytosis in comparison to the control cells and those treated only with FITC.

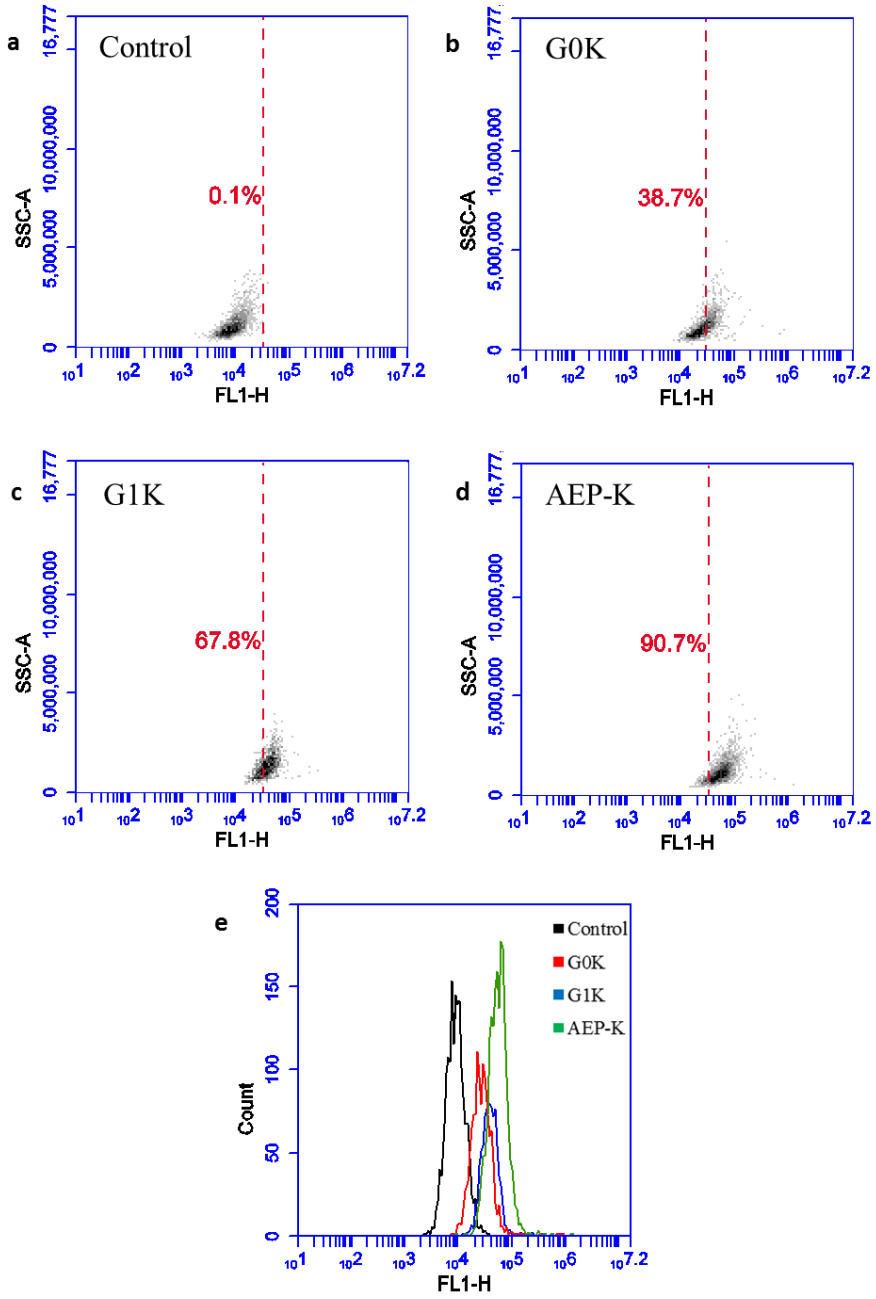

Fig.5.11: Analysis of FITC-labelled G0K, G1K and AEP-K by flow cytometry. The analysis was carried out through FL1-H channel for FITC detection in comparison to negative control cells. The a-d figures represent the dots blots for each negative control, G0K, G1K and AEP-K, while the e figure represents the single-parameter counting histogram shows the shifting of peaks of G0K, G1K and AEP-K from the control peak according to the florescence intensity.

5.4.3 Examination of the penetration of FP-integrated dendronised molecules across the in vitro BBB model using HPLC

A series of dilutions of FP, G0K-FP, G1K-FP and AEP-K-FP in DMEM (phenol red-free) solution were analysed using HPLC and the relative standard curves constructed to allow the quantitative determination of the transport of each molecule across the bEnd.3 monolayer (Fig.5.12 - 5.15).

5.4.3.1 Examination of the microporous membrane permeability

The results of examination of the resistance of Transwell® membrane alone (cell-free) for permeability showed that FP and FP-attached molecules amounts in the basal chambers were approximately half (49-51%) of the initial concentration at the apical chamber after 1 hr of incubation. These results indicate that the microporous membrane alone is permeable leading to equilibrium between both chambers. Thus the microporous membrane has no any impact on the permeability of the molecules and does not by itself represent an obstacle.

5.4.3.2 Examination of the permeability across bEnd.3 monolayer cultured on Transwell membrane

The HPLC analysis of the penetration of free FP and FP-loaded molecules across the bEnd.3 monolayer culture with Transwell system were carried out after 1 and 4 hr incubation periods (Table 5.2). For free drug, the amount that permeated was only 2.69% of its initial apical upload concentration after 1hr and increased to be not more than 8.6% after 4 hrs. No significant differences ($P>0.05$) were found in the both 1 and 4 hrs of G0K-FP values (5.2 and 12.3% respectively) from that of the free drug and also of the G1K-FP values. While the calculated amounts for the permeability of G1K-FP were: 4.2% after 1 hr and 14.7 % after 4 hr which are significantly different ($P<0.05$) from that of the free FP at both time intervals. The results of AEP-K-FP penetration analysis showed the permeability has boosted more than 6 times (16.3%) after 1 hr and 4 times (35.9%) after 4 hr from that of free FP values with significant differences ($P<0.001$) from that of all other values of free FP, G0K-FP and G1K-FP (Table 5.2).

However, it is worth mentioning that both G0K-FP and AEP-K-FP bearing 2 drug moieties while G1K-FP having 4, in turn this could increase the amount of the permeated drug upon dissociation at target tissue.

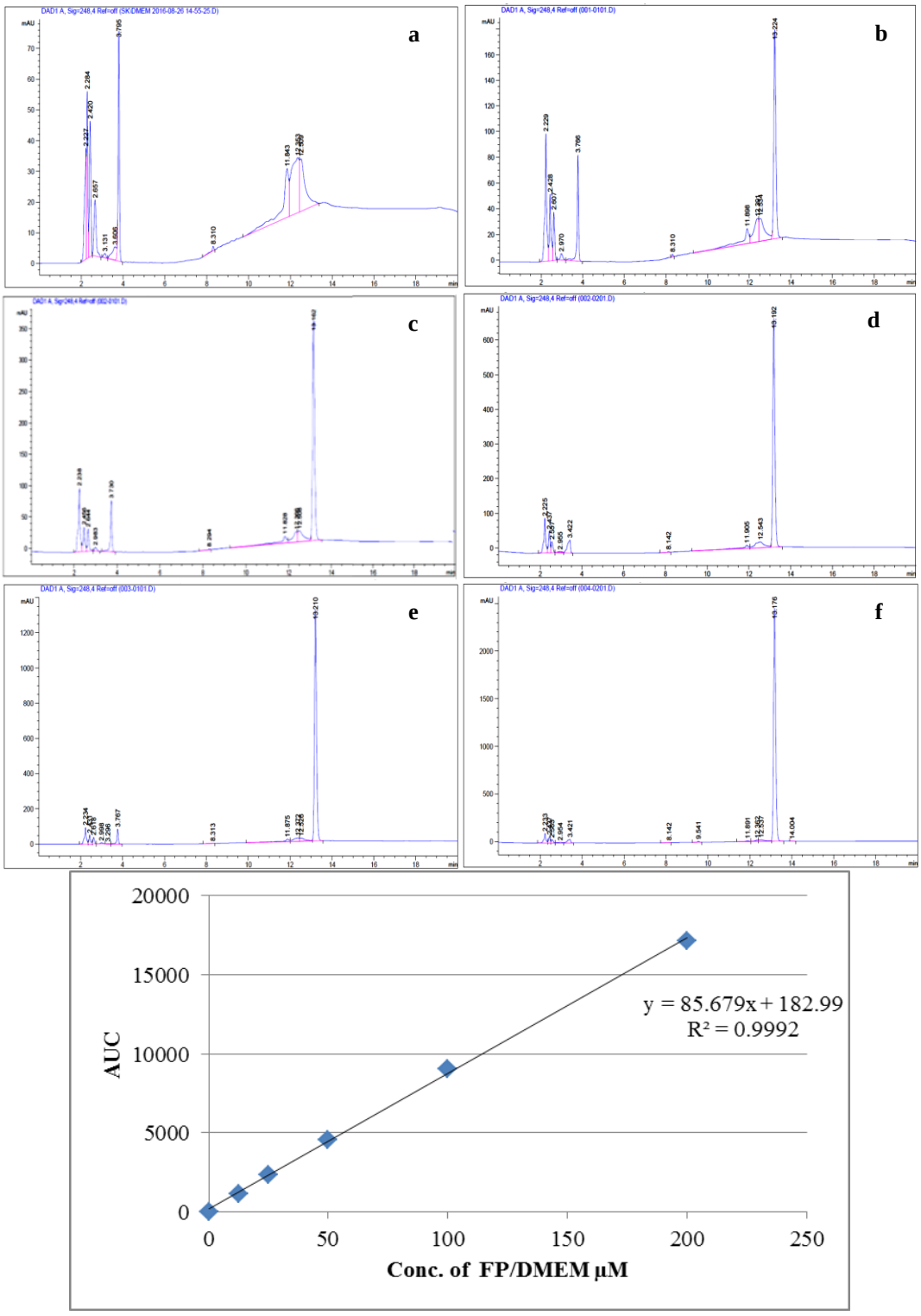

Fig.5.12: The standard curve of FP. The 6 upper graphs represent the HPLC results of analysing the FP in DMEM: a. 0 µM, b. 12.5 µM, c. 25 µM, d. 50 µM, e. 100 µM, f. 200 µM, with their corresponding standard curve (at the bottom) .

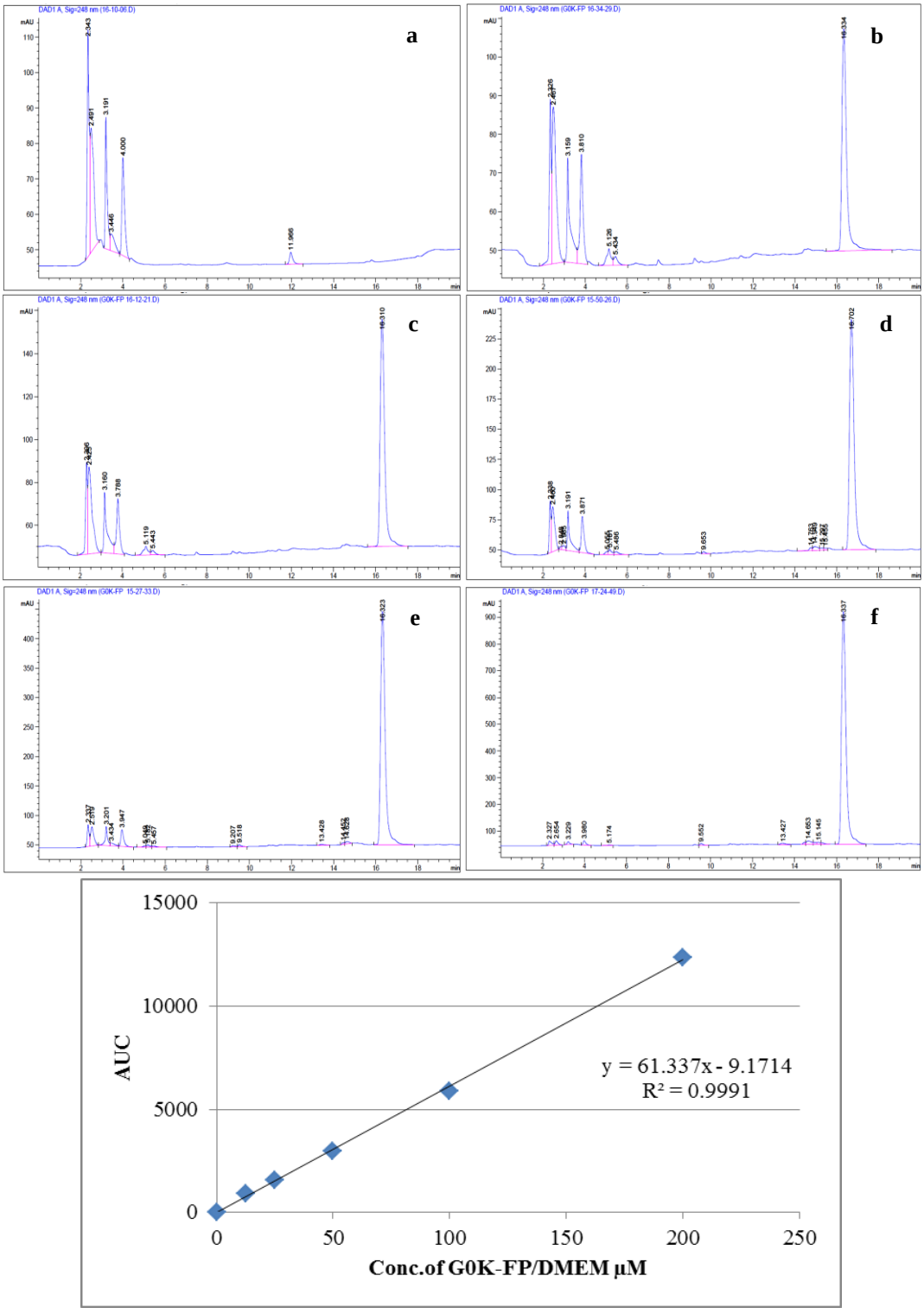

Fig.5.13: The standard curve of G0K-FP. The 6 upper graphs represent the HPLC results of analysing the G0K- FP in DMEM: a. 0 µM, b. 12.5 µM, c. 25 µM, d. 50 µM, e. 100 µM, f. 200 µM,, with their corresponding standard curve (at the bottom).

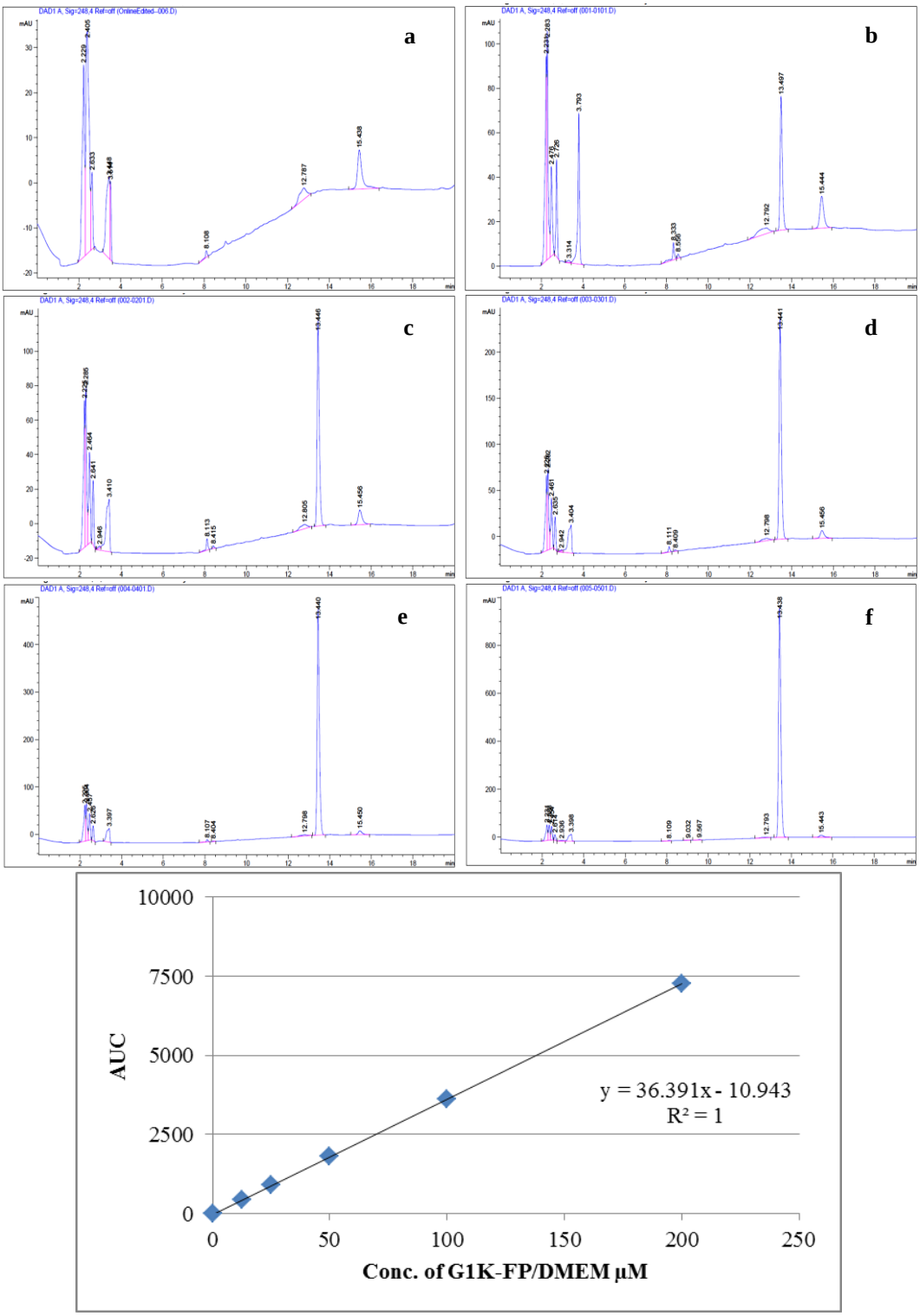

Fig.5.14: The standard curve of G1K-FP. The 6 upper graphs represent the HPLC results of analysing the G1-FP in DMEM: a. 0 µM, b. 12.5 µM, c. 25 µM, d. 50 µM, e. 100 µM, f. 200 µM, with their corresponding standard curve (at the bottom).

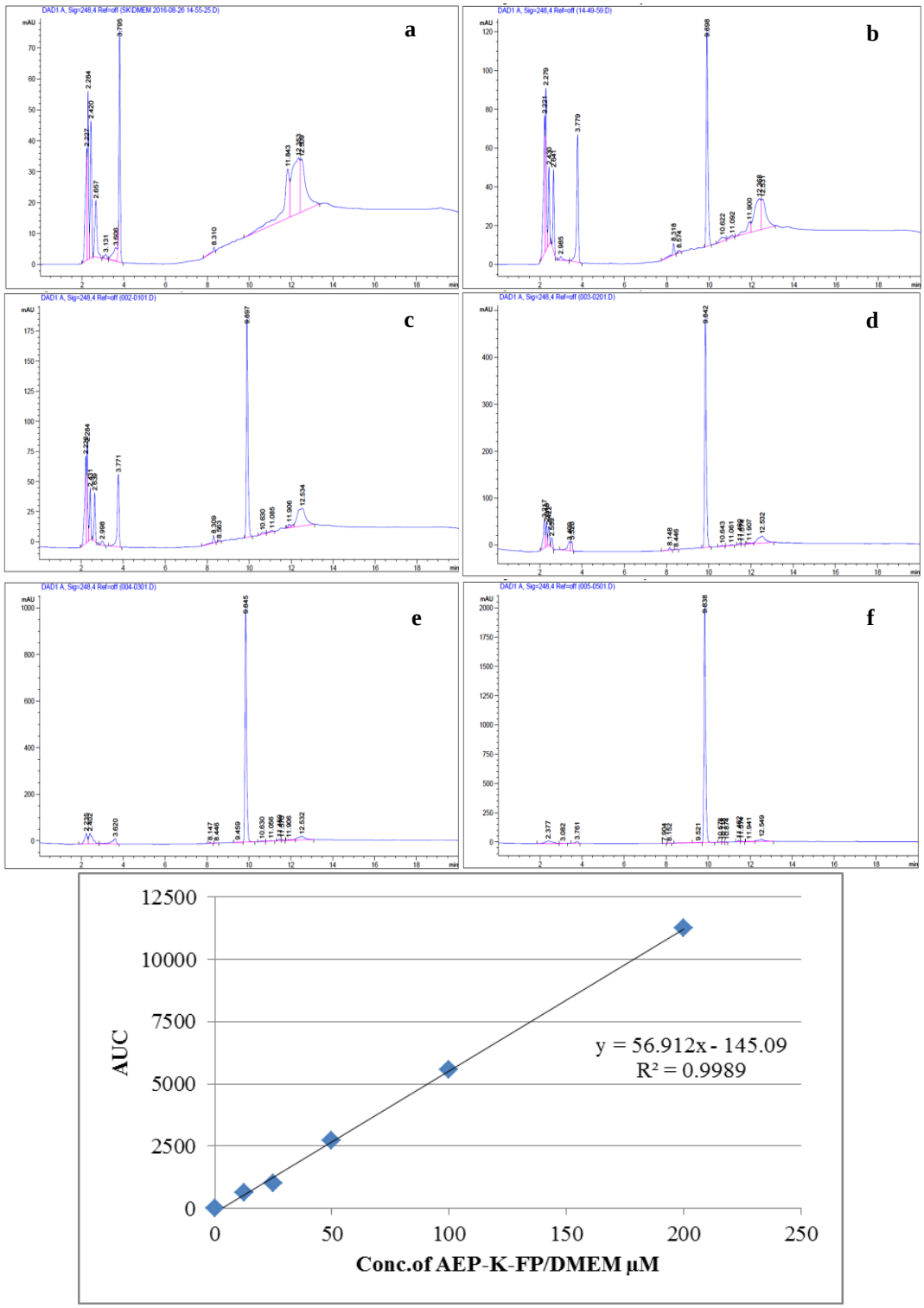

Fig.5.15: The standard curve of AEP-K-FP. The 6 upper graphs represent the HPLC results of analysing the AEP-K-FP in DMEM: a. 0 µM, b. 12.5 µM, c. 25 µM, d. 50 µM, e. 100 µM, f. 200 µM, with their corresponding standard curve (at the bottom).

Table 5.2: The results of HPLC analysis of molecules across the *in vitro* BBB model.

Molecule	***Time***	***No. of readings***	***Range***	***% Of permeability (Mean ± SD)***	***P-value to FP***	***P-value to G0K-FP***	***P-value to G1K-FP***
FP	**1 hr**	8	0.73 - 4.8	2.69 ± 1.64			
	4 hr	8	4.17 - 13.43	8.60 ± 3.12			
G0K-FP	**1 hr**	8	2.10 - 11.62	5.19 ± 3.37	>0.05		
	4 hr	8	6.75 - 21.38	12.34 ± 4.24	>0.05		
G1K-FP	**1 hr**	8	2.74 - 5.65	4.26 ± 1.05	<0.05	>0.05	
	4 hr	8	9.94 - 25.52	14.76 ± 6.01	<0.05	>0.05	
AEP-K-FP	**1 hr**	8	11.26 - 23.67	16.35 ± 4.56	<0.001	<0.001	<0.001
	4 hr	8	16.82 - 49.83	35.98 ± 11.76	<0.001	<0.001	<0.001

5.5 Discussion

The BBB is known for its efficient partitioning role and impenetrability. However, it is the main brain gateway as it grants access only to necessary nutrients, ions and hormones (Oller *et al.*, 2016). Currently, most strategies that circumvent the BBB in drug delivery are either invasive, resulting in high risk of brain damage or the need to very small and lipid soluble drugs to be eligible for diffusion (Chen *et al.*, 2012) (see Section 1.5). The endogenous transport systems available for the BBB are potentially the most efficient and safest way to deliver molecules into the brain. Indeed, certain peptides and some macromolecules can pass through the BBB via transcytosis mechanisms either by adsorption or receptor mediation (Oller *et al.*, 2016). In this process, the formed vesicle arising from molecule-membrane interaction circulates across the cytoplasm, bypassing the lysosomal digestion and eventually releases the content into the abluminal side by exocytosis (see Section 5.1).

Generally, endocytosis in AMT is promoted by the interaction of the cationic molecule with membrane phospholipids and the glycocalyx, while that in RMT is evoked by ligand-receptor interaction (Tuma *et al.*, 2003).

Transporters which trigger BBB receptors should have the following merits: receptor overexpression in the brain vasculature in relation to other tissues; ability to mediate transcytosis and maintain the physiological role of the transporter (Oller *et al.*, 2016). In this regard, LDLrs have been extensively exploited in transport and signalling at the BBB. These receptors, particularly LRP1, are highly expressed in the brain and in tumours (Huang *et al.*, 2008; Molino *et al.*, 2017).

Since the bioavailability and trafficking of any drug-loaded molecules determine their targeting efficiency, their design requires a full comprehension of how the interaction with the target can happen (Leupold *et al.*, 2008).

To screen the transport efficiency of any carrier system across the BBB, a validated model should be used. Several *in vitro* BBB models have been developed based on the physiology and pathology of this barrier and most of them are based on cultured brain endothelial cells. Cell-based BBB models emerged in the early 1990s as a potential physiological tool in preclinical and pharmaceutical research (Naik *et al.*, 2012). These models are characterised by a number of advantages through giving relatively high

throughput with lower cost and easier in use than *in vivo* models (Omidi *et al.*, 2003). An appropriate *in vitro* BBB model should mimic the *in vivo* anatomical environment, demonstrating the functional expression of essential transport mechanisms of the BBB (Brown *et al.*, 2007) and possess a typical architecture and biochemistry resembling the brain endothelium, including TJ proteins with paracellular transport restriction (Oller *et al.*, 2016). BEnd.3 cells have been widely utilised as a model for *in vitro* vascular endothelial cells and in permeability studies, with many scientific studies assessing the validity of this cell line for simulation to the *in vivo* situation (Brown *et al.*, 2007; Omidi *et al.*, 2003; Pachter *et al.*, 2003).

It is crucial to characterise the model in order to determine its validity to be used for drug transport studies. It has already been postulated that the TEER measurement can act as an indicator of TJ formation signifying the formation of a continuous cell layer that prevent the paracellular permeability (Patabendige *et al.*, 2013). This transcellular resistance reflects the ability of small ions carrying electrical current to penetrate and is inversely proportional to permeability (Patabendige *et al.*, 2013).

In the current study, the bEnd.3 *in vitro* model was firstly characterised by TEER measurements and found to be > 150 Ω cm^2 by day 6 of culture, greater than that of HUVEC and membrane only (Fig.5.6). Thus, suggesting a sufficient formation of TJs to produce an integral cell layer. TEER values also showed no changes after incubation with the synthesised molecules asserting no adverse effect was exerted on the monolayer integrity. Those TEER readings are in agreement with that previously published for different primary brain endothelial cells (Brown *et al.*, 2007; Raub *et al.*, 1992; Vries *et al.*, 1996) which ranged 50-180 Ω cm^2. These values also fall within the range for the same cell line from previous studies (Brown *et al.*, 2007; Omidi *et al.*, 2003) and also are higher than those reported for other immortalised brain endothelial cell lines such as b.End clone and bEnd.5 (Brown *et al.*, 2007; Kannan *et al.*, 2000; Romero *et al.*, 2003).

Further validation of the model characterisation was carried out in terms of the restrictiveness of the paracellular permeability to sucrose. Sucrose permeability was found at its lowest values in a Transwell cultured with bEnd.3 when compared to that in HUVEC and membrane alone (Table 5.1) signifying the formation of TJs which are capable of limiting the paracellular transport. It was reported that the permeability of sucrose (the paracellular marker) decreased in confluent brain endothelial cell cultures owing to the

tightness generated from TJs formation. According to experimental studies, the low sucrose permeability values were considered an acceptable indicator for BBB model to be used for the transport studies (Pierre *et al.*, 1996). These results are consistent with previous research which showed a limited sucrose transport using the immortalised brain capillary endothelial cells (Eigenmann *et al.*, 2013; Patabendige *et al.*, 2013).

BEnd.3 has also been characterised in terms of morphology using CLSM (Fig.5.9), which underlined the subcellular localisation of the actin structure (a TJ protein) forming a continuous cellular layer with no gaps when compared to the HUVEC. This outcome is in agreement with other studies which showed the display of bEnd.3 to different TJ proteins (Brown *et al.*, 2007).

Thus in the present work, the bEnd.3 cultured on Transwell membrane appear to be a suitable BBB model and the optimal available to mimic the *in vivo* environment. This model expresses appropriate TJ proteins resulting in a tight barrier between the apical and the basolateral chambers in turn increasing the electrical resistance. Furthermore, it formed a functional barrier to sucrose, a paracellular permeability marker which is commonly used in both *in vivo* and *in vitro* investigations (Brown *et al.*, 2007; Patabendige *et al.*, 2013). Repeating the experiment using human cell line-based BBB model may reveal some differences on recognition of LDLr by the targeting AEP. However, in previous studies, mouse bEnd.3 cell line has successfully recognised this targeting AEP in carrier systems (Wagner *et al.*, 2012; Zensi *et al.*, 2009).

Consequently, the uptake and permeability examination was implemented at the peak day of bEnd.3 culture. To study the cellular uptake and endocytosis of the peptide, the CLSM was used. The cellular binding and uptake of G0 and G1 dendrons were proven as both molecules showed positive interaction in comparison to the control demonstrating an unspecific binding. It has been theorised that amino dendrimers can be internalised, possibly via cationic adsorption (Kolhe *et al.*, 2003; Patri *et al.*, 2012; Sadekar *et al.*, 2013). After the bEnd.3 cells incubation with AEP-K, a clear intracellular uptake and accumulation of FITC-labelled peptide could be observed by CLSM in comparison to the control (untreated cells) (Fig.5.10). These results proposed the receptor-mediated uptake of the AEP decorated dendron. In turn, the expression of lipoprotein receptors was possibly verified by this BBB model. This is in agreement with other studies which showed that

NPs decorated with AEP were internalised by bEnd.3 cell line via interaction with LDLr (Wagner *et al.*, 2012; Zensi *et al.*, 2009).

This work finding of cellular uptake of the synthesised peptides obtained by CLSM was supported using flow cytometry. It is of note that the G1K uptake is nearly double than G0K dendron, it is proposed that the increased numbers of amino branches on G1K likely facilitating its electrostatic internalisation. It has previously been found that the cellular entry of dendrimers increased with their generation owing to more peripheral amino groups (Najlah *et al.*, 2006). It should be remarked that a significant higher uptake by the bEnd.3 was displayed by AEP-functionalised dendron than that of the dendron alone (Fig.5.11). This suggests that this carrier system enters into bEnd.3 cells, most likely by a receptor-mediated pathway. This speculation is supported by other experiments devoted to assess the ApoE derived peptide intracellular distribution which showed that their uptake is presumably mediated by receptor endocytosis (Bana *et al.*, 2014; Re *et al.*, 2011; Wagner *et al.*, 2012). Previous studies focused on the binding domain of ApoE residue (141-150) found it to be able to induce an endocytosis via LDLr-engagement in a primary cultures of brain tissue (Wang *et al.*, 1997). As well ApoE derived peptide-decorated NL has been shown to be efficiently taken up by brain endothelium of rat after 30 min incubation when compared to free NL (Sauer *et al.*, 2005). The NLs decorated with ApoE residue (141-150) have successfully enhanced the brain uptake of antioxidants (Gobbi *et al.*, 2010) and curcumin (Re *et al.*, 2011). Published results of CLSM and flow cytometry analysis have clearly shown a specific cellular binding after 1 hr incubation of bEnd.3 cells with NPs covalently linked to ApoE in comparison to the unlinked NPs (Wagner *et al.*, 2012; Zensi *et al.*, 2009).

In order to assess the potential of dendrons and AEP-functionalised dendron in transporting FP to the other side of endothelial cells after endocytosis, the permeability of free drug and drug-loaded molecules were examined across this Transwell insert-cultured bEnd.3 model. Taking into consideration, the resistance of the Transwell insert itself was excluded by conferring free passage of molecules through the cell-free membrane and the paracellular transport was also precluded.

An improvement was seen in the permeability when FP was attached to the carrier systems (Table 5.2). Unattached FP was found to penetrate less than 9% of its initial payload; a finding, to some extent, similar to previous study results which revealed the FP diffusion

through bEnd.3 cells monolayer was approximately 10% and is insufficient to induce its pharmacological effect (Meister *et al.*, 2013).

A slight increase in penetration was observed by HPLC analysis for FP-conjugated dendrons (G0K-FP and G1K-FP) when compared to free drug. The positive charges of the amine groups of dendrons are vital in the exploration of their ability to be delivering vehicles, which facilitate cellular transport. Earlier investigations found that cationic dendrimers such as poly lysine, PPI and PAMAM could interact electrostatically with the negative charges of the biological membranes leading to a profound applicability for intracellular drug delivery (Prashant, 2014). As documented previously, folic acid was efficiently delivered to the target when conjugated with PEG5000-dendrimer (Srinivas *et al.*, 2014). Furthermore, the paclitaxel (anticancer) when conjugated with PAMAM demonstrated 12 fold greater permeability across brain endothelial cells and Caco-2 cell monolayers than paclitaxel alone (Teow *et al.*, 2013). In addition, the permeation of ketoprofen and diflunisel through skin tissue improved when integrated into PAMAM dendrimers (Cheng *et al.*, 2007), while G0 PAMAM-conjugated to naproxen showed high permeability across Caco-2 cells (Najlah *et al.*, 2007).

Cationic peptides can enter cells and mostly undergo endocytosis through different mechanisms. It is assumed that they undergo AMT to cross the BBB (Herve *et al.*, 2008). However, their exocytosis from the brain endothelia is more controversial than in RMT and they might accumulate inside the cells as reported previously for lectins, another positively charged protein (Oller *et al.*, 2016). Combining the results from the uptake and permeability studies, it can be suggested that dendrons could efficiently carry the loaded drug inside cells, however, only 12-14% conjugated molecules here were transported to the other side (basolateral chamber) during the short time considered by the *in vitro* model. This low permeability may be explained to longer time needed for exocytosis than other pathways (Najlah *et al.*, 2006). This may give preference for the sustained release of drug delivery as supported by many scientists who demonstrated that dendrimers enhance cellular uptake with consequent release of cargo into target cells (Kesharwani *et al.*, 2011; Prashant, 2014). It has also been reported that anticancer drug (doxorubicin) loaded on G5 poly lysine dendrimer has given prolonged antitumor activity (Kaminskas *et al.*, 2012) and that rifampicin-dendrimer complex has shown sustained release of antitubercular drug (Kumar *et al.*, 2006). Kolhe *et al.*, (2003) have observed that the ibuprofen-dendrimer

complex was rapidly taken up by cells with sustained release and suggested the ability of dendrimers to be efficiently exploited for intracellular targeting of substances (Kolhe *et al.*, 2003). Further findings have demonstrated that the conjugate of PAMAM dendrimers with erythromycin or azithromycin were having high drug payload and sustained release (Bosnjakovic *et al.*, 2011).

Another explanation for the low penetration is the low branching generation of the dendrons used in this work. As a previous study has reviewed that the cationic PAMAM dendrimers (G0-G4) permeability across Caco-2 cell monolayers increased with generation (Kitchens *et al.*, 2005). In another study, G3-NH_2 dendrimer was found to have lower rate of cellular entry when compared with G4-NH_2 due to fewer surface charges (Najlah *et al.*, 2006). However, it is worth reiterating that the toxicity of dendrimers increases with the generation and size. Even if the percentage of permeability might only slightly increased, the excess molar of drug conjugated within dendrons (2 more in G0 and 4 more in G1) should be taken in to account as it can increase the final drug concentration at the target site.

Different profile of transport across this *in vitro* model was seen when dendron was further functionalised with AEP (AEP-K-FP) highlighting that the permeability was significantly higher than that measured for both the drug alone and the unfunctionalised dendrons (G0K-FP and G1K-FP). Once more, the percentage of permeated molecules might not reflect the exact drug amount that could dissociate later from carrier system, as the drug and other fragments of dendron which are linked via biodegradable amide bond, ensures eventual release of more active principle upon hydrolysis. As clearly illustrated in Table 5.2, the AEP-K-FP molecule crossed the bEnd.3 monolayer barrier into the basolateral chamber. This signifies that the molecule has been internalised by the endothelial cells and then undergone exocytosis to the external side of the cells presumably via receptor-mediated pathway. The results are supported by earlier suggestions in which the AEP-decorated molecules transport across the BBB is due to a mechanism of RMT with a selective ApoE binding to a member of the LDLr family (Kreuter *et al.*, 2002; Zensi *et al.*, 2009).

The BBB endothelium is rich in the LDLr relative to other tissues (Banks, 2012; Dehouck *et al.*, 1994). It acts in the transcytotic uptake of lipoproteins into the brain and ApoE is one of its ligands. The ApoE sequence (141-150) is considered the recognition domain that

successfully interacts with the cellular surface and it is later internalised. The ApoE-derived peptide complexing with liposomes and NPs are successfully used for specific drug applications such as in tumour therapy (Rensen *et al.*, 2001; Sauer *et al.*, 2006). Many drugs have been efficiently transported into the brain using an ApoE-functionalised carrier system including dalargine, curcumin and doxorubicin (Kreuter *et al.*, 2002; Re *et al.*, 2011; Sauer *et al.*, 2006). Hence, in this work, functionalisation of dendron with AEP has been synergising drug (FP) transport across BBB in addition to improve the targeting of the brain.

As reported before, the functionalisation of PAMAM dendrimers with TfR ligand enhanced the brain targeting of doxorubicin (Huang *et al.*, 2008), on same pattern, OX26-functinalised dendrimer was utilised for opioid (Yuan *et al.*, 2011), whereas angiopep-2-functinalised PAMAM was used efficiently in delivering and targeting genes (Ke *et al.*, 2009; Shixian *et al.*, 2011).

Dendronised carriers are thus able to transport FP across the BBB, with more potentiation for AEP-functionalisation, and deliver the drug to the brain, this cannot normally take place. Hence, this novel design can be optimised to be used in the treatment of AD.

An attractive aspect of the RMT strategy for CNS drug delivery is its ability to direct a drug to specific organs containing specific receptors, thus; avoiding other body tissues and decreasing undesirable systemic effects. In other words, through this behaviour, AEP-dendron is able to carry the drug molecules directly to the site of interest inside the brain through recognition of the LDLr, thereby avoiding interaction with other organs in the body and enhancing the amounts of drug that can reach the target. Using less specific approaches of drug delivery would lead to a rapid clearance of the drug from the circulation as a consequences of its wide distribution and resulting into inadequate amounts being delivered to the brain (Chen *et al.*, 2012; Khawli *et al.*, 2013). In this regards, a decreased dose of drug (FP) could be used in the case of its conjugation with AEP-dendron still exerting a pharmacological action at the target tissue. Thence, the side effects associated with high dose could be avoided.

In addition to FP, a wide range of other poor penetrating drugs, proteins and peptides could also be transported by this novel carrier system, the AEP-dendron, as it is able to carry a high payload of molecules with site specific targeting into the brain.

5.6 Conclusion

In this work, confluent bEnd.3 cells cultured on Transwell membrane offered a valid *in vitro* BBB model by expressing appropriate biochemical properties. This making it a functional barrier between the apical and basolateral chambers allowing its use in the permeability studies of the novel drug conjugates of this project.

The presented data provide the evidence that a dendronised carrier system could induce endothelial uptake and endocytosis of the drug with the possibility of sustained exocytosis.

Moreover, the functionalisation of dendron with ApoE peptide derived from binding domain to the LDLr was shown to facilitate translocation of the drug across the *in vitro* BBB model assuming that ApoE-evoked transport occurs via a specific interaction with the receptor.

Yet, the results of this chapter provide a novel contribution to knowledge, showing the AEP-dendron carrier system improves BBB permeability and targeting and can act as a key to selectively allowing therapeutics to cross the BBB. This finding has significant potential not only for the treatment of AD but also for other CNS diseases, as this attractive strategy for brain delivery can be applied for a wide range of drugs, genes and diagnostic agents.

The biochemical activity and biodegradability of the drug carriers will be the focus of the next chapter towards the validation of their efficiency on the target neuronal cells.

Chapter 6. Biochemical Investigation of the FP-Integrated Dendronised molecules Activity on γ-secretase Enzyme and Their Biodegradability

6.1 Introduction

Over the last few decades, a significant amount of evidence has accumulated supporting the hypothesis that the aggregation of Aβ protein in the brain has the causal role in the development of AD. This aggregation leads to a pathological cascade that eventually results in neuronal dysfunction and death (Jakob *et al.*, 2009). Different peptides are generated from the APP through sequential proteolytic cleavages mediated by β and γ secretases (Turner *et al.*, 2003). Secretase type γ is one of the intramembrane cleaving proteases which cleaves the peptide bond within the lipid bilayer (Wolfe, 2012). APP is cleaved by γ-secretase at γ- and ε- sites resulting in numerous Aβ species with different number of amino acids (37-46) (Eriksen *et al.*, 2003) (see Section 1.1.6.1). The Aβ42 isomer has been implicated as the most pathogenic in AD, resulting from the final cleavage event by γ-secretase activity. This variant aggregates much more readily than other shorter species and these aggregates forming cytotoxic SPs (Ballard *et al.*, 2011) (Fig.6.1).

Recently, interest in the effect of NSAIDs, specifically Flurbiprofen, as GSM has increased due to their potential to act as disease modifying agents in AD (Crump *et al.*, 2013), where they were found to selectively decrease the Aβ42 secretion (Eriksen *et al.*, 2003). This effect is independent of their anti-inflammatory action on COX, rather they act by subtly altering γ-secretase activity without significant impairment in Notch signalling or other APP processing pathways (Weggen *et al.*, 2003). Conversely, the γ-secretase inhibitors block the whole enzyme leading to many adverse effects (Crump *et al.*, 2013).

The quartet of proteins that assembles to form this intramembranous γ-secretase complex; Aph-1, nicastrin, PSENs and Pen-2, with different numbers of domains, are obligatory for its cellular activity (Bergmans *et al.*, 2010) (Fig.6.1). Nevertheless, the PSEN 1 and 2, the catalytic subunits of γ-secretase, are initially involved in APP cleavage, then the production of Aβ42 (Crump *et al.*, 2013; McLendon *et al.*, 2000). Studies have shown that the deactivation of PSEN1 resulted in the reduction of Aβ42 levels (Saftig *et al.*, 1998). Other studies have demonstrated that mutations of components in PSENs also decreased

Aβ42 production and increased shorter peptides, confirming that PSENs expression is essential in Aβ42 formation (McLendon *et al.*, 2000; Smith *et al.*, 2000).

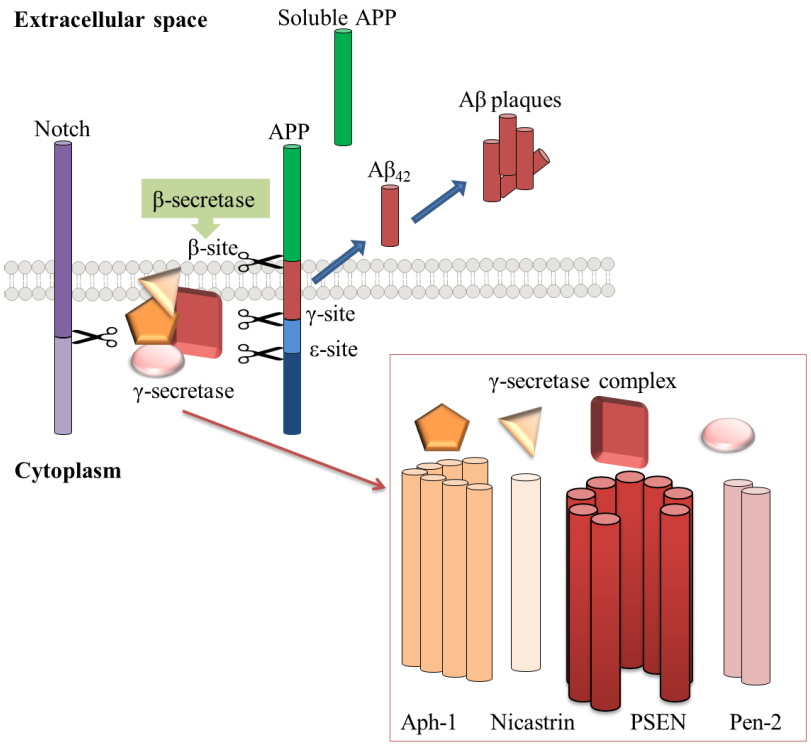

Fig.6.1: Schematic representation of amyloidogenic processing of APP. APP is first cleaved by BACE, resulting in extracellular soluble APP; the remaining membrane-bound fragment is further cleaved at the γ- and ε- sites by γ-secretase enzyme producing short Aβ and Aβ42. Aβ42 accumulates readily extracellularly forming SPs. Notch is also cleaved by γ-secretase resulting in the release of Notch intracellular domain. The magnified area shows the components of γ-secretase complex in which each one has different domains with the PSEN being the largest.

Further findings have shown that PSEN1gene mutations can lead to different effects on γ- and ε-cleavage sites, thus, altering Aβ42 and Aβ38 levels (Crump *et al.*, 2013; Cruts *et al.*, 1998). In this respect, NSAIDs are theorised to act only on PSENs in γ-secretase to reduce amyloid plaques alongside their action on neuro inflammation (Sastre *et al.*, 2008). The exact molecular mechanisms of action of NSAIDs and how they interact with the PSENs in γ-secretase have not been elucidated to date. It has however been proposed that NSAIDs or GSMs binding to γ-secretase increases the distance between terminal fragments of

PSEN thus suggesting that a conformational change may be instrumental in its inhibition (Crump *et al.*, 2013).

Nevertheless, the low transepithelial permeability of FP has led to its failure in crossing the BBB and in reaching its target so preventing its further development as an AD therapy (Green *et al.*, 2009; Meister *et al.*, 2013). In previous chapters of this work, FP was covalently bound to the dendrons and AEP-dendron via amide linkage. This conjugation, in particular the AEP-dendronised drug complex, has enabled the drug to cross the *in vitro* BBB model. However, the question remains regarding whether the drug retains its functional activity while attached to the carrier. In this regard, biochemical investigation of γ-secretase activity of neuroglial cells exposed to the FP conjugates was conducted.

One of the cell lines commonly used in neurological studies for cellular mechanisms is the C6, a cell line retaining most of the phenotypic features of the neuroglial cells (Hook *et al.*, 1998). C6 cell cultures have also been exploited in a range of AD research aimed at investigating secretase enzymes and APP to further understand the disease mechanisms and identifying new therapies (Refolo *et al.*, 1995). These studies support the rationale for using C6 cell line in this project to investigate the effect of FP-linked molecules on γ-secretase activity.

Certain drugs can exert their action while still conjugated to the carrier systems. For instance, an aspirin-linked polymer has shown the same potency as free aspirin, while ibuprofen was found to achieve prolonged activity and an increased plasma half-life while conjugated to a polymer (Silverman *et al.*, 2014). However, this depends on type of drug, type of conjugate and their linking.

Covalent polymer-drug conjugates, including dendrimers, are distinctive DDS where the drug or other bioactive molecules are covalently conjugated to the backbone of the carrier through a physiologically labile linkage (Ringsdorf, 1975). The biodegradable peptide linkage in between the building units of the dendrimer and of the peptides which also serves to covalently link them with the drug ensures the conjugate stability in the circulation and its eventual gradual degradation (Fig.6.2). This type of bond makes the conjugated systems interesting for various applications (Elvira *et al.*, 2005).

Previous studies presenting the conjugation of Tf to liposome via the amide linkage arm of PEG resulted interestingly in increased time of biodistribution and high bioavailability in brain tumour (Osamu *et al.*, 2001). Other studies have described that the formation of amide bonds between ligands with liposome or micelle were employed efficiently in the targeting delivery of the drugs (Karolina *et al.*, 2015; Zeng *et al.*, 2006). Additionally, the PAMAM dendrimer was covalently conjugated with antibody-carbon nanotube complexes and applied successfully in targeted gene therapy (Baoling *et al.*, 2010; Karolina *et al.*, 2015). Likewise, Doxorubicin was attached to the dendrimer using the amide bond and showed improved efficacy by increasing cytotoxic activity against cancer cells in comparison to free drug (Lai *et al.*, 2007).

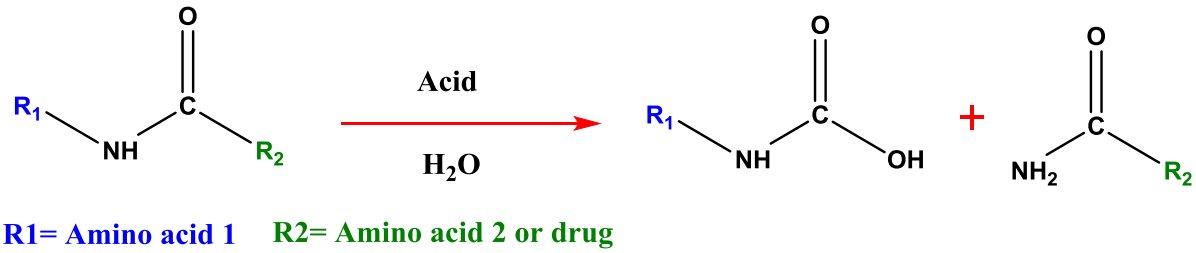

Fig.6.2: Peptide degradation by hydrolytic enzymes in acidic environment. The peptide is hydrolysed into its building monomers such as amino acids in addition to releasing the free drug in case of conjugation.

The dendrimers can be covalently conjugated to drugs through some spacers, such as PEG, or biodegradable linkages including amide or ester bonds. Different researchers have successfully conjugated different drugs such as penicillin V, venlafaxine, naproxen, propranolol with dendrimers, which have resulted in the enhanced controlled release of these drugs in comparison to the free form (Madaan *et al.*, 2014; Najlah *et al.*, 2007; Yang *et al.*, 2003). The conjugates also showed improved therapeutic action and exhibited long blood residence by reducing premature metabolism and excretion (Madaan *et al.*, 2014; Pasut *et al.*, 2005).

The amide bonds are very stable in aqueous solution and physiological pH and it has been proposed that, of all the proteases, cathepsin B is primarily responsible for the cleavage of the amide linkage (Souza *et al.*, 2004). Further study on the peptide linkage has found it to be stable in plasma but cleavable by cellular cathepsin B (Duncan *et al.*, 1985). Pharmacokinetic evaluation of dendrimers has shown high initial volumes of distribution

and rapid initial clearance, particularly in the case of poly lysine dendrimers (Prashant, 2014). A successful release of doxorubicin and/or methotrexate from carrier systems has been reported when using the dipeptide Phe-Lys or the tripeptide Ala-Phe-Lys which are recognised by proteases for hydrolysis (Khandare *et al.*, 2011).

Thus, drug molecules covalently bound via amide or ester linkage can be released in a site-specific manner. Likewise, dendrimer are completely biodegraded and metabolised via hydrolytic enzymes over time therefore can be eliminated easily from the body (Groot *et al.*, 2003; Khandare *et al.*, 2011).

6.2 Aim of the chapter

To show the effect of the novel FP-conjugated dendronised systems on γ-secretase enzyme and the possibility of the free drug release upon degradation, this chapter assessed the effect of the conjugates on neuroglial cells as well as their degradation to release free dug. In particular, this chapter aimed to:

1. Quantify the γ-secretase enzyme in C6 cells biochemically in response to exposure to the drug-attached dendronised molecules, and to compare with that of cells exposed to free drug using γ-secretase sandwich enzyme-linked immune-sorbent assay (ELISA).
2. Examine the biochemical fate and degradability of the drug-attached dendronised carrier systems to ensure its safety and to define the possibility of the drug release through amide linkage cleavage.

6.3 Materials and Experimental methods

6.3.1 Preparation of C6 glial cells

The complete growth medium was made according to the ATCC-product sheet by addition of FBS to a final concentration of 2.5% $^{v}/_{v}$ and horse serum (Gibco by life technology) to a final concentration of 15% $^{v}/_{v}$ to F-12K medium.

C6 glial cells (ATCC- LGC,UK) were seeded in T-75 tissue culture flasks in a density of $5x10^{4}$ cells per cm^{2} and incubated at 37˚C and 5% CO_2. The flasks were checked daily using light microscope and the culture media was changed every 3 days. Experiments were performed when cells reached 75-85% confluence. The passage numbers of C6 cells were less than 20 in all experiments.

6.3.2 Freezing and Thawing cell stocks

Cells were cryopreserved in a freezing solution containing 5% $^{v}/_{v}$ DMSO and 95% $^{v}/_{v}$ complete culture medium (with FBS and horse serum). Cells were frozen to -70˚C before being transferred to liquid nitrogen for long term storage.

Frozen cells were thawed according to the ATCC-product sheet, by applying gentle agitation in a water bath (37˚C) for 2 min and fresh media was added before centrifugation, finally the cell pellet was resuspended with complete culture media to be ready for culturing.

6.3.3 Passaging and Subculturing of the cells

Routine cell passaging was performed by firstly removing the media, rinsing the adhered cells with PBS then trypsinising for 5 min at 37˚C and cells were viewed under the light microscope to check detachment of the cells from the flask. Once detached, the trypsin was neutralised using the twice volume of complete culture media and transferred to centrifuge tubes. The trypsinised cells were then centrifuged at 500 rpm for 5 min. The supernatant was aspirated and the cells pellets resuspended in 1 mL fresh culture media prior to counting using the haemocytometer to be cultured again.

6.3.4 Principle and Treatment protocols of the quantification of γ-secretase enzyme

The investigation is based on sandwich ELISA technology using γ-secretase enzyme kit (Abbexa Ltd., UK). The 96-well plate is pre-coated with γ-secretase capture antibody. On

addition of the samples to the wells, the target antigen is bound to the capture antibody, and the unbound sample is washed away. The biotin conjugated antibody is added for detection, it binds to the captured antigen complex in each well. This is following by the addition of horseradish peroxidase (HRP) whereas tetramethylbenzidine (TMB) is added to visualise HRP enzymatic reaction (Fig.6.3).

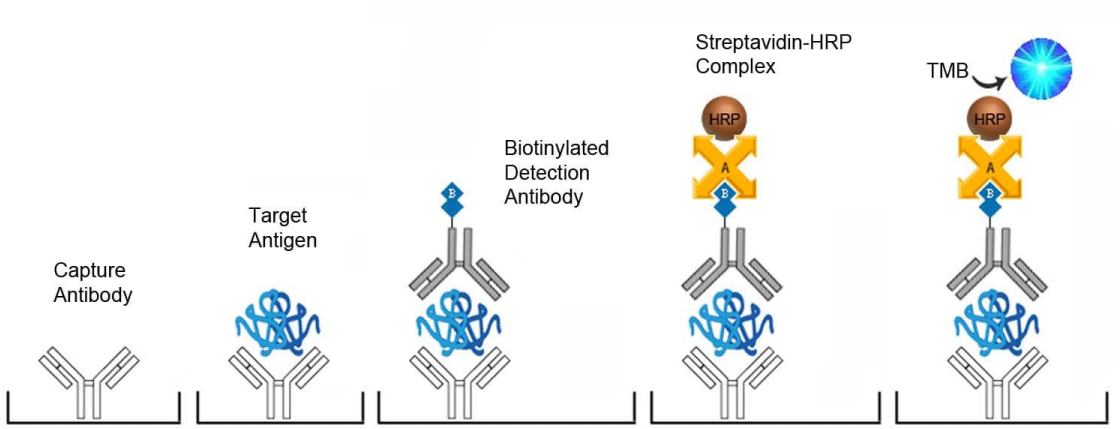

Fig.6.3: The principle of sandwich ELISA kit (picture taken from https://www.lsbio.com/elisakits)

TMB is a chromogenic substrate for peroxidases which reduces hydrogen peroxide to water forming a blue reaction product (diamine). The reaction can be stopped with acidic solution, such as sulfuric acid resulting in a yellow reaction product (Mesulam *et al.*, 1984) (Fig.6.4). The density of yellow which is measured spectrophotometrically at 450 nm is proportional to the amount of γ-secretase in the sample captured in the plate.

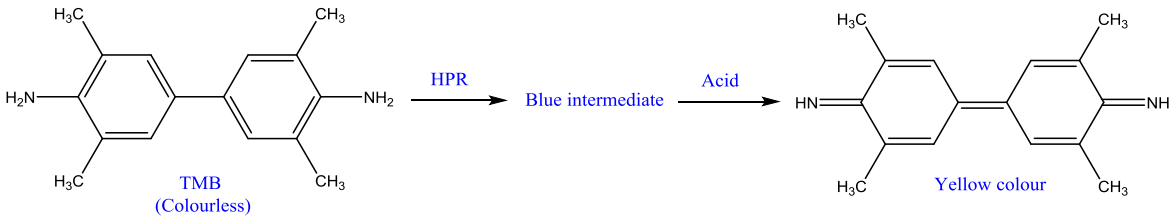

Fig.6.4: Reaction of HRP with TMB. TMB reduces the hydrogen peroxide forming a blue intermediate (diamine), which can be stopped with the addition of acid resulting in a final yellow reaction product.

6.3.4.1 Preparation of samples for γ-secretase enzymatic activity assay

C6 glial cells were cultured in 24-well plates at density $5x10^4$ cells per cm^2, after reaching confluence, they were treated with 200 µM FP, G0K-FP, G1K-FP or AEP-K-FP dissolved

in F-12K media. Each sample was filtered using micro unit filter of 0.2 µm pore size before use. Wells containing untreated C6 cells were also included as a control. After 4 hr incubation, cells were washed with PBS and lysed via freezing to -20˚C and thawing to room temperature 3 times. The well plates were centrifuged at 1500 x g for 10 min to remove any cellular debris and the supernatant was collected for assaying the γ-secretase activity (according to kit instructions). The collected samples were used immediately to avoid any degradation and denaturalisation.

6.3.4.2 Preparation of the Wash buffer

The concentrated wash buffer was diluted 25 fold with DW prior to use according to kit instructions.

6.3.4.3 Preparation of γ-secretase standard

The standard solution was freshly prepared prior to the experiment by adding 1 mL of sample/standard diluent buffer (supplied with the kit) into the standard tube (supplied with the kit) to produce 500 pg/mL of γ-secretase standard solution. The solution was kept for 10 min at room temperature with thorough mixing. A series of dilutions 250 - 7.81 pg/mL were prepared to construct the standard curve of γ-secretase.

6.3.4.4 Preparation of biotin conjugated antibody solution

Biotin binds covalently to protein, nucleic acid or other molecule such as streptavidin with an extremely high affinity and specificity (Barat *et al.*, 2007). Biotin conjugated antibody solution was prepared less than 1 hour before its use by diluting the biotin conjugated antibody (supplied with the kit) 100 fold with antibody diluent buffer (supplied with the kit) and mixing thoroughly.

6.3.4.5 Preparation of HRP streptavidin conjugate (SABC) solution

SABC is designed specifically for immunochemistry and other immunedetection analyses in displaying the antigens distribution in cells. Complexation of streptavidin with peroxidase offers strong affinity to biotin molecules with high specificity (Weber *et al.*, 1989). SABC solution was also prepared less than 1 hour before its use by diluting SABC (supplied with the kit) 100 fold with SABC diluent buffer (supplied with the kit) and mixing thoroughly.

6.3.4.6 Assay procedure for quantification of γ-secretase enzyme

The 96-well plate of the kit was washed twice before adding samples in duplicate. Firstly, a 100 µL aliquots of each of; the prepared standard solutions, sample/standard diluent buffer (as background) and the samples of the collected supernatants (of treated cells) were added, and the plate was covered and left for 90 min at 37˚C. Once completed, the cover was removed and the solution discarded prior to adding 100 µL of biotin conjugated antibody into each well. The plate was then sealed and incubated at 37˚C. After 60 min, the plate was washed 3 times with washing buffer, and 100 µL of SABC solution was added into each well, and then incubated at 37˚C for 30 min. The solution was then discarded and washed 5 times with washing buffer prior to the addition of 90 µL of TMB substrate into each well. Finally, the plate was incubated at 37˚C in dark conditions for 20 min, the reaction was terminated by the addition of 50 µL of stop solution into each well with thorough mixing, and the colour changed from blue to yellow immediately. The colour absorbance was read spectrophotometrically at 450 nm using a microplate reader. The standard curve of γ-secretase standards was constructed and the concentration of γ-secretase was calculated for each sample.

6.3.5 Degradation analysis of FP-conjugated dendronised molecules

Dendrimer and peptides were synthesised by coupling amino acids residues, as well the drug via amide linkage as discussed in Section 2.3 and 4.3. As the peptide breaks down at acidic pH encountered in lysosomal enzyme (Mindell, 2012; Souza *et al.*, 2004), the biodegradability of synthesised peptides and dissociation of the attached drug was ensured by using acidic buffer solution.

The acidic buffer solution was prepared according to manufacturer's instructions, by dissolving an acidic buffer tablet (Honeywell Fluka) in 100 mL of DW with shaking until a clear solution was obtained and the pH was adjusted to 4.5 using sodium hydroxide solution. The G0K-FP, G1K-FP and AEP-K-FP were dissolved in this acidic buffer solution to concentrations of 200 µM and incubated for 24 hr in 37˚C. Samples of 100 µL were collected and filtered with a 0.22 µm filter prior to analysis by HPLC technique. HPLC analysis was performed (as detailed in 2.3.2.4 and 4.3.2) for free FP, G0K-FP, G1K-FP and AEP-K-FP, buffer alone samples also included as background.

6.3.6 Statistical analysis

Data are expressed as average values of number of reproducibility (n) ± the SD and were processed using Microsoft Office Excel. Significant differences between means were assessed using one-way analysis of variance (ANOVA) and Tukey's test, with a 95% confidence interval, P-values of < 0.05 were considered significant statistically.

6.4 Results

6.4.1 Standard curve of γ-secretase

Spectrophotometric results of a series of dilutions 250 -7.81 pg/mL of γ-secretase standard with blank wells (0 pg/mL) were collected and the standard curve was constructed (Fig.6.5). Absorbance values from wells containing sample/standard diluent buffer only were subtracted from all other absorbance values and a standard curve constructed in Excel. The amounts of γ-secretase enzyme from tested samples were calculated according to the equation of the line.

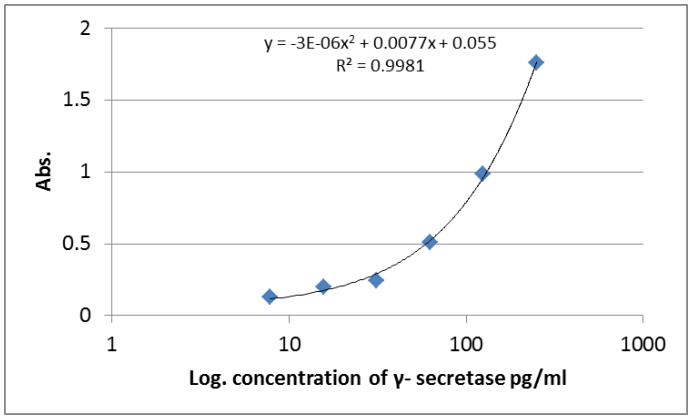

Fig.6.5: The standard curve of γ-secretase.

6.4.2 Quantification of γ-secretase enzyme by ELISA

C6 glial cell line was cultured routinely (Fig.6.6) and the γ-secretase enzyme was quantified using a sandwich ELISA kit. Colour density obtained from the reaction of tested samples (control C6 cells, FP, G0K-FP, G1K-FP and AEP-K-FP) were observed via spectrophotometer and the levels of γ-secretase were calculated.

As demonstrated in Table 6.1; values obtained for the amount of γ-secretase from set of C6 control cells were 28.4 pg/mL, while treatment cells with FP significantly decreased ($P<0.05$) the amount to 8.2 pg/mL.

The results of quantification of γ-secretase also showed that the cells treated with G0K-FP significantly decreased ($P<0.05$) the levels of the enzyme to an average of 12.7 pg/mL, when compared to that of the control cells, with insignificant difference ($P>0.05$) from FP. The analysis also found a significant decrease ($P<0.05$) in γ-secretase for both set of cells

that were incubated with G1K-FP and AEP-K-FP in comparison to the control untreated cells, with average values of 16.0 pg/mL and 14.6 pg/mL respectively. Furthermore, these decreases were also significant ($P<0.05$) compared to the levels of the free drug.

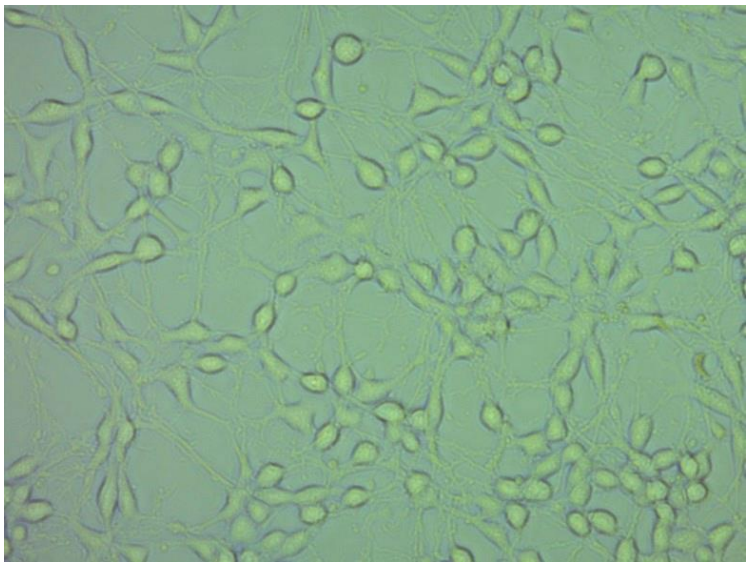

Fig.6.6: Light microscopic image of C6 glial cells (image scale is 200 μm).

Table 6.1: Results of quantification of γ-secretase enzyme after exposure to free FP, G0K-FP, G1K-FP and AEP-K-FP.

Factor	**No.**	**Conc. range pg/mL**	**Average ± SD pg/mL**	**P-value to FP**	**P-value to Control**
Control	6	17.69-36.66	28.43±8.32	< 0.05	
FP	6	3.57-12.40	8.20±3.80		
G0K-FP	6	8.27-19.16	12.69±4.85	>0.05	<0.05
G1K-FP	6	12.99-20.34	16.04±3.18	<0.05	<0.05
AEP-K-FP	6	11.22-19.64	14.60±3.51	<0.05	<0.05

6.4.3 Degradation analysis

To ensure the degradability of synthesised peptides and dissociation of the attached drug, acidic buffer was used. After 24 hr in 37˚C incubation of G0K-FP, G1K-FP and AEP-K-FP in acidic buffer, a qualitative HPLC analysis was carried out. The results of the analyses demonstrated that there are various peaks appeared in each spectra indicating that the hydrolysis of peptide into various products has occurred. As illustrated in the Fig.6.7, the peaks at the beginning of the HPLC run, before 6 min, are related to the solvent (background), whereas at 13.1 min elution represents the dissociated drug as reported in Section 2.4.3.

Moreover, the analysis also demonstrated that some of the whole drug-attached molecules remained without degradation and appeared at their related elution time as demonstrated in their initial analysis. In this regards, the peaks at 16.5 and 14.3 min correspond to the G0K-FP and G1K-FP respectively (Fig.6.7. b and c), while that at time 9.8 min is related to AEP-K-FP. The remaining detected peaks are likely to represent the amino acid residues used in the assembly of the dendrons and peptide including lysine, phenylalanine, leucine and arginine or the shorter peptides that formed due to the breakdown. These hydrolysed products have been detected with a reduction in retention time which is due to their lower MW and hydrophobicity resulting in their earlier elution.

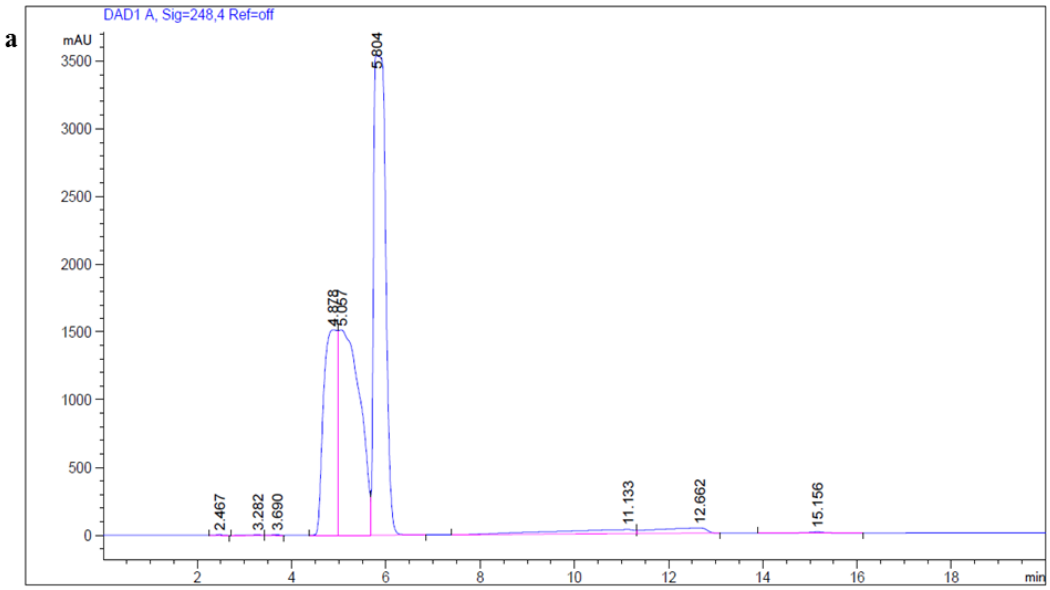

Fig.6.7: HPLC analysis of G0K-FP, G1K-FP and AEP-K-FP degradation after acid incubation. a. buffer only (the background). The analysis method was performed on a hydrophobic C18 column, at 25˚C, 20 µL of injection volume, and the flow rate was 0.6 ml/min. The HPLC mobile phase solvents gradient started with 75:25 of water: acetonitrile over 20 min.

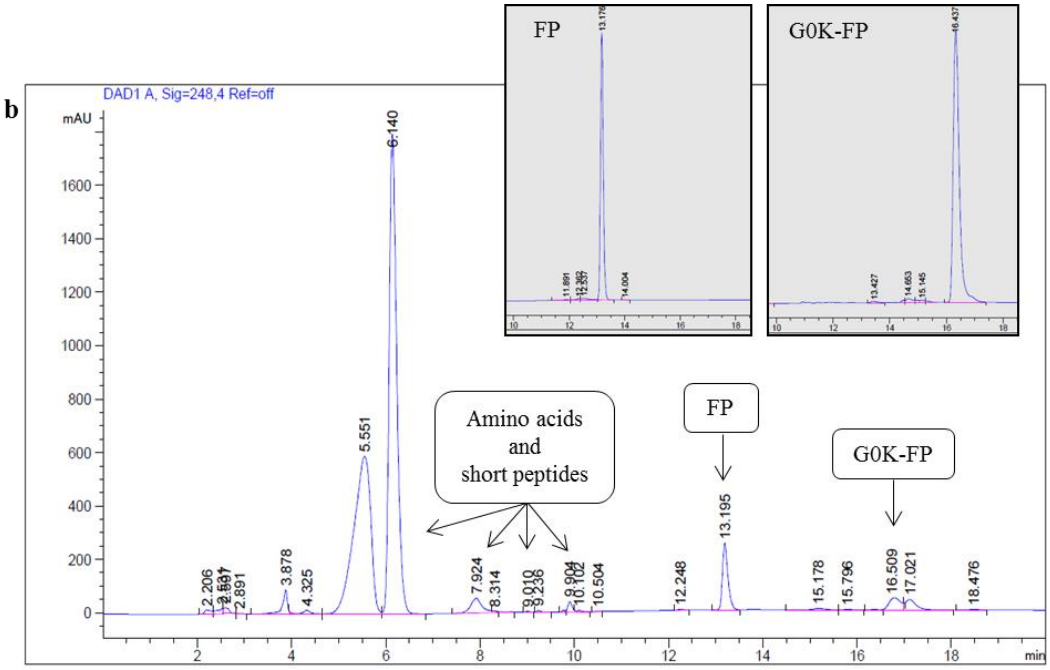

Fig.6.7. b: HPLC analysis of G0K-FP degradation. The inserts show the elution of the initial G0K-FP and free FP.

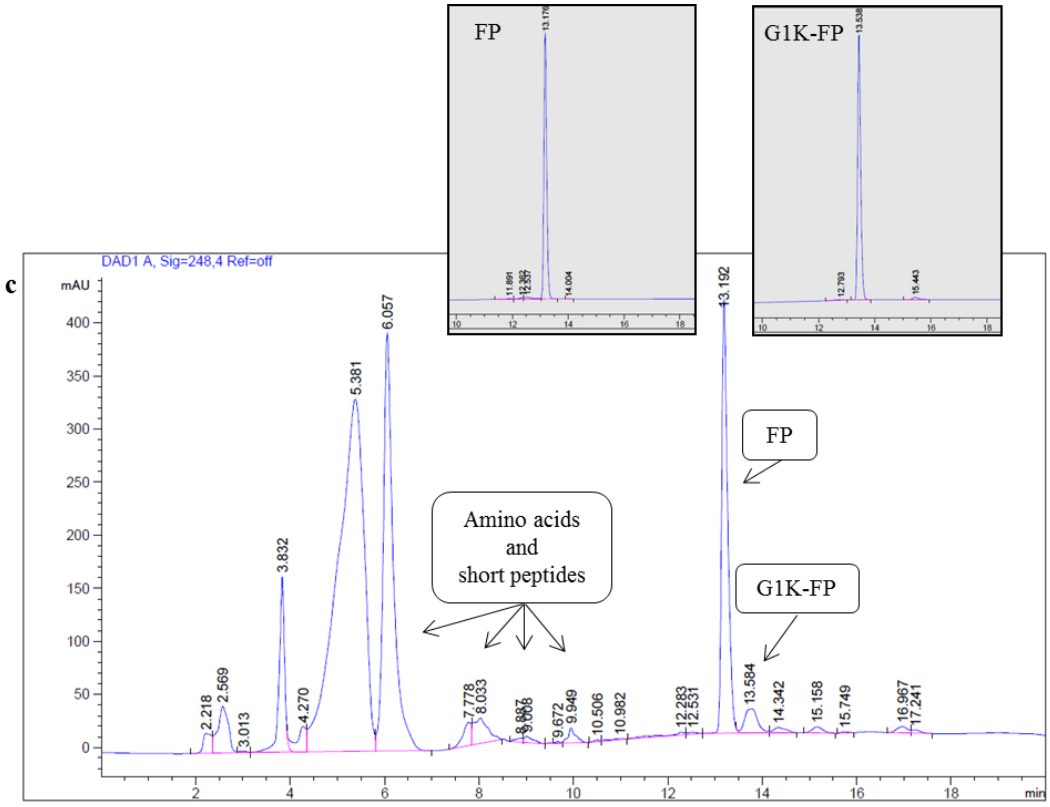

Fig.6.7. c: HPLC analysis of G1K-FP degradation. The inserts show the elution of the initial G1K-FP and free FP.

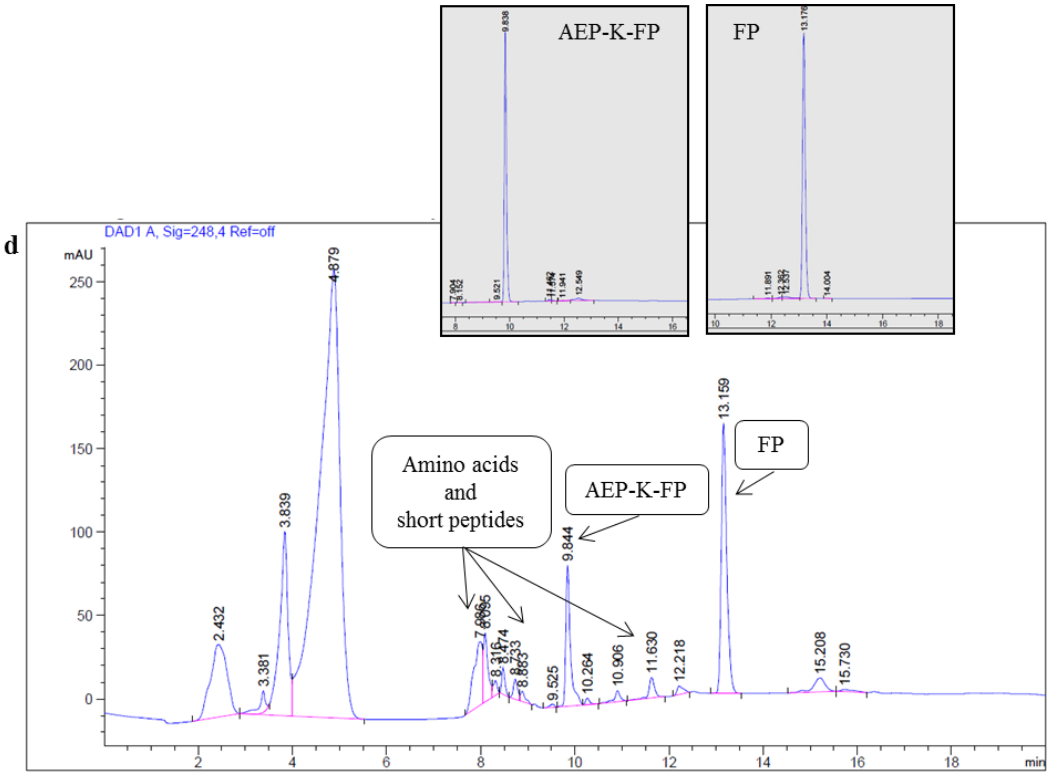

Fig.6.7. d: HPLC analysis of AEP-K-FP degradation. The inserts show the elution of the initial AEP-K-FP and free FP.

6.5 Discussion

FP and other GSMs have emerged at the forefront of AD therapy as potential disease modifying agents. Despite their unclear mechanism of action, GSMs selectively reduce the production of the pathogenic Aβ42 isomer and yet without affecting the total amount of Aβ formed (Crump *et al.*, 2013). Furthermore, they have little effect on other γ-secretase-dependent processing including the Notch pathway as they have been shown no inhibitory effect on the generation of Notch intracellular domain (Weggen *et al.*, 2003). This action is contrary to non-selective γ-secretase inhibition by other inhibitor therapies which drastically affects the metabolism of total amyloid proteins which act to regulate various neuronal and synaptic functions (Crump *et al.*, 2013). It has been stated that the action of the GSMs is solely on PSEN, the part of γ-secretase responsible for the production of Aβ42 isomer which is the underlying cause of AD (Crump *et al.*, 2013). It has been found that FP primarily acts on the PSEN site of the γ-secretase complex which potentially reduces neurotoxic Aβ42 isomer (Eriksen *et al.*, 2003). In addition to the above, formation of Aβ42 in rat-cultured neuroblastoma cells decreased in response to the FP incubation as a selective γ-secretase inhibitor (Gasparini *et al.*, 2004).

On the other hand, clinical trials have demonstrated that the FP failed to improve cognition and other Alzheimer's symptoms due to the existence of BBB. It has been found that the permeability of the drug through the BBB is so low that it cannot reach the target cells inside the brain to exert its pharmacological action (Green *et al.*, 2009; Wilcock *et al.*, 2008). Hence, in this work it was coupled with low generation lysine-dendrons (G0 and G1) and AEP-dendron (Chapter 2 and 4) that has been shown to have the potential to improve BBB penetration and targeting using *in vitro* model (Chapter 5).

Despite this remarkable achievement in the drug permeability, drug conjugation to the dendronised carrier might result in some molecular or structural modifications that may influence its activity (Silverman *et al.*, 2014). For this reason, C6 glial cells were cultured to investigate the quantity of γ-secretase enzyme liberated after cell lysis following the incubation with the FP-attached dendronised carrier systems in relation to the free form of the drug molecule.

The C6 cell line possesses most of the regulatory control mechanisms and characteristic features of the neuroglial cells. It has been used in many neurological studies for basic cellular mechanisms and as a model that mimics the *in vivo* situation or primary brain cell culture for several research aspects such as hormonal action (Hook *et al.*, 1998). These cells were found to express similarity to the *in vivo* cells in terms of multiple factors including stereotypical astroglial markers, glial fibrillary acid protein and fibronectin fragments as well as presenting an astrocyte phenotype (Reichert, 2008). In addition, gene and proteins analysis for this neuronal glial cells have showed the cellular expression of APP and secretases (Nord *et al.*, 2010). C6 cell cultures have also been used in AD research to examine the response of γ-secretase to different inhibitory treatments which significantly reduced the secretory cleavage of APP (Refolo *et al.*, 1995).

Since the study presented here represents the first attempt that successfully coupled FP with a carrier system, there are no previous studies demonstrating the efficacy of FP in its conjugated form. A recent trial that has been conducted regarding enhancing FP cellular uptake was by its entrapment in PEG-micelles rather than chemical coupling (Mu *et al.*, 2013), but the study was devoid of secretase activity examination. A further study looked to embed FP in NP that only disguised its cytotoxic effect to allow high concentrations to be transported across the BBB (Meister *et al.*, 2013) also provided no direct evidence of its effect on the enzyme activity.

In this work, the results generated from the γ-secretase enzyme quantification using a sandwich ELISA kit showed a reduction in enzymatic activity of C6 cells due to the use of the free drug with a significant difference ($P<0.05$) from the levels of the control. As demonstrated, FP as one of GSMs has the ability to act on γ-secretase thus reducing amyloidogenic Aβ42 levels in numerous *in vivo* and *in vitro* studies without perturbing other signalling of the enzyme (Weggen *et al.*, 2003).

Alternatively, the FP-bound carriers showed a reduction in enzymatic activity of more than 50% in the case of G0K-FP which was not significantly different ($P>0.05$) from that of the free drug. The results achieved using G1K-FP and AEP-K-FP, however, were shown to be less effective than free drug, however these drug-integrated molecules still demonstrated a significant effect ($P<0.05$) in decreasing the quantity of γ-secretase in comparison to that of untreated cells (Table 6.1).

The steric hindrance which occurs within large sized molecule may prevent specific chemical reactions and change the reactivity patterns (Silverman *et al.*, 2014). This is perhaps the most likely reason behind the moderate efficacy observed in the case of FP-bound molecules. In spite of having 4 more molar excess of drug moieties, G1K-FP showed the more moderate reduction in enzymatic activity, probably attributed to the spatial arrangement of the chemical groups as it has a more branched structure and the active sites of the drug are probably less exposed to the target.

As reported previously, some drugs have been shown to lose part or all of their activity in conjugation form. For instance, the steroid hormone (testosterone) lacked its androgenic effect when it was linked to a polymer due to the steric hindrance (Silverman *et al.*, 2014). A further study showed that the *in vitro* doxorubicin-conjugate potency varied and increased with increasing amounts of drug loaded (Hamblett *et al.*, 2004). Instead, a variety of approaches and chemistries have been employed to develop a design for DDS by attaching drugs to different carrier systems covalently via a spacer, such as lysine, through a biodegradable linkage to ensure drug release and to ascertain its subsequent action (Karolina *et al.*, 2015; Khandare *et al.*, 2011).

Although encapsulating the drug in a dendrimer or another DDS is thought to be useful as it keeps the drug molecules intact, the drug could be quickly released from such system under physiological conditions (Safari *et al.*, 2014). Alternatively, covalent conjugation of drugs to the periphery of dendrimers can lead to a slower release rate compared to those entrapped by electrostatic interactions (Cheng *et al.*, 2007; Najlah *et al.*, 2007). Therefore, the complexation of the drug via hydrolytically labile linkages including amide, carbamate and ester linkages is more suitable for a better control of drug release over time and targeting than that can be achieved by encapsulation/electrostatic complexation alone (Li *et al.*, 2012; Safari *et al.*, 2014).

The structure of the carrier system and the drug or ligand is the most important factor that determines the type of suitable linking reaction, and it facilitates the chemical conjugation via the formation of the functionalities such as amide, ester, acetyl-hydrazone or disulfide groups (Karolina *et al.*, 2015). It is noteworthy to mention that FP molecular structure containing a carboxyl group facilitated its coupling to G0 and G1 lysine dendron and AEP-lysine via amide linkage (Chapter 2 and 4) which offers the preferential drug release.

To provide supporting evidence that the drug can dissociate from the dendronised carrier system and to determine the fate of molecules, a biochemical investigation of drug-bound carrier degradation was performed by HPLC analysis. The analysis was carried out using acidic buffer solution (of pH 4.5) mimicking the lysosomal situation in which the peptide and amide linkage are hydrolysed (Mindell, 2012; Souza *et al.*, 2004). The results highlighted that very small portions of original integrated molecules remained undegraded whereas the majority of drug molecules were liberated in the solution alongside numerous breakdown products (amino acids and small peptides residues) (Fig.6.7). This was suggested by the early elution of peaks from the HPLC column. According to the elution principle of the reverse phase HPLC this practically depends on the affinity of the material to the hydrophobic stationary phase, in turn the more non-polar compound being the most strongly retained as its attraction to the stationary phase is higher. In contrast, small fragments are more water soluble compounds and as a consequences they are weakly retained, so being eluted earlier in the aqueous mobile phase moving fast through the column (Pare *et al.,* 1997). Hence, the peaks observed in the HPLC chromatographs that are not related to the free drug or drug-bound carriers are most likely attributed to the amino acids, the building units of peptide, or to short peptides resulting from the breakdown of the original peptide or dendron.

These data suggest the hydrolysis of the drug-dendronised molecules and release the free drug and they are consistent with other studies which have confirmed the degradation of dendrimers. Indeed, a conjugate of doxorubicin to aminoethyl polyacrylamide resulted in the release of doxorubicin at pH 4.0 in less than 24 hr, and more than 96 hr at pH 7.5. The amide linkage was found to be cleaved at the acidic pH encountered in proteolytic enzyme action and stable at physiological pH (Souza *et al.*, 2004). A further study has found that cationic G2 and G3 dendrons were biodegraded into their building monomers using acidic buffer solution with a rate decreasing with the higher generation number (Lee *et al.*, 2006). Our results are also supported by previous findings of methotrexate coupling to poly-L-lysine polymer via amide linkage which revealed full drug pharmacological action so signified degradation of linkage as the action of the drug requires detachment from polymer (Silverman *et al.,* 2014). Likewise, pharmacokinetic and biodistribution investigation of intravenous administration of cationic poly-L-lysine-dendrimers in rats revealed the appearance of radiolabeled form of free lysine and larger products (but non

intact dendrimer) in plasma, suggesting that biodegradation of the dendrimer to L-lysine and short peptides. The radiolabelled L-lysine dendrimer was also found to be widely distributed throughout the major organs, with selective exception for organs of the reticuloendothelial system (Boyd *et al.*, 2006).

The degradation tendency of the dendrons and the peptide used in this project can facilitate their metabolism and eventual excretion; therefore decrease the cytotoxicity that may instead occur due to accumulation inside the body. This property is important for future *in vivo* trials that aim to prove benefit of this conjugate over other types of carrier systems or other types of building units of dendrons.

Findings from several studies have also demonstrated that polyamide dendrimers, in comparison to other types of linkages, have higher stability due to their relatively lower rate of hydrolysis in blood circulation (Khandare *et al.*, 2011). Direct amide linking of naproxen with PAMAM dendrimer showed a higher chemical stability in plasma and liver homogenate and in different pH buffers including 7.4 and 1.2, than that of ester linking (Najlah *et al.*, 2007). This feature is necessary to minimise the non-specific interaction of dendrimers with systemic circulation thus asserting that the drug-loaded dendronised system will not be cleared rapidly and so achieving intracellular delivery of bioactives. That would ensure the drug circulates in blood without degradation and reaches the target site in sufficient amount in turn decreasing the administered dose. As mentioned previously, high doses of FP leads to several side effects such as gastric ulcer and haemorrhage which can be avoided by attaching FP covalently to the dendron (Bjarnason *et al.*, 1993; Meister *et al.*, 2013). This could also help the future *in vivo* investigation when the FP-loaded dendronised system is used as intravenous formulation rather than local injection. In addition, this conjugation could offer a prolonged drug effect due to the stability of the conjugate in the circulation and as a consequence, a less frequent drug administration.

Hence, the FP conjugation to lysine dendron and its bifunctionalisation with AEP provide advantages over other types of conjugates as it is likely favour the drug release at the site specific with higher bioavailability and eventual biodegradation.

6.6 Conclusion

In this chapter, FP-bound dendronised carriers were investigated biochemically for their potential ability to reduce the γ-secretase activity in relation to the free drug. The drug in its conjugated form in the entire complex molecules tested still retained the capability of reducing the cellular enzymatic activity. This demonstration provides the potential of the synthesised molecule (G0K-FP, G1K-FP and AEP-K-FP) to induce a substantial AD therapeutic action resulting in lowering the pathogenic amyloidogenesis responsible for the disease.

Moreover, the biodegradable building monomers that have been used in the synthesis of these peptides, alongside the biodegradable amide linkage that linked them with each other and with drug, supports the dissociation of the drug over time. Therefore, the pharmacological activity of the dug can be boosted in the long term leading to a greater reduction in the enzymatic activity of γ-secretase.

Over all, the activity of the bound FP at the time of administration with the later release of free drug from degrading complexes highlights the benefit of using a dendron as a carrier system with more preference when functionalised with AEP.

Ultimately, these biodegradable dendrons are good candidates for drug delivery and other different biomedical applications arising from their ability to promote therapeutic activity on the target cells without any significant cytotoxic effect.

Chapter 7. General Discussion and Conclusions

7.1 Discussion

AD, a neurodegenerative brain disorder, represents one of the greatest healthcare challenges of this century; a fact that is exacerbated by the continuously growing life expectancy (Aparicio *et al.*, 2016) and has arguably become one of the most dreaded conditions of older people (Wyss, 2016). AD leads to a devastating and progressive loss of memory and cognition, for which there is no curative treatment. The main pathological hallmarks of the disease are aggregates of extracellular Aβ peptides that form SPs (Canter *et al.*, 2016). In healthy individuals, the Aβ peptide level remains at a steady-state and does not lead to the generation of amyloid plaques due to metabolism of the peptides (Jakob *et al.*, 2009).

CNS disorders such as AD are considered among the most lengthy and resource-consuming diseases with unmet medical needs (Aparicio *et al.*, 2016). The high failure rate of the current treatment is due to a great extent to persistence of the BBB which impedes the access of therapeutic compounds into the brain, leading to insufficient exposure for the drug (Wyss, 2016). FP is one of these poorly penetrating drugs.

FP is an arylpropionic acid derivative member of the NSAIDs, FDA-approved, and commercially available as an effective pain reliever and anti-inflammatory (McGeer *et al.*, 2007). It is a well absorbed drug with 4 hr biological half-life and it is fully excreted from the body within 24 hr (Davies, 1995). Studies have confirmed the FP's potential as a treatment for AD through the selective reduction of Aβ42 via the modulation of γ-secretase (Crump *et al.*, 2013). However, FP's limited penetration through the BBB, which has led to its discontinuing use, is a challenge to be overcome in order to deliver effective doses into the brain.

The present project aimed to improve the brain permeability of FP by designing a non-cytotoxic and biodegradable carrier system able to aid the passage of the drug across the BBB and reach the target to reduce the pathogenic Aβ in AD.

The brain endothelial barrier is tight at the brains interface with the neuroglial cells and, in normal conditions, can only be passed through via endogenous transporters including

solute carriers, active efflux transport and adsorptive and/or receptor mediated transport (Wim *et al.*, 2008) (details in Section 1.4). Many strategies have been proposed to circumvent this formidable obstacle to drug penetration to the brain and enable active molecules to reach their targets in relevant therapeutic amounts, however to date none has provided a satisfactory balance in efficiency and safety (Carlotta *et al.*, 2017). Direct or local drug injection into the brain carries a high risk, whereas enhancing the diffusion of drugs across the barrier through modification is only applicable for some low MW (<400 Da) molecules with high lipophilicity (Chen *et al.*, 2012). Among the alternative, non-invasive approaches, are the use of BBB shuttles or Trojan horses via AMT and RMT, in which a wider variety of cargoes can be transported into the brain without affecting the integrity of the BBB (Aparicio *et al.*, 2016). In recent years, the Trojan horse approach has made a significant progress in the field of drug delivery to the brain with improved potential targeting capacity. In addition, a plethora of BBB shuttle peptides and drug carriers have emerged that offer a great promise for the development of more efficacious treatments for NDs such as AD (Oller *et al.*, 2016).

Dendrimers are a class of drug carriers with growing interest in this area of application. They are hyper branched polymers offering the possibility of the creation of well-characterised complexes with different payloads including drugs and ligands (Neelov *et al.*, 2016). Currently, dendrimers are widely used in a variety of industrial and biomedical applications, specifically in drug and gene delivery (Ebelegi *et al.*, 2017; Srinivas *et al.*, 2014) (see Section 1.6.4.2). To date, only three different types of dendrimers; PAMAM, PPI and poly (lysine)-based, have been widely used as drug transporters with interesting outcomes in the treatment of CNS disorders (Gagliardi, 2017).

Synthesis and characterisation of FP-integrated dendronised carrier systems

In the present study low generation lysine dendrons (G0 and G1) were designed and synthesised, then successfully integrated with FP molecules via attachment to the amino groups at the branches to pursue their potential to be used as drug carrier systems across the BBB. Moreover, the adaptable architecture of the G0 lysine dendron allowed it to be further successfully bifunctionalised with AEP. AEP is a 10 amino acids peptide of sequence LRKLRKRLLR derived from the ApoE peptide molecule (the 141-150 amino acids residues) (Datta *et al.*, 2000). This short peptide mimics the active ApoE-binding

domain with cell surface LDLr that has demonstrated the best performance for receptor binding and the potential to transport a wide range of substances across the BBB when used to functionalise several carrier systems (Re *et al.*, 2011) (see Chapter 4).

Here, microwave Fmoc-based SPPS was employed to synthesise dendrons and the peptide as well as coupling them to the drug molecules (Chapter 2 and 4). The basic amino acid monomer, lysine, is stable in solution, inexpensive and contains an alkyl amino side-chain enabling the introduction of multiple branching units. The assembly was performed on TentaGel-NH_2 resin as illustrated in Chapter 2. This method has ensured a faster and efficient synthesis process when compared to non-aided microwave conventional SPPS method. In addition, this microwave-assisted SPPS method with Fmoc chemistry was shown to be a valuable tool that offered peptide assembly with a high degree of purity as demonstrated in TLC and HPLC analysis (Chapter 2 and 4).

The chemical structure of FP consisting of carboxyl group also facilitated the successful formation of amide linkage and integration with the dendronised carrier systems as shown in MS and FTIR analysis (Chapter 2 and 4).

For the first time, the precise control of the synthetic method combined with optimised techniques of characterisation led to the production of novel FP-integrated dendronised carrier systems. In addition, these synthesised products have appropriate linkages assured later degradation and drug release upon hydrolysis. Furthermore, these findings show that the FP-integrated dendrons and functionalisation with AEP can be produced successfully using automated SPPS method, achieving a high degree of purity and reproducibility in a time and cost efficient manner. Consequently, a wide range of other peptides may benefit from this method of synthesis and coupling to different drugs of similar chemical structure to FP (such as ibuprofen and methylprednisolone) and used in a variety of applications (Kolhe, 2003).

Cytotoxicity studies

This work set out to further the knowledge relating to the biocompatibility of the FP-conjugated dendronised carriers to understand the effects of these novel biomaterials on biological systems. This was achieved by testing the cytotoxicity of each of these synthesised molecules towards the brain endothelial cell line (bEnd.3) using MTT analysis

for metabolic activity and LDH assay for membrane integrity, in addition to the cell death assessment using HPI. The results found there to be no cytotoxic effect even after incubation for 48 hr and up to 400 µM (Chapter 3 and 4). These findings support those of the previous published literatures which have revealed lower cytotoxicity of low generation dendrons when compared to higher generations (Menjoge *et al.*, 2010) (details in Chapter 3), while studies using AEP have also confirmed its low cytotoxicity (Re *et al.*, 2011) (details in Chapter 4).

Moreover, using lysine, which is a naturally occurring amino acid residue, to synthesise dendrimers of different generations, may be considered as the safest choice in comparison to other dendrimers due to its lack of cytotoxicity (Neelov *et al.*, 2016).

The data documented in this thesis identify the properties of these novel materials in terms of cellular response, such as viability or metabolic activity and membrane integrity, which in turn suggested their safety as drug carrier systems. This can stand as an important contribution to knowledge not only for the future *in vivo* studies of FP brain delivery but also for long-term or high-dose therapeutic applications. In this regard, FP-conjugated dendronised carriers may be applied for sustained release in anti-inflammatory therapy since it can circulate in the blood for long time without harmful effect.

In vitro BBB model validation

The main aim of this thesis was to explore the potential of the designed dendronised carriers to improve the permeability of FP across an *in vitro* BBB model. To achieve this aim the validation of this model was first tested. The cell-based model must faithfully recapitulate the *in vivo* transcytotic criteria such as cellular organisation and TJ permeability (Patabendige *et al.*, 2013).

The cell line used in the study (bEnd.3) that cultured on microporous Transwell® inserts has previously been shown to have great potential as a BBB model for drug transport studies (He *et al.*, 2010). In order to confirm the validity of the model, TJs formation, a particular feature of brain endothelia and thought to be influential in the efficiency of the model to paracellular transport, was examined. Cellular monolayer integrity was confirmed using TEER measurements, cell morphology by CLSM and the restriction to sucrose paracellular permeability using HUVEC cells as a negative control. Findings from all

examined parameters in this study confirmed that the model expressed an integral cell layer due to appropriate TJs formation. These findings are in agreement with other studies which have proved the validity of this type *in vitro* BBB model for drug transport study (Brown *et al.*, 2007; Omidi *et al.*, 2003) (more details in Chapter 5).

The low number of passages that have been used here for the bEnd.3 (< 20 passages) and the optimised culturing conditions also helped in assurance the maintenance of the primary cellular barrier features. As previously documented, the paracellular leakage increased due to invalid TJs formation with increasing passage number particularly over 35 (Brown *et al.*, 2007).

It was not possible to co-culture the bEnd.3 with C6 glial cells due to each cell type requiring different culturing media. The delicate nature of the bEnd.3 cultures made it difficult to grow them in using different culture media. However, earlier investigations of bEnd.3 monolayers have shown them to possess functional TJs when cultured alone with no significant differences in comparison to those obtained when co-cultured with glial cells (Omidi *et al.*, 2003; Weksler *et al.*, 2005).

As facilities to measure paracellular permeability utilising radio isotopes as used in previous studies (Patabendige *et al.*, 2013) was not available, paracellular permeability for sucrose was measured using a more difficult method but with same reported reliability (Teixeira *et al.*, 2012).

Hence, the bEnd.3 monolayer cultured on Transwell membrane at confluence displayed the merits that allowed its worthwhile use as *in vitro* BBB model for drug transport studies. Using cell-based *in vitro* models to study transcytosis possesses many advantages. *In vitro* models can be easily manipulated and allow the measurement of different variables, such as temperatures and pharmacological agents and explore the molecular mechanisms of transcytosis with higher precision. The complexity of living organisms makes the identification of interactions between the components and the exploration of the basic biological functions a great barrier so that most studies have been conducted using cell-based model as it simplifies the system under study and can be focusing on a small number of components (Vignais *et al.*, 2010), also it can be used as an alternative to reduce ethically controversial animal models. In addition, it allows fast and relatively inexpensive

screening (Price *et al.*, 2009). For these reasons, an *in vitro* model of BBB was used in this work. However, *in vitro* models still lack the *in vivo* context that could provide some level of body regulation, so that further *in vivo* investigation required for future studies.

Cellular uptake and Permeability investigations

The transport of drugs or other substances across the BBB via regulated transcytosis is an attractive strategy as it enables the passage of macromolecular complexes that are not normally achievable (Mager *et al.*, 2017; Zuchero *et al.*, 2016).

One of the crucial areas of concern in RMT is to find receptors that are (a) selective to the BBB vasculature, and (b) highly expressed in the desired site. An additional challenge is to find ligands that are capable of taking advantage of these receptors in the transcytosis for drug delivery (Mager *et al.*, 2017). It is well stated that the BBB endothelium is rich in the LDLr in comparison to other tissues making this receptor an eligible to be exploited for targeting brain delivery (Dehouck *et al.*, 1994; Molino *et al.*, 2017).

To confirm that the synthesised dendronised carrier systems are able to be endocytosed, CLSM and flow cytometry analysis were used in which the uptake by the cells could be visualised via fluorescent-labelling. In the confocal images, fluorescent accumulation in the cytoplasm was observed in bEnd.3 cells that were treated with G0 and G1dendrons when compared to that of the control cells (Fig.5.10). Whereas the flow cytometry analysis (Fig.5.11) of bEnd.3 showed that both (G0 and G1) dendrons were internalised by the cells in a similar manner to those demonstrated in previous studies that identified the cellular localisation of dendrimers using a range of different cell lines including fibroblasts, Caco-2 cells (Yang *et al.*, 2007) and lung epithelial cell line A549 (Khandare *et al.*, 2005). This internalisation is due to electrostatic interactions between the negatively charged cellular membranes with the cationic dendrons (Xu *et al.*, 2014) (details in 5.1.1). This is also supported by previous findings in which the uptake of several drugs including folic acid (Choi *et al.*, 2005), ibuprofen (Kolhe *et al.*, 2003) and camptothecin (Sadekar *et al.*, 2013) have successfully internalised after being conjugated with dendrimers (Patri *et al.*, 2012).

Our data from CLSM and flow cytometry also revealed a significant higher uptake by the bEnd.3 was displayed by the dendron when was further functionalised with AEP and proposed for a lipoprotein receptor-mediated uptake (Chapter 5). This is in agreement with

other studies which showed that AEP-decorated NP and NL have undergone increased cellular uptake when compared to undecorated carrier systems (details in Section 5.1). These studies have also investigated the cellular interaction of the bEnd.3 cell line which verified the location of the LDLr via which the binding of AEP-decorated carrier systems occurred (Wagner *et al.*, 2012). Furthermore, it was also found that these formulations' cellular uptake were by a caveolae-mediated mechanism rather than late-endosomes or early-lysosomes; thus also indicating receptor-mediating endocytosis for AEP complexes (Re *et al.*, 2010).

In order to examine the permeability of the FP-loaded molecules across this *in vitro* BBB model, HPLC analysis was used. The method was optimised to be appropriate not only for FP but also for FP-conjugated molecules after identification of λ_{max} and the mobile phase solvents gradient (Chapter 2 and 4). The measurements included both free and conjugated drug, and they were considered after exclusion of the resistance of the Transwell® insert itself. An improvement was seen in the permeability when FP was attached to the dendronised carrier systems and the highest percentage of permeability was observed with AEP-functionalised dendron (Chapter 5).

Cationic peptides or dendrons are thought to be able to cross the biological membranes. Their positively-charged amine groups support its electrostatic interaction with negative charges of cell membrane followed by a clathrin- and caveolae-mediated endocytosis then transcytosis to the other site of the cell (Herve *et al.*, 2008). Thus the cationic dendrimers such as poly lysine, PPI and PAMAM have been widely exploited in drug delivery (Prashant, 2014). As previously reported that cationic dendrimer enhanced paclitaxel and naproxen permeability across brain endothelial cells and Caco-2 cell monolayers (Najlah *et al.*, 2007; Teow *et al.*, 2013).

Even though the permeability across cellular membranes could increase with higher generations of dendrons as reviewed by earlier studies (Kitchens *et al.*, 2005; Najlah *et al.*, 2006), low generations were used in the present work to avoid any cytotoxicity that is associated with increased generation and size of dendrimers (Yang *et al.*, 2009).

Functionalisation of the G0-dendron with AEP significantly boosted the permeability across the *in vitro* BBB model, which could be attributed to RMT via LDLr. The AEP is

the binding domain of the ApoE peptide that can be recognized by the receptor at the cell membrane. These findings are supported by earlier investigations in which carriers grafted with this ApoE sequence (141-150), were successfully internalised and then transported across the BBB due to RMT mechanism with a selective cellular surface binding to a the LDLr (Kreuter *et al.*, 2002; Sauer *et al.*, 2005). ApoE-functionalisation has been efficiently employed to transport many drugs into the brain such as dalargine, curcumin and doxorubicin using different carriers (Kreuter *et al.*, 2002; Re *et al.*, 2011; Sauer *et al.*, 2006). In RMT, the cargo can get access into the brain by "piggybacking" in which the ligand binds to the membrane receptor forming a caveolae subsequently resulting in small vesicle formation followed by its exocytosis into the external cellular side (Xiao *et al.*, 2013) (Fig.4.3).

However, these permeability values do not reflect the real amount of drug that passed through the *in vitro* BBB model, as the molar excess of drug conjugated within the dendronised carrier systems (2 more in G0 and AEP-functionalised dendron and 4 more in G1) can increase the final free drug concentration after dissociation. This can ensure delivery of high drug payload to the brain increasing its bioavailability at the site of action.

Thus, conjugation of FP with the dendronised carrier systems provides the possibility of re-using the drug after discontinuing it in the treatment of AD because of its limited permeability to the BBB, as the dendronised carrier systems enabled the drug to pass through this barrier. Moreover, the side effects that associated with high doses of the unconjugated drug required to induce the action can be avoided. Therefore, the frequency of drug administration could be decreased which is more comfortable for patients.

Using AEP-functionalised dendron in crossing the BBB via RMT is an attractive strategy for brain targeting (Mager *et al.*, 2017). Alternative entry routes such as direct injection into the cerebrospinal fluid or temporary opening to the BBB are limited by the requirement of hospitalisation and increased infection risk and pathogen entry to the brain (Chen *et al.*, 2012; Jones *et al.*, 2007). Peptides, including AEP, are affordable, easily obtained and characterised with their amenability to chemical synthesis which opens up the possibility of applying a variety of modifications and of introducing multiple functional groups for site specific conjugation (Oller *et al.*, 2016). Furthermore, in the case of RMT, most peptide ligands neither compete with endogenous compounds nor stay bound to the

receptor when compared to some antibodies that have been previously used as a carrier (Oller *et al.*, 2016; Xiao *et al.*, 2013). Thus receptor-based BBB transporters have so far provided promising achievements in preclinical brain delivery (Mager *et al.*, 2017; Molino *et al.*, 2017).

Moreover, utilising this targeting approach would help in delivering the drug solely to the desirable organ, thereby avoiding interactions with other body tissues and subsequently decreasing the undesirable systemic effects alongside reducing the dosage required of the drug. This is unlike other approaches that lack such properties which may lead to drug's wide distribution in all tissues and inadequate amount delivered to the brain (Jones *et al.*, 2007; Mager *et al.*, 2017).

Hence, functionalisation of dendron with AEP facilitates the transport of FP and its targeting to the brain; beneficial properties that can be further used for the treatment of other CNS disorders, as a wide range of poorly penetrating drugs and genes can be transported by this carrier system.

The data presented in this work provides the first direct evidence that dendronised carrier systems, in particular the AEP-functionalised dendron, could induce endothelial uptake and endocytosis of the drug with improving BBB permeability and targeting.

Quantification of γ-secretase enzyme in response to exposure to the FP-integrated molecules and the degradation of these integrated molecules

Further to the demonstration of improved transport of FP across the *in vitro* model of the BBB, another study was conducted to investigate the activity of the drug in its conjugated form before its dissociation from the carrier system.

As mentioned before, FP as one of GSMs, is a profound disease modifying agent in AD by selectively decreasing the production of the amyloidogenic Aβ42 (Crump *et al.*, 2013). Its action lies in altering γ-secretase activity in a way that does not affect other Notch signalling or other APP processing pathways (Lleo *et al.*, 2004). This is an advantageous property of the drug over other γ-secretase inhibitors, as it keeps the normal activity of the other APP processes (Turner *et al.*, 2003). FP has been found to act primarily on the PSEN

site of the γ-secretase complex preventing formation of neurotoxic Aβ42 isomer during APP cleavage (Crump *et al.*, 2013; Gasparini *et al.*, 2004; Weggen *et al.*, 2003).

In this study, quantification of γ-secretase enzyme in response to exposure to the FP-integrated molecules was carried out using a sandwich ELISA following incubation of glial C6 cells line with free FP and FP-attached dendronised carrier systems. The results showed that the drug-conjugates still retained the drug action in decreasing the activity of γ-secretase with significant differences ($P<0.05$) in comparison to that of untreated cells (Table 6.1). Whilst they are not as active as the free drug, this might be explained due to the steric hindrance that occurs within the large size molecule and the spatial arrangement of functional groups which could change the reactivity of the drug. Several previous studies provided a line of support to this explanation in which therapeutic agents lacked their usual efficiency upon conjugation due to steric hindrance (Hamblett *et al.*, 2004; Silverman *et al.*, 2014). Instead, some others were able to maintain their activity while they still attach to the carrier molecules (Silverman *et al.*, 2014) (more details in Chapter 6) .

To provide a support for a full activity of the drug in the long term, the degradation of the FP-integrated dendronised carriers was investigated using HPLC analysis proving later drug dissociation from the carriers. The key point in this project was the use of biodegradable materials including amino acids which are linked through a hydrolysable amide linkage, a bond that also linked the FP molecules to the dendrons.

Researchers have reported that dendrimers or peptides with such backbones, are completely broken down into their building-block monomers thereby releasing the entire moieties including the drug payloads (Khandare *et al.*, 2011; Souza *et al.*, 2004). Moreover, it has been stated that the introduction of biodegradable units during the construction of the carrier molecules not only helps in their final dissociation but also will aid a reduction in their toxicity as the bonds can be proteolysed by cellular enzymes (Elvira *et al.*, 2005; Xu *et al.*, 2014). In fact, the peptide and poly amino acid type-dendrimers biodegrade through the hydrolysis of their amide linkage into parent carboxylic acids and the appropriate amines that are normally metabolised and eliminated from the body (Boyd *et al.*, 2006).

In the case of poly amino acid dendrons as carrier systems, providing benefits over other DDS by offering this direct biodegradable linking with drug molecule. This is supported by previous finding of methotrexate coupled to poly lysine polymers via amide linkages which revealed full drug pharmacological action upon degradation of the linkages (Silverman *et al.*, 2014). Likewise, testosterone has been found to be ineffective when linked directly to a polymer but it retained its activity when linked via a biodegradable spacer (Silverman *et al.*, 2014). This finding shows considerable promise for the use of poly lysine dendrons as carrier systems or as a spacer arms with other carrier systems to conjugate the active compounds and assure their efficacy.

It has been also shown that dendrimers can protect drugs against systemic degradation ensuring the stability of the conjugate in the circulation and in turn reducing their contact with healthy tissues during the delivery process and lowering their systemic toxicity (Neelov *et al.*, 2016). Previously studied drugs-dendrimers conjugates via amide linking have demonstrated a relative low hydrolysis in blood circulation (Khandare *et al.*, 2011; Najlah *et al.*, 2007). This suggests that the formulation FP in conjugation with dendronised carrier systems produced in this study could be suitable for administration as a parenteral injection and circulating in the blood for enough time without losing the drug activity or affecting the healthy organs.

In addition, FP like other NSAIDs, is extensively bound to plasma proteins in its noncovalent binding form resulting in only a small amount reaching the target (Parepally *et al.*, 2006) and high doses needed for therapeutic effect can be cytotoxic and exert a number of side effects (Biswas *et al.*, 2017). Therefore, this conjugation of the FP molecules alongside the high upload capability of the poly lysine dendrons that passed it through the BBB could also make FP more potent than the free form.

Previous attempts to enhance FP permeability, which were also conducted *in vitro*, relied on either its entrapment in PEG-micelles using the Tf ligand for RMT (Mu *et al.*, 2013) or by embedding FP in NP that only could disguise its cytotoxic effect to enable transport in high concentrations (Meister *et al.*, 2013). In comparison to these studies, the present dendronised carriers showed an advantage of relatively low MW and reduced cytotoxicity with a covalent conjugation preventing rapid drug release that occurs during entrapping or encapsulation (Cheng *et al.*, 2007; Safari *et al.*, 2014). For this reason, these complexes can

be used for sustained release or prolonged use application allowing recommendation for the drug to be given as a single dose rather than multiple-dose regimen for more convenience and less cost.

Together the findings of this thesis offer a straightforward explanation of the advantages of the use of the AEP-dendronised carrier system with remarkable potentiation of FP permeability and targeting to the brain. This could encourage its re use in the treatment of AD providing a promise for modifying the disease cause rather than only symptomatic relief.

7.2 General conclusions

In conclusion, non-cytotoxic and biodegradable dendronised FP conjugates were prepared using a rapid Fmoc-SPPS method with high purity and reproducibility which minimised the batch-to-batch variations that are usually associated with synthesis. The study succeeded in improving FP penetration across the *in vitro* BBB model and targeting the brain via AEP functionalisation with a prospective optimal concentration that should minimise side effects seen with current high dose therapy.

In turn, this would reduce the Aβ peptide aggregation and prevent SPs formation and thus facilitate the body metabolism and clearance of the pre-formed Aβ peptides. In this way the primary underlying cause of AD will be treated, unlike the currently available therapy or drugs that are only capable of improving symptoms of the disease.

Ultimately, this novel AEP-functionalised dendron carrier system is a promising candidate in fulfilling the search for enhanced drug delivery to the brain. This molecule presents considerable potential as a drug carrier across the BBB. It is hoped that outcomes of this work will enable future studies for effective brain delivery for a variety of drugs, genes and imaging and diagnostic agents in AD and other NDs.

Chapter 8. Contribution to Knowledge and Future Studies

8.1 Original Contribution to Knowledge

In the last few years, there is a worldwide effort underway and the research is active to find better methods for the treatment of AD, delaying its onset, and preventing it from developing. Current available drugs are only capable of improving symptoms, but do not have profound disease-modifying effects. However, in recent years, several approaches have been developed aimed at targeting the Aβ aggregation or to sequester the peptide.

Due to the low BBB permeability of most drugs used for the treatment of AD, such as FP, it is essential to incorporate them with an appropriate carrier system to ensure their optimum pharmacological activity. This project aimed to address the limitations of current drug therapies for the treatment of AD through the development of new class of drug delivery method that will provide the following contributions to knowledge:

1. Design and production of dendronised molecule capable of acting as a carrier for a drug with poor BBB penetration with high degree of purity and reproducibility via using adapted SPPS method with Fmoc chemistry.
2. Possibility of conjugation of the dendronised carrier system for the first time with FP via amide linkage that enables it to reach the site of action. In addition to the possibility of providing higher payload of the drug.
3. Proof of improving the endothelial uptake, transportation and brain targeting via functionalisation of the dendron, for the first time, with ApoE-derived peptide. This peptide acts as a ligand that can be recognised by LDL receptors which are widely expressed in brain endothelial cells. Thence, enhance the drug permeability and targeting the brain.
4. Provision of evidence of the safety and non-cytotoxicity of these novel drug conjugates with brain endothelia. In addition to the evidences of their degradability and breaking down to their building monomers.
5. Use of bEnd.3 as a validated *in vitro* model to examine the BBB permeability of synthesised molecules by measuring parameters that mimic the *in vivo* model.
6. Provision of evidence of the ability of drug conjugates to exert action on the targeted enzymatic activity with proof of eventual release of free drug molecules.

8.2 Future Studies

From the findings of this thesis, a number of future research projects are envisaged leading to further development of drug delivery research and development of future treatments of NDs and other related conditions.

Moreover, further research is required to definitively address the gap of knowledge following the permeability improvement which can be formulated as new questions:

1. Can higher generations of dendrons be used to improve the payload of FP with acceptable cytotoxic effects?

Employing dendrons of higher generation (3 and up) can be used to load more FP molecules and, in turn, increase its bioavailability at the target due to more amine branching that upload more drug molecules, while increasing the rate of permeability with increasing generation. Permeability and cytotoxicity studies of such relatively large MW molecules require additional investigation to shed light on these issues.

2. What is the permeability profile of the FP-loaded carrier systems using *in vivo* BBB models and animal studies?

Although using an *in vitro* BBB model for the permeability studies could mimic the *in vivo* model, complete replication cannot be achieved. Thence measuring the permeability and the bioavailability of the drug in the animal brain is a crucial step to promote further validation of these synthesised molecules and taking them forward to clinical studies.

3. Is it possible to use these novel dendronised carrier systems for other poorly brain-penetrating drugs?

After the successful attachment of FP and proving its improved permeability through the *in vitro* BBB model, these dendronised carrier systems, specifically AEP-dendron, have the potential to be used for other drugs with limited BBB penetration. For instance, other NSAIDs, other drugs used for treatment of NDs such as methylprednisolone, anti-cancer drugs (such as doxorubicin) and in gene therapy might be able to be conjugated using the same carrier system for better permeability across the BBB. However, such utilisation requires further investigation about the methods of drug attachment to these carrier systems, the cytotoxicity and biocompatibility of the final molecules, drug activity and drug dissociation from the carrier system.

4. What are the permeability and pharmacological activity of the FP-loaded carrier systems using other epithelial layers or addressing other targets rather than BBB?

Since FP is one of available anti-inflammatory, fever and pain relieving drugs, its penetration across other physiological barriers, such as the intestinal epithelial barrier, is also limited thus requiring a high dose of drug to reach the target in its effective pharmacological concentration. Enabling the drug to cross the epithelial barriers, enhancing its cellular entry and targeting it to a particular tissue or organ is a promising strategy that would lower the dose used and, in turn, avoid the side effects associated with NSAIDs such as gastrointestinal ulcers and haemorrhage.

5. What are the stability patterns of these synthesised molecules in different storage conditions?

It is also worthwhile further investigation of the stability of the final molecule in different physical and biological conditions such as the effect of time, different temperatures and humidity and plasma protein binding. These investigations could help in drug formulation to be used by the drug industry.

References

2014 Alzheimer's Disease Facts and Figures. (2014). *Alzheimers Dement, 10*(2), e47-92.

Abbasi, E., Aval, F., Akbarzadeh, A., Milani, M., *et al.* (2014). Dendrimers: Synthesis, Applications, and Properties. *Nanoscale Res Lett, 9*(1), 247. doi: 10.1186/1556-276x-9-247

Abbott. (2014). Anatomy and Physiology of the Blood–Brain Barriers. In M. Hammarlund-Udenaes, E. C. M. de Lange & R. G. Thorne (Eds.), *Drug Delivery to the Brain* (Vol. 10, pp. 3-21): Springer New York.

Abbott, & Friedman. (2012). Overview and Introduction: The Blood-Brain Barrier in Health and Disease. *Epilepsia, 53 Suppl 6*, 1-6. doi: 10.1111/j.1528-1167.2012.03696.x

Abbott, N., Patabendige, A., Dolman, D., Yusof, S., *et al.* (2010). Structure and Function of the Blood-Brain Barrier. *Neurobiol Dis, 37*(1), 13-25. doi: 10.1016/j.nbd.2009.07.030

Akbarzadeh, A., Rezaei-Sadabady, R., Davaran, S., Joo, S. W., *et al.* (2013). Liposome: Classification, Preparation, and Applications. *Nanoscale Res Lett, 8*(1), 102. doi: 10.1186/1556-276x-8-102

Albericio, F. (2000). *Solid-Phase Synthesis: A Practical Guide* Boca Raton: CRC Press.

Alberts, B. (2007). *Molecular Biology of the Cell Bruce Alberts* New York: Garland Science.

Allcock, H. R. (2011). *Introduction to Materials Chemistry*: John Wiley & Sons.

Alzheimer's, A. (2017). 2017 Alzheimer's Disease Facts and Figures. *Alzheimer's & Dementia, 13*(4), 325-373. doi: https://doi.org/10.1016/j.jalz.2017.02.001

Alzheimer's Society. (2016). 2017, from https://www.alzheimers.org.uk/

Aparicio, J., Martin, C., & Torres, I. (2016). In Vitro Screening of Nanomedicines through the Blood Brain Barrier: A Critical Review. *BIOMATERIALS, 103*, 229-255. doi: 10.1016/j.biomaterials.2016.06.051

Armulik, A., Genove, G., Mae, M., Nisancioglu, M. H., *et al.* (2010). Pericytes Regulate the Blood-Brain Barrier. *Nature, 468*(7323), 557-561. doi: 10.1038/nature09522

Aulenta, F., Hayes, W.,Rannard, S. . (2003). Dendrimers: A New Class of Nanoscopic Containers and Delivery Devices. *Euro Pol J, 39*, 1741-1771.

Bai, S., Thomas, C., & Ahsan, F. (2007). Dendrimers as a Carrier for Pulmonary Delivery of Enoxaparin, a Low-Molecular Weight Heparin. *J Pharm Sci, 96*(8), 2090-2106. doi: 10.1002/jps.20849

Balda, S., & Matter, K. (2016). Tight Junctions as Regulators of Tissue Remodelling. *Curr Opin Cell Biol, 42*, 94-101. doi: http://dx.doi.org/10.1016/j.ceb.2016.05.006

Ballabh, P., Braun, A., & Nedergaard, M. (2004). The Blood-Brain Barrier: An Overview: Structure, Regulation, and Clinical Implications. *Neurobiol Dis, 16*(1), 1-13. doi: 10.1016/j.nbd.2003.12.016

Ballard, C., Gauthier, S., Corbett, A., Brayne, C., *et al.* (2011). Alzheimer's Disease. *The Lancet, 377*(9770), 1019-1031.

Bana, L., Minniti, S., Salvati, E., Sesana, S., *et al.* (2014). Liposomes Bi-Functionalized with Phosphatidic Acid and an Apoe-Derived Peptide Affect Aβ Aggregation Features and Cross the Blood–Brain-Barrier: Implications for Therapy of Alzheimer Disease. *Nanomedicine: Nanotechnology, Biology and Medicine, 10*(7), 1583-1590. doi: http://dx.doi.org/10.1016/j.nano.2013.12.001

Banks, W. (2012). Drug Delivery to the Brain in Alzheimer's Disease: Consideration of the Blood–Brain Barrier. *Advanced Drug Delivery Reviews, 64*(7), 629-639.

Banks, W., Farr, S., Morley, J., Wolf, K., *et al.* (2007). Anti-Amyloid Beta Protein Antibody Passage across the Blood-Brain Barrier in the Samp8 Mouse Model of Alzheimer's Disease: An Age-Related Selective Uptake with Reversal of Learning Impairment. *Exp Neurol, 206*(2), 248-256. doi: 10.1016/j.expneurol.2007.05.005

Baoling, Z., Chen, Q., Tang, H., Xie, Q., *et al.* (2010). Characterization of and Biomolecule Immobilization on the Biocompatible Multi-Walled Carbon Nanotubes Generated by Functionalization with Polyamidoamine Dendrimers. *Colloids and Surfaces B: Biointerfaces, 80*(1), 18-25.

Barat, B., & Wu, A. (2007). Metabolic Biotinylation of Recombinant Antibody by Biotin Ligase Retained in the Endoplasmic Reticulum. *Biomol Eng, 24*(3), 283-291. doi: 10.1016/j.bioeng.2007.02.003

Barres, B., Daneman, R., Zhou, L., Agalliu, D., *et al.* (2010). The Mouse Blood-Brain Barrier Transcriptome: A New Resource for Understanding the Development and Function of Brain Endothelial Cells. *PLoS One, 5*(10), e13741. doi: 10.1371/journal.pone.0013741

Barten, D., Guss, V., Corsa, J., Loo, A., *et al.* (2005). Dynamics of {Beta}-Amyloid Reductions in Brain, Cerebrospinal Fluid, and Plasma of {Beta}-Amyloid Precursor Protein Transgenic Mice Treated with a {Gamma}-Secretase Inhibitor. *J Pharmacol Exp Ther, 312*(2), 635-643. doi: 10.1124/jpet.104.075408

Bartsch, M., Weeke-Klimp, A. H., Meijer, D. K., Scherphof, G. L., *et al.* (2005). Cell-Specific Targeting of Lipid-Based Carriers for Odn and DNA. *J Liposome Res, 15*(1-2), 59-92. doi: 10.1081/lpr-64961

Bateman, R., Munsell, L., Morris, J., & Swarm, R. (2006). Human Amyloid-Beta Synthesis and Clearance Rates as Measured in Cerebrospinal Fluid in Vivo. *Nat Med, 12*(7), 856-861. doi: 10.1038/nm1438

Bauer, H., & Traweger, A. (2016). Tight Junctions of the Blood-Brain Barrier - a Molecular Gatekeeper. *CNS & Neurological Disorders - Drug Targets (Formerly Current Drug Targets, 15*(9), 1016-1029.

Becker, R., Greig, N., & Giacobini, E. (2008). Why Do So Many Drugs for Alzheimer's Disease Fail in Development? Time for New Methods and New Practices? *J Alzheimers Dis, 15*(2), 303-325.

Begley, D. J. (2004). Delivery of Therapeutic Agents to the Central Nervous System: The Problems and the Possibilities. *Pharmacol Ther, 104*(1), 29-45. doi: 10.1016/j.pharmthera.2004.08.001

Bereczki, E., Re, F., Masserin, E., Winblad, B., *et al.* (2011). Liposomes Functionalized with Acidic Lipids Rescue Aβ-Induced Toxicity in Murine Neuroblastoma Cells. *Nanomedicine: Nanotechnology, Biology, and Medicine, 7*(5), 560-571. doi: 10.1016/j.nano.2011.05.009

Bergmans, B., & De Strooper, B. (2010). Gamma-Secretases: From Cell Biology to Therapeutic Strategies. *Lancet Neurol, 9*(2), 215-226. doi: 10.1016/s1474-4422(09)70332-1

Bernacki, J., Dobrowolska, A., Nierwinska, K., & Malecki, A. (2008). Physiology and Pharmacological Role of the Blood-Brain Barrier. *Pharmacol Rep, 60*(5), 600-622.

Berridge, M., & Tan, A. (1993). Characterization of the Cellular Reduction of 3-(4,5-Dimethylthiazol-2-Yl)-2,5-Diphenyltetrazolium Bromide (Mtt): Subcellular Localization, Substrate Dependence, and Involvement of Mitochondrial Electron Transport in Mtt Reduction. *Arch Biochem Biophys, 303*(2), 474-482. doi: 10.1006/abbi.1993.1311

Best, J., Jay, M., Otu, F., Churcher, I., *et al.* (2006). In Vivo Characterization of Abeta(40) Changes in Brain and Cerebrospinal Fluid Using the Novel Gamma-Secretase Inhibitor N-[Cis-4-[(4-Chlorophenyl)Sulfonyl]-4-(2,5-Difluorophenyl)Cyclohexyl]-1,1,1-Trifl Uoromethanesulfonamide (Mrk-560) in the Rat. *J Pharmacol Exp Ther, 317*(2), 786-790. doi: 10.1124/jpet.105.100271

Best, J., Jay, M., Otu, F., Ma, J., *et al.* (2005). Quantitative Measurement of Changes in Amyloid-Beta(40) in the Rat Brain and Cerebrospinal Fluid Following Treatment with the Gamma-Secretase Inhibitor Ly-411575 [N2-[(2s)-2-(3,5-Difluorophenyl)-2-Hydroxyethanoyl]-N1-[(7s)-5-Methyl-6-Oxo-6,7-D Ihydro-5h-

Dibenzo[B,D]Azepin-7-Yl]-L-Alaninamide]. *J Pharmacol Exp Ther*, *313*(2), 902-908. doi: 10.1124/jpet.104.081174

Bhaskar, S., Razansky, D., Tian, F., Stoeger, T., *et al.* (2010). Multifunctional Nanocarriers for Diagnostics, Drug Delivery and Targeted Treatment across Blood-Brain Barrier: Perspectives on Tracking and Neuroimaging. *Particle and fibre toxicology, 7*(1), 3-3. doi: 10.1186/1743-8977-7-3

Biricova, V., & Laznickova, A. (2009). Dendrimers: Analytical Characterization and Applications. *Bioorg Chem, 37*(6), 185-192. doi: 10.1016/j.bioorg.2009.07.006

Biswas, G., Kim, W., Kim, K.-T., Cho, J., *et al.* (2017). Synthesis of Ibuprofen Conjugated Molecular Transporter Capable of Enhanced Brain Penetration. *Journal of Chemistry, 2017*, 10. doi: 10.1155/2017/4746158

Bjarnason, I., Hayllar, J., Macpherson, A. N. d. J., & Russell, A. N. t. S. (1993). Side Effects of Nonsteroidal Anti-Inflammatory Drugs on the Small and Large Intestine in Humans. *Gastroenterology, 104*(6), 1832-1847. doi: http://dx.doi.org/10.1016/0016-5085(93)90667-2

Boas, U., & Heegaard, P. M. H. (2004). Dendrimers in Drug Research. *Chemical Society reviews, 33*(1), 43-63. doi: 10.1039/b309043b

Boer, A., & Gaillard, P. (2007). Drug Targeting to the Brain. *Annu Rev Pharmacol Toxicol, 47*, 323-355. doi: 10.1146/annurev.pharmtox.47.120505.105237

Borger, E., Aitken, L., Zhang, W., & Yan, S. (2013). Is Amyloid Binding Alcohol Dehydrogenase a Drug Target for Treating Alzheimer's Disease? *CURRENT ALZHEIMER RESEARCH, 10*(1), 21-29.

Bosnjakovic, A., Mishra, M. K., Ren, W., Kurtoglu, Y. E., *et al.* (2011). Poly(Amidoamine) Dendrimer-Erythromycin Conjugates for Drug Delivery to Macrophages Involved in Periprosthetic Inflammation. *Nanomedicine, 7*(3), 284-294. doi: 10.1016/j.nano.2010.10.008

Boyd, B., Kaminskas, L., Karellas, P., Krippner, G., *et al.* (2006). Cationic Poly-L-Lysine Dendrimers: Pharmacokinetics, Biodistribution, and Evidence for Metabolism and Bioresorption after Intravenous Administration to Rats. *Mol Pharm, 3*(5), 614-627. doi: 10.1021/mp060032e

Bracci, L., Falciani, C., Lelli, B., Lozzi, L., *et al.* (2003). Synthetic Peptides in the Form of Dendrimers Become Resistant to Protease Activity. *J Biol Chem, 278*(47), 46590-46595. doi: 10.1074/jbc.M308615200

Brown, R., Morris, A., & O'Neil, R. (2007). Tight Junction Protein Expression and Barrier Properties of Immortalized Mouse Brain Microvessel Endothelial Cells. *Brain Res, 1130*(1), 17-30. doi: 10.1016/j.brainres.2006.10.083

Calderon, M., & Strumia, M. (2013). Hyperbranched and Hiperfunctionalized Materials from Dendritic Chemistry. *LatinAm. Metal. Mat., 33*(1), 2-14.

Canovi, M., Duyckaerts, C., Flores, O., Gobbi, M., *et al.* (2011). The Binding Affinity of Anti-Aβ1-42 mab-Decorated Nanoliposomes to Aβ1-42 peptides In vitro and to Amyloid Deposits in Post-Mortem Tissue. *BIOMATERIALS, 32*(23), 5489-5497. doi: 10.1016/j.biomaterials.2011.04.020

Canter, R., Penney, J., & Tsai, L. (2016). The Road to Restoring Neural Circuits for the Treatment of Alzheimer's Disease. *Nature, 539*(7628), 187-196. doi: 10.1038/nature20412

Cao, X., Sudhof, T. C. (2004). Dissection of Amyloid-Beta Precursor Protein-Dependent Transcriptional Transactivation. *J Biol Chem, 279*(23), 24601-24611. doi: 10.1074/jbc.M402248200

Carlmark, A., Hawker, C.,Hult, A.,Malkoch, M. (2009). New Methodologies in the Construction of Dendritic Materials. *Chem Soc Rev, 38*(2), 352-362. doi: 10.1039/b711745k

Carlotta, M., Rinaldi, F., Hanieh, P. N., Di Marzio, L., *et al.* (2017). Drug Delivery in Overcoming the Blood–Brain Barrier: Role of Nasal Mucosal Grafting. *Drug design, development and therapy, 11*, 325.

Carman, A., Mills, J., Krenz, A., Kim, D., *et al.* (2011). Adenosine Receptor Signaling Modulates Permeability of the Blood-Brain Barrier. *J Neurosci, 31*(37), 13272-13280. doi: 10.1523/jneurosci.3337-11.2011

Carreras, I., McKee, A. C., Choi, J. K., Aytan, N., *et al.* (2013). R-Flurbiprofen Improves Tau, but Not Ass Pathology in a Triple Transgenic Model of Alzheimer's Disease. *Brain Res, 1541*, 115-127. doi: 10.1016/j.brainres.2013.10.025

Carruthers, A., DeZutter, J., Ganguly, A., & Devaskar, S. U. (2009). Will the Original Glucose Transporter Isoform Please Stand Up! *Am J Physiol Endocrinol Metab, 297*(4), E836-848. doi: 10.1152/ajpendo.00496.2009

Chen, Y., & Liu, L. (2012). Modern Methods for Delivery of Drugs across the Blood-Brain Barrier. *Advanced Drug Delivery Reviews, 64*(7), 640-665. doi: 10.1016/j.addr.2011.11.010

Chêne, G., Beiser, A., Au, R., Preis, S. R., *et al.* (2015). Gender and Incidence of Dementia in the Framingham Heart Study from Mid-Adult Life. *Alzheimer's & Dementia, 11*(3), 310-320. doi: http://dx.doi.org/10.1016/j.jalz.2013.10.005

Cheng, Y., Man, N., Xu, T., Fu, R., *et al.* (2007). Transdermal Delivery of Nonsteroidal Anti-Inflammatory Drugs Mediated by Polyamidoamine (Pamam) Dendrimers. *J Pharm Sci, 96*(3), 595-602. doi: 10.1002/jps.20745

Cheng, Z., Zhang, J., Liu, H., Li, Y., *et al.* (2010). Central Nervous System Penetration for Small Molecule Therapeutic Agents Does Not Increase in Multiple Sclerosis- and Alzheimer's Disease-Related Animal Models Despite Reported Blood-Brain Barrier Disruption. *Drug Metab Dispos, 38*(8), 1355-1361. doi: 10.1124/dmd.110.033324

Cheung, Z., Gong, K., Ip, N. (2008). Cyclin-Dependent Kinase 5 Supports Neuronal Survival through Phosphorylation of Bcl-2. *J Neurosci, 28*(19), 4872-4877.

Choi, Y., Thomas, T., Kotlyar, A., Islam, M., *et al.* (2005). Synthesis and Functional Evaluation of DNA-Assembled Polyamidoamine Dendrimer Clusters for Cancer Cell-Specific Targeting. *Chem Biol, 12*(1), 35-43. doi: 10.1016/j.chembiol.2004.10.016

Choi, Y., Youngseon, C., Almut, M., Bradford, O., *et al.* (2004). DNA-Directed Synthesis of Generation 7 and 5 Pamam Dendrimer Nanoclusters. *Nano Let., 4*, 391-397.

Cirrito, J., Deane, R., Fagan, A., Paul, S., *et al.* (2005). P-Glycoprotein Deficiency at the Blood-Brain Barrier Increases Amyloid-Beta Deposition in an Alzheimer Disease Mouse Model. *J Clin Invest, 115*(11), 3285-3290. doi: 10.1172/jci25247

Cirrito, J., May, P., ODell, M., Cramer, J., *et al.* (2003). In Vivo Assessment of Brain Interstitial Fluid with Microdialysis Reveals Plaque-Associated Changes in Amyloid-Beta Metabolism and Half-Life. *J Neurosci, 23*(26), 8844-8853.

Clark, D. (2003). In Silico Prediction of Blood-Brain Barrier Permeation. *Drug Discov Today, 8*(20), 927-933.

Cole, S., & Vassar, R. (2007). The Alzheimer's Disease Beta-Secretase Enzyme, Bace1. *Mol Neurodegener, 2*, 22. doi: 10.1186/1750-1326-2-22

Colucci, L., & F., M. (2014). Alzheimer's Disease Costs: What We Know and What We Should Take into Account. *Journal of Alzheimer's Disease, 42*(4), 1311-1324. doi: 10.3233/JAD-131556

Cooper, G. (2000). *The Cell: A Molecular Approach*. Sinauer Associates: Sunderland (MA).

Cooper, J. (1987). Effects of Cytochalasin and Phalloidin on Actin. *J Cell Biol, 105*(4), 1473-1478.

Crump, J., Johnson, S., & Li, Y. (2013). Development and Mechanism of Γ-Secretase Modulators for Alzheimer's Disease. *Biochemistry, 52*(19), 3197-3216. doi: 10.1021/bi400377p

Cruts, M., & Van, C. (1998). Presenilin Mutations in Alzheimer's Disease. *Hum Mutat, 11*(3), 183-190. doi: 10.1002/(sici)1098-1004(1998)11:3<183::aid-humu1>3.0.co;2-j

Cruz, M., Simoes, S., & Lima, M. (2004). Improving Lipoplex-Mediated Gene Transfer into C6 Glioma Cells and Primary Neurons. *Exp Neurol, 187*(1), 65-75. doi: 10.1016/j.expneurol.2003.12.013

Dallas, S., Miller, D. S., & Bendayan, R. (2006). Multidrug Resistance-Associated Proteins: Expression and Function in the Central Nervous System. *Pharmacol Rev, 58*(2), 140-161. doi: 10.1124/pr.58.2.3

Daneman, R., Zhou, L., Kebede, A., & Barres, B. (2010). Pericytes Are Required for Blood-Brain Barrier Integrity During Embryogenesis. *Nature, 468*(7323), 562-566. doi: 10.1038/nature09513

Datta, G., Chaddha, M., Garber, D. W., Chung, B. H., *et al.* (2000). The Receptor Binding Domain of Apolipoprotein E, Linked to a Model Class a Amphipathic Helix, Enhances Internalization and Degradation of Ldl by Fibroblasts. *Biochemistry, 39*(1), 213-220.

Dauchy, S., Dutheil, F., Weaver, R. J., Chassoux, F., *et al.* (2008). Abc Transporters, Cytochromes P450 and Their Main Transcription Factors: Expression at the Human Blood-Brain Barrier. *J Neurochem, 107*(6), 1518-1528. doi: 10.1111/j.1471-4159.2008.05720.x

Davies, N. M. (1995). Clinical Pharmacokinetics of Flurbiprofen and Its Enantiomers. *Clinical pharmacokinetics, 28*(2), 100-114.

Dean, M., Rzhetsky, A., & Allikmets, R. (2001). The Human Atp-Binding Cassette (Abc) Transporter Superfamily. *Genome Res, 11*(7), 1156-1166. doi: 10.1101/gr.184901

Deane, R., Wu, Z., & Zlokovic, B. (2004). Rage (Yin) Versus Lrp (Yang) Balance Regulates Alzheimer Amyloid Beta-Peptide Clearance through Transport across the Blood-Brain Barrier. *Stroke, 35*(11 Suppl 1), 2628-2631.

Deane, R., & Zlokovic, B. (2007). Role of the Blood-Brain Barrier in the Pathogenesis of Alzheimer's Disease. *Curr Alzheimer Res, 4*(2), 191-197.

Dehouck, B., Dehouck, M., Fruchart, J., & Cecchelli, R. (1994). Upregulation of the Low Density Lipoprotein Receptor at the Blood-Brain Barrier: Intercommunications between Brain Capillary Endothelial Cells and Astrocytes. *J Cell Biol, 126*(2), 465-473.

DeMattos, R., Bales, K., Cummins, D., Paul, S., *et al.* (2002). Brain to Plasma Amyloid-Beta Efflux: A Measure of Brain Amyloid Burden in a Mouse Model of Alzheimer's Disease. *Science, 295*(5563), 2264-2267. doi: 10.1126/science.1067568

Dillen, K., Annaert, W. (2006). A Two Decade Contribution of Molecular Cell Biology to the Centennial of Alzheimer's Disease: Are We Progressing toward Therapy? *Int Rev Cytol, 254*, 215-300. doi: 10.1016/s0074-7696(06)54005-7

Dovey, H., John, V., Anderson, J., Chen, L., *et al.* (2001). Functional Gamma-Secretase Inhibitors Reduce Beta-Amyloid Peptide Levels in Brain. *J Neurochem, 76*(1), 173-181.

Downard, K. (2004). *Mass Spectrometry: A Foundation Course* UK: Royal society of Chemistery.

Doyle, W. (1992). Principles and Applications of Fourier Transform Infrared (Ftir) Process Analysis. *Process control and quality, 2*(1), 11-41.

Duncan, R., Rejmanova, P., Kopecek, J., & Lloyd, J. B. (1985). Stability in Rat Plasma and Serum of Lysosomally Degradable Oligopeptide Sequences in N-(2-Hydroxypropyl) Methacrylamide Copolymers. *BIOMATERIALS, 6*(1), 45-48. doi: http://dx.doi.org/10.1016/0142-9612(85)90037-7

Dyer, C., Cistola, D., Parry, G., & Curtiss, L. (1995). Structural Features of Synthetic Peptides of Apolipoprotein E That Bind the Ldl Receptor. *J Lipid Res, 36*(1), 80-88.

Ebelegi, N., Ekubo Tobin, Ayawei Nimibofa, & Donbebe., W. (2017). A Review of Synthesis, Characterization and Applications of Functionalized Dendrimers. *American Journal of Polymer Science, 7*(1), 8-14.

Edmond, H., & Stroobant, V. (2007). *Mass Spectrometry: Principles and Applications*: John Wiley & Sons.

Eigenmann, D., Xue, G., Kwang, K., Moses, A., *et al.* (2013). Comparative Study of Four Immortalized Human Brain Capillary Endothelial Cell Lines, Hcmec/D3, Hbmec, Ty10, and Bb19, and Optimization of Culture Conditions, for an in Vitro Blood–Brain Barrier Model for Drug Permeability Studies. *Fluids and Barriers of the CNS*, 10:33.

El-Sayed, M., Ginski, M., Rhodes, C., & Ghandehari, H. (2002). Transepithelial Transport of Poly(Amidoamine) Dendrimers across Caco-2 Cell Monolayers. *J Control Release, 81*(3), 355-365.

Elvira, C., Gallardo, A., Roman, J. S., & Cifuentes, A. (2005). Covalent Polymer-Drug Conjugates. *Molecules, 10*(1), 114-125.

Eriksen, J., Sagi, S., Smith, T., Weggen, S., *et al.* (2003). Nsaids and Enantiomers of Flurbiprofen Target Gamma-Secretase and Lower Abeta 42 in Vivo. *J Clin Invest, 112*(3), 440-449. doi: 10.1172/jci18162

Feliu, N., Walter, M. V., Montanez, M. I., Kunzmann, A., *et al.* (2012). Stability and Biocompatibility of a Library of Polyester Dendrimers in Comparison to Polyamidoamine Dendrimers. *BIOMATERIALS, 33*(7), 1970-1981. doi: 10.1016/j.biomaterials.2011.11.054

Fields, G., Williams, P., White, P., Kates, S., *et al.* (2014). *Solid-Phase Peptide Synthesis-Tips and Tricks Forsolid Phase Peptide Synthes* (T. E. A. BACHEM Ed.): Global Marketing, Bachem Group.

Furuse, M., Furuse, K., Sasaki, H., & Tsukita, S. (2001). Conversion of Zonulae Occludentes from Tight to Leaky Strand Type by Introducing Claudin-2 into Madin-Darby Canine Kidney I Cells. *J Cell Biol, 153*(2), 263-272.

Furuse, M., Hirase, T., Itoh, M., Nagafuchi, A., *et al.* (1993). Occludin: A Novel Integral Membrane Protein Localizing at Tight Junctions. *J Cell Biol, 123*(6 Pt 2), 1777-1788.

Gabathuler, R. (2010). Approaches to Transport Therapeutic Drugs across the Blood-Brain Barrier to Treat Brain Diseases. *Neurobiol Dis, 37*(1), 48-57. doi: 10.1016/j.nbd.2009.07.028

Gagliardi, M. (2017). Recent Advances in Preclinical Studies and Potential Applications of Dendrimers as Drug Carriers in the Central Nervous System. *CURRENT PHARMACEUTICAL DESIGN, 23*, 1-15. doi: http://dx.doi.org/10.2174/1381612823666170313124811

Ganguli, M., Dodge, H., Shen, C., & DeKosky, S. (2005). Alzheimer Disease and Mortality: A 15-Year Epidemiological Study. *Arch Neurol, 62*, 779-784.

Gao, H., Pang, Z., Fan, L., Hu, K., *et al.* (2010). Effect of Lactoferrin- and Transferrin-Conjugated Polymersomes in Brain Targeting: In Vitro and in Vivo Evaluations. *Acta Pharmacol Sin, 31*(2), 237-243.

Gasparini, L., Rusconi, L., Xu, H., del Soldato, P., *et al.* (2004). Modulation of Beta-Amyloid Metabolism by Non-Steroidal Anti-Inflammatory Drugs in Neuronal Cell Cultures. *J Neurochem, 88*(2), 337-348.

Ghosh, K., Brindisi, M., & Tang, J. (2012). Developing B-Secretase Inhibitors for Treatment of Alzheimer's Disease. *Journal of neurochemistry, 120*(Suppl 1), 71-83. doi: 10.1111/j.1471-4159.2011.07476.x

Giannini, G., Rappuoli, R., & Ratti, G. (1984). The Amino-Acid Sequence of Two Non-Toxic Mutants of Diphtheria Toxin: Crm45 and Crm197. *Nucleic Acids Res, 12*(10), 4063-4069.

Gingrich, M., & Traynelis, S. (2000). Serine Proteases and Brain Damage - Is There a Link? *Trends Neurosci, 23*(9), 399-407.

Gleeson, M. P. (2008). Generation of a Set of Simple, Interpretable Admet Rules of Thumb. *J Med Chem, 51*(4), 817-834. doi: 10.1021/jm701122q

Gobbi, M., Gasco, P., Salmona, M., Masserini, E., *et al.* (2010). Lipid-Based Nanoparticles with High Binding Affinity for Amyloid-Beta1-42 Peptide. *BIOMATERIALS, 31*(25), 6519.

Godlee, C., & Kaksonen, M. (2013). Review Series: From Uncertain Beginnings: Initiation Mechanisms of Clathrin-Mediated Endocytosis. *J Cell Biol, 203*(5), 717-725. doi: 10.1083/jcb.201307100

Goulatis, L. I., & Shusta, E. V. (2017). Protein Engineering Approaches for Regulating Blood–Brain Barrier Transcytosis. *Current Opinion in Structural Biology, 45*(Supplement C), 109-115. doi: https://doi.org/10.1016/j.sbi.2016.12.005

Green, R., Schneider, L., Amato, D., Beelen, A., *et al.* (2009). Effect of Tarenflurbil on Cognitive Decline and Activities of Daily Living in Patients with Mild Alzheimer Disease: A Randomized Controlled Trial. *Jama, 302*(23), 2557-2564. doi: 10.1001/jama.2009.1866

Greenwood, J., Amos, C., Walters, C., Couraud, P., *et al.* (2003). Intracellular Domain of Brain Endothelial Intercellular Adhesion Molecule-1 Is Essential for T Lymphocyte-Mediated Signaling and Migration. *J Immunol, 171*(4), 2099-2108.

Groot, F., Albrecht, C., Koekkoek, R., Beusker, P., *et al.* (2003). "Cascade-Release Dendrimers" Liberate All End Groups Upon a Single Triggering Event in the Dendritic Core. *Angewandte Chemie International Edition, 42*(37), 4490-4494. doi: 10.1002/anie.200351942

Grosch, S., Tegeder, I., Schilling, K., Maier, T. J., *et al.* (2003). Activation of C-Jun-N-Terminal-Kinase Is Crucial for the Induction of a Cell Cycle Arrest in Human Colon Carcinoma Cells Caused by Flurbiprofen Enantiomers. *Faseb j, 17*(10), 1316-1318. doi: 10.1096/fj.02-0919fje

Haass, C. (2004). Take Five--Bace and the Gamma-Secretase Quartet Conduct Alzheimer's Amyloid Beta-Peptide Generation. *Embo j, 23*(3), 483-488. doi: 10.1038/sj.emboj.7600061

Habeck, M. (2002). New Insights into Alzheimer's Disease. *Drug Discovery Today, 7* (8), 441-442.

Hamblett, K., Senter, P., Chace, D., Sun, M., *et al.* (2004). Effects of Drug Loading on the Antitumor Activity of a Monoclonal Antibody Drug Conjugate. *Clin Cancer Res, 10*(20), 7063-7070. doi: 10.1158/1078-0432.ccr-04-0789

Hansson, E., Ronnback, L., & Abbott, N. (2006). Astrocyte-Endothelial Interactions at the Blood-Brain Barrier. *Nat Rev Neurosci, 7*(1), 41-53.

Hartman, R., Izumi, Y., Bales, K., Paul, S., *et al.* (2005). Treatment with an Amyloid-Beta Antibody Ameliorates Plaque Load, Learning Deficits, and Hippocampal Long-Term Potentiation in a Mouse Model of Alzheimer's Disease. *J Neurosci, 25*(26), 6213-6220. doi: 10.1523/jneurosci.0664-05.2005

Hawkes, C., & McLaurin, J. (2007). Immunotherapy as Treatment for Alzheimer's Disease. *Expert Rev Neurother, 7*(11), 1535-1548. doi: 10.1586/14737175.7.11.1535

Hawkins, R., O'Kane, R., Simpson, I., & Vina, J. (2006). Structure of the Blood-Brain Barrier and Its Role in the Transport of Amino Acids. *J Nutr, 136*(1 Suppl), 218s-226s.

He, F., Yin, F., Peng, J., Li, K., *et al.* (2010). Immortalized Mouse Brain Endothelial Cell Line Bend.3 Displays the Comparative Barrier Characteristics as the Primary Brain Microvascular Endothelial Cells]. *Chinese journal of contemporary pediatrics, 12*(6), 474-478.

Heather, A., Ruth, H., Haskamp, A., Chevelle, C., *et al.* (2011). Evaluation of Biotinylated Pamam Dendrimer Toxicity in Models of the Blood Brain Barrier: A Biophysical and Cellular Approach. *Journal of Biomaterials and Nanobiotechnology, 2*(5), 485-493. doi: 10.4236/jbnb.2011.225059

Hecimovic, S., Wang, J., Dolios, G., & Goate, A. (2004). Mutations in App Have Independent Effects on Abeta and Ctfgamma Generation. *Neurobiol Dis, 17*(2), 205-218. doi: 10.1016/j.nbd.2004.04.018

Herve, F., Ghinea, N., & Scherrmann, J. M. (2008). Cns Delivery Via Adsorptive Transcytosis. *Aaps j, 10*(3), 455-472. doi: 10.1208/s12248-008-9055-2

Hills, I., & Vacca, J. (2007). Progress toward a Practical Bace-1 Inhibitor. *Curr Opin Drug Discov Devel, 10*(4), 383-391.

Hirase, T., Kawashima, S., Wong, E. Y., Ueyama, T., *et al.* (2001). Regulation of Tight Junction Permeability and Occludin Phosphorylation by Rhoa-P160rock-Dependent and -Independent Mechanisms. *J Biol Chem, 276*(13), 10423-10431. doi: 10.1074/jbc.M007136200

Hirase, T., Staddon, J., Saitou, M., Y., A., *et al.* (1997). Occludin as a Possible Determinant of Tight Junction Permeability in Endothelial Cells. *J Cell Sci, 110 (Pt 14)*, 1603-1613.

Holstein, M. (1996). Alzheimer's Disease and Senile Dementia, 1885-1920: An Interpretive History of Disease Negotiation. *Journal of Aging Studies, 11*(1), 1-13.

Hong, S., Bielinska, A., Mecke, A., Keszler, B., *et al.* (2004). Interaction of Poly(Amidoamine) Dendrimers with Supported Lipid Bilayers and Cells: Hole Formation and the Relation to Transport. *Bioconjug Chem, 15*(4), 774-782. doi: 10.1021/bc049962b

Hook, G., & Lucier, G. (1998). *Reviews in Environmental Health: Toxicological Defence Mechanisms*: Diane Publishing CO.

Huang, R., Ke, W., Liu, Y., Jiang, C., *et al.* (2008). The Use of Lactoferrin as a Ligand for Targeting the Polyamidoamine-Based Gene Delivery System to the Brain. *BIOMATERIALS, 29*(2), 238-246. doi: 10.1016/j.biomaterials.2007.09.024

Huber, D., Balda, M., & Matter, K. (2000). Occludin Modulates Transepithelial Migration of Neutrophils. *J Biol Chem, 275*(8), 5773-5778.

Issa, R., Meikle, S., James, S., & Cooper, I. (2015). Poly(E-Lysine) Dendrons as Modulators of Quorum Sensing in Pseudomonas Aeruginosa. *Journal of Materials Science: Materials in Medicine, 26*(5), 1-7. doi: 10.1007/s10856-015-5508-1

Jakob, R., & Jacobsen, H. (2009). Alzheimer's Disease: From Pathology to Therapeutic Approaches. *ANGEWANDTE CHEMIE-INTERNATIONAL EDITION, 48*(17), 3030-3059. doi: 10.1002/anie.200802808

Jia, L., Xu, Y., Fang, Q., Cao, A., *et al.* (2007). Novel Symmetric Amphiphilic Dendritic Poly(L-Lysine)-B-Poly(L-Lactide)-B-Dendritic Poly(L-Lysine) with High Plasmid DNA Binding Affinity as a Biodegradable Gene Carrier. *Biomacromolecules, 8*(5), 1409-1416. doi: 10.1021/bm0701806

Jones, A., & Shusta, E. (2007). Blood-Brain Barrier Transport of Therapeutics Via Receptor-Mediation. *Pharm Res, 24*(9), 1759-1771. doi: 10.1007/s11095-007-9379-0

Jurima, M., Crawford, K., & Huang, H. S. (1994). Comparative Cytotoxicity of Non-Steroidal Anti-Inflammatory Drugs in Primary Cultures of Rat Hepatocytes. *Toxicol In Vitro, 8*(1), 55-66.

Kalaria, R. (2010). Vascular Basis for Brain Degeneration: Faltering Controls and Risk Factors for Dementia. *Nutr Rev, 68*(2), S74-87.

Kaminskas, L., McLeod, V., Kelly, B., Sberna, G., *et al.* (2012). A Comparison of Changes to Doxorubicin Pharmacokinetics, Antitumor Activity, and Toxicity Mediated by Pegylated Dendrimer and Pegylated Liposome Drug Delivery Systems. *Nanomedicine, 8*(1), 103-111. doi: 10.1016/j.nano.2011.05.013

Kannan, R., Chakrabarti, R., Tang, D., Kim, K. J., *et al.* (2000). Gsh Transport in Human Cerebrovascular Endothelial Cells and Human Astrocytes: Evidence for Luminal Localization of Na+-Dependent Gsh Transport in Hcec. *Brain Res, 852*(2), 374-382.

Karolina, W., Winiewski, M., Terzyk, A., & Furmaniak, S. (2015). The Chemistry of Bioconjugation in Nanoparticles-Based Drug Delivery System. *Advances in Condensed Matter Physics, 2015*, 27. doi: 10.1155/2015/198175

Ke, W., Jiang, C., Shao, K., Huang, R., *et al.* (2009). Gene Delivery Targeted to the Brain Using an Angiopep-Conjugated Polyethyleneglycol-Modified Polyamidoamine Dendrimer. *BIOMATERIALS, 30*(36), 6976-6985. doi: 10.1016/j.biomaterials.2009.08.049

Kesharwani, P., Tekade, R. K., Gajbhiye, V., Jain, K., *et al.* (2011). Cancer Targeting Potential of Some Ligand-Anchored Poly(Propylene Imine) Dendrimers: A Comparison. *Nanomedicine, 7*(3), 295-304. doi: 10.1016/j.nano.2010.10.010

Khandare, J., Kolhe, P., Pillai, O., Kannan, S., *et al.* (2005). Synthesis, Cellular Transport, and Activity of Polyamidoamine Dendrimer-Methylprednisolone Conjugates. *Bioconjug Chem, 16*(2), 330-337. doi: 10.1021/bc0498018

Khandare, J., & Kumar, S. (2011). Biodegradable Dendrimers and Dendritic Polymers *Handbook of Biodegradable Polymers* (pp. 237-262): Wiley-VCH Verlag GmbH & Co. KGaA.

Khawli, L., & Prabhu, S. (2013). Drug Delivery across the Blood-Brain Barrier. *MOLECULAR PHARMACEUTICS, 10*(5), 1471-1472. doi: 10.1021/mp400170b

Khyati, M., & Deepshikha, P. (2016). Shared Links between Type 2 Diabetes Mellitus and Alzheimer's Disease: A Review. *Diabetes & Metabolic Syndrome: Clinical Research & Reviews, 10*(2), S144-S149. doi: http://dx.doi.org/10.1016/j.dsx.2016.01.021

Kim, M., Maeng, H., Yu, K., Lee, K., *et al.* (2010). Evidence of Carrier-Mediated Transport in the Penetration of Donepezil into the Rat Brain. *J Pharm Sci, 99*(3), 1548-1566. doi: 10.1002/jps.21895

Kitchens, K., El-Sayed, M., & Ghandehari, H. (2005). Transepithelial and Endothelial Transport of Poly (Amidoamine) Dendrimers. *Adv Drug Deliv Rev, 57*(15), 2163-2176. doi: 10.1016/j.addr.2005.09.013

Klein, J. (2007). Phenserine. *Expert Opin Investig Drugs, 16*(7), 1087-1097. doi: 10.1517/13543784.16.7.1087

Kojro, E., & Fahrenholz, F. (2005). The Non-Amyloidogenic Pathway: Structure and Function of Alpha-Secretases. *Subcell Biochem, 38*, 105-127.

Kolhe, P., Ekta, M., Kannan, R., Sujatha, K., *et al.* (2003). Drug Complexation, in Vitro Release and Cellular Entry of Dendrimers and Hyperbranched Polymers. *Int J Pharm, 259*(1-2), 143-160.

Konsman, J., Drukarch, B., & VanDam, A. (2007). (Peri)Vascular Production and Action of Pro-Inflammatory Cytokines in Brain Pathology. *Clin Sci (Lond), 112*(1), 1-25. doi: 10.1042/cs20060043

Kou, L., Sun, J., Zhai, Y., & He, Z. (2013). The Endocytosis and Intracellular Fate of Nanomedicines: Implication for Rational Design. *Asian Journal of Pharmaceutical Sciences, 8*(1), 1-10. doi: https://doi.org/10.1016/j.ajps.2013.07.001

Kreuter, J., Shamenkov, D., Petrov, V., Ramge, P., *et al.* (2002). Apolipoprotein-Mediated Transport of Nanoparticle-Bound Drugs across the Blood-Brain Barrier. *J Drug Target, 10*(4), 317-325. doi: 10.1080/10611860290031877

Kryscio, R., Abner, E., Caban, A., Lovell, M., *et al.* (2017). Association of Antioxidant Supplement Use and Dementia in the Prevention of Alzheimer's Disease by

Vitamin E and Selenium Trial. *JAMA Neurol, 74*(5), 567-573. doi: 10.1001/jamaneurol.2016.5778

Kumar, P., Asthana, A., Dutta, T., & Jain, N. (2006). Intracellular Macrophage Uptake of Rifampicin Loaded Mannosylated Dendrimers. *J Drug Target, 14*(8), 546-556. doi: 10.1080/10611860600825159

Kuo, Y., Emmerling, M., Kasunic, T., Ball, M., *et al.* (1996). Water-Soluble a Beta (N-40, N-42) Oligomers in Normal and Alzheimer Disease Brains. *JOURNAL OF BIOLOGICAL CHEMISTRY, 271*(8), 4077-4081.

Lai, P., Lou, P., Peng, C., Pai, C., *et al.* (2007). Doxorubicin Delivery by Polyamidoamine Dendrimer Conjugation and Photochemical Internalization for Cancer Therapy. *Journal of Controlled Release, 122*(1), 39-46.

Lanz, T., Karmilowicz, M., Wood, K., Pozdnyakov, N., *et al.* (2006). Concentration-Dependent Modulation of Amyloid-Beta in Vivo and in Vitro Using the Gamma-Secretase Inhibitor, Ly-450139. *J Pharmacol Exp Ther, 319*(2), 924-933. doi: 10.1124/jpet.106.110700

Lawther, K., Kumar, S., & Krovvidi, H. (2011). Blood–Brain Barrier. *Continuing Education in Anaesthesia, Critical Care & Pain, 11*(4), 128-132. doi: 10.1093/bjaceaccp/mkr018

Lee, H., Zhu, X., Castellani, R., Nunomura, A., *et al.* (2007). Amyloid-Beta in Alzheimer Disease: The Null Versus the Alternate Hypotheses. *J Pharmacol Exp Ther, 321*(3), 823-829. doi: 10.1124/jpet.106.114009

Lee, J., & Nan, A. (2012). Combination Drug Delivery Approaches in Metastatic Breast Cancer. *J Drug Deliv, 2012*, 915375. doi: 10.1155/2012/915375

Lee, S., Huh, J., Ahn, H., Lee, M., *et al.* (2006). Synthesis of Novel Biodegradable Cationic Dendrimers. *Macromolecular rapid communications, 27*(18), 1608-1614.

Leupold, E., Nikolenko, H., Beyermann, M., & Dathe, M. (2008). Insight into the Role of Hspg in the Cellular Uptake of Apolipoprotein E-Derived Peptide Micelles and Liposomes. *Biochimica et Biophysica Acta (BBA) - Biomembranes, 1778*(12), 2781-2789. doi: http://dx.doi.org/10.1016/j.bbamem.2008.09.008

Li, Y., He, H., Jia, X., Lu, W.-L., *et al.* (2012). A Dual-Targeting Nanocarrier Based on Poly(Amidoamine) Dendrimers Conjugated with Transferrin and Tamoxifen for Treating Brain Gliomas. *BIOMATERIALS, 33*(15), 3899-3908. doi: 10.1016/j.biomaterials.2012.02.004

Lichtenthaler, S., Dominguez, D., Westmeyer, G., Reiss, K., *et al.* (2003). The Cell Adhesion Protein P-Selectin Glycoprotein Ligand-1 Is a Substrate for the Aspartyl Protease Bace1. *J Biol Chem, 278*(49), 48713-48719. doi: 10.1074/jbc.M303861200

Lichtenthaler, S., & Haass, C. (2004). Amyloid at the Cutting Edge: Activation of Alpha-Secretase Prevents Amyloidogenesis in an Alzheimer Disease Mouse Model. *J Clin Invest, 113*(10), 1384-1387. doi: 10.1172/jci21746

Liebner, S., & Plate, K. H. (2010). Differentiation of the Brain Vasculature: The Answer Came Blowing by the Wnt. *J Angiogenes Res, 2*, 1. doi: 10.1186/2040-2384-2-1

Liu, G., Men, P., Kudo, W., Perry, G., *et al.* (2009). Nanoparticle-Chelator Conjugates as Inhibitors of Amyloid-Beta Aggregation and Neurotoxicity: A Novel Therapeutic Approach for Alzheimer Disease. *Neurosci Lett, 455*(3), 187-190. doi: 10.1016/j.neulet.2009.03.064

Liu, L., Valerie, D., Jessica, W., Menno, P., *et al.* (2012). Trans-Synaptic Spread of Tau Pathology in Vivo. *PLoS One, 7*(2), e31302. doi: 10.1371/journal.pone.0031302

Liu, X., Tu, M., Kelly, S., Chen, C., *et al.* (2004). Development of a Computational Approach to Predict Blood-Brain Barrier Permeability. *Drug Metab Dispos, 32*(1), 132-139. doi: 10.1124/dmd.32.1.132

Lleo, A., Berezovska, O., Herl, L., Raju, S., *et al.* (2004). Nonsteroidal Anti-Inflammatory Drugs Lower Abeta42 and Change Presenilin 1 Conformation. *Nat Med, 10*(10), 1065-1066. doi: 10.1038/nm1112

Longmire, M., Ogawa, M., Choyke, P., & Kobayashi, H. (2011). Biologically Optimized Nanosized Molecules and Particles: More Than Just Size. *Bioconjug Chem, 22*(6), 993-1000. doi: 10.1021/bc200111p

Lovestone, S. (1998). *Early Diagnosis and Treatment of Alzheimer`S Disease*. london,UK: Martin Dunitz.

Luchsinger, J., Tang, M., Stern, Y., Shea, S., *et al.* (2001). Diabetes Mellitus and Risk of Alzheimer's Disease and Dementia with Stroke in a Multiethnic Cohort. *Am J Epidemiol, 154*(7), 635-641.

Madaan, K., Kumar, S., Poonia, N., Lather, V., *et al.* (2014). Dendrimers in Drug Delivery and Targeting: Drug-Dendrimer Interactions and Toxicity Issues. *Journal of Pharmacy & Bioallied Sciences, 6*(3), 139-150. doi: 10.4103/0975-7406.130965

Made, V., Els-Heindl, S., Beck-Sickinger, A. G. (2014). Automated Solid-Phase Peptide Synthesis to Obtain Therapeutic Peptides. *Beilstein J Org Chem, 10*, 1197-1212. doi: 10.3762/bjoc.10.118

Magali, J., Anaies, H., & Amelie, M. (2009). N-Terminus Fitc Labeling of Peptides on Solid Support: The Truth Behind the Spacer. *J-GLOBAL, 50*(3), 2-263.

Mager, I., Meyer, A., Li, J., Lenter, M., *et al.* (2017). Targeting Blood-Brain-Barrier Transcytosis–Perspectives for Drug Delivery. *Neuropharmacology, 120*, 4-7.

Mahley, R. W. (1988). Apolipoprotein E: Cholesterol Transport Protein with Expanding Role in Cell Biology. *Science, 240*(4852), 622-630.

Majno, G., & Joris, I. (1995). Apoptosis, Oncosis, and Necrosis. An Overview of Cell Death. *Am J Pathol, 146*(1), 3-15.

Malik, N., Wiwattanapatapee, R., Klopsch, R., Lorenz, K., *et al.* (2000). Dendrimers: Relationship between Structure and Biocompatibility in Vitro, and Preliminary Studies on the Biodistribution of 125i-Labelled Polyamidoamine Dendrimers in Vivo. *J Control Release, 65*(1-2), 133-148.

Maloney, B., Lahiri, D., Chen, D., Holloway, H., *et al.* (2007). The Experimental Alzheimer's Disease Drug Posiphen [(+)-Phenserine] Lowers Amyloid-Beta Peptide Levels in Cell Culture and Mice. *J Pharmacol Exp Ther, 320*(1), 386-396. doi: 10.1124/jpet.106.112102

Maqsood, M., Matin, M., Bahrami, A., & Ghasroldasht, M. (2013). Immortality of Cell Lines: Challenges and Advantages of Establishment. *Cell Biol Int, 37*(10), 1038-1045. doi: 10.1002/cbin.10137

Martin, J., & Haefely, W. (1993). Pharmacology of Aniracetam. *Drug Investigation, 5*(1), 4-49. doi: 10.1007/bf03258426

Mass Spectrometry. (2015). 2015, from http://www.premierbiosoft.com/tech_notes/mass-spectrometry

Matter, K., & Balda, M. S. (2003). Signalling to and from Tight Junctions. *Nat Rev Mol Cell Biol, 4*(3), 225-236. doi: 10.1038/nrm1055

McGeer, P., & McGeer, E. (2007). Nsaids and Alzheimer Disease: Epidemiological, Animal Model and Clinical Studies. *Neurobiol Aging, 28*(5), 639-647. doi: 10.1016/j.neurobiolaging.2006.03.013

McLendon, C., Xin, T., Ziani-Cherif, C., Murphy, M. P., *et al.* (2000). Cell-Free Assays for Gamma-Secretase Activity. *Faseb j, 14*(15), 2383-2386. doi: 10.1096/fj.00-0286fje

Meikle, S., Perugini, V., Guildford, A., & Santin, M. (2011). Synthesis, Characterisation and in Vitro Anti-Angiogenic Potential of Dendron Vegf Blockers. *Macromol Biosci, 11*(12), 1761-1765. doi: 10.1002/mabi.201100267

Meikle, S., Pineiro, Y., Banobre Lopez, Rivas, J., *et al.* (2016). Surface Functionalization Superparamagnetic Nanoparticles Conjugated with Thermoresponsive Poly(Epsilon-Lysine) Dendrons Tethered with Carboxybetaine for the Mild Hyperthermia-Controlled Delivery of Vegf. *Acta Biomater, 40*, 235-242. doi: 10.1016/j.actbio.2016.04.043

Meister, S., Zlatev, I., & Pietrzik, C. (2013). Nanoparticulate Flurbiprofen Reduces Amyloid-Beta42 Generation in an in Vitro Blood-Brain Barrier Model. *Alzheimer's Research & Therapy, 5*(6), 51.

Menjoge, A., Kannan, R., & Tomalia, D. (2010). Dendrimer-Based Drug and Imaging Conjugates: Design Considerations for Nanomedical Applications. *Drug Discov Today, 15*(5-6), 171-185. doi: 10.1016/j.drudis.2010.01.009

Merrifield, R. (1965). Automated Synthesis of Peptides. *Science, 150*(3693), 178-185.

Mesulam, M., Martin, T., & Mufson, E. (1984). The Light Side of Horseradish Peroxidase Histochemistry. *Journal of Histochemistry & Cytochemistry, 32*(7), 793-793. doi: 10.1177/32.7.6736628

Michael, B., & Wittwer, C. (2000). Flow Cytometry: Principles and Clinical Applications in Hematology. *Clinical Chemistry, 46*(8), 1221-1229.

Michikawa, M. (2003). Cholesterol Paradox: Is High Total or Low Hdl Cholesterol Level a Risk for Alzheimer's Disease? *J Neurosci Res, 72*(2), 141-146.

Mills, S., Cowin, A., & Kaur, P. (2013). Pericytes, Mesenchymal Stem Cells and the Wound Healing Process. *Cells, 2*(3), 621-634. doi: 10.3390/cells2030621

Mindell, J. A. (2012). Lysosomal Acidification Mechanisms. *Annu Rev Physiol, 74*(1), 69-86. doi: 10.1146/annurev-physiol-012110-142317

Mitchell, A. (2008). Studies in Solid-Phase Peptide Synthesis: A Personal Perspective. *Biopolymers, 90*(3), 215-233. doi: 10.1002/bip.20812

Mitic, L., & Anderson, J. (1998). Molecular Architecture of Tight Junctions. *Annu Rev Physiol, 60*, 121-142. doi: 10.1146/annurev.physiol.60.1.121

Molino, Y., David, M., Varini, K., Jabès, F., *et al.* (2017). Use of Ldl Receptor–Targeting Peptide Vectors for in Vitro and in Vivo Cargo Transport across the Blood-Brain Barrier. *The FASEB Journal*. doi: 10.1096/fj.201600827R

Montesano, R., Pepper, M., Mohle, U., Risau, W., *et al.* (1990). Increased Proteolytic Activity Is Responsible for the Aberrant Morphogenetic Behavior of Endothelial Cells Expressing the Middle T Oncogene. *Cell, 62*(3), 435-445.

Morgan, D., Diamond, D., Gottschall, P., Ugen, K. E., *et al.* (2000). A Beta Peptide Vaccination Prevents Memory Loss in an Animal Model of Alzheimer's Disease. *Nature, 408*(6815), 982-985. doi: 10.1038/35050116

Morita, K., Sasaki, H., Furuse, M., & Tsukita, S. (1999). Endothelial Claudin: Claudin-5/Tmvcf Constitutes Tight Junction Strands in Endothelial Cells. *J Cell Biol, 147*(1), 185-194.

Mosmann, T. (1983). Rapid Colorimetric Assay for Cellular Growth and Survival: Application to Proliferation and Cytotoxicity Assays. *J Immunol Methods, 65*(1-2), 55-63.

Mourtas, S., Antimisiaris, S., Canovi, M., Zona, C., *et al.* (2011). Curcumin-Decorated Nanoliposomes with Very High Affinity for Amyloid-Beta 1-42 Peptide. *BIOMATERIALS, 32*(6), 1635-1645. doi: 10.1016/j.biomaterials.2010.10.027

Mu, C., Dave, N., Hu, J., Desai, P., *et al.* (2013). Solubilization of Flurbiprofen into Aptamer-Modified Peg-Pla Micelles for Targeted Delivery to Brain-Derived Endothelial Cells in Vitro. *J Microencapsul, 30*(7), 701-708. doi: 10.3109/02652048.2013.778907

Murphy, S., Xu, J., & Kochanek, K. (2013). National Vital Statistics Reports. *National Center for Health Statistics data, 61*.

Nachlas, M., Margulies, S., Goldberg, J., & Seligman, A. (1960). The Determination of Lactic Dehydrogenase with a Tetrazolium Salt. *Anal Biochem, 1*, 317-326.

Naik, P., & Cucullo, L. (2012). In Vitro Blood–Brain Barrier Models: Current and Perspective Technologies. *Journal of Pharmaceutical Sciences, 101*(4), 1337-1354. doi: 10.1002/jps.23022

Najlah, M., & D'Emanuele, A. (2006). Crossing Cellular Barriers Using Dendrimer Nanotechnologies. *Curr Opin Pharmacol, 6*(5), 522-527. doi: 10.1016/j.coph.2006.05.004

Najlah, M., Freeman, S., Attwood, D., & D'Emanuele, A. (2007). In Vitro Evaluation of Dendrimer Prodrugs for Oral Drug Delivery. *Int J Pharm, 336*(1), 183-190. doi: 10.1016/j.ijpharm.2006.11.047

Neelov, I., & Popova, E. (2016). Molecular Dynamics Simulation of Lysine Dendrimer and Oppositely Charged Semax Peptides. *Natural Science, 8*(12), 499-510.

Nelson, P., Alfafuzoff, I., Biqio, E., Davies, P., *et al.* (2012). Correlation of Alzheimer Disease Neuropathologic Changes with Cognitive Status: A Review of the Literature. *J Neuropathol Exp Neurol, 71*(5), 362-381. doi: 10.1097/NEN.0b013e31825018f7

Nord, L., Sundqvist, J., Andersson, E., & Fried, G. (2010). Analysis of Oestrogen Regulation of Alpha-, Beta- and Gamma-Secretase Gene and Protein Expression in Cultured Human Neuronal and Glial Cells. *Neurodegener Dis, 7*(6), 349-364. doi: 10.1159/000282279

Oller, B., Sanchez, M., Giralt, E., & Teixido, M. (2016). Blood-Brain Barrier Shuttle Peptides: An Emerging Paradigm for Brain Delivery. *Chem Soc Rev, 45*(17), 4690-4707. doi: 10.1039/c6cs00076b

Omidi, Y., Campbell, L., Barar, J., Connell, D., *et al.* (2003). Evaluation of the Immortalised Mouse Brain Capillary Endothelial Cell Line,B.End3, as an in Vitro Blood–Brain Barrier Model for Drug Uptake and Transport Studies. *Brain research, 990*( ), 95-112.

Osamu, I., Maruyama, K., Tanahashi, H., Iwatsuru, M., *et al.* (2001). Liposomes Bearing Polyethyleneglycol-Coupled Transferrin with Intracellular Targeting Property to the Solid Tumors in Vivo. *Pharm Res, 18*(7), 1042-1048.

Pachter, S., & Song, L. (2003). Culture of Murine Brain Microvascular Endothelial Cells That Maintain Expression and Cytoskeletal Association of Tight Junction-Associated Proteins. *In Vitro Cell Dev Biol Anim, 39*(7), 313-320.

Panyam, J., & Labhasetwar, V. (2003). Biodegradable Nanoparticles for Drug and Gene Delivery to Cells and Tissue. *Adv Drug Deliv Rev, 55*(3), 329-347.

Pardridge, W. M. (2005). The Blood-Brain Barrier: Bottleneck in Brain Drug Development. *NeuroRx, 2*(1), 3-14. doi: 10.1602/neurorx.2.1.3

Pardridge, W. M., Eisenberg, J., & Yang, J. (1985). Human Blood-Brain Barrier Insulin Receptor. *J Neurochem, 44*(6), 1771-1778.

Pare, J., MR, J., & Sigouin, M. (1997). High Performance Liquid Chromatography (Hplc): Principles and Applications. *Techniques and Instrumentation in Analytical Chemistry, 18*, 37-59.

Parepally, J., Mandula, H., & Smith, Q. (2006). Brain Uptake of Nonsteroidal Anti-Inflammatory Drugs: Ibuprofen, Flurbiprofen, and Indomethacin. *Pharm Res, 23*(5), 873-881. doi: 10.1007/s11095-006-9905-5

Park, K. (2008). Trojan Monocytes for Improved Drug Delivery to the Brain. *J Control Release, 132*(2), 75. doi: 10.1016/j.jconrel.2008.10.009

Pasut, G., Scaramuzza, S., Schiavon, O., Mendichi, R., *et al.* (2005). Peg-Epirubicin Conjugates with High Drug Loading. *Journal of bioactive and compatible polymers, 20*(3), 213-230.

Patabendige, A., Skinner, R., Morgan, L., & Abbott, N. (2013). A Detailed Method for Preparation of a Functional and Flexible Blood–Brain Barrier Model Using Porcine Brain Endothelial Cells. *Brain research, 1521*, 16-30. doi: http://dx.doi.org/10.1016/j.brainres.2013.04.006

Patri, A., & Simanek, E. (2012). Biological Applications of Dendrimers. *Mol Pharm, 9*(3), 341. doi: 10.1021/mp300057m

Pawley, J. (2006). *Handbook of Biological Confocal Microscopy* (22-40 Ed. 3 ed.). US: Springer.

Pedziwiatr, E., Fuentes, E., Dzmitruk, V., Sanchez-Nieves, J., *et al.* (2013). Novel 'Si-C' Carbosilane Dendrimers as Carriers for Anti-Hiv Nucleic Acids: Studies on Complexation and Interaction with Blood Cells. *Colloids Surf B Biointerfaces, 109*, 183-189. doi: 10.1016/j.colsurfb.2013.03.045

Peppiatt, C., Howarth, C., Mobbs, P., & Attwell, D. (2006). Bidirectional Control of Cns Capillary Diameter by Pericytes. *Nature, 443*(7112), 700-704. doi: 10.1038/nature05193

Perugini, V. (2013). *Poly-Ɛ-Lysine Dendron Aptamers as Regulators of Angiogenesis in Tissue Regeneration.* (Doctor of Philosophy), University of Brighton, eprints.brighton.ac.uk.

Petty, M. (2002). Junctional Complexes of the Bloodbrain Barrier: Permeability Changes in Neuroinflammation. *Prog Neurobiol, 68*, 311-323.

Pierre, C., & Daniel, S. (1996). *Biology and Physiology of the Blood-Brain Barrier* (1 ed.): Springer US.

Pissarnitski, D. (2007). Advances in Gamma-Secretase Modulation. *Curr Opin Drug Discov Devel, 10*(4), 392-402.

Prashant, K., Keerti, J., Narendra, K. (2014). Dendrimer as Nanocarrier for Drug Delivery. *Progress in Polymer Science, 39*, 268-307.

Price, C., & Jacqueline, N. (2009). *Exploring Proteins: A Student's Guide to Experimental Skills and Methods*. Oxford: Oxford University Press.

Prince, M., Comas-Herrera, A., Knapp, M., Guerchet, M., *et al.* (2016). World Alzheimer Report 2016: Improving Healthcare for People Living with Dementia: Coverage, Quality and Costs Now and in the Future.

Quignot, N., Hamon, J., & Bois, F. (2014). *Extrapolating in Vitro Results to Predict Human Toxicity, in in Vitro Toxicology Systems*. New York, USA: Springer Science.

Raub, T., Kuentzel, S., & Sawada, G. (1992). Permeability of Bovine Brain Microvessel Endothelial Cells in Vitro: Barrier Tightening by a Factor Released from Astroglioma Cells. *Exp Cell Res, 199*(2), 330-340.

Re, F., Cagnotto, A., Salmona, M., Masserini, M., *et al.* (2011). Functionalization of Liposomes with Apoe-Derived Peptides at Different Density Affects Cellular Uptake and Drug Transport across a Blood-Brain Barrier Model. *Nanomedicine : nanotechnology, biology, and medicine, 7*(5), 551-559. doi: 10.1016/j.nano.2011.05.004

Re, F., Gregori, M., & Masserini, M. (2012). Nanotechnology for Neurodegenerative Disorders. *Nanomedicine: Nanotechnology, Biology and Medicine, 8, Supplement 1*(0), S51-S58.

Re, F., Sancini, G., Cambianica, I., Sesana, S., *et al.* (2010). Functionalization with Apoe-Derived Peptides Enhances the Interaction with Brain Capillary Endothelial Cells of Nanoliposomes Binding Amyloid-Beta Peptide. *Journal of biotechnology, 156*(4), 341-346. doi: 10.1016/j.jbiotec.2011.06.037

Refolo, L., Sambamurti, K., Efthimiopoulos, S., Pappolla, M., *et al.* (1995). Evidence That Secretase Cleavage of Cell Surface Alzheimer Amyloid Precursor Occurs after Normal Endocytic Internalization. *Journal of Neuroscience research, 40*(5), 694-706.

Reichert, W. M. (2008). Indwelling Neural Implants: Strategies for Contending with the in Vivo Environment (pp. 97). Boca Raton (FL): CRC Press/Taylor & Francis Taylor & Francis Group, LLC.

Reid, G., Wielinga, P., Zelcer, N., van der Heijden, I., *et al.* (2003). The Human Multidrug Resistance Protein Mrp4 Functions as a Prostaglandin Efflux Transporter and Is Inhibited by Nonsteroidal Antiinflammatory Drugs. *Proc Natl Acad Sci U S A, 100*(16), 9244-9249. doi: 10.1073/pnas.1033060100

Reitz, C., Mayeux, R. (2014). Alzheimer Disease: Epidemiology, Diagnostic Criteria, Risk Factors and Biomarkers. *Biochem Pharmacol, 88*(4), 640-651. doi: 10.1016/j.bcp.2013.12.024

Rensen, P., de Vrueh, R., Kuiper, J., Bijsterbosch, M., *et al.* (2001). Recombinant Lipoproteins: Lipoprotein-Like Lipid Particles for Drug Targeting. *Adv Drug Deliv Rev, 47*(2-3), 251-276.

Rezai, K., Shytle, D., Sun, N., Mori, T., *et al.* (2005). Green Tea Epigallocatechin-3-Gallate (Egcg) Modulates Amyloid Precursor Protein Cleavage and Reduces Cerebral Amyloidosis in Alzheimer Transgenic Mice. *J Neurosci, 25*(38), 8807-8814. doi: 10.1523/jneurosci.1521-05.2005

Richard, M., & Yaakov, S. (2012). Epidemiology of Alzheimer Disease. *Cold Spring Harbor perspectives in medicine, 8*(2).

Ringsdorf, H. (1975). Structure and Properties of Pharmacologically Active Polymers. *J Polym Sci Polym Symp, 51*.

Rip, J., Schenk, G., & de Boer, A. (2009). Differential Receptor-Mediated Drug Targeting to the Diseased Brain. *Expert Opin Drug Deliv, 6*(3), 227-237. doi: 10.1517/17425240902806383

Rocha, S. (2013). Targeted Drug Delivery across the Blood Brain Barrier in Alzheimer's Disease. *CURRENT PHARMACEUTICAL DESIGN, 19*(37), 6635-6646.

Rodriguez, H., Suarez, M.,Albericio, F. (2010). A Convenient Microwave-Enhanced Solid-Phase Synthesis of Short Chain N-Methyl-Rich Peptides. *J Pept Sci, 16*(3), 136-140. doi: 10.1002/psc.1209

Romero, I., Radewicz, K., Jubin, E., Michel, C., *et al.* (2003). Changes in Cytoskeletal and Tight Junctional Proteins Correlate with Decreased Permeability Induced by Dexamethasone in Cultured Rat Brain Endothelial Cells. *Neurosci Lett, 344*(2), 112-116.

Rothman, S. S. (2002). *Lessons from the Living Cell: The Culture of Science and the Limits of Reductionism*. New York: McGraw-Hill.

Ruth, D., & Lorella, I. (2005). Dendrimer Biocompatibility and Toxicity. *Advanced Drug Delivery Reviews, 57*, 2215- 2237.

Sadekar, S., Thiagarajan, G., Bartlett, K., Hubbard, D., *et al.* (2013). Poly(Amido Amine) Dendrimers as Absorption Enhancers for Oral Delivery of Camptothecin. *International journal of pharmaceutics, 456*(1), 175-185. doi: 10.1016/j.ijpharm.2013.07.071

Safari, J., & Zarnegar, Z. (2014). Advanced Drug Delivery Systems: Nanotechnology of Health Design a Review. *Journal of Saudi Chemical Society, 18*(2), 85-99.

Saftig, P., De Strooper, B., Craessaerts, K., Vanderstichele, H., *et al.* (1998). Deficiency of Presenilin-1 Inhibits the Normal Cleavage of Amyloid Precursor Protein. *Nature, 391*(6665), 387-390. doi: 10.1038/34910

Sahoo, S., Parveen, S., & Panda, J. (2007). The Present and Future of Nanotechnology in Human Health Care. *Nanomedicine, 3*(1), 20-31. doi: 10.1016/j.nano.2006.11.008

Saito, T., Iwata, N., Tsubuki, S., Takaki, Y., *et al.* (2005). Somatostatin Regulates Brain Amyloid Beta Peptide Abeta42 through Modulation of Proteolytic Degradation. *Nat Med, 11*(4), 434-439. doi: 10.1038/nm1206

Sandoval, K., Farr, S., Banks, W., Niehoff, M., *et al.* (2011). Chronic Peripheral Administration of Somatostatin Receptor Subtype-4 Agonist Nnc 26-9100 Enhances Learning and Memory in Samp8 Mice. *Eur J Pharmacol, 654*(1), 53-59. doi: 10.1016/j.ejphar.2010.12.013

Saraiva, A., Cardoso, I., Pereira, M., Coelho, M., *et al.* (2010). Controlling Amyloid-Beta Peptide(1-42) Oligomerization and Toxicity by Fluorinated Nanoparticles. *Chembiochem, 11*(13), 1905-1913. doi: 10.1002/cbic.201000237

Sastre, M., Walter, J., & Gentleman, S. M. (2008). Interactions between App Secretases and Inflammatory Mediators. *J Neuroinflammation, 5*, 25. doi: 10.1186/1742-2094-5-25

Satoh, H., Zhong, Y., Isomura, H., Saitoh, M., *et al.* (1996). Localization of 7h6 Tight Junction-Associated Antigen Along the Cell Border of Vascular Endothelial Cells Correlates with Paracellular Barrier Function against Ions, Large Molecules, and Cancer Cells. *Exp Cell Res, 222*(2), 269-274. doi: 10.1006/excr.1996.0034

Sauer, I., Dunay, I. R., Weisgraber, K., Bienert, M., *et al.* (2005). An Apolipoprotein E-Derived Peptide Mediates Uptake of Sterically Stabilized Liposomes into Brain Capillary Endothelial Cells. *Biochemistry, 44*(6), 2021-2029. doi: 10.1021/bi048080x

Sauer, I., Nikolenko, H., Keller, S., Abu Ajaj, K., *et al.* (2006). Dipalmitoylation of a Cellular Uptake-Mediating Apolipoprotein E-Derived Peptide as a Promising Modification for Stable Anchorage in Liposomal Drug Carriers. *Biochimica et Biophysica Acta (BBA) - Biomembranes, 1758*(4), 552-561. doi: http://dx.doi.org/10.1016/j.bbamem.2006.03.017

Sawyer, S., & Krantz, S. (1986). Transferrin Receptor Number, Synthesis, and Endocytosis During Erythropoietin-Induced Maturation of Friend Virus-Infected Erythroid Cells. *J Biol Chem, 261*(20), 9187-9195.

Schenk, D., Barbour, R., Dunn, W., Gordon, G., *et al.* (1999). Immunization with Amyloid-Beta Attenuates Alzheimer-Disease-Like Pathology in the Pdapp Mouse. *Nature, 400*(6740), 173-177. doi: 10.1038/22124

Schilrreff, P., Mundina, C., Romero, E. L., & Morilla, M. J. (2012). Selective Cytotoxicity of Pamam G5 Core--Pamam G2.5 Shell Tecto-Dendrimers on Melanoma Cells. *Int J Nanomedicine, 7*, 4121-4133. doi: 10.2147/ijn.s32785

Schmitt, F., Ryan, M., & Cooper, G. (2007). A Brief Review of the Pharmacologic and Therapeutic Aspects of Memantine in Alzheimer's Disease. *Expert Opin Drug Metab Toxicol, 3*(1), 135-141. doi: 10.1517/17425255.3.1.135

Schofield, P., Tang M, Marder K, Bell K, Dooneief G, Chun M, et al. . (1997). Alzheimer's Disease after Remote Head Injury: An Incidence Study. *J Neurol Neurosurg Psychiatry, 62*(2), 119-124.

Scholz, M., Cinatl, J., Schadel-Hopfner, M., & Windolf, J. (2007). Neutrophils and the Blood-Brain Barrier Dysfunction after Trauma. *Med Res Rev, 27*(3), 401-416. doi: 10.1002/med.20064

Selkoe, D., Wolfe, M. . (2007). Presenilin: Running with Scissors in the Membrane. *Cell, 131*(2), 215-221. doi: 10.1016/j.cell.2007.10.012

Serlin, Y., Shelef, I., Knyazer, B., & Friedman, A. (2015). Anatomy and Physiology of the Blood Brain Barrier. *Seminars in Cell & Developmental Biology, 38*(0), 2-6.

Seshadri, S., & Beiser, A., et al. (2006). The Lifetime Risk of Stroke: Estimates from the Framingham Study. *Stroke, 37*, 345-350.

Sevigny, J., Chiao, P., Bussière, T., Weinreb, P. H., *et al.* (2016). The Antibody Aducanumab Reduces Aβ Plaques in Alzheimer's Disease. *Nature, 537*, 50. doi: 10.1038/nature19323

https://www.nature.com/articles/nature19323#supplementary-information

Sherma, J., & Fried, B. (2003). *Handbook of Thin-Layer Chromatography* (Vol. 89): CRC press.

Shin, D., Kim, D., Chung, W. J., & Lee, Y. (2005). Combinatorial Solid Phase Peptide Synthesis and Bioassays. *J Biochem Mol Biol, 38*(5), 517-525.

Shir, A., Ogris, M., Wagner, E., & Levitzki, A. (2006). Egf Receptor-Targeted Synthetic Double-Stranded Rna Eliminates Glioblastoma, Breast Cancer, and Adenocarcinoma Tumors in Mice. *PLoS Med, 3*(1), e6. doi: 10.1371/journal.pmed.0030006

Shityakov, S., Salvador, E., & Förster, C. (2013). In Silico, in Vitro and in Vivo Methods to Analyse Drug Permeation across the Blood–Brain Barrier: A Critical Review. . *OA Anaesthetics, 1*(2), 13.

Shixian, H., Li, J., Han, L., Liu, S., *et al.* (2011). Dual Targeting Effect of Angiopep-2-Modified, DNA-Loaded Nanoparticles for Glioma. *BIOMATERIALS, 32*(28), 6832-6838. doi: 10.1016/j.biomaterials.2011.05.064

Silverman, R., & Holladay, M. (2014). Prodrugs and Drug Delivery Systems *The Organic Chemistry of Drug Design and Drug Action (Third Edition)* (pp. 423-468). Boston: Academic Press.

Smith, T., Murphy, M., Uljon, S., Fraser, P., *et al.* (2000). Presenilin 1 Regulates Pharmacologically Distinct Gamma-Secretase Activities: Implications for the Role of Presenilin in Gamma-Secretase Cleavage. *J Biol Chem, 34*.

Solfrizzi, V., Scafato, E., Gandin, C., Maggi, S., *et al.* (2011). Metabolic Syndrome, Mild Cognitive Impairment, and Progression to Dementia. The Italian Longitudinal Study on Aging. *Neurobiol Aging, 32*(11), 1932-1941.

Song, Y., Kwon, J., Kim, B., Jeon, Y., *et al.* (2011). Physicobiological Properties and Biocompatibility of Biodegradable Poly(Oxalate-Co-Oxamide). *J Biomed Mater Res A, 98*(4), 517-526. doi: 10.1002/jbm.a.33135

Souza, A., & Topp, E. (2004). Release from Polymeric Prodrugs: Linkages and Their Degradation. *J Pharm Sci, 93*(8), 1962-1979. doi: 10.1002/jps.20096

Srinageshwar, B., Peruzzaro, S., Andrews, M., Johnson, K., *et al.* (2017). Pamam Dendrimers Cross the Blood-Brain Barrier When Administered through the Carotid Artery in C57bl/6j Mice. *Int J Mol Sci, 18*(3). doi: 10.3390/ijms18030628

Srinivas, N., Anusha, G., Malath, K., & Preetika, A. (2014). Dendrimer - for Novel Drug Delivery System- a Review Article. *INDO AMERICAN JOURNAL OF PHARMACEUTICAL SCIENCES, 1*(5), 295-304.

Steinert, S., Shay, J., & Wright, W. (2000). Transient Expression of Human Telomerase Extends the Life Span of Normal Human Fibroblasts. *Biochem Biophys Res Commun, 273*(3), 1095-1098. doi: 10.1006/bbrc.2000.3080

Strum, J., Shehee, R., Virley, D., Richardson, J., *et al.* (2007). Rosiglitazone Induces Mitochondrial Biogenesis in Mouse Brain. *J Alzheimers Dis, 11*(1), 45-51.

Suehs, B., & Shah, S. (2014). Household Members of Persons with Alzheimer's Disease: Health Conditions, Healthcare Resource Use, and Healthcare Costs. *Journal of the American Geriatrics Society, 62*(3), 435-441. doi: 10.1111/jgs.12694

Takeichi, M. (1995). Morphogenetic Roles of Classic Cadherins. *Curr Opin Cell Biol, 7*(5), 619-627.

Taylor, M., Gregori, M., Allsop, D., Moore, S., *et al.* (2011). Effect of Curcumin-Associated and Lipid Ligand-Functionalized Nanoliposomes on Aggregation of the Alzheimer's a Beta Peptide. *NANOMEDICINE-NANOTECHNOLOGY BIOLOGY AND MEDICINE, 7*(5), 541-550. doi: 10.1016/j.nano.2011.06.015

Teixeira, A., Ribeiro, L., Rezende, S., Barros, E., *et al.* (2012). Development of a Method to Quantify Sucrose in Soybean Grains. *Food Chemistry, 130*(4), 1134-1136. doi: http://dx.doi.org/10.1016/j.foodchem.2011.07.128

Teow, H., Zhou, Z., Najlah, M., Yusof, S., *et al.* (2013). Delivery of Paclitaxel across Cellular Barriers Using a Dendrimer-Based Nanocarrier. *Int J Pharm, 441*(1-2), 701-711. doi: 10.1016/j.ijpharm.2012.10.024

Tiwari, G., Tiwari, R., Sriwastawa, B., Bhati, L., *et al.* (2012). Drug Delivery Systems: An Updated Review. *International journal of pharmaceutical investigation, 2*(1), 2. doi: 10.4103/2230-973X.96920

Tomalia, D. (1991). Dendrimer Research. *Science, 252*(5010), 1231. doi: 10.1126/science.252.5010.1231-b

Tomalia, D., Baker, H., Dewald, J., Hall, M., *et al.* (1985). A New Class of Polymers: Starburst-Dendritic Macromolecules. *Polym J, 17*.

Tomalia, D., & Svenson, S. (2005). Dendrimers in Biomedical Applications--Reflections on the Field. *Adv Drug Deliv Rev, 57*(15), 2106-2129. doi: 10.1016/j.addr.2005.09.018

Touzani, R. (2011). Dendrons, Dendrimers New Materials for Environmental and Science Applications. *Mater. Environ. Sci, 2*(3), 201-214.

Traber, M., Vliet A, Reznick Z, & E., C. (2000). Tobacco-Related Diseases. Is There a Role for Antioxidant Micronutrient Supplementation? . *Clin Chest Med, 21*(1), 173-187.

Tsukita, S., Furuse, M., & Itoh, M. (2001). Multifunctional Strands in Tight Junctions. *Nat Rev Mol Cell Biol, 2*(4), 285-293. doi: 10.1038/35067088

Tuma , P., & Hubbard, A. (2003). Transcytosis: Crossing Cellular Barriers. *Physiological Reviews, 83*(3), 871-932. doi: 10.1152/physrev.00001.2003

Turner, P., & O'Connor, K. (2003). Roles of Amyloid Precursor Protein and Its Fragments in Regulating Neural Activity, Plasticity and Memory. *Prog Neurobiol, 70*(1), 1-32.

Ulmer, D., Vallee, B., & Wacker, W. (1956). Metalloenzymes and Myocardial Infarction. Malic and Lactic Dehydrogenase Activities and Zinc Concentrations in Serum. *N Engl J Med, 255*(10), 450-456.

Van, I., Christina, M., & Anderson, M. (2014). Architecture of Tight Junctions and Principles of Molecular Composition. *Cell & Developmental Biology, 36*, 157-165. doi: http://dx.doi.org/10.1016/j.semcdb.2014.08.011

Vignais, V., & Paulette, M. (2010). *Discovering Life, Manufacturing Life. How the Experimental Method Shaped Life Sciences*. Berlin: Springer.

Vorbordt, A. (2004). Molecular Anatomy of Interendothelial Junctions in Human Blood-Brain Barrier Microvessels. *Folia Histochem Cytobiol, 42*, 67-75.

Vries, H., Blom, M., Oosten, M., Boer, A., *et al.* (1996). The Influence of Cytokines on the Integrity of the Blood-Brain Barrier in Vitro. *J Neuroimmunol, 64*(1), 37-43.

Wagner, S., Zensi, A., Wien, S., Tschickardt, S., *et al.* (2012). Uptake Mechanism of Apoe-Modified Nanoparticles on Brain Capillary Endothelial Cells as a Blood-Brain Barrier Model. *PLoS One, 7*(3), e32568. doi: 10.1371/journal.pone.0032568

Wallen, C., Higashikubo, R., & Roti, J. (1983). Comparison of the Cell Kill Measured by the Hoechst-Propidium Iodide Flow Cytometric Assay and the Colony Formation Assay. *Cell Tissue Kinet, 16*(4), 357-365.

Wang, X., Ciraolo, G., Morris, R., & Gruenstein, E. (1997). Identification of a Neuronal Endocytic Pathway Activated by an Apolipoprotein E (Apoe) Receptor Binding Peptide. *Brain Res, 778*(1), 6-15.

Watson, G., Peskind, E., Plymate, S., & Craft, S. (2003). Insulin Increases Csf Abeta42 Levels in Normal Older Adults. *Neurology, 60*(12), 1899-1903.

Weber, P., Ohlendorf, D., Wendoloski, J., & Salemme, F. (1989). Structural Origins of High-Affinity Biotin Binding to Streptavidin. *Science, 243*(4887), 85-88.

Weggen, S., Eriksen, J., Sagi, S., Pietrzik, C., *et al.* (2003). Evidence That Nonsteroidal Anti-Inflammatory Drugs Decrease Amyloid Beta 42 Production by Direct Modulation of Gamma-Secretase Activity. *J Biol Chem, 278*(34), 31831-31837. doi: 10.1074/jbc.M303592200

Weisgraber, K. (1994). Apolipoprotein E: Structure-Function Relationships. *Adv Protein Chem, 45*, 249-302.

Weksler, B., Subileau, E., Perriere, N., Charneau, P., *et al.* (2005). Blood-Brain Barrier-Specific Properties of a Human Adult Brain Endothelial Cell Line. *Faseb j, 19*(13), 1872-1874. doi: 10.1096/fj.04-3458fje

White, P., & Chan, W. (2000). *Fmoc Solid Phase Peptide Synthesis. A Practical Approach*: Oxford university Inc. press.New York.

Whitmer, A., Sidney, S., Selby, J., Johnston, S., *et al.* (2005). Midlife Cardiovascular Risk Factors and Risk of Dementia in Late Life. *Neurology, 64*(2), 277-281.

Wilcock, G., Black, S., Hendrix, S., Zavitz, K., *et al.* (2008). Efficacy and Safety of Tarenflurbil in Mild to Moderate Alzheimer's Disease: A Randomised Phase Ii Trial. *Lancet Neurol, 7*(6), 483-493. doi: 10.1016/s1474-4422(08)70090-5

Williams, D. (2008). On the Mechanisms of Biocompatibility. *BIOMATERIALS, 29*(20), 2941- 2953.

Wim, H., & Paul, J. (2008). Drug Delivery and Nanoparticles: Applications and Hazards. *Int.J.Nanomedicine, 3*(2), 133-149.

Wolburg, H., & Lippoldt, A. (2002). Tight Junctions of the Blood-Brain Barrier: Development, Composition and Regulation. *Vascul Pharmacol, 38*(6), 323-337.

Wolfe, M. (2012). Gamma-Secretase as a Target for Alzheimer's Disease. *Adv Pharmacol, 64*, 127-153. doi: 10.1016/b978-0-12-394816-8.00004-0

Wyss, T. (2016). Ageing, Neurodegeneration and Brain Rejuvenation. *Nature, 539*(7628), 180-186. doi: 10.1038/nature20411

Xia, C., Boado, R., & Pardridge, W. (2009). Antibody-Mediated Targeting of Sirna Via the Human Insulin Receptor Using Avidin-Biotin Technology. *Mol Pharm, 6*(3), 747-751. doi: 10.1021/mp800194y

Xiao, G., & Gan, L. (2013). Receptor-Mediated Endocytosis and Brain Delivery of Therapeutic Biologics. *International Journal of Cell Biology, 2013*, 14. doi: 10.1155/2013/703545

Xing, Y., Zhao, J., Conti, P., & Chen, K. (2014). Radiolabeled Nanoparticles for Multimodality Tumor Imaging. *Theranostics, 4*(3), 290-306. doi: 10.7150/thno.7341

Xu, L., Zhang, H., & Wu, Y. (2014). Dendrimer Advances for the Central Nervous System Delivery of Therapeutics. *ACS Chemical Neuroscience, 5*(1), 2-13. doi: 10.1021/cn400182z

Yaffe, K., Weston, A., Blackwell, T., & Krueger, K. (2009). The Metabolic Syndrome and Development of Cognitive Impairment among Older Women. *Arch Neurol, 66*(3), 324-328.

Yang, H., & Kao, W. (2007). Synthesis and Characterization of Nanoscale Dendritic Rgd Clusters for Potential Applications in Tissue Engineering and Drug Delivery. *Int J Nanomedicine, 2*(1), 89-99.

Yang, H., Liu, C., Yang, D., Zhang, H., *et al.* (2009). Comparative Study of Cytotoxicity, Oxidative Stress and Genotoxicity Induced by Four Typical Nanomaterials: The Role of Particle Size, Shape and Composition. *J Appl Toxicol, 29*(1), 69-78. doi: 10.1002/jat.1385

Yang, H., & Lopina, S. (2003). Penicillin V-Conjugated Peg-Pamam Star Polymers. *J Biomater Sci Polym Ed, 14*(10), 1043-1056.

Ye, Y., Li, H., Jiang, X., Fan, C., *et al.* (1999). 3-(Diethoxyphosphoryloxy)-1,2,3-Benzotriazin-4(3h)-One (Depbt): A New Coupling Reagent with Remarkable Resistance to Racemization. *Org Lett, 1*(1), 91-93.

Yuan, Q., Fu, Y., Kao, W., Janigro, D., *et al.* (2011). Transbuccal Delivery of Cns Therapeutic Nanoparticles: Synthesis, Characterization, and in Vitro Permeation Studies. *ACS Chem Neurosci, 2*(11), 676-683. doi: 10.1021/cn200078m

Zbinden, G., & Flury-Roversi, M. (1981). Significance of the Ld50-Test for the Toxicological Evaluation of Chemical Substances. *Arch Toxicol, 47*(2), 77-99.

Zeng, F., Lee, H., & Allen, C. (2006). Epidermal Growth Factor-Conjugated Poly (Ethylene Glycol)-Block-Poly (Δ-Valerolactone) Copolymer Micelles for Targeted Delivery of Chemotherapeutics. *Bioconjug Chem, 17*(2), 399-409.

Zensi, A., Begley, D., Pontikis, C., Legros, C., *et al.* (2009). Albumin Nanoparticles Targeted with Apo E Enter the Cns by Transcytosis and Are Delivered to Neurones. *Journal of Controlled Release, 137*(1), 78-86. doi: http://dx.doi.org/10.1016/j.jconrel.2009.03.002

Zhang, E., Knipp, G., Ekins, S., & Swaan, P. (2002). Structural Biology and Function of Solute Transporters: Implications for Identifying and Designing Substrates. *Drug Metab Rev, 34*(4), 709-750. doi: 10.1081/dmr-120015692

Zuchero, Y., Chen, X., Bien, N., Bumbaca, D., *et al.* (2016). Discovery of Novel Blood-Brain Barrier Targets to Enhance Brain Uptake of Therapeutic Antibodies. *Neuron, 89*(1), 70-82. doi: 10.1016/j.neuron.2015.11.024

Dissemination

1. Improving Brain Permeability and Targeting of Drug Used For the Treatment of Alzheimer's Disease. S. Al-Azzawi, H. Bachtarzi, G. Phillips, M. Santin. Poster presentation/ Brighton doctoral college research student conference, 2014.

2. Using Dendron as A Carrier For Improving Brain Permeability of Drug Used For The Treatment Of Alzheimer's Disease. S. Al-Azzawi, A. Guildford, G. Phillips, M. Santin. Poster presentation /UK society for biomaterials 14th annual conference and postgraduate day –Belfast, 2015.

3. Bifunctionalisation of the Dendronised Carrier System with Apo-E Peptide and Drug Used In the Treatment of Alzheimer's Disease For Enhancing Blood Brain Barrier Permeability And Targeting. S. Al-Azzawi, A. Guildford, G. Phillips, M. Santin. Oral presentation / Brighton doctoral college research student conference, 2016.

4. Designing and Characterisation A Biocompatible Carrier System To Improve Drug Permeability and Targeting To The Blood Brain Barrier. S. Al-Azzawi, A. Guildford, G. Phillips, M. Santin. Poster presentation / RIC – Caen, France, 2016.

5. Functionalization of the Dendron-Based Carrier System With Apoe-Derived Peptide For Enhancing Blood-Brain Barrier Targeting And Permeability of Drug Used in the Treatment of Alzheimer’s Disease. S. Al-Azzawi, A. Guildford, G. Phillips, M. Santin. Oral presentation /3rd World Congress on Pharmacology - Birmingham, UK, 2016.

6. Dendrimeric Poly(epsilon-Lysine) Carriers for the Enhanced Permeability of Flurbiprofen across the Blood-Brain Barrier in Alzheimer’s Disease: Molecular Design and In vitro Cell Models. S. Al-Azzawi, A. Guildford, G. Phillips, M. Santin. Rapid fire and poster presentation / 28th annual conference of the European Society for Biomaterials (ESB) - Athens, Greece, 2017.